The University Of Sheffield.

Department of Civil and Structural Engineering.

Bioelectrochemically-enhanced Remediation of Contaminated Groundwater

by

Petra Hedbavna

March 2016

Supervisors: Dr Steven F. Thornton, Dr Stephen A. Rolfe and Dr Wei E. Huang

Dissertation submitted to the University of Sheffield in fulfilment of the requirements for the degree of

Doctor of Philosophy

"You do experiments, and 90% of them aren't going to work. Nobody warned me about that."

- Andrew Hires -

(Woolston, 2015)

Abstract

Plumes of organic chemicals in groundwater are frequently anaerobic due to limitations in the availability and aqueous solubility of oxygen. As biodegradation rates for anaerobic processes are usually slower than for aerobic processes, plumes of organic contaminants may persist in groundwater. A novel, but under-developed, approach to enhance the anaerobic bioremediation of organic compounds in groundwater is to couple the exchange of electrons between bacteria and solid state electrodes. In this case, electrodes inserted into the subsurface serve as an inexhaustible electron acceptor for microbial metabolism of organic compounds.

It was shown in laboratory bioelectrochemical systems (BESs) that the presence of an electrode can enhance biodegradation of organic contaminants such as petroleum hydrocarbons, phenol, benzene, naphthalene, phenanthrene and pyrene. However, these laboratory experiments used inocula from sources other than groundwater and often supplied bacteria with mineral media, nutrients, vitamins and single carbon sources. This fails to represent the *in situ* conditions in most aquifers.

In this thesis, the biodegradation rate of phenols and their metabolites in contaminated groundwater was evaluated in a laboratory-scale microbial fuel cell (MFC). The groundwater microbial community development in the MFC was studied subsequently. The tested contaminated groundwater contained a mixture of phenolic compounds (phenol and isomers of cresols and xylenols) and acetate as a product of fermentation of phenols. The electro-active bacteria, likely to be *Desulfuromonas* sp. from Geobacteraceae family, attached to the electrode and used acetate as an electron donor for electricity generation (~1.8 mW/m^2 of projected electrode surface area). Biodegradation of acetate was enhanced in the presence of an electrode acting as an electron acceptor. Enhanced biodegradation of phenols occurred after complete acetate removal. The original groundwater microbial community was more diverse than the community developed in the MFCs as only a few bacterial species were dominating the latter.

The results demonstrate that it is crucial to identify compound(s) utilised by exoelectrogens as electron donor(s) to implement bioelectrochemically-enhanced remediation of organic contaminants. It is likely that electro-active bacteria will not directly degrade the contaminants but utilise their metabolites. Microbial community will undergo significant changes after the introduction of BES electrodes in the aquifer. Hence, knowledge of biodegradation pathways of the parent compound(s) to the electron donating metabolite and their regulation, as well as the cell-cell interactions and carbon flow in the microbial community, is critical for successful application of remediation BESs at the field scale.

In this place, I would like to thank my supervisors, Dr. Steven F. Thornton, Dr. Stephen A. Rolfe and Dr. Wei E. Huang, for scientific support during the project and my colleagues in GPRG office for creating a nice working atmosphere. Last but not least, I would like to thank my friends, family and my partner Darren for their support during this time.

Content

List of Figures

List of Tables

Nomenclature

4H3MB acid - 4-hydroxy-3-methylbenzoic acid

4HB acid - 4-hydroxybenzoic acid

acetyl-CoA - acetyl coenzyme A

AMMI - additive main effects and multiplicative interaction

ANOVA - analysis of variance

ATP - adenosine triphosphate

BES - bioelectrochemical system

bp - base pair

BTEX - benzene, toluene, ethylbenzene and xylenes

CCV - closed circuit voltage

CC-MFC - closed-circuit microbial fuel cell

CE - Coulombic efficiency

COD - chemical oxygen demand

DCA - dichlorethane

DCE - dichloroethene, dichloroethylene

DNA - deoxyribonucleic acid

DO - dissolved oxygen

EET - extracellular electron transfer

EPS - extracellular polymeric substances

FISH - fluorescence in situ hybridisation

GW - groundwater

HPLC - high performance liquid chromatography

ICP - interaction principle component

ICP-MS - inductively coupled plasma mass spectrometry

M3C - microbial 3-electrode cell

mbgl - meters below ground level

MEC - microbial electrolysis cell

ME+S-MFC - mature electrode in sterile microbial fuel cell

MFC - microbial fuel cell

mRNA - messenger ribonucleic acid

NA - not applicable

NAD^+ ($NADH+H^+$) - nicotinamide adenine dinucleotide

ND - not detected

OC-MFC - open-circuit microbial fuel cell

OCV - open circuit voltage

OD_{600} - optical density at 600 nm

OTU - operational taxonomic unit

PAHs - polyaromatic hydrocarbons

PCA - principal component analysis

PCoA - principal coordinates analysis

PCE - tetrachloroethene

PCP - pentachlorophenol

PCR - polymerase chain reaction

PES - polyether sulphone

PICRUSt - phylogenetic investigation of communities by reconstruction of unobserved states

PRB - permeable reactive barrier

PTFE - polytetrafluoroethelene

q-RT-PCR - quantitative reverse transcription polymerase chain reaction

rRNA - ribosomal ribonucleic acid

RT-PCR - reverse transcription polymerase chain reaction

SE+CC-MFC - sterile electrode in closed-circuit microbial fuel cell

SEM - scanning electron microscopy

SHE - standard hydrogen electrode

SIP - stable isotope probing

S-MFC - sterile microbial fuel cell

TCA - tricarboxylic acid

TCE - trichloroethene

TFF - tangential flow filtration

TRF - terminal restriction fragment

T-RFLP - terminal restriction fragment length polymorphism

Chapter 1

Introduction

Groundwater is an important source of drinking water as about 75% of EU residents depend on groundwater for their water supply. Groundwater also greatly contributes to the river flow with up to 90% of river flow consisting of groundwater in the summer season (European Commission, 2008). If contaminants are released from factories, underground petrol tanks or other sources, they can be transported through soil and reach groundwater, compromising its quality and potentially causing harm to humans and the environment (Panagos et al., 2013).

Around 340,000 sites around Europe were reported to be contaminated in 2013, with the estimate of up to 2.5 million potentially contaminated sites. Around 60% of contaminated groundwater sites are polluted by organic chemicals. The main groups of organic contaminants are petroleum hydrocarbons, benzene, toluene, ethylbenzene and xylenes also known as BTEX, polyaromatic hydrocarbons (PAHs), phenolic compounds and chlorinated solvents. Exposure to these chemicals can seriously affect human health, causing for example different types of cancer, liver and kidney damage, respiratory irritation and damage of central nervous system (Panagos et al., 2013).

Various groundwater remediation techniques have been developed and are implemented at contaminated sites. In principle, they can be divided into *ex situ* and *in situ* technologies depending on where the treatment is taking place, i.e. outside or within the aquifer, respectively (Federal Remediation Technologies Roundtable, n.d.). *In situ* remediation has been identified as the most sustainable approach for many contaminated sites (http://www.theadvocateproject.eu/). Bacteria naturally present in the environment have developed the ability to use organic chemicals as a carbon source for their energy metabolism and growth, while degrading the pollutants to carbon dioxide or other harmless chemicals. This process of biodegradation has the potential to clean up groundwater *in situ*. Monitored natural attenuation is one of the *in situ* bioremediation techniques utilising the ability of bacteria to degrade contaminants. However, its application is limited to the sites with conditions favourable for successful biodegradation (Federal Remediation Technologies Roundtable, n.d.).

Bacteria gain energy for their metabolism through redox reactions; coupled chemical half-reactions that involve transfer of electrons from one molecule to another. The half-

reactions are characterised by a redox potential which shows the tendency of a substance to donate electrons. Reactants with higher redox potential (electron acceptors) acquire electrons from those with lower potential (electron donors). The bigger the difference in redox potentials between the electron donor and acceptor, the higher the energy gain for bacteria (Eweis et al., 1998).

Most organic compounds (petroleum hydrocarbons, PAHs, BTEX, phenols etc.) have low redox potentials and serve as electron donors. Hence, a suitable electron acceptor to receive the electrons is needed for biodegradation to occur. In the environment, the most efficient electron acceptor for biodegradation of organic pollutants is oxygen due to its high redox potential. However, plumes of organic chemicals in groundwater are frequently anaerobic due to limitations in the availability and aqueous solubility of oxygen. Biodegradation under anaerobic conditions, using electron acceptors such as nitrate, manganese and iron oxides, sulphate and carbon dioxide, is usually slower than aerobic biodegradation. Furthermore, the potential depletion of these electron acceptors slows biodegradation even more (Atlas and Philp, 2005). Some contaminants, such as trichloroethene (TCE) and tetrachloroethene (PCE), have a high redox potential, close to oxygen, and therefore cannot be utilised by bacteria as electron donors. Instead, bacteria use these pollutants as electron acceptors and therefore they require suitable electron donors for biodegradation (Grindstaff, 1998).

In the environment, some bacterial species developed the ability to transfer electrons to insoluble electron acceptors such as iron(III) and manganese(IV) oxides, highly abundant in aquifer sediments. These bacteria have to transport electrons outside their cells in order to reach the solid electron acceptor (Mehta et al., 2005; Reguera et al., 2005). This phenomenon is universal and enables electron transfer from bacteria to solid electrodes in bioelectrochemical systems. Depending on the potential of the electrode, transfer of electrons from electrodes to bacteria is also possible (Rabaey et al., 2010) and it has been proposed that some of the electro-active bacteria can perform extracellular transfer of electrons over long distances (up to 2 cm) (Nielsen et al., 2010; Revil et al., 2010).

Similarly, carbon electrodes could be installed in the subsurface to provide bacteria with an electron acceptor or donor for enhanced bioremediation of groundwater, i.e. bioelectrochemically-enhanced remediation (Lovley, 2011; Lovley and Nevin, 2011; Aulenta and Majone, 2010). This is potentially a promising and sustainable technique to enhance bioremediation of groundwater, but it is still in its infancy.

This thesis firstly discusses the state-of-the-art of bioelectrochemically-enhanced remediation and, as it is apparent from the literature review, there is much research needed to move the technology from laboratory experiments to groundwater application. The laboratory-scale studies mostly test artificial groundwater systems amended with nutrients, vitamins and sole carbon sources, and waste water or single strain bacteria as an inoculum. Other research is focused on bioelectrochemically-enhanced remediation of soils or sediments. This thesis fills in the gap in our understanding of interaction of groundwater microbial community with the electrodes and its effect on biodegradation of a mixture of groundwater contaminants (phenolic compounds) without any amendments with nutrients.

Chapter 2

Literature review and fundamentals

The rate of biodegradation of organic pollutants in groundwater can be limited by the lack of readily available electron acceptors/donors for microbial metabolism. Technologies currently implemented to enhance *in situ* bioremediation by addition of electron acceptors/donors include for example biosparging, addition of nitrate or carbohydrates (e.g. molasses). Biosparging requires a continuous electricity source to power the air pumping under the ground, nitrate can potentially create additional pollution and the mass transfer of oxygen, nitrate and carbohydrates in the aquifer porous media is hard to control (Zhang et al., 2010; Eweis et al., 1998). Application of BES (bioelectrochemical system) electrodes can overcome these problems as they serve as an inexhaustible electron acceptor/donor. Low maintenance costs after BES installation and the possibility of electricity production from organic contaminants make this technology highly sustainable (Zhang et al., 2010).

A bioelectrochemical system is a device in which an oxidation or reduction reaction on the electrode is enhanced by biological catalyst (microorganisms, enzymes, DNA) (Schröder et al., 2015). For the purposes of this thesis, BESs employ extracellular electron transfer (EET) between bacteria and electrodes (Rabaey et al., 2010). The transfer of electrons from bacteria to electrodes was first studied in microbial fuel cells (MFCs), 'bacterial batteries'. It is a group of BESs which produce electrical current by the metabolic activity of microorganisms. MFCs were believed to be a possible sustainable source of energy in the future. However, research has shown that the power produced by MFCs is limited. More recent publications focus on other BES applications which may have additional value other than electricity generation, or applications where electricity generation is not the primary aim (Rosenbaum et al., 2011). One example is the use of BESs to enhance the bioremediation of organic contaminants in groundwater (Rabaey et al., 2010). This application has been largely unexplored to date.

2.1 BES technical concept

In principle, there are three types of BESs (Rosenbaum et al., 2011; Rabaey et al., 2010; Logan, 2008):

- Microbial 3-electrode cells (M3Cs). The working electrode interacts with bacteria and its potential is controlled by a potentiostat with respect to the known potential of the reference electrode (Figure 2-1). The counter electrode completes the circuit. The working electrode can work as both, anode (electron acceptor) or cathode (electron donor) depending on the value of its potential which can be set to keep favourable conditions for biodegradation. Electricity is needed to power the potentiostat. Electrical current is produced when the anode accepts electrons, whereas the cathode requires a power source.

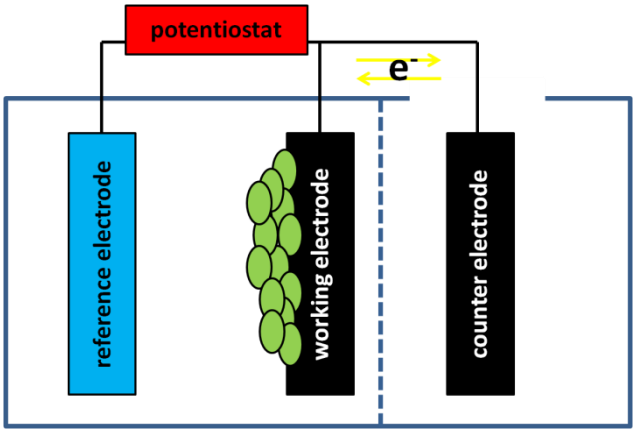

Figure 2-1 A schematic of a microbial three-electrode cells (M3C).

- Microbial fuel cells (MFCs). MFCs consist of an anode, cathode and the circuit is completed by the load, e.g. resistor (external resistance) (Figure 2-2). Bacteria can occupy either of the two electrodes (bio-anode vs. bio-cathode), although most research has been focused on bio-anode applications due to the possibility of electricity production. The electrode potential is influenced by external resistance, bacterial enzymes interacting with the electrode and a chemical reaction taking place on the other electrode. The bio-cathode application requires a source of electrons to the anode.

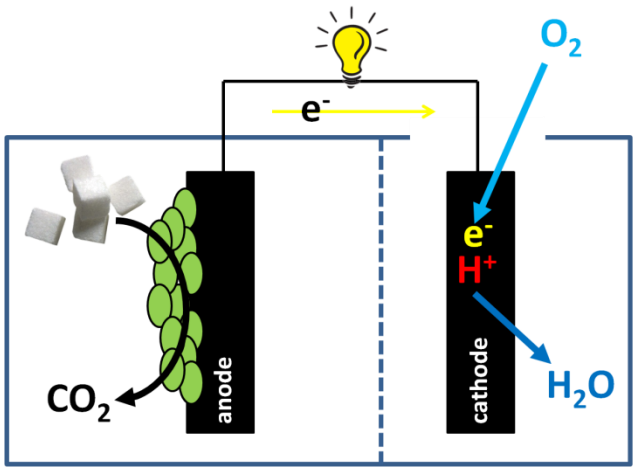

Figure 2-2 A schematic of a microbial fuel cells (MFC)

- Microbial electrolysis cells (MECs). The potential developed between the two electrodes due to bacterial action is increased by > 0.2 V using a potentiostat (Figure 2-3). Increasing the potential difference between the two electrodes helps catalyze reaction on the cathode where no oxygen is needed. MECs are used for example for hydrogen production but they are not main focus of this thesis.

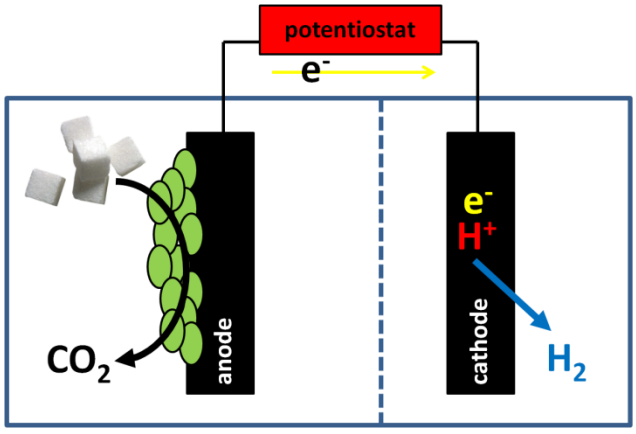

Figure 2-3 A schematic of a microbial electrolysis cell (MEC).

BES designs vary greatly. Most laboratory systems are built as either single-chamber or dual-chamber BESs. In a single-chamber BES, all electrodes share the same chamber. Working and reference electrode/anode are in a chamber separated from the counter electrode/cathode chamber in a dual-chamber BES. In most cases, the chambers are divided by a membrane and electrodes are made of graphite or carbon (Logan, 2008). The simplest and cheapest dual-chamber BES can be constructed using two Schott bottles

connected by a semi-permeable membrane to give an H-type BES (Figure 2-4). This design is typically used in experiments exploring basic parameters, for example new materials, different microbial communities and biodegradation of specific compounds (Logan, 2012; Logan and Regan, 2006). It is ideal for first proof-of-concept bioremediation experiments. More information about BES designs and set-ups can be found for example in Li et al. (2011), Zhou et al. (2011) and Logan (2008).

Figure 2-4 H-type microbial fuel cell.

BES performance can be characterised by different variables. One is power density, calculated as the ratio of power production over limiting electrode surface (unit W/m^2) or reactor volume (unit W/m^3). The same applies for the current density (unit A/m^2 or A/m^3) (Chae et al., 2008; Bullen et al., 2006; Logan et al., 2006). Coulombic efficiency (CE) reflects the efficiency of electron transfer between the organic compound and an electrode. It is calculated as a proportion of electrons recovered from the given organic compound(s) on the anode. For the cathode, it is the number of electrons reducing the soluble electron donor(s) relative to number of electrons provided on the electrode (Rabaey et al., 2010; Chae et al., 2008; Du et al., 2007). Removal efficiency of target compound(s) is a useful parameter for wastewater or bioremediation application of BESs (Rabaey et al., 2010).

Many carbon sources, e.g. glucose and also contaminants such as phenols, BTEX and alkanes, are firstly activated then metabolised to acetyl-CoA by bacterial processes. Acetyl-coA can then be used for building biomass or to produce energy in the form of ATP from the TCA cycle and respiratory chain. Acetyl-CoA entering the TCA cycle is metabolised to carbon dioxide and hydrogen atoms are carried by nicotinamide adenine dinucleotide (NAD^+) in the form of $NADH+H^+$ to the respiratory chain. Electrons released from the respiratory chain are transferred to the terminal electron acceptor (Madigan et al., 2011). The amount of energy bacteria gain (ΔG) from this is directly proportional to the potential

difference between the final electron acceptor reduction and $NAD^+/NADH+H^+$ reaction which delivers electrons to the respiratory chain (Equation 1).

$$\Delta G = -nFE \quad (1)$$

where n is the number of electrons transferred, F is Faraday constant (96630 J/V) and E is redox potential of the reaction defined by Nernst-equation (Equation 2) as

$$E = E^{\emptyset} - \frac{RT}{nF} lnQ_R \quad (2)$$

where $E^{\emptyset}$ is standard potential of the reaction, R is gas constant (8.314 J/(mol·K)), T is temperature in Kelvin and Q_R is the reaction quotient (Logan, 2008).

In BESs, the electrons can be transferred to the anode. Its potential can be either set in an M3C or it can develop based on the potential of redox proteins involved in respiratory chain interacting with the anode in an MFC (Rosenbaum et al., 2011; Logan, 2008). Electrons are transported to the cathode/counter electrode via the wire and in an MFC interact with the protons reducing the present soluble electron acceptor, in most cases oxygen (Figure 2-5) (Logan, 2008).

2.1.1 MFC efficiency

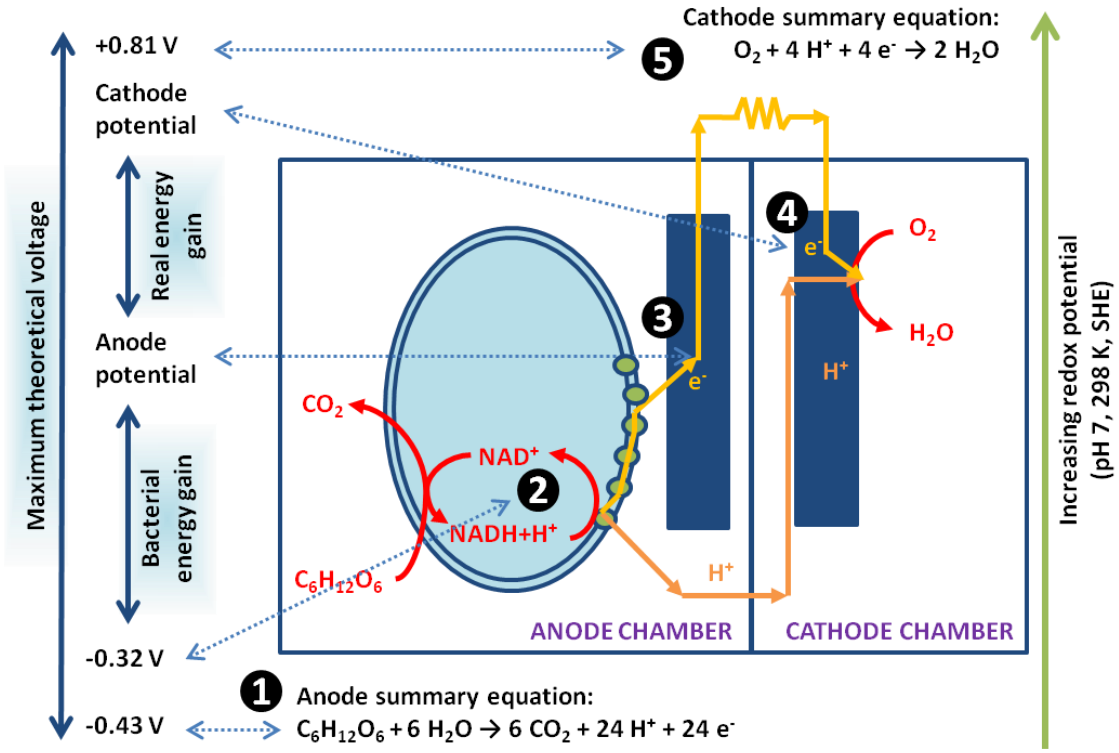

Figure 2-5 Schematic of a dual-chamber MFC and redox potentials in the system. 1 - anode summary equation for glucose oxidation, 2 - nicotinamide adenin dinucleotid (NAD^+) reduction/oxidation, 3 - anode potential, 4 - cathode potential, 5 - cathode summary equation for oxygen reduction. SHE - standard hydrogen electrode. Extracellular electron transfer mechanisms not shown. Not to scale.

In an MFC, the theoretical voltage ($E^{\emptyset}_{cell}$) can be calculated from Equation 3 as

$$E^{\emptyset}_{cell} = E^{\emptyset}_{cat} - E^{\emptyset}_{an} \quad (3)$$

where $E^{\emptyset}_{cat}$ is the standard potential of a reaction occurring on the cathode and $E^{\emptyset}_{an}$ is the standard potential of a reaction taking place on the anode (Figure 2-5).

For an MFC degrading glucose on the anode and oxygen reduction taking place on the cathode, the theoretical maximum voltage is

$$E^{\emptyset}_{cell} = E^{\emptyset}_{cat} - E^{\emptyset}_{an} = 0.81 - (-0.43) = 1.24\,V \quad (4)$$

However, as mentioned previously, bacteria harvest part of the chemical energy in the form of ATP from the transfer of electrons to the anode and the potential of the cathode is lower due to potential losses. Hence, the measured open circuit voltage (without the resistor) is always lower than expected (Logan, 2008).

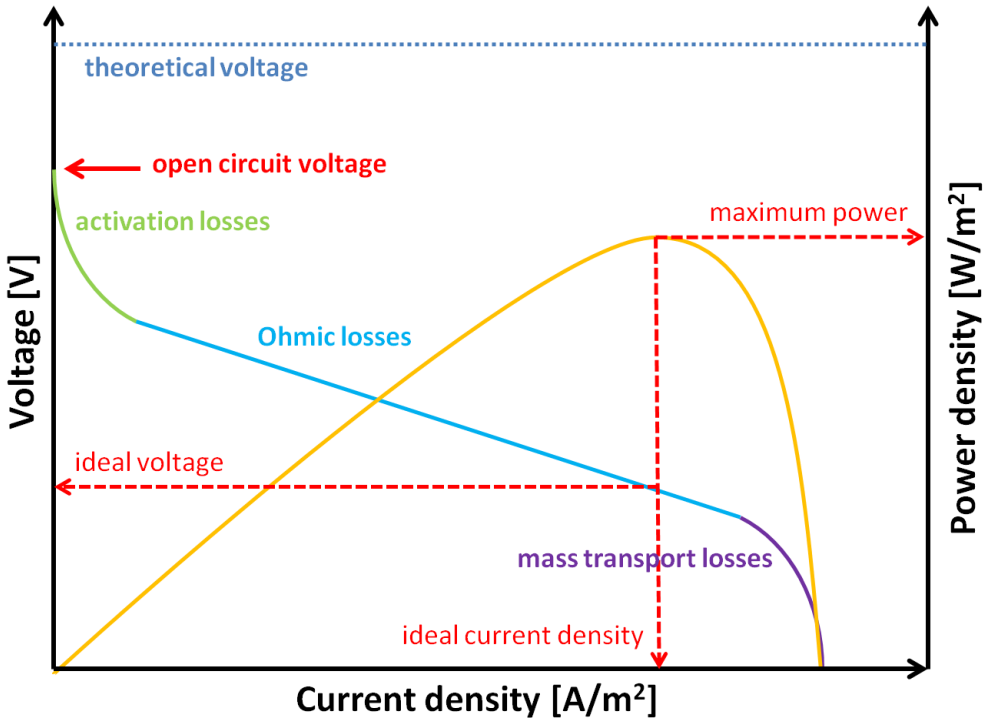

Figure 2-6 Polarisation and power curve.

If the electrodes are connected by the wire and the resistor or another load is introduced, the voltage drops. The extent of the decrease depends on the current density flowing through the system. This can be regulated by external resistance used in the MFC system or by a potentiostat and a so-called 'polarisation curve' can be measured (Figure 2-6). It characterises the decrease of measured voltage as the current density increases for a given resistance (from Ohm's law). The initial rapid voltage decrease is caused by the activation losses under low current densities. These losses reflect the energy needed for the

reaction initiation on the electrode. The next drop has a near linear form and appears under medium current densities. These voltage losses, called Ohmic losses, result from the electrical resistances present in the system, e.g. electrolyte, membrane, electrodes, biofilm, wires, etc. The final rapid voltage drop occurs at high current densities due to the mass transfer limitations of reactants to the electrode and products from the electrodes, including hydrogen protons through the membrane. These losses are called mass transport losses. The activation losses and Ohmic losses contribute to the internal resistance of an MFC (Zhao et al., 2009; Clauwaert et al., 2008; Logan et al., 2006). The highest power density possible can be found for a certain current density when the external and internal resistance are equal (Figure 2-6) (Chae et al., 2008; Bullen et al., 2006; Logan et al., 2006). The voltage losses can be minimised by changing various factors, mainly material and design features (Table 2-1) (Clauwaert et al., 2008). When scaling-up MFCs, the electrode surface area and electrode spacing limit the MFC performance the most (Logan, 2010).

Further information on the various factors which affect MFC performance is provided in Lovley (2012), Li et al. (2011), Zhou et al. (2011), Franks et al. (2010), Pant et al. (2010), Torres et al. (2010), Logan (2008), Rinaldi et al. (2008).

Table 2-1 Factors which positively affect the electrical performance of MFCs (Clauwaert et al. 2008).

Activation losses	High specific electrode surface area
	High ratio of anode surface covered by anode reducing bacteria to total anode surface
	Application of catalysts on cathode surface
	Microorganisms capable of efficient electron transfer to the anode
Ohmic losses	Highly conductive electrodes and wires
	High concentration of ions with high mobility
	Low electrode spacing
	No membrane or high membrane surface area
Mass transport losses	High specific electrode surface area
	High buffering capacity or fast H^+ transport to the cathode
	Stirring

2.1.2 Extracellular electron transfer

Bacteria build biofilm on the BES electrodes (Logan, 2008). Electrons are released from the cells and transported to the anode via different EET mechanisms (Schröder et al., 2015; Logan et al., 2006; Logan and Regan, 2006). The mechanisms discovered to date include direct contact of the cell with the electrode via c-type cytrochromes or nanowires (bacterial

conductive *pili*) and electron mediators/shuttles (soluble compounds which can be reduced and oxidised again after releasing electrons to the anode). A bacterial species can use one or a combination of these mechanisms. Some microorganisms cannot transfer electrons to the anode on their own but can use electron mediators produced by other bacteria (Franks and Nevin, 2010; Torres et al., 2010; Lovley, 2006a).

Two mechanisms of electron transfer from electrodes to bacteria have been discovered. These are direct contact provided by cytochromes and electron shuttle transfer. The mechanism of electron transfer from the bacteria to the final soluble electron acceptors remains unknown (L. Huang et al., 2011b). In general, the electron transport mechanisms between bacteria and electrodes are not fully resolved and more research needs to be done in this area.

Geobacter sp. are some of the most studied bacteria in BES research due to ease of culturing and ability to produce high current densities in pure culture. Geobacteraceae transfer electrons to electrodes via c-type cytochromes and nanowires (Reguera et al., 2006). Due to their ability to efficiently transfer electrons to the electrode bacteria *Geobacter* sp. usually dominate the bio-anode communities in BESs (Chae et al., 2009; Jung and Regan, 2007; Lovley, 2006a; Bond et al., 2002). Above all, *Geobacter*-like species are capable of using the low potential electrodes as electron donors to reduce electron acceptors with a higher redox potential (e.g. nitrate, fumarate) (Rosenbaum et al., 2011).

Another genus of culturable exoelectrogens, *Shewanella* sp., has also been examined in detail. These bacteria transfer electrons to electrodes by producing electron mediators and c-type cytochromes (Franks et al. 2010; Schaetzle et al. 2008; Rabaey et al. 2007; Gorby et al. 2006). Nevertheless, microorganisms other than the previously mentioned examples are capable of electron transport to the electrode. Most bacteria which utilise insoluble iron(III) oxides as an electron acceptor can in principle produce electricity in BESs. However, not every current producer can transfer electrons to iron(III) oxides. In addition to *Geobacter* spp., *Shewanella* spp., other microorganisms which can utilise electrodes in BESs as an electron acceptor include *Geothrix fermentas*, *Pseudomonas* spp., *Aeromonas hydrophilia*, *Clostridium* spp., *Rhodoferax ferrireducens*, *Desulfobulbus propionicus*, *Escherichia coli*, bacteria of the Firmicutes phylum etc. (Franks et al., 2010).

2.2 *In situ* BESs for enhanced bioremediation

Many microbial, environmental and technical factors affect the efficiency of bioremediation. These include the presence of biodegrading microorganisms, bioavailability

of contaminants, electron acceptors (their redox potential) and nutrients, pH, media buffering capacity and temperature (Alvarez and Illman, 2006; Atlas and Philp, 2005). One aim of bioremediation techniques is to enhance the metabolic activity of indigenous microorganisms capable of biodegrading a specific organic compound/s, either by bioaugmentation (laboratory culturing and inoculation back into the environment) or biostimulation (modifying environmental factors which positively influence microbial metabolism) (Scow and Hicks, 2005). Application of BESs in bioremediation is a biostimulation technique, as they provide unlimited availability of an energetically favourable electron acceptor/donor for microbial metabolism. In addition, graphite electrodes can adsorb contaminants, offering the possibility to concentrate the electron acceptor/donor supply, biodegrading microorganisms and organic contaminants in one location to enhance bioremediation performance (Lovley and Nevin, 2011).

In principle, two types of BES could be installed in the field. The M3C system would require a power source for the potentiostat[*] and also to deliver electrons for bioremediation if needed. The electrical energy could be produced from renewable sources (e.g. solar or wind) (Aulenta et al., 2013). The advantage of the three-electrode approach is the possibility to set the electrode potential to control the biodegradation rate and use the electrode as both electron acceptor or donor. Any electricity gained from the biodegradation of contaminants could be stored (Franks and Nevin, 2010) and reused, for example for powering the potentiostat. It is also possible to set the potential of the electrode to promote hydrogen or oxygen development for enhanced biodegradation. However, this is not the main focus of this review.

The MFCs are passive systems which do not rely on any power source. They are more practical for enhanced *in situ* biodegradation of contaminants on the anode than on the cathode. The cathode would require a source of electrons. They would have to come from an anode, either from a chemical or biological reaction, which would be difficult to implement in the field. An anode could be placed within the contamination plume, in contact with biodegraders and contamination; the cathode could be installed within the oxygenated uncontaminated groundwater, reducing oxygen to water. Any current produced could be collected (Franks and Nevin, 2010) and reused, e.g. for monitoring purposes. The limiting factor in electricity production will be the internal resistance of the system.

[*] A cost-effective and field-ready potentiostat has already been constructed for monitoring of bacterial respiration by subsurface electrodes (Friedman et al., 2012).

2.2.1 Influence of electrode potential on biodegradation rate

Although electricity production is not the main focus of BES-bioremediation applications, the electricity production efficiency can potentially affect bioremediation efficiency. The microbial metabolic rate can be influenced by two factors: the electrode potential and the current flowing through the system (Aelterman et al., 2008). Considering the bio-anode application, a higher anode potential is more thermodynamically favourable for bacteria. In theory, this is reflected by an increased propensity for bacteria to transfer electrons to the anode, resulting in a higher current density and increased substrate biodegradation rate. However, several studies show that current generation can be improved under low anode potentials (Wagner et al., 2010).

A low anode potential also implies a higher voltage gain from an MFC. Although decreasing the anode potential looks desirable, by increasing the voltage gain for external use, it may result in preferential use of other electron acceptors with higher redox potential by the bacteria. Therefore the CE of the system decreases (Logan, 2008; Rabaey and Verstraete, 2005). In MFC applications, the important factor influencing the anode potential and current density flowing through the systems will most likely be external resistance. The anode potential can reach high values under lower external resistance when current density is increased. This is also likely to facilitate transfer of electrons from bacteria to the anode (Katuri et al., 2011). Theoretically the higher the current flow, the faster the biodegradation of contaminants.

Similarly as with the anode, the cathode potential will affect the biodegradation rate of contaminants in bio-cathode applications. The studies focusing on the effect of the cathode potential on bioremediation are discussed later (Chapter 2.3).

In situ bioremediation-BESs differ from laboratory-BESs in key aspects, such as biodegraded substrates/contaminants, microorganisms present, environmental conditions and design. These factors, which potentially influence the performance of bioremediation-BESs in the terms of electricity production and therefore bioremediation, are considered below.

2.2.2 Substrates

As defined previously, the amount of electricity produced by BESs is affected by the substrate degraded by bacteria. Coulombic efficiency (CE) quantifies how many electrons were recovered from a given substrate. CE of a given substrate depends on the metabolic

pathway used in its biodegradation and its biodegradability (Kiely et al., 2011; Pant et al., 2010; Chae et al., 2009). Experiments by Luo et al. (2009) showed that the CE of MFCs which biodegrade contaminants such as phenol can be lower than for a readily biodegradable substrate such as glucose.

Contaminated land typically contains a mixture of organic chemicals requiring treatment (Pant et al., 2010; Alvarez and Illman, 2006; Atlas and Philp, 2005). MFCs biodegrading complex substrate mixtures produce lower power densities than MFCs biodegrading simple substrates (Liu and Logan, 2004). An MFC used to biodegrade mixtures of more recalcitrant organic contaminants in the environment will therefore produce lower energy than when biodegrading simple readily biodegradable substrates.

The low biodegradation potential of many hydrophobic organic compounds is often related to their low aqueous solubility and therefore bioavailability (Cameotra and Makkar, 2010). Hydrophobic organic compounds can adsorb onto graphite electrodes in BESs and be metabolised by microorganisms, as shown by Zhang et al. (2010) using [^{14}C]-toluene. However, the mechanism of toluene uptake by the microbes was not deduced.

2.2.3 Microbial community

Microorganisms already present in the environment will be involved in the substrate biodegradation and electron transfer. The microbial community within the bioremediation-BES must therefore be able to oxidise/reduce a specific contaminant and transfer the electrons to/from the electrode. In the anode biofilm community, the non-electricity producing bacteria can convert various complex substrates into simpler compounds, which are further utilised by exoelectrogens (bacteria capable of extracellular electron transfer to and from the electrode) (Pant et al., 2010; Chae et al., 2009; Logan and Regan, 2006; Lovley, 2006a). Some exoelectrogens are capable of both, biodegrading complex organic contaminants while reducing the anode (Wang et al., 2012; Zhang et al., 2010). In this case metabolic cooperation between different microbial species is not required.

The best known exoelectrogens are *Geobacter* sp. and *Shewanella* sp., both abundant in the environment (Lovley et al., 2011; Hau and Gralnick, 2007). Although *Geobacter*-like bacteria prefer simple substrates such as acetate and transfer electrons to the anode (Chae et al., 2009), they also contribute to the biodegradation of aromatic hydrocarbons (Rooney-Varga et al., 1999). For example, the bacterium *Geobacter metallireducens* transfers electrons to the anode but also degrades aromatic compounds such as benzoate and toluene (Zhang et al., 2010; Tender et al., 2002). In pure culture, *Geobacter metallireducens* can colonise the anode surface while using toluene as a sole carbon source and achieving a CE of 91%

(Zhang et al., 2010). The genus *Geobacter* is likely to play an important role in bioremediation-BESs. *Geobacter lovleyi* can transfer electrons from an electrode with a low redox potential to chemical compounds with higher potential. This principle has been applied in biocathode-BESs for the reductive biodegradation of chlorinated solvents (Aulenta et al., 2009; Strycharz et al., 2008).

Possible exoelectrogenic bacteria in bioremediation-BESs also include *Pseudomonas* spp. which produces electron shuttles (Franks et al., 2010; Pham et al., 2008). These bacteria have the potential to metabolise various hydrocarbon compounds (Hamme et al., 2003; Samanta et al., 2002; Margesin and Schinner, 2001; Allard and Neilson, 1997). These properties make them potentially abundant in communities of bioremediation-BESs. Experimental studies support this theory. Morris et al. (2009) analyzed the biofilm community of a diesel-biodegrading MFC using DNA sequencing of 16S rRNA genes. The community comprised mainly denitrifying bacteria, including *Pseudomonas* sp., along with the exoelectrogen *Shewanella* sp. Bacteria of genus *Pseudomonas* sp. were also identified in a nitrobenzene-biodegrading MFC with glucose as a co-substrate (Li et al., 2010).

Considering groundwater bioremediation using BESs, two mechanisms of electron transfer are preferable; direct contact with the electrode via cytochromes and nanowires. Soluble electron shuttles may not be effective depending on the groundwater flow rate.

2.2.4 Environmental conditions

Environmental factors which typically influence bioremediation efficiency *in situ* are the availability of electron acceptors and their redox potential, nutrients, pH, media buffering capacity of soil or groundwater and temperature (Alvarez and Illman, 2006; Atlas and Philp, 2005). Potential effects of these factors on bioelectrochemically-enhanced remediation are discussed below.

The presence of alternative electron acceptors in the environment may decrease the energy efficiency of bioremediation-BESs due to competition with the anode for electron transfer (Nevin et al., 2008; Logan et al., 2006; Rabaey and Verstraete, 2005). Even if bacteria have a preference for other electron acceptors, the anode provides a long-term high concentration electron acceptor which cannot be depleted like other electron acceptors (Morris et al., 2009). BES technology can be used in combination with nutrient or other electron acceptor amendments. Biodegradation rates can be higher, despite the possibility of a decrease in CE due to electron transfer to these alternative electron acceptors. Experiments by Yan et al. (2012) showed that the combination of MFC technology and addition of ferric hydroxide to sediment resulted in a higher bioremediation

efficiency of a persistent compound such as phenanthrene (99.5%), compared with MFC technology in isolation (96.1%), ferric hydroxide addition (87.6%) and natural attenuation (80.3%) in 240 days.

Most groundwater has a near-neutral pH but specific contaminants such as organic acids or inorganic acid-organic chemical mixtures can cause extreme pH conditions (pH 3–11) (Andrews et al., 2004; Chapelle, 2001). Laboratory studies show that pH influences the BES performance. However, the exact effect of pH on BES efficiency is quite unpredictable. Despite an optimum pH for bacterial growth, several BES studies show that electricity generation is enhanced by increasing the pH in the anode chamber to pH 9 (Yuan et al., 2011; Puig et al., 2010; He et al., 2008; Logan, 2008; Ren et al., 2007). For this reason, the influence of pH on electricity production and bioremediation enhancement within the BES is difficult to predict. The buffering capacity of contaminated groundwater will also be important.

Most studies of bioremediation-BESs considered in this review have been carried out under a laboratory temperature between 22 and 30°C, typically much higher than that of groundwater (depending on the variation in season, vegetation, heat capacity of the media and subsurface depth) (Kasenow, 2001; Killham, 1994). Considering the preceding analysis (Behera et al., 2011; Liu et al., 2011; Michie et al., 2011; Ahn and Logan, 2010; Larrosa-Guerrero et al., 2010), the power density achieved by *in situ* BES technologies will probably be lower than implied in comparable laboratory studies.

2.2.5 Designs

There are many differences in the design of laboratory, wastewater treatment and groundwater BES devices. Laboratory BESs are small-scale reactors with capacities in the order of 0.2–10 litres. Wastewater treatment deals with larger volumes and complex mixtures of substrates. However, in comparison with groundwater BESs, the conditions (pH, temperature, stirring etc.) in BESs treating wastewater are easier to control.

2.2.5.1 BES-permeable reactive barrier

In groundwater, the working electrode (anode or cathode) will be installed within the contamination plume, providing close contact between microorganisms, contaminants and the electron acceptor/donor to enhance biodegradation. Due to the groundwater flow, bioremediation of contaminated groundwater using BESs is a continuous process. In this respect, the working electrode of a BES used in groundwater bioremediation must support biodegradation of contaminants in flowing groundwater, in addition to fulfilling general

material requirements (being conductive and allow attachment of bacteria naturally present in groundwater). A possible solution is the use of graphite granules to construct an electrode, arranged as a permeable reactive barrier (conductive 'BES-PRB' as shown in Figure 2-7).

Granule size varies and should allow the adjustment of hydraulic conditions in the electrode to those in the host aquifer. The variable structure of the graphite granule particles can provide different specific areas for microbial growth and therefore affect the BES-PRB performance (Arends et al., 2012). It is assumed that indigenous microorganisms will attach to the electrode material. A restriction may be the low specific area of the graphite granules for microbial growth relative to other electrode materials. Additionally, connecting such material to the wire gathering/providing the electrons is a technical challenge. The granules are connected to each other by a small fraction of their total area due to their shape and porosity of the packed bed. The contact with the current collector is also limited. For these reasons incomplete electron transfer may occur (Zhou et al., 2011; Logan, 2008). The possibility of installing more gathering wires into large volume electrodes could be examined.

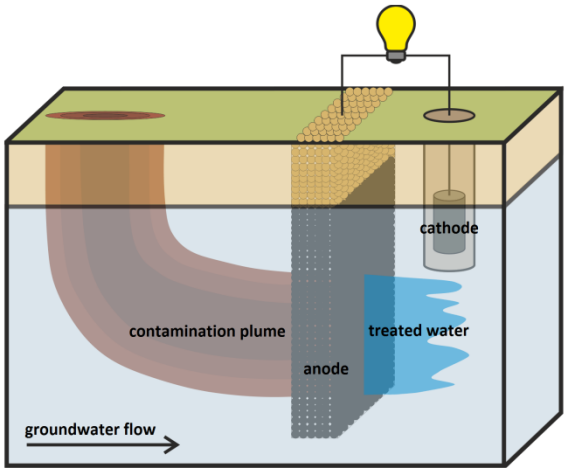

Figure 2-7 Conceptual model of bioremediation-MFC.

Technical aspects such as residence time, treatment rate, and implementation of conductive PRB materials, e.g. barrier size, location relative to plume and temporal changes in discharge, should be considered as per traditional PRB technology. Similarly, this conductive BES-PRB could suffer from potential fouling by microbial biomass accumulation. Clogging of BESs has been reported in systems which have used graphite granules as the electrode material (Zhang et al., 2011).

To reduce construction costs a PRB based on graphite granules could be developed as a funnel-gate system where the size of the reactive 'gate' is much smaller and contaminants

are directed through the treatment zone (BES-PRB) by the 'funnel' system (Grindstaff, 1998). It has been shown that it is also possible to mix the graphite granules with aquifer material which would reduce the cost of the system. Arends et al. (2012) mixed the graphite granules with sand in different ratios. It was shown that a 2:1 ratio of graphite granules to sand does not decrease the performance significantly.

The BES-PRB can be connected to the counter electrode/cathode placed near the surface for easy maintenance. Considering oxygen in air is the only environmentally-friendly and sustainable electron acceptor (Rismani-Yazdi et al., 2008), the cathode of a bioremediation-MFC will require access to oxygen as electron acceptor for cathode reaction (Figure 2-7). In such field-scale MFC, the natural presence of bacteria at the cathode would potentially allow biologically catalyzed reduction of oxygen (Logan et al., 2006).

2.2.5.2 Sequential BES-PRB

Bioremediation of some contaminants might require both a suitable electron donor and acceptor. Biodegradation of PCE is an example of such process. PCE is first reduced through TCE to *cis*-DCE (*cis*-dichloroethene), which can then be oxidised to carbon dioxide. BESs with regulated electrode potential provide both an electron donor and acceptor for both sequential steps of biodegradation. Figure 2-8 shows two PRBs; the first one enhancing reduction of PCE to *cis*-DCE which then migrates down-gradient to the next PRB where its oxidation takes place (Aulenta and Majone, 2010).

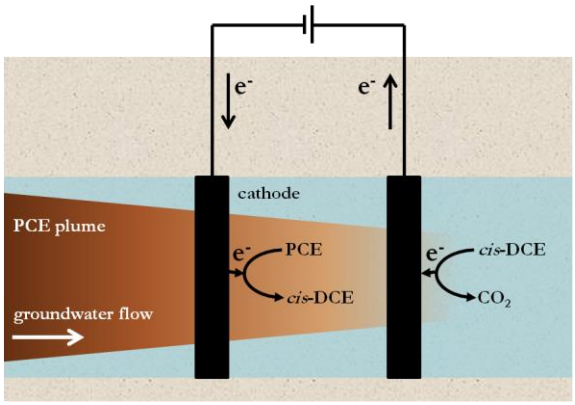

Figure 2-8 Conceptual model of BES for biodegradation of chlorinated solvents. The electrodes are constructed as PRBs and their potential is regulated (adapted from Aulenta & Majone 2010).

2.2.5.3 Bioremediation-MFCs

The following text discusses the field application of bioremediation-MFCs. No membrane is required in the system as the electrodes are naturally separated by the material

between them. This is similar to benthic-MFC/sediment-MFC applications where the anode is buried in the anaerobic marine sediment with the cathode in the overlying oxygenated water (Tender et al., 2008; Lovley, 2006a, 2006b). The *in situ* sediment-MFCs are proven to be a viable source of electricity for low-power monitoring devices. Organic matter for these MFCs is provided by natural oceanic productivity and oxygen is supplied to the overlying water by diffusion (Tender et al., 2008). The cathode of a bioremediation-MFC can be, for example, placed in a borehole in uncontaminated groundwater or embedded in soil with unlimited oxygen access to it. Organic matter will be provided as organic contaminants from the groundwater flux past the device.

The scale of bioremediation-MFCs is likely to be much larger than laboratory examples or sediment-MFCs. Many factors which influence MFC efficiency (Table 2-1) cannot be easily controlled in field applications. The material present between the electrodes, its specific resistance, water saturation and salinity, porosity etc. and the distance between the electrodes will influence the Ohmic losses and internal resistance of the system. An important design requirement for bioremediation-MFCs is to decrease the internal resistance of the system by decreasing the electrode distance to maximise electricity production and consequently the bioremediation efficiency.

It has been proposed that the anode and cathode must be connected, perhaps by a proton bridge, to enhance proton transport between them. Morris & Jin (2008) tested the influence of proton bridge length on power production, simulating an electrode distance of up to 9 m in the environmental application of an MFC, and found that power production decreased as the proton bridge length increased. Nevertheless, it has been proven that sufficient electricity production is possible even without using a specially designed connection between the electrodes. Williams et al. (2010) used an MFC to monitor *in situ* acetate-stimulated reduction of uranium(VI). The maximum current density achieved was 40 mA/m^2, even with a 6-m electrode separation distance (implying high internal resistance and slow proton transport between the electrodes). The current density achieved was higher than within some sediment-MFCs (Tender et al., 2002). Williams et al. (2010) in their test found good correlation between electricity production and uranium(VI) removal; proving that MFCs can be used as biosensors, providing real-time data for biological activity and electron donor (in this case acetate) availability.

The distance between the electrodes does not only imply an increase in the internal resistance of an MFC. When tested in sediments, the redox conditions change with the depth of the embedded anode which influences the overall cell potential (Reimers et al.,

2001). As shown by An et al. (2013), the sediment-MFC performance increases with increasing distance of the electrodes up to 10 cm (although the internal resistance increases) due to increased open circuit voltage (OCV). Hence, redox conditions in the contaminant plume may affect the bioremediation-MFC performance. However, the distance between the electrodes can be much greater than 10 cm and the effect of internal resistance more significant.

As in traditional MFC technology, the cathode could be a factor limiting the achievement of higher power densities in this application. The cathode will have to be designed for high energy efficiency and low cost. Using platinum as a catalyst is an expensive solution. Graphite brush cathodes with high specific surface area and porosity could be applied. This cathode could be placed in the saturated zone close to the anode to reduce the internal resistance. A borehole leading to it would enable efficient oxygen transfer to the cathode which would be limited by the oxygen diffusion from air to groundwater. A half-submerged cathode might enable better oxygen transfer to it (Morris and Jin, 2012). In the field, it will operate as a bio-cathode as it is impossible to keep it aseptic.

For future applications of bioremediation-MFCs, the external resistance will have to be set to maintain a certain anode potential. This will allow control of the MFC performance, biodegradation rate and electricity production, but the optimum value of the anode potential/external resistance will depend on the indigenous microbial community, materials used and environmental conditions (Oh et al., 2010; Wagner et al., 2010).

2.2.5.4 The snorkels

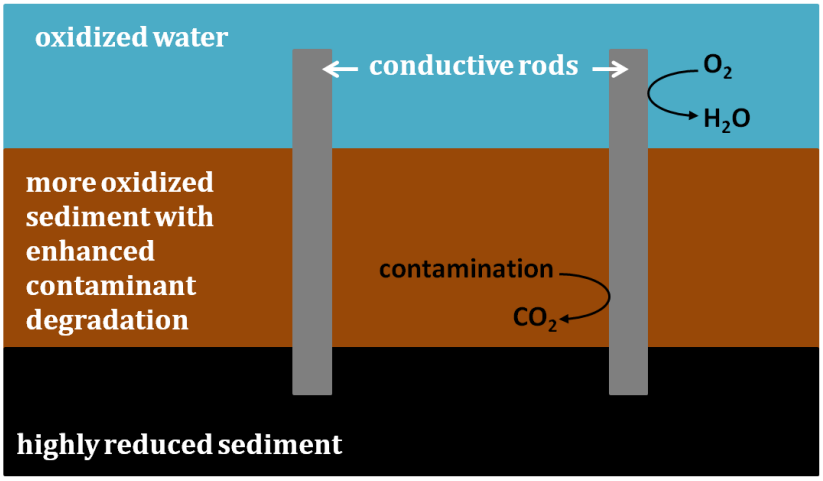

Figure 2-9 Subsurface snorkel for stimulating bioremediation of organic contaminants in sediments, as shown in Lovley (2011).

Lovley (2011) designed snorkels for bioremediation of sediments (Figure 2-9). The snorkels are simple graphite rods. Their base is in contact with contaminants, the top in contact with oxygen. Their own conductivity enables the flow of electrons from the basal "anode" part to the top "cathode" part. The limiting factor in groundwater application of snorkels is the mass transfer of the contaminants to the microorganisms and electron transfer between the microorganisms and snorkel. Although there are possible ways to enhance bacterial electron transfer,[*] capturing the whole contaminant plume by snorkels would be very difficult; most polluted groundwater would just flow past them without being treated. Hence, a PRB based on the snorkel concept with its top in contact with air looks more promising than the snorkels themselves. The advantage of snorkel-PRB is the ease of installation in comparison with bioremediation-BESs, with no need for power source as in M3Cs and no limitation by electricity production as in MFCs.

2.3 Laboratory tests - a pathway to *in situ* applications

The use of BESs for enhanced bioremediation was first proposed more than 10 years ago (Bond et al., 2002). In this laboratory study a pure culture of bacterium *Geobacter metallireducens* in a sediment-M3C (+400 mV vs. SHE) was used to degrade benzoate (0.48 mM) to carbon dioxide, while producing electricity and achieving a CE of 84%. Since then, further studies have been done on bioremediation-BES technology.

Laboratory tests of bioremediation-BESs are necessary as a proof that the bioremediation of various contaminants is enhanced, to test different BES designs and evaluate the influence of environmental conditions on bioremediation efficiency. When considering different BES set-ups, MFCs were mostly used in studies where the contaminants serve as electron donor in the anode chamber (e.g. D.-Y. Huang et al. 2011;

[*] The possibility of electron transfer from bacteria to electrodes over long distances, e.g. 2 cm which is 20,000 times the average size of a microbial cell, via nanowires or nanowires in combination with iron minerals has been proposed (Nielsen et al., 2010; Revil et al., 2010). Some bacteria, including previously mentioned iron and anode reducers *Geobacter* sp. and *Shewanella* sp., can transport electrons to other bacterial species, bulk particles of iron-oxide minerals or electrodes, via nanoparticles of iron-oxide minerals (e.g. ferrihydrite, magnetite, goethite or hematite) which are naturally present in the environment. The exact mechanism responsible for this 'long-distance' electron transfer depends on the properties of these minerals. Soluble iron species released from these oxide minerals by microbial activity can function as electron shuttles. Conductive or semi-conductive minerals can act as an electrical conduit and non-conductive minerals may be changed by microbial metabolism into semi-conductive forms (Bosch et al., 2010a, 2010b; Kato et al., 2012; Nakamura et al., 2009). Above all, filamentous bacteria from the family Desulfobulbaceae, which can act as living 'micro-cables' and enhance electron transport from sulfide to oxygen over a distance of 2 cm, have been recently discovered (Pfeffer et al., 2012). The presence of iron-oxide minerals as nanoparticles in the environment and bacteria with potential to transfer electrons over relatively long distances could enhance the distance of electron transfer from microorganisms to the electrode in BESs/snorkels. Hence, the contaminants and microorganisms could be present further from the solid electron acceptor for greater treatment potential.

Luo et al. 2009; Morris et al. 2009), whereas the M3Cs are preferred for bio-cathode applications (e.g. Strycharz et al. 2010; Aulenta et al. 2009; Strycharz et al. 2008). The laboratory studies of sediment- and soil-BES test designs that could potentially be applied in the field (Cruz Viggi et al., 2014; Morris and Jin, 2012; Wang et al., 2012; Yan et al., 2012; D.-Y. Huang et al., 2011) while the first proof-of-concept experiments for enhanced groundwater bioremediation with BESs used traditional single- or dual-chamber BES designs (Morris et al., 2009; Morris and Jin, 2008). Researchers at Sapienza University of Rome have been developing BESs for enhanced bioremediation of chlorinated solvents. They have designed a laboratory BES reactor based on the field conceptual model. Firstly, the 'conventional' laboratory BESs were operated under continuous mode (Aulenta et al., 2011) and after that a flow-through column BES reactor with porous electrodes simulating the field conditions was developed (Figure 2-10) (Lai et al., 2014; Majone et al., 2013).

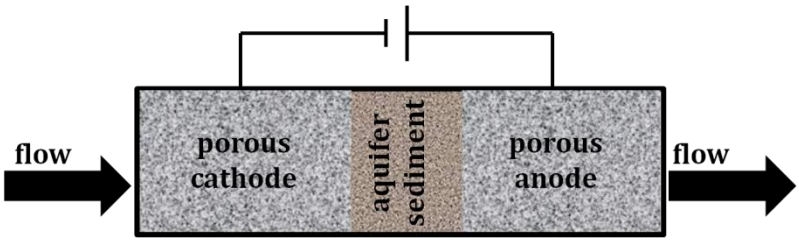

Figure 2-10 A flow-through column BES reactor with porous electrodes designed based on the conceptual model shown in Aulenta & Majone (2010).

Laboratory studies of bioremediation-MFC concepts have used many different communities of bacteria and pure cultures of microorganisms depending on the experimental set-up and scientific objective. Examples include bacterium *Geobacter* sp. (Bond et al., 2002; Strycharz et al., 2008; Zhang et al., 2010), anaerobic sludge and wastewater (L. Huang et al., 2011a; Mohan and Chandrasekhar, 2011; Li et al., 2010; Luo et al., 2009; Zhu and Ni, 2009), contaminated groundwater (Morris et al., 2009; Morris and Jin, 2008), sediments (Cruz Viggi et al., 2014; Morris and Jin, 2012; Yan et al., 2012; Zhang et al., 2010; Aulenta et al., 2009) and soil (Wang et al., 2012; D.-Y. Huang et al., 2011) (Table 2-2).

Comparing the enhancement of bioremediation achieved by different BESs is not straightforward due to variation in experimental set-up, such as system design, set-up of controls, or media supporting bacterial growth (Table II). Some studies compare the biodegradation rate in the BES with simple anaerobic biodegradation, whereas some use an open circuit control (a BES without wires connected). In this case electrons cannot be transported from the anode/to the cathode. Comparing the published energy efficiency of

BESs used for bioremediation of contaminants is also complicated due to differences in presentation of the relevant electricity and performance data. Power density rather than CE is published in some studies. All of the experiments in Table II were run in laboratory scale reactors (up to 3 litres).

Various groups of organic compounds have been evaluated as substrates in BES studies to demonstrate enhanced bioremediation. These include petroleum hydrocarbons, phenol, toluene, benzene, polyaromatic hydrocarbons (naphthalene, phenanthrene, pyrene), chlorinated hydrocarbons (1,2-dichlorethane, trichlorethene, tetrachlorethene, pentachlorophenol) (Wang et al., 2012; Yan et al., 2012; D.-Y. Huang et al., 2011; L. Huang et al., 2011a; Mohan and Chandrasekhar, 2011; Zhang et al., 2010; Luo et al., 2009; Morris et al., 2009; Pham et al., 2009).

The feasibility of applying bioremediation-MFC technology to enhance the bioremediation of **petroleum hydrocarbons** has been examined in several studies (Morris & Jin 2012; Wang et al. 2012; Mohan & Chandrasekhar 2011; Morris et al. 2009). All report improved treatment performance compared with the control systems regardless of the host media, e.g. liquid, soil or sediment. Some studies have also considered individual compounds, including polyaromatic hydrocarbons (discussed below). Cruz Viggi et al. (2014) tested the application of snorkels for bioremediation of oil-spills in microcosm experiments, reporting enhanced biodegradation of petroleum hydrocarbons compared to control systems.

The biodegradation of phenol as a model representative of a large group of **phenolic compounds** has been studied in an MFC containing liquid media (Luo et al., 2009), waterlogged soil (D.-Y. Huang et al., 2011) and in a M3C with the anode poised to 320 mV vs. SHE reference electrode (Friman et al., 2013). In the first study, phenol biodegradation was enhanced by 15% compared with an open circuit control. The second study showed a 12-fold increase in phenol biodegradation rate in a soil-MFC compared with open circuit conditions. The residual phenol concentration in the open circuit control systems was 47–78% higher than in the working M3C in the last study.

Table 2-2 Performance comparison of different bioremediation-BES experiments.

Contaminant	Source of inoculum	Bioremediation efficiency	Maximum electrical efficiency	Reference
Petroleum hydrocarbons 28.3 g/kg soil	Soil	120% enhancement close to the anode (<1 cm)	0.85 mW/m², 1 kΩ,155 mV	(Wang et al., 2012)
Petroleum hydrocarbons 16 g/kg sediment	Sediment	24% in MFC while 2% in open circuit control in 66 days	2162 mW/m³, 1 kΩ, up to 190 mV	(Morris and Jin, 2012)
Petroleum hydrocarbons (2.5 g/l) incl. PAHs	Anaerobic sludge	Two times higher (41% in 17 days) than anaerobic biodegradation	53.11 mW/m², 100 Ω, OCV 343 mV	(Mohan and Chandrasekhar, 2011)
Petroleum hydrocarbons	Sediment	Enhanced in comparison with anaerobic microcosms	Not applicable, snorkels	(Cruz Viggi et al., 2014)
Diesel (C8-C25) (300 mg/l)	Diesel-contaminated groundwater	82% removal (31% for open circuit control) over 21 days	Up to 31 mW/m² cathode, 1 kΩ, up to 160 mV	(Morris et al., 2009)
Phenol (400 mg/l)	1:1 mixture of aerobic and anaerobic sludge	8–15% increase in comparison with open circuit control	Up to 9.1 mW/m² anode, 1 kΩ, 121 mV average	(Luo et al., 2009)
Phenol (80 mg/l)	Soil	13 times higher than open circuit MFC	29.45 mW/m² - max on power curve, 100 Ω, 520 mV OCV	(D.-Y. Huang et al., 2011)
Phenol (100–400 mg/l)	*Cupriviadus basilensis*	Residual phenol 47–78% higher in the control system	Electrode poised to +320 mV vs. SHE, 478 mA/m²	(Friman et al., 2013)
Benzoate (0.48 mM)	*Geobacter metallireducens*	Complete biodegradation within 17 days	Electrode poised to+ 400 mV vs. SHE, CE 84%	(Bond et al., 2002)
Toluene (376 µM)	*Geobacter metallireducens*	Per single cell 100x faster compared with Fe(III) oxide as an electron acceptor	Electrode poised to +500 mV vs. SHE, CE 91%	(Zhang et al., 2010)
Toluene (10 µM), benzene (9 µM), naphthalene (100 µM)	Sediment	Complete biodegradation within 7–10 days, enhanced by the electrode presence	Electrode poised to +500 mV vs. SHE, not reported	(Zhang et al., 2010)
Phenanthrene (10 mg/kg), pyrene (5 mg/kg)	Sediment	96% or 92% (80% or 75% for natural attenuation) in 240 days	16.5 ± 8.9 mV average, 100 Ω	(Yan et al., 2012)
1,2-dichlorethane (99 mg/l)	Acetate-enriched anodophilic consortium or contaminated site community	95% or 85% (53% or 3% in open circuit control) in two weeks, respectively	CE 43% or 25% respectively, 20 Ω	(Pham et al., 2009)
***cis*-dichloroethene (85 µM)**, ethene (10 µM) as co-substrate	Activated sludge	Negligible biodegradation at 1.0 V, enhanced at 1.5 V by oxygen production	+1.0 or 1.5 V vs. SHE	(Aulenta et al., 2013)
Trichlorethene	Enriched brackish sediments	Trichloroethene biodegraded predominantly to cis-DCE but also to ethane and ethane	Electrode poised to -450 mV vs. SHE or -550 mV vs. SHE	(Aulenta et al., 2010, 2009)
	Geobacter lovleyi	Trichloroethene biodegraded only to *cis*- dichloroethene	Electrode poised to -450 mV vs. SHE	
Trichloroethene (35 µM)	TCE-to-ethene dechlorinating culture	100% removal at -750 mV vs. SHE by hydrogen production, 60% removal at -250 mV vs. SHE to *cis*-dichloroethene	-250 mV–750 mV vs. SHE, highest CE (95%) at -250 mV vs. SHE	(Aulenta et al., 2011)
Tetrachlorethene (200-400 µM)	*Geobacter lovleyi*	25 µmol/day (biodegradation only to *cis*-dichloroethene)	Electrode poised to -300 mV vs. SHE	(Strycharz et al., 2008)
2-chlorophenol (80 µM)	*Anaeromyxobacter dehalogenans*	Reductive dechlorination to phenol, approx. 90% loss after 6 days (60% in sterile system)	Electrode poised to -300 mV vs. SHE	(Strycharz et al., 2010)
Pentachlorophenol (0-20 mg/l) acetate and glucose as co-substrates	Domestic wastewater	Approx. two times higher (for 15 mg/l of PCP) compared with open circuit conditions	500 Ω, 2.0 W/m³ - max on power curve - decreasing with PCP concentration, lower for glucose than with acetate as co-substrate	(L. Huang et al., 2011a)

Table II (continued) Performance comparison of different bioremediation-BES experiments.

Contaminant	Source of inoculum	Bioremediation efficiency	Maximum electrical efficiency	Reference
Pentachlorophenol (0-20 mg/l) acetate and glucose as co-substrates	Domestic wastewater	Complete mineralization, biodegradation rate proportional to PCP initial concentration	Power decreasing with PCP concentration (max. 264 ± 39 mW/m^2, acetate)	(Huang et al., 2012b)
Pentachlorophenol (5 – 40 mg/l) bio -cathode	Domestic wastewater	Complete mineralization, biodegradation rate 0.263 ± 0.05 mg/L-h	2.5 ± 0.03 W/m^3	(Huang et al., 2012a)
Pentachlorophenol (75 µM in bio-anode, 86 µM in bio-cathode)	Domestic wastewater	Bio-anode: at +200 mV vs. SHE, degradation enhanced by 28.5% compare to MFC Bio-cathode: -300 mV vs. SHE, degradation enhanced by 21.5% compare to MFC	Bio-anode: -200 mV – +300 mV vs. SHE, 500 Ω for MFC Bio-cathode: -500 mV – +100 mV vs. SHE, 200 Ω for MFC	(Huang et al., 2013)
***p*-nitrophenol (1 mM)**	Anaerobic sludge (glucose as carbon source)	Total biodegradation in cathode chamber within 12 days	143 mW/m^2 - max on power curve, 350 mV, 1 kΩ	(Zhu and Ni, 2009)
Nitrobenzene (0-250 mg/l)	1:1 aerobic and anaerobic sludge in anode chamber	Complete biodegradation within 24 hours when using glucose as co-substrate	1 kΩ, low electricity production without glucose, 8.5–28.6 W/m^3 with glucose (decreases with increasing PCP concentration)	(Li et al., 2010)
Nitrobenzene (250 mg/l)	1:1 aerobic and anaerobic sludge in anode chamber (glucose as carbon source)	Complete biodegradation within 24 hours in cathode chamber	1 kΩ, 400 mV, 6.3 W/m^3 - max on power curve	(Li et al., 2010)

The enhanced BES-biodegradation of **BTEX** (benzene, toluene, ethylbenzene and xylenes), as a component group of petroleum hydrocarbons, has only focused on benzene and toluene. Biodegradation of both organic chemicals was enhanced in a petroleum-contaminated sediment-M3C (the anode poised to +500 mV vs SHE). Using [^{14}C] labeled compounds, toluene and benzene were completely biodegraded to carbon dioxide after initial adsorption on the electrode. Biodegradation of toluene as a sole carbon source has been evaluated in M3Cs with liquid media using a pure culture of *Geobacter metallireducens*. The biodegradation rate per single bacterial cell was 100-times faster than when using Fe(III)-oxide as an electron acceptor, reaching a CE of 91% (Zhang et al., 2010).

Polyaromatic hydrocarbons (PAHs) are often an important component of contamination by petroleum hydrocarbons (Wang et al., 2012). Naphthalene is often tested as a model compound to evaluate the biodegradation potential of PAHs. When tested in a petroleum-contaminated sediment-M3C (+500 mV vs. SHE), the naphthalene biodegradation rate was increased compared with control systems, and 40% was recovered as carbon dioxide (Zhang et al., 2010). The bioremediation of structurally more complex PAHs such as phenanthrene and pyrene was enhanced in a sediment-MFC in comparison with natural attenuation (Yan et al., 2012). The bioremediation of PAH mixtures has been also studied. Mohan & Chandrasekhar (2011) examined biodegradation of PAHs in a liquid

media MFC and observed enhanced metabolism of large 4, 5, and 6-ring PAHs to smaller 2- and 3-ring PAHs, relative to an anaerobic control.

Biodegradation of **chlorinated hydrocarbons** has also been studied in BESs; some of these compounds can function as electron acceptors for microbial metabolism due to their high redox potential (Alvarez and Illman, 2006). In a BES, these contaminants can be biodegraded either in the anode chamber using another electron donor as a co-substrate which may decrease the electrical efficiency of the system (L. Huang et al., 2011a) or using the bio-cathode principle (Strycharz et al., 2010; Aulenta et al., 2009; Strycharz et al.2008).

1,2-dichlorethane (1,2-DCA) can either serve as an electron donor for microbial metabolism or as an electron acceptor depending on the microbial community involved in biodegradation. Pham et al. (2009) used two different communities for a bioremediation-MFC where 1,2-DCA served as electron donor in the anode chamber. In both cases, bioremediation of 1,2-DCA was enhanced by the MFC compared with an open circuit control. On the other hand, it was shown that the *cis*-dichloroethene (*cis*-DCE), containing one unsaturated bond, could not be oxidised on the electrode and required oxygen for biodegradation (Aulenta et al., 2013).

Anaerobic biodegradation of tetrachloroethene (PCE) and trichloroethene (TCE) can be enhanced in an M3C by poising the electrode to low redox potentials (-750 – -250 mV vs. SHE). Depending on the inoculum the biodegradation can be complete to ethene and ethane when using mixed culture containing *Dehalococcoides* spp., or partial to *cis*-DCE when a pure culture of *Geobacter lovleyi* is used (Aulenta et al., 2011, 2010, 2009; Strycharz et al., 2008). However, at very low electrode potentials, water electrolysis on the electrode is supported, resulting in low CE, TCE biodegradation enhanced by hydrogen development on the electrode and intense methanogenesis. It is therefore preferable to keep the electrode potentials at higher values (Aulenta et al., 2011).

Reductive dechlorination of 2-chlorophenol by *Anaeromyxobacter dehalogenans* using the electrode as electron donor (poised at -300 mV vs. SHE) was tested by Strycharz et al. (2010). Dechlorination stopped when the cathode was disconnected from the source of current. This experiment shows that other species than Geobacteraceae can exchange electrons with electrodes.

Researchers at Dalian University of Technology (China) explored various aspects of pentachlorophenol (PCP) biodegradation in BESs. Preliminary studies focused on pentachlorophenol bioremediation in a dual-chamber (L. Huang et al., 2011a) and single-chamber (Huang et al., 2012b) MFC when acetate or glucose were used as co-substrates in

the anode chamber. The following experiments examined PCP biodegradation in bio-cathode MFC (Huang et al., 2012a) and the effect of the start-up electrode potential on the MFC start-up times and biodegradation rate in a bio-anode and bio-cathode M3Cs (Huang et al., 2013). PCP biodegradation was enhanced in comparison with open circuit conditions. Optimum electrode potential was determined (+200 mV vs. SHE for bio-anode, -300 mV vs. SHE for bio-cathode), increasing the PCP biodegradation rate by 28.5% and 21.5%, respectively, in comparison with MFC conditions. A negative potential (-200 mV vs. SHE) on bio-anode and positive potential (+100 mV vs. SHE) had a negative effect on PCP biodegradation.

Various **nitrogen-containing compounds** also have a relatively high redox potential and can serve as electron acceptors (Alvarez and Illman, 2006). Biodegradation of these compounds in BESs is influenced by the same principles as biodegradation of chlorinated compounds. They may be biodegraded in the anode chamber when adding co-substrates as electron donors (Li et al., 2010). Power generation decreases with increasing concentration of nitrobenzene in the anode chamber when using glucose as co-substrate. Nitrogen-containing compounds can be also degraded abiotically in the cathode chamber. The required electrons can be supplied by biodegradation of other organic compounds in the anode chamber (Li et al., 2010). In a study performed by Zhu & Ni (2009), *p*-nitrophenol was oxidised by the hydroxyl radicals developed in the cathode chamber. These radicals were generated by the Fenton's reaction of hydrogen peroxide (formed by oxygen reduction on the carbon felt electrode) with Fe^{2+} ions. Biodegradation in a biocathode-BES may be problematic due to toxicity of nitroaromatics (Li et al., 2010).

2.4 Identified research gaps

Considering the literature on BESs and requirements for *in situ* application of this technology discussed above, the research needed to develop BESs for future applications in enhanced bioremediation of groundwater is outlined below.

Future application of BES technology for enhanced *in situ* bioremediation requires understanding of microbial community structure and function, which is currently very limited in the context of groundwater bioremediation BESs. Most studies on bioremediation BESs did not use groundwater as inoculum (Section 2.3, Table 2-2). Microbial communities in successful bioremediation BES systems will be capable of using the electrodes as electron acceptors/donors for contaminant biodegradation. Information about the development of the anode community obtained from the inoculum under certain

conditions and metabolic interactions between microorganisms in the biofilm is needed to provide insight into the community function (Oh et al., 2010), potentially illustrating ways to enhance the bioremediation process.

Microbial adaptation to new conditions is presumed after first introducing the electrodes into the environment before an enhancement of bioremediation is expected. This adaptation time and mechanism should be explored in experiments. The possibility of using bioaugmentation could also be explored (Arends et al., 2012). Bacteria capable of contaminant biodegradation and electron transfer can be grown in the laboratory and added to the environment to evaluate their performance in this context. *Geobacter* sp. are of special interest as certain species appear to manage both tasks.

Most exoelectrogens belong to iron reducers (Torres et al., 2010) and therefore *in situ* redox conditions are likely to influence the activity of these microorganisms. Different redox zones will typically exist in groundwater contaminant plumes due to sequential consumption of available electron acceptors during biodegradation of organic compounds (Christensen et al., 2000). Depending on the redox conditions, functionally different microorganisms are distributed in the plume with potential to utilise the electron acceptors present within a certain redox zone (Alvarez and Illman, 2006; Atlas and Philp, 2005). Considering the evidence concerning exoelectrogens, the Fe(III)-reduction zone may contain microorganisms with the ability to use electrodes in BESs as electron acceptors/donors. The redox conditions in a plume can also affect the OCV of an MFC. The placement of the BES electrodes based on the presence of exoelectrogenic microorganisms and OCV of MFCs must be investigated in further research.

Contaminants in the environment occur in mixtures and research should move from studying simple model compounds (most of the current studies, Section 2.3) to these mixtures, e.g. petroleum hydrocarbons, phenols, BTEX, PAHs, etc. The biodegradation rate of individual compounds within these mixtures should be determined including effects related to their specific biodegradation behaviour, such as the sequence of biodegradation, metabolites and CE. Bioavailability of the hydrophobic contaminants could be increased by applying surface-active compounds (Cameotra and Makkar, 2010). However, the presence of these surfactants could affect biofilm development on the electrode by interaction with bacteria and the electrode surface (Neu, 1996). The influence of other environmental factors such as pH, temperature and nutrients and electron acceptor availability on bioremediation and electricity efficiency of BESs should be determined. The possibility of enhancing the performance of these BESs by addition of nutrients should be examined.

New cost-effective designs of BESs for groundwater bioremediation should be developed, considering important issues such as internal resistance of the system and mass transfer limitations. The sustainability of this system, considering bioremediation efficiency and cost of installation should be evaluated. Experimental studies should move from testing purely laboratory BES designs to concepts which are similar to the field BESs with respect to relevant construction.

For future applications of bioremediation-BESs, the optimum electrode potential will have to be found. This will allow control of the BES performance, biodegradation rate and electricity production. The optimum value of the electrode potential (external resistance in the case of MFCs) will depend on the indigenous microbial community, materials used and environmental conditions (Oh et al., 2010; Wagner et al., 2010). The effect of electrode potential, current density in all BESs, or external resistance in MFCs on microbial community development and biodegradation rate of contaminants should be studied in more detail. The amount of electricity needed for powering a potentiostat, setting electrode potential and donating electrons for biodegradation must be evaluated by future experiments and field tests. However, it has been reported that the amount of current necessary for supporting reductive dechlorination can be low (Strycharz et al., 2010).

The energy efficiency of MFCs may be increased by combining several units in series to provide higher voltage outputs (Logan et al., 2006). This innovation should be studied simulating the field conditions where anodes will not be separated by a physical barrier as it is in laboratory MFC stacks.

The research gaps identified here are broad and were therefore further refined for the purposes of this project. The main focus of the thesis is on biodegradation of a mixture of contaminants and their metabolites as present in contaminated groundwater, with subsequent study of microbial community development. Thesis aims and objectives developed based on these knowledge gaps are discussed in the following chapter.

Chapter 3

Thesis aims, objectives and structure

3.1 Thesis aims

Bioelectrochemical systems (MFCs and M3Cs) can enhance the biodegradation of organic chemicals such as petroleum hydrocarbons (Morris and Jin, 2012; Wang et al., 2012; Mohan and Chandrasekhar, 2011; Morris et al., 2009), phenol (Friman et al., 2013; D.-Y. Huang et al., 2011; Luo et al., 2009), benzene, toluene and naphthalene (Zhang et al., 2010), and phenanthrene and pyrene (Yan et al., 2012), by providing bacteria with an electrode that acts as an inexhaustible electron acceptor. This has been demonstrated at laboratory scale using pure cultures of bacteria, wastewater, sediment or soil, often amended with nutrients and vitamins. However, the potential role of BES technology in the treatment of contaminated groundwater has been limited to one study of petroleum hydrocarbon-contaminated groundwater, enriched with phosphate buffer and surfactants (Morris et al., 2009). This is an important knowledge gap in the development of bioelectrochemically-enhanced treatment of groundwater contaminants in terms of both scientific understanding of the processes involved and engineering applications.

Organic contaminants in groundwater typically occur in mixtures with different potential for biodegradation (Wang et al., 2012; Cameotra and Makkar, 2010; Wiedemeier et al., 1999). An example is phenolic compounds (phenol, cresols, xylenols) but only biodegradation of phenol has been examined in MFCs (Friman et al., 2013; D.-Y. Huang et al., 2011; Luo et al., 2009). The performance of BES technology in the treatment of natural groundwater containing a mixture of phenols (phenol, isomers of cresols and xylenols) and their metabolites, electron acceptors and an indigenous microbial community is to date unknown. The influence of different organic compounds, which may compete with target contaminants as alternative carbon sources for bacteria in biodegradation processes, is of particular interest. This is important as bioremediation may be limited by preferential metabolism of alternative substrates, causing catabolite repression (Görke and Stülke, 2008), despite an adequate supply of electron acceptors for complete metabolism (Wiedemeier et al., 1999).

Previous studies of phenol biodegradation in MFCs have demonstrated the basic concept of enhanced bioremediation (Friman et al., 2013; D.-Y. Huang et al., 2011; Luo et al., 2009) but the metabolic pathways and mechanism of phenol removal were not studied.

Insight into the interaction of indigenous groundwater microbial community with the electrode is also limited, with only one study using groundwater as MFC inoculum and sequencing 16S rRNA genes (Morris et al., 2009). The main aim of this thesis is therefore to examine the chemical and biological processes that occur in an MFC used to treat groundwater contaminated by phenols.

3.2 Thesis objectives

The thesis objectives are as follows:

1) **To develop methodology and MFC design which will provide good quality electricity and chemistry data and enable monitoring of changes in microbial community structure in groundwater contaminated by phenolic compounds.** H-type MFCs were previously used in our laboratory. However, their design was rather simple, sampling procedure potentially affected the processes within the anode chamber, electricity data was measured only once a day and the removal of electrodes for DNA extraction and microscopy was not possible. Biosludge community from wastewater treatment plant was initially used to evaluate phenol biodegradation within this H-type MFC. The intention was to move from the biosludge community to indigenous groundwater microbial community.
2) **To provide insight into biodegradation pathways of phenols in an MFC inoculated with contaminated groundwater.** For successful application of BESs in enhanced bioremediation, it is essential to understand the interaction between the bacteria and electron donors and acceptors within the BESs. Groundwater used in this thesis contained phenol, cresols and xylenols and acetate as a fermentation product of phenols (Watson et al., 2005; Thornton et al., 2001b). Any of these chemical compounds could in principle serve as an electron donor for electricity production. Changes in concentrations of these chemicals and other potential metabolites of phenols linked with electricity generation and utilisation of alternative electron acceptors can provide the basis for a conceptual model of MFC function and mass balance. Understanding the fundamental processes driving the biodegradation in MFCs, highlighted in a conceptual model, is the first step to engineered bioelectrochemically-enhanced remediation.
3) **To link microbial community structure with its function in biodegradation of phenols in MFCs.** That is to deepen the understanding of the processes occurring in the MFCs inoculated with groundwater contaminated by phenolic compounds. Twenty-five percent of the planktonic microbial community of the groundwater used

in this thesis consists of *Geobacter* sp. (unpublished data), implying that the community could be electro-active (Rabaey et al., 2010; Logan, 2008). Based on the literature review on EET (Section 2.1.2), it was hypothesised that the groundwater microbial community would use the anode of an MFC as an electron acceptor after forming a biofilm on it. *Geobacter* sp. are often dominant in MFCs fed by acetate (Zhu et al., 2014; Kiely et al., 2011) but can also degrade aromatic compounds (Zhang et al., 2010; Bond et al., 2002; Rooney-Varga et al., 1999). *Geobacter* sp. could therefore be a dominant species in electrode biofilm, utilising phenols or acetate as electron donors. The bacterial species living in electrode biofilm and planktonic form were identified, with the potential link to their function within the microbial community.

3.3 Thesis structure

The experimental work is divided into four main chapters (Chapter 4 – Chapter 7).

Chapter 1: Introduction

The chapter introduces the concept of bioelectrochemically-enhanced remediation in the context of electron-accepting and donating processes needed for successful bioremediation of groundwater.

Chapter 2: Literature review and fundamentals

The knowledge of bioelectrochemical systems fundamental to understanding of this project is summarised in this chapter. Literature on the application of BESs in enhanced bioremediation and related topics is reviewed. Important knowledge gaps in the terms of practical *in situ* application of BESs in groundwater bioremediation are identified.

Chapter 3: Thesis aims, objectives and structure

Thesis aims and objectives are listed as well as the thesis structure.

Chapter 4: Methodology development

This chapter addresses the objective No. 1. At the end of this chapter, MFC design and experimental procedures are fully developed for the future experimentation in Chapter 5 and 6. Some of the results presented in this chapter were published as ADVOCATE bulletin No. 3 (http://www.theadvocateproject.eu/files/AB3_Petra%20(1).pdf) (Appendix A) and a conference paper 'Hedbavna P., Thornton S.F., Huang W. (2013) *Enhanced groundwater bioremediation using microbial fuel cell concepts*. Proceedings of the 2nd European Symposium, Water Technology & Management, Belgium.' (Appendix B).

Chapter 5: Biodegradation of phenolic compounds and their metabolites in contaminated groundwater using MFCs

The main focus of this chapter is on the thesis objective No. 2 and the role of electrode biofilm in electricity generation as part of the objective No. 3. The results presented in this chapter have been published in the following paper (Appendix C):

Hedbavna, P., Rolfe, S.A., Huang, W.E., Thornton, S.F., 2016. *Biodegradation of phenolic compounds and their metabolites in contaminated groundwater using microbial fuel cells*. Bioresource Technology 200, 426–434.

Chapter 6: Microbial community structure in an MFC degrading phenolic compounds and their metabolites

Insight into the microbial community structure and function within the objective No. 3 is provided. It is also intended to submit this chapter as a journal paper.

Chapter 7: Groundwater microbial fuel cell: *in situ* experiment.

Based on the positive results in Chapter 5, a follow-up pilot-scale MFC was installed within the plume of phenolic compounds in the sandstone aquifer.

Chapter 8: Thesis synthesis, future research and conclusion.

The conclusions of the different chapters are summarised and discussed in wider context. Future research needs, as identified from the experiments performed in this thesis, are highlighted. The final conclusion of the project is presented.

Chapter 4

Methodology development

The main aim of this chapter is to develop methodology for MFC set-up and operation which would provide good quality data of electricity production, chemical changes in MFCs and biological samples. At the end of the process, the MFCs were to be run with groundwater contaminated by phenolic compounds, containing indigenous microbial community.

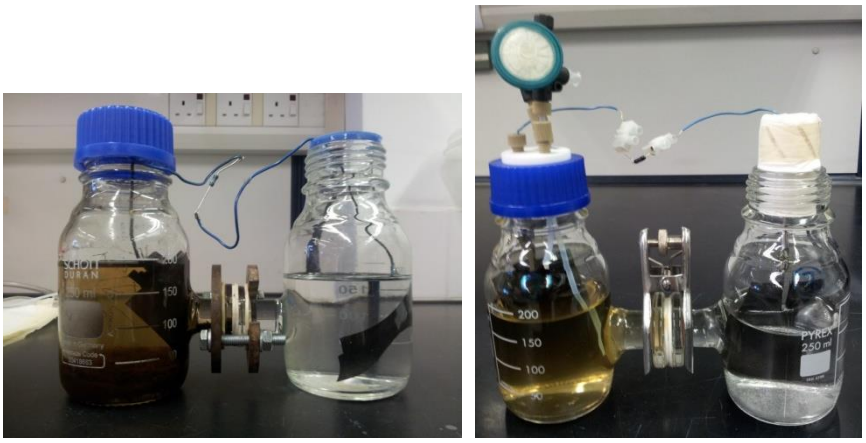

Figure 4-1 First MFC design used in our laboratory (left), improved MFC design (right).

H-type dual-chamber MFCs with the chambers separated by a proton exchange membrane, Nafion 117, were chosen as an easy-to-build and cost-effective design. They were previously used in our laboratory to explore electricity production by a biosludge community from a coke wastewater treatment plant in Scunthorpe using naphthalene as a sole carbon source (Huang, 2011). However, the MFC design did not provide the opportunity to take samples from the anode chamber without opening the chamber and disrupting the anaerobic conditions in it. Manipulation with these MFCs was rather complicated, electrodes could not easily be changed, cathode chamber could not be kept sterile and flow of oxygen into the system could not be monitored (Figure 4-1, left). These aspects were therefore improved (Figure 4-1, right):

- The anode chambers were equipped with the lids which enabled anaerobic sampling without opening the chamber. 0.2 μm sterile PES syringe filters were attached to the sampling ports to prevent biological contamination.
- Pinch clamps were used to connect the chambers while holding the membrane.
- The electrodes were connected to the wires by crocodile clips.

- The cathode chamber was closed by a cotton stopper.
- Both chambers were equipped with oxygen sensor spots to monitor the dissolved oxygen level inside. The oxygen sensor spot was attached with silicon glue inside the Schott bottle. When illuminated by an LED, the sensor spot emits fluorescent light which is detected by an optical sensor. Presence of oxygen limits the amount of fluorescence emitted (http://www.presens.de/).

Carbon cloth was chosen as an ideal electrode material. It enables attachment of electrogenic biofilm in the anode chamber (Logan, 2010). Although it may limit cathode performance to some extent (Logan et al., 2006), carbon cloth would be cost effective at a large scale and is less prone to poisoning than Pt catalysts (Logan, 2010; He and Angenent, 2006).

4.1 Materials and methods

Table 4-1 Experimental set-up.

Name	Live/sterile	Oxygen access	MFC	Expected electricity production	Expected biodegradation
CC-MFC	Live	?	1 kΩ resistor	Yes	Faster than anaerobic
OC-MFC	Live	?	Wires not connected	No	Slower than closed circuit
S-MFC	Sterile	?	1 kΩ resistor	No	None
Anaerobic system	Live	None	NA	NA	Very slow
Anaerobic control	Sterile	None	NA	NA	None
Aerobic system	Live	From air (not limited)	NA	NA	Fastest
Aerobic control	Sterile	From air (not limited)	NA	NA	None (volatalisation possible)

The biodegradation rate of phenols was to be measured in different MFC and non-MFC devices to observe the influence of electrode presence/electricity production on biodegradation (Table 4-1). Closed-circuit MFC (CC-MFC) had the electrodes connected via the 1 kΩ resistor, meaning that the electrons could be transferred from the anode chamber to the cathode chamber. The biodegradation rate of phenols should theoretically be faster in an anode chamber of a CC-MFC than in an open-circuit MFC (OC-MFC), which lacked the connection between the electrodes. No biodegradation should occur in a sterile MFC (S-MFC). The biodegradation performance in MFCs was compared with

biodegradation under aerobic and anaerobic conditions in Schott bottles and their sterile controls. All the MFC components were sterilised prior to experimentation by autoclaving (121 °C, 0.15 MPa, 20 min), including the Nafion membrane which was during sterilisation inserted in ultra-high quality (UHQ) water.

Biosludge

The first MFC experiment on phenol biodegradation (Section 4.2) was conducted using biosludge from a coke wastewater treatment plant in Scunthorpe managed by Tata Steel Europe, Ltd. The composition of the main contaminants in the biosludge can be seen in Table 4-2.

Table 4-2 Scunthorpe biosludge chemical composition prior to treatment.

Chemical	Concentration [mg/l]	Chemical	Concentration [µg/l]
Total phenols	180–375	Anthracene	5–15
Monophenol	150–320	Pyrene	100–200
Total NH_3	50–70	Benzo[a]pyrene	100–170
Thiocyanate	120–250	Naphthalene	320–460
Free cyanide	0.5–1.0		
COD	~2500		

20 ml of biosludge/15 ml of autoclave-sterilised biosludge was taken and centrifuged (4588 x g, 10 min). The supernatant was removed and minimal media was added up to 40 ml and the cuvette was vortexed to wash of the organics staying in the biosludge biomass. Samples were centrifuged again and the supernatant removed. Minimal media was added again up to 40 ml and this mixture was added into 160 ml of minimal media in the MFCs or control bottles.

Minimal media

Minimal media of the following composition (Huang, 2011) was used in a few initial experiments (Section 4.2 and 4.3).

Salt solutions A and B (10 ml of each) were sterilised through 0.2 µm filter and added into 1 L of autoclaved deionised water.

Solution A:

250 g/l Na_2HPO_4

250 g/l KH_2PO_4

Solution B:

100 g/l $(NH_4)_2SO_4$

10 g/l $MgSO_4 \cdot 7\ H_2O$

100 ml Bauchop & Elsden solution

900 ml water

Bauchop & Elsden solution:

10.75 g/l $MgSO_4 \cdot 7\ H_2O$

4.5 g/l $FeSO_4 \cdot 7\ H_2O$

2.0 g/l $CaCO_3$

1.44 g/l $ZnSO_4 \cdot 7\ H_2O$

1.12 g/l $MnSO_4 \cdot 4\ H_2O$

0.25 g/l $CuSO_4 \cdot 5\ H_2O$

0.28g/l $CoSO_4 \cdot 7\ H_2O$

0.06 g/l H_3BO_3

51.3 ml concentrated HCl into 1 l of deionised water

Anaerobic set-up

The oxygen level in the anode chamber of MFC and anaerobic controls had to be below detection limit at the start of experimentation. To ensure this, the bottles were either degassed or set up in anaerobic chamber. Degassing (experiments in Section 4.2 and 4.3.2) was performed after MFCs/anaerobic controls were fully set up, i.e. contained inoculum, minimal media and carbon source. The liquid in the anode chamber was sparged with filter-sterilised (0.22 μm PES, Millex®, Merck KGaA) nitrogen gas which was introduced in the bottle via sterile PTFE tube covered by 0.22 μm sterile PES syringe filter. MFCs containing groundwater (experiments in Section 4.3.3 and 4.4) were set up in the anaerobic chamber flushed with sterile nitrogen gas prior to working. In the case MFCs contained any dissolved oxygen after being set up in the anaerobic chamber, the anode chambers were degassed using sterile nitrogen gas as previously described.

Analysis of phenolic compounds

Samples for analysis of phenol(s) (phenol, cresols and xylenols) were taken through 0.2 μm PES syringe filters to remove bacteria. The frequency of changing these filters was different for each experiment (Section 4.2, 4.3.2, 4.3.3 and 4.4). As shown by the initial data (Section 4.2) it is critical to replace the syringe filters at each sampling point prior to taking the sample.

Phenolic compounds (phenol in Section 4.2 and 4.3.2; phenol, isomers of cresols and xylenols in Section 4.3.3 and 4.4) were analyzed by reversed-phase high performance liquid chromatography (HPLC) using a PerkinElmer instrument with a UV detector (wavelength 280 nm) and C18 column (Thermo Scientific™ Hypersil™ ODS-2, particle size 5μm, 250 mm x 4.6 mm I.D.) and C18 guard column. The sample injection loop was 10 μL. The eluent was an 80:20 mixture of acetic acid and acetonitrile, with 1.6 mL/min flow rate, changing to 1.0 ml/min between 4.7–5.7 min, followed by a 12 min gradient to a 60:40 ratio for another 4 min. The detection limit was 1 mg/L, with an analytical precision of ± 7%.

Groundwater

Groundwater used in initial experiments (Section 4.3 and 4.4) was sampled from a plume of phenolic compounds in the UK Permo-Triassic sandstone aquifer (Lerner et al., 2000; S F Thornton et al., 2001). Samples were collected from different depths in the aquifer using a multilevel sampler (MLS) equipped with monitoring points at 1 m intervals (Thornton et al., 2001b). The groundwater was collected in sterile (autoclaved), nitrogen-purged 2.5 L amber glass bottles, which were filled completely. Samples were stored at 4 °C prior to use in the experiments.

Initial tests on biodegradation of phenol by the groundwater community (Section 4.3) used groundwater from 4 different depths of the aquifer, 12, 13, 14 and 17 meters below ground level (mbgl). This groundwater was chosen for testing as it originated from the active part of the plume, the plume fringe. In this zone, contaminated groundwater mixes with uncontaminated groundwater, creating ideal conditions for biodegradation of phenols. Biodegradation rate of phenols is highest at the plume fringe due to the supply of oxygen and nitrate from the uncontaminated groundwater (Thornton et al., 2001b). Tested contaminated groundwater contained total phenols of concentration lower than 500 mg/l (Figure 4-2) and oxygen concentration was below detection limit (data not shown). The

concentration of phenols in uncontaminated groundwater used in the cathode chamber (Section 4.3.3 and 4.4) was below detection limit (Figure 4-2).

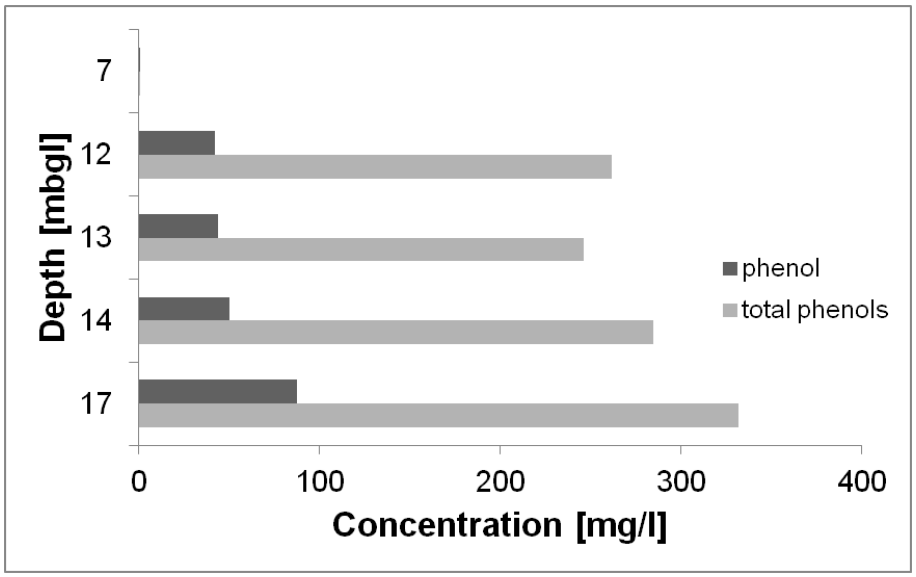

Figure 4-2 Concentration of phenol and total phenols at different depths of the aquifer, data from March 2012 measured by Lukasz Cieslak. The concentration of phenol and total phenols in the plume core can reach up to 2 g/l and 5 g/l, respectively (Thornton et al., 2001b).

Groundwater for sterile controls needed to be sterilised in a way which does not affect its chemical composition or changes it as little as possible. Tangential flow filtration (TFF) was used to reduce the number of bacteria in the groundwater prior to 0.1 μm filter sterilisation (Figure 4-16) or sodium azide addition. A TFF unit (Pall Centratmate, Supor PES membrane, 0.1 μm) was sterilised with chlorine solution for 15 min prior to groundwater filtration. The TFF system was then flushed with sterile degassed water. The groundwater (12 mbgl), which was sparged with sterile nitrogen in the 2.5 L bottle, was then connected to the feed of the TFF unit. The first part of retentate and permeate was discarded as it contained the flushing water. After this, retentate was returned back to the original bottle and permeate was collected in a fresh sterile 2.5 L bottle which was being degassed with sterile nitrogen gas (Figure 4-3).

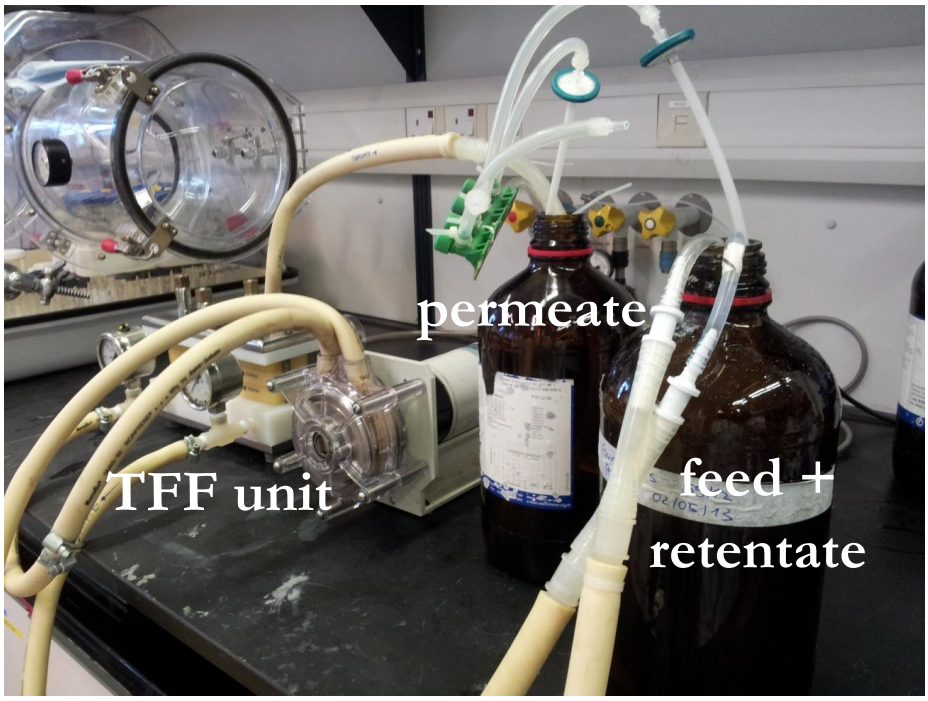

Figure 4-3 Tangential flow filtration set-up for groundwater pre-sterilisation.

MFC incubation

Typical groundwater temperatures in the UK are around 10 °C (Shah et al., 2009). However, all the MFCs were incubated at laboratory temperature to ensure faster rate of biochemical reactions and therefore shorter duration of experiments. The MFCs were firstly not stirred (Section 4.2) and later shaken at 100 rpm (Section 4.3.3 and 4.4). Stirring would increase the rate of mass transfer within the anode/cathode chamber (see Chapter 5, Section 5.2.1).

Voltage measurement

Initially the voltage was measured by a voltmeter (Section 4.2 and 4.3). Closed circuit voltage (CCV) across the 1 kΩ resistor and open circuit voltage (OCV) were measured every day. Polarisation curve was determined by the constant resistance discharge technique. Starting at open circuit (infinite resistance) and decreasing the resistance, different resistors were connected to the MFCs. The measurement was taken once the voltage stabilised (Zhao et al., 2009). The equipment was then upgraded to what is used in MFC publications as a standard, i.e. a data logger (NI USB-6251, National Instruments) was used to measure the closed circuit voltage every 10 min and the polarisation curve was determined by the potentiostatic discharge technique. During the potentiostatic measurement, the voltage is controlled by a computer, decreasing from OCV, and the resulting current is measured (Zhao et al., 2009). The equipment for this was custom made

by Dr. Paul Bentley from the Department of Civil and Structural Engineering at the University of Sheffield.

The results presented in this chapter come from five different experiments. Each experiment had its own aim and led to an improvement in the procedures carried out during MFC operation. Statistical comparison of presented data was completed with one-way ANOVA ($\alpha = 0.05$) in SigmaPlot 12.0.

4.2 Biosludge MFC

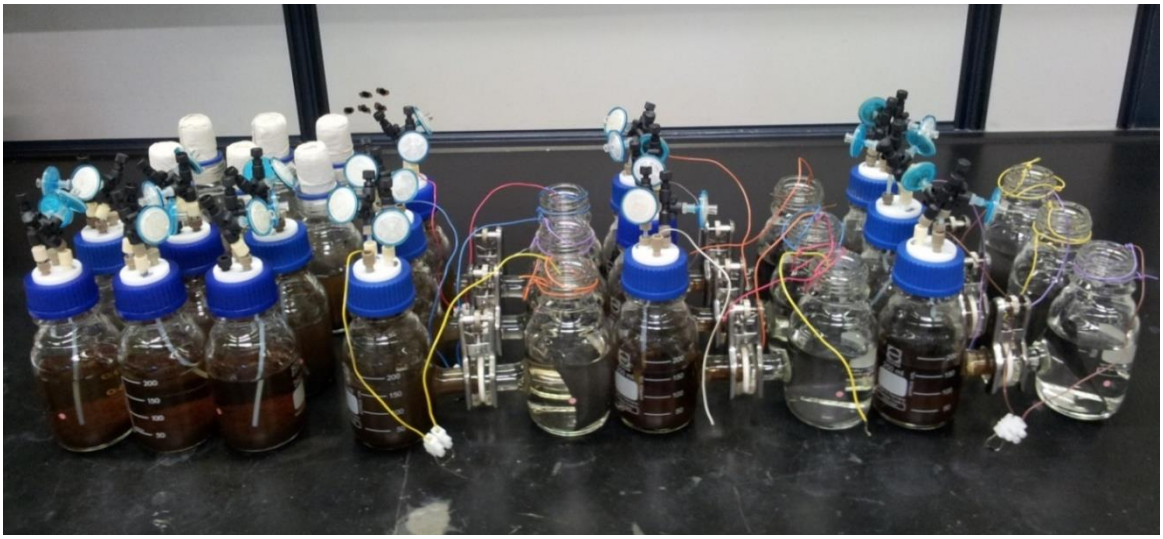

Figure 4-4 Biosludge MFC experiment with all the controls.

Improved MFC design (described at the beginning of this chapter) was firstly tested to explore its electrical performance and basic chemistry parameters, i.e. changes in ion and carbon source concentration. Phenol, a model chemical representing the group of phenolic compounds, was chosen as a sole carbon source. All other parameters were kept the same as in previous tests with naphthalene. MFCs and the Schott bottles (triplicates) (Figure 4-4) were inoculated with the Scunthorpe biosludge (Section 4.1) using minimal media and 5 mM phenol. Biosludge in sterile controls was sterilised in an autoclave. The cathode chamber contained sterilised disodium hydrogen phosphate (12.5 g/L of deionised water) and was open to air. All the anaerobic bottles and MFC anode chambers were degassed prior to the start of the experiment.

Samples for chemical analysis were taken through the 0.2 μm syringe filter. The filters got blocked by biosludge biomass and were therefore changed once a week but for economical reasons were not changed for each sampling point. Minimal media was added in the systems with a syringe after the sampling to keep the volume in the systems stable.

Unfortunately, it was impossible to add it through the filter due to the biosludge blockage so the filters were taken off for the minimal media addition.

CCV and OCV were measured every day by a voltmeter. CCV (Figure 4-5) increased slightly during the first 10 days for all the systems. During this period, there was no significant difference in the measured voltage between the MFC systems ($P > 0.05$). After 10 days, the CCV of CC-MFCs increased, reaching the maximum CCV of 87 ± 12 mV at day 19. Polarisation curve was measured at this point (see below for detailed description). MFCs were discharged during the polarisation curve measurement which was likely to have caused the rapid drop in CCV after day 19. OC-MFCs produce significantly less electricity ($P < 0.05$) than CC-MFCs after day 10, with the average CCV being 20 ± 2 mV. S-MFCs generated a limited amount of electricity with a peak at 19 days. It is not clear why this peak in electricity generation would occur in a sterile MFC system. However, as can be seen from data on phenol degradation (see below), S-MFCs were probably contaminated by bacteria. This would explain why S-MFCs were active in the terms of electricity generation.

OCV started at approx. 100 mV and increased immediately in CC- and OC-MFCs (Figure 4-5). As the electrodes were not connected during incubation of OC-MFC, there was no pressure on the present microbial community to discharge electrons to the electrode. This is likely to have resulted in faster increase of OCV. The maximum OCV for CC-MFCs was 464 ± 34 mV and 432 ± 30 mV for OC-MFCs. A drop in OCV of OC-MFCs occurred at day 14. The reason for this was not known. There was no significant difference in OCV between the CC- and OC-MFCs after day 17 ($P > 0.05$). The OCV of S-MFCs decreased below zero at days 3 and 4, but started increasing after this initial period. As mentioned before, the increase in CCV and therefore OCV can be explained by biological contamination of S-MFCs and consequently increased activity of the system.

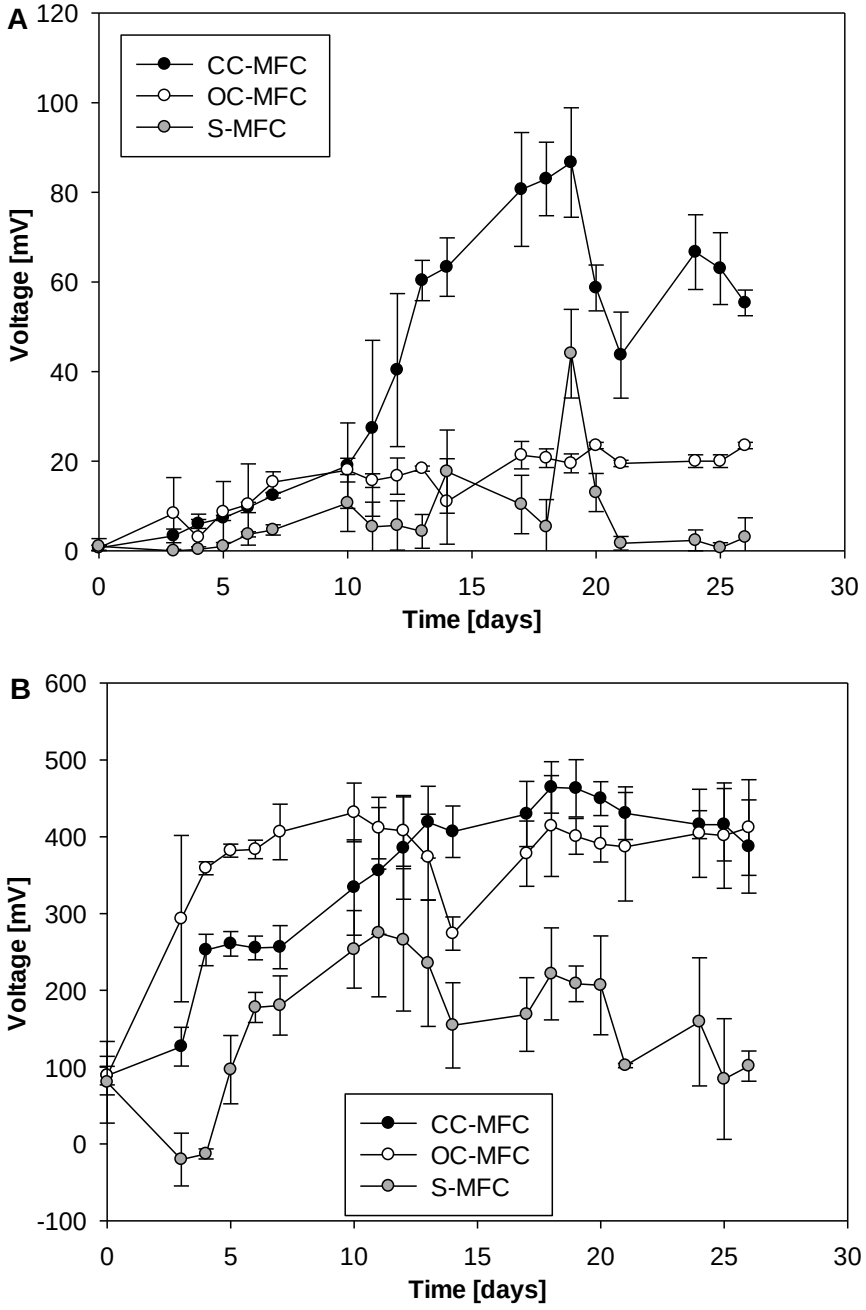

Figure 4-5 Closed circuit voltage (A) and open circuit voltage (B) measured in biosludge experiment.

Polarisation curve was measured when highest CCV of the experiment was achieved (day 19). By changing the external resistance, the current density flowing through the system was controlled and a different voltage value was measured. Power density was calculated from Equation 5:

$$P_{dens} = \frac{V_{MFC}^2}{R_{ext} \cdot A} \quad (5)$$

where P_{dens} is the power density, V_{MFC} is the measured voltage over the resistor, R_{ext} is the value of external resistance and A is the projected electrode surface area (Logan, 2008).

With increasing current density, the voltage of an OC-MFC and an S-MFC dropped rapidly and the maximum power density achieved was considerably less (0.20 ± 0.02 mW/m^2). Only the CC-MFC was capable of higher power production (1.7 ± 0.6 mW/m^2) and the voltage drop with increasing current density was slower (Figure 4-6). This shows that, although the OCV was similar in CC- and OC-MFC, only the microbial community in CC-MFC was adapted to electricity production. The power density achieved was comparable with the usual power production by H-type MFCs with aqueous cathodes using dissolved oxygen. The typical power density values range between 0.17–45.00 mW/m^2, depending on whether the cathode chamber is being sparged with oxygen, and on the types of electrodes and separators used (Logan, 2008).

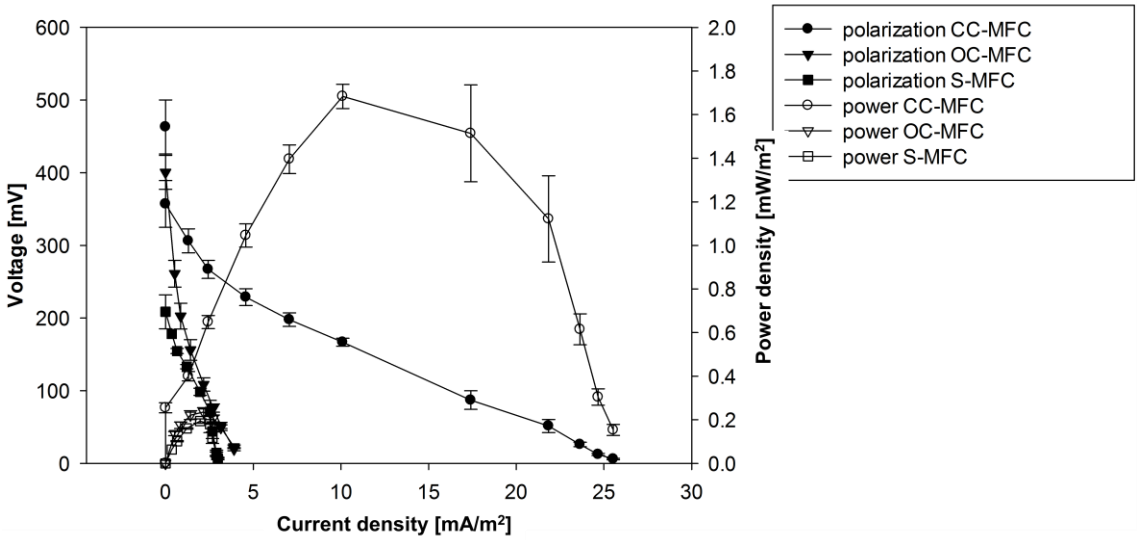

Figure 4-6 Polarisation and power curves measured at day 19 of the biosludge MFC experiment.

Phenol biodegradation under aerobic conditions was fastest, as could be expected (Figure 4-7). Phenol concentration did not decrease in the aerobic control system showing that phenol could not be removed by non-biological processes (e.g. evaporation, adsorption on biosludge material). Biodegradation under anaerobic conditions did not appear to occur. Phenol concentration in the S-MFCs decreased faster than in the CC-MFCs and OC-MFCs. This unexpected phenomenon indicated that there was a problem with the experimental set-up. This was confirmed by the dissolved oxygen (DO) concentration in the sterile systems (data not shown). It decreased to zero as well as in the aerobic system containing live biosludge; any oxygen entering the bottle was immediately consumed by respiring bacteria. Biological contamination of sterile systems including the S-MFC was likely to occur during sampling and minimal media addition. The 0.2 μm syringe filters were removed and a single syringe was used to add minimal media in all the systems which could have potentially caused biological cross-contamination of the systems.

Removal of the filters for minimal media addition was to be avoided in the next experiment.

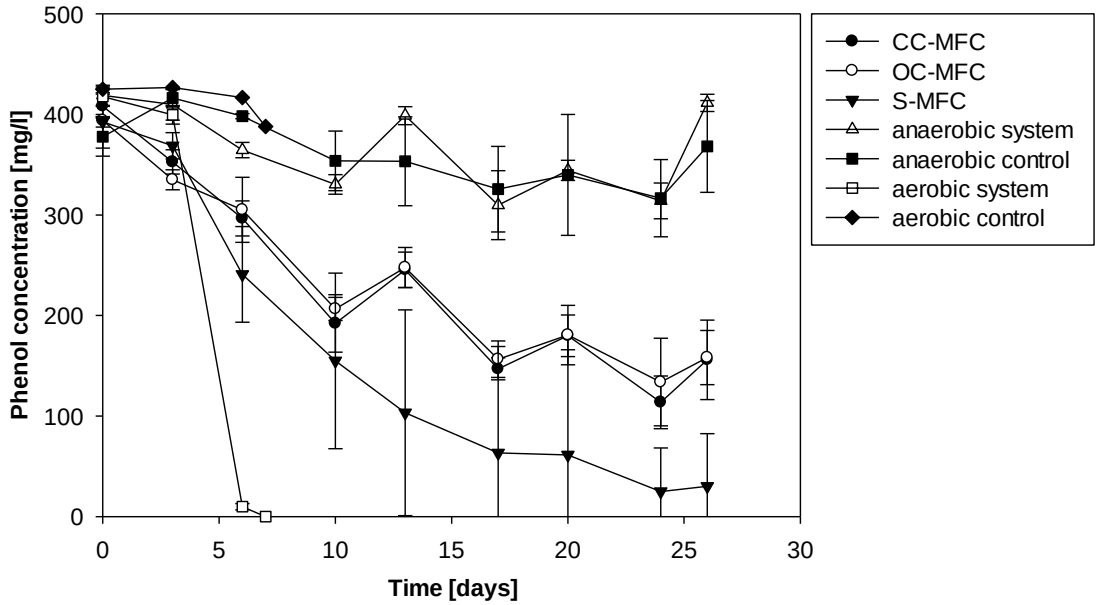

Figure 4-7 Phenol degradation during the first biosludge MFC experiment.

Nafion 117, as a cation exchange membrane, preferentially transfers cations. However, movement of anions across the membrane in the direction of concentration gradient was observed (Appendix D). Measured pH values did not show significant difference between the systems and no significant difference over time ($P > 0.05$) (data not shown). The laboratory temperature varied at 21.9 ± 0.5 °C.

The cathode chamber got contaminated by microorganisms after a period of time which was apparent from increased turbidity. The cathode chamber was open to air with no lid. The ions and very likely phenol as a carbon source were transported from the anode chamber to the cathode chamber via the Nafion membrane. This was likely to be a reason for microbial contamination. The cathode chamber needed to be kept sterile in all subsequent experiments to be able to observe and quantify diffusion of substrates and nutrients through the Nafion membrane.

The biosludge MFC experiment was repeated, this time making sure that the addition of minimal media did not cause any problems with biological contamination by keeping the 0.2 μm syringe filters on the valves. They got unblocked by the flow of minimal media into the system and were therefore kept on for longer period of time (up to 3 sampling points). Cathode chambers were covered by a cotton stopper to prevent biological contamination. Electricity production in CC- and OC-MFCs followed a similar trend as in the first

experiment (Figure 4-8). CCV increased rapidly in the CC-MFCs after 12 days of experimentation, reaching the maximum of 46 ± 11 mV. OC-MFC produced 11 ± 4 mV on average. CCV produced by S-MFCs stayed near zero. Similarly, the OCV of the S-MFCs fluctuated around zero value. The OCV of the CC-MFCs increased at a slower rate than in the OC-MFCs, as previously shown.

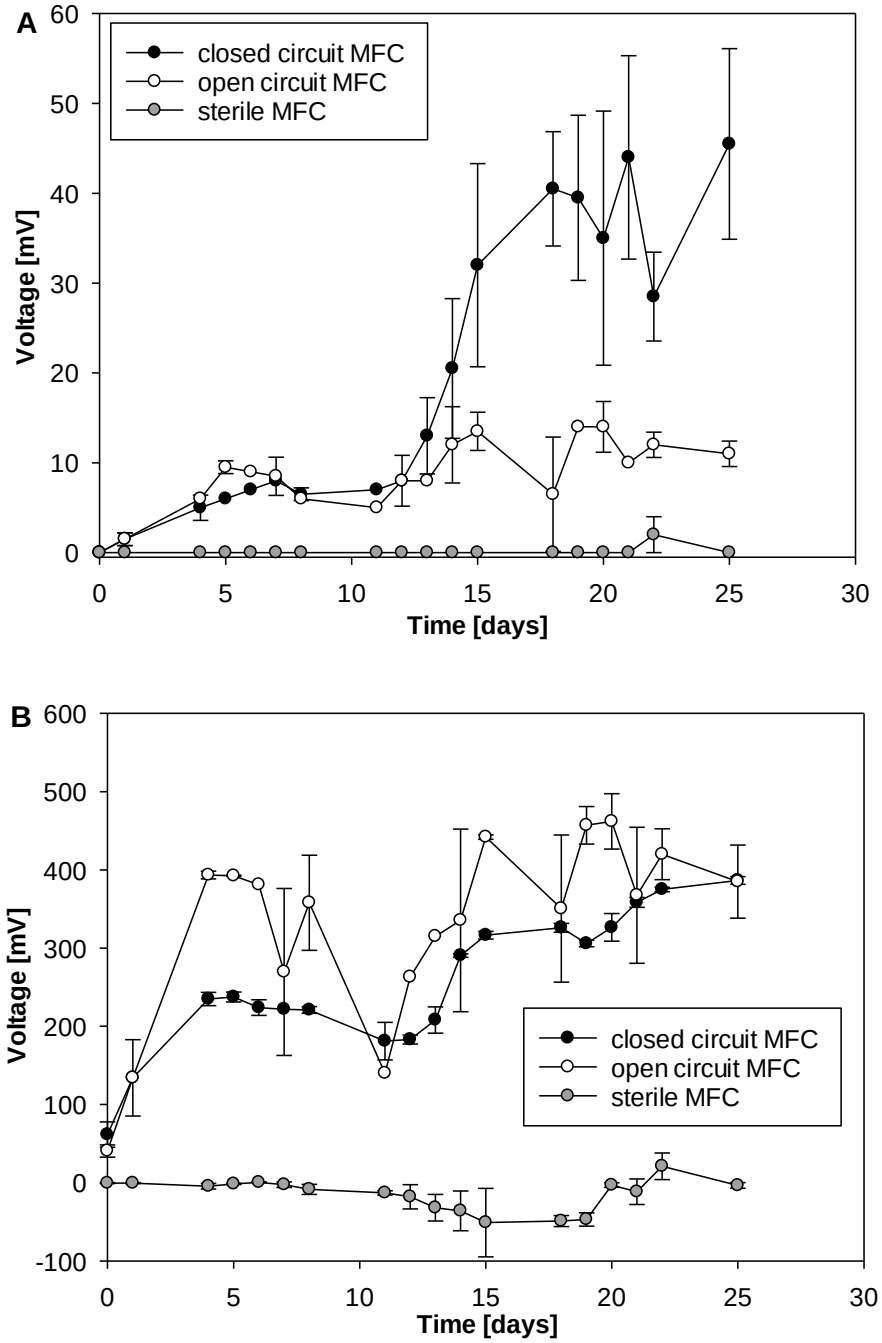

Figure 4-8 Closed circuit voltage (A) and open circuit voltage (B) measured in repeated biosludge experiment.

Oxygen diffusion through the membrane was observed in the S-MFC (Figure 4-9). The measured values closely followed the theoretical calculated (Equations 6 and 7) trend, based on the measurements by Kim et al. (2007). This is given by

$$V\frac{dc_2}{dt} = J_c A = \frac{D_{Cm}A}{L_t}(c_1 - c_2) \tag{6}$$

which is integrated using the separation of variables, assuming constant oxygen concentration in the cathode chamber $c_{1,0}$ ($c_1 = c_{1,0}$) and no oxygen initially present in the anode chamber ($c_{2,0} = 0$),

$$c_2 = c_{1,0}\left(1 - e^{-\frac{D_{Cm}At}{VL_t}}\right) \tag{7}$$

where V is the volume of each chamber [cm^3], J_c the flux of oxygen [mg/cm^{3}s], A the membrane area [cm^2], D_{Cm} the diffusion coefficient [cm^2/s] and L_t the membrane thickness [cm]. It was assumed that no reaction in the anode chamber was consuming oxygen (Kim et al., 2007). Diffusion coefficient D_{Cm} as calculated from the measured data can be found in Appendix E.

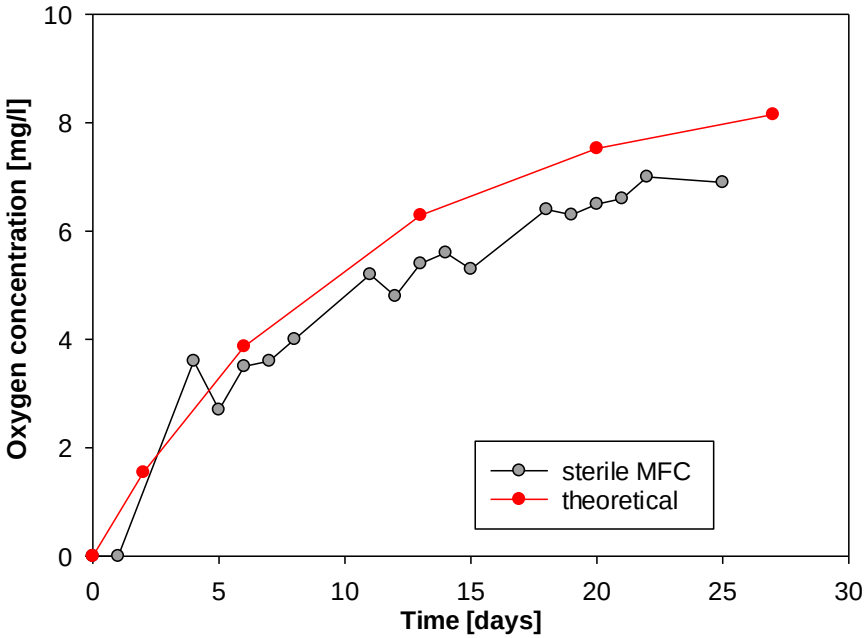

Figure 4-9 Oxygen diffusion to the anode chamber of biosludge S-MFC (repeated experiment) and the theoretical calculated rate of diffusion based on (Kim et al., 2007).

Phenol concentration decreased in all the MFCs (Figure 4-10). Phenol could have therefore diffused from the anode chamber to the cathode chamber via the Nafion membrane. However, the large error in the data prevented any reasonable comparison between the systems and interpretation. It was suspected that the poor quality of the data was caused by the microbial contamination of the 0.2 μm syringe filters on the sampling

valves. After the sampling, the filters were not changed and therefore the outside facing side contained phenol as a carbon source and minimal media to support microbial growth. Air-borne bacteria could have therefore entered the filter and thrived. During the next sampling, these bacteria could have been transferred in the samples and degraded phenol, causing the large variation in phenol concentration data. The MFCs themselves did not get contaminated. The 0.2 μm syringe filters on the valves were therefore changed prior to sampling during the following MFC experiments (Section 4.3.2, 4.3.3 and 4.4) and no problems with phenol data quality occurred.

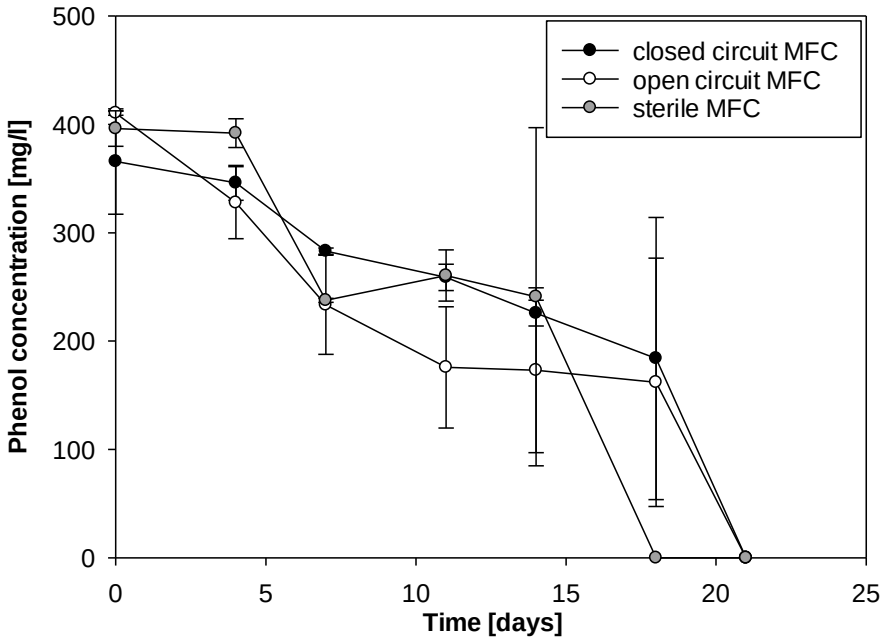

Figure 4-10 Changes in phenol concentration in the anode chamber of biosludge MFCs (repeated experiment).

4.3 Preliminary groundwater tests

The Scunthorpe biosludge microbial community degrades phenol and other contaminants under aerobic conditions. It was expected that it would be able to degrade phenol in MFCs due to the oxygen entering the anode chamber through the membrane. There would be no oxygen nearby the anode in the field BES application. It was therefore intended to use groundwater contaminated by coal tar (phenolic compounds) extracted from the oxygen depleted zone of the plume as an inoculum in the next experiments. Microbial community from this zone is adapted to grow under anaerobic conditions.

4.3.1 Inoculum testing

The main aim of this experiment was to find reasonable phenol concentration and inoculum for MFCs. The groundwater comes from a coal tar contaminated field (Section

4.1). Groundwater from four different depths (borehole 59, depth 12 mbgl, 13 mbgl, 14 mbgl and 17 mbgl) was tested as potential inoculum for MFCs. The depths were chosen based on the data collected in March 2012 by Lukasz Cieslak. The following criteria had to be met:

- Concentration of total phenols lower than 500 mg/l because microbial growth may be suppressed by the toxicity of phenols above this concentration (Spence et al., 2001).
- Minimum total cell count 10^7/ml to ensure good activity of microorganisms. The presence of *Geobacter* spp. should be beneficial for electricity production.
- Oxygen concentration below detection limit. The microbial community from this depth should be capable of phenol degradation under anaerobic conditions.

The growth rate of groundwater microorganisms as optical density at 600 nm (OD_{600}) under aerobic conditions was measured in a micro-titration plate by a plate reader (Synergy II multimode, BioTek Instruments, Inc.). The groundwater was 10x diluted by minimal media (Section 4.1) and the phenol concentration was varied between 0 and 1500 mg/l. Using a micro-titration plate (micro-cultivation) is a quick and efficient method to test how different conditions affect microbial growth. Unfortunately, it is not possible to keep the conditions within the plate anaerobic. Tests under anaerobic conditions would have taken considerably longer and would be much more laborious. The quality of data from the micro-cultivation was satisfactory for the purposes of this research.

When no phenol was added some growth of microorganisms was noticed in all the tested depths of the aquifer (Figure 4-11). This was likely to be caused by the presence of growth substrates (phenols and acetate) in the groundwater. As the phenol concentration was increased up to 500 mg/l, the final OD_{600} also increased and the lag-phase prolonged. The growth of the microorganisms above 500 mg/l of phenol was likely to be suppressed by phenol toxicity (Lerner et al., 2000). The results for the depths 12 mbgl, 13 mbgl and 14 mbgl show a similar trend; when 700 mg/l of phenol is applied no significant growth of microorganisms was apparent. However, when using groundwater from 17 mbgl and 700 mg/l phenol microorganisms started growing after 200 hours. This might have been caused by the adaptation of microorganisms from depth 17 mbgl on a higher total phenolics concentration (approx. 200 mg/l in depths 12 mbgl, 13 mbgl, 14 mbgl and 300 mg/l in depth 17 mbgl, Figure 4-2).

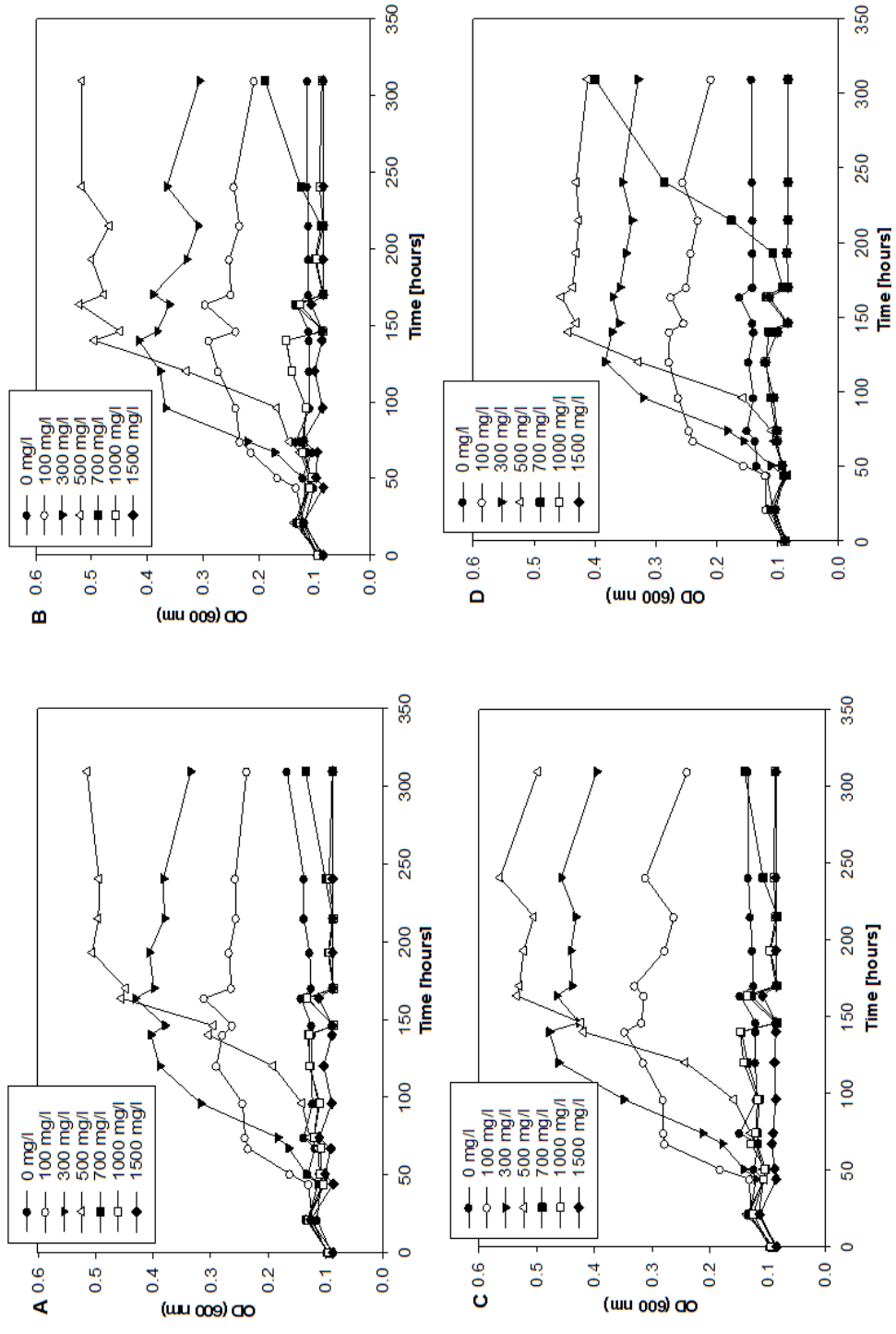

Figure 4-11 Microbial growth (as OD 600 nm) at different phenol concentrations with inoculums from different depth of the aquifer; (A) 12, (B) 13, (C) 14 and (D) 17 mbgl.

The groundwater from 12 mbgl was chosen as an inoculum for the following experiments (Section 4.3.2 onwards). There were two reasons for this choice. Firstly, 12 mbgl did not perform very differently in terms of biodegradation of phenol in comparison with other groundwater (13, 14 and 17 mbgl). Secondly and more importantly, 16S rRNA gene sequencing data was available for this depth, showing that 25% of microbial community at 12 mbgl consists of *Geobacter* sp. It was hypothesised that the presence of this bacterium would be beneficial for MFC performance (Chapter 3, Section 3.2).

4.3.2 Further MFC design testing

It was previously shown in the literature and in biosludge MFC experiments (Chapter 4.2) that oxygen is transported via the membrane to the anode chamber and also substrate can escape into the cathode chamber through the membrane (Kim et al., 2007). In principle, there would be no transfer of oxygen to the anode in the field application of BESs. The mass transfer of the contaminants between the chambers could therefore complicate their mass balance and interpretation of biodegradation data. Hence, the second MFC experiment looked at the possibility of eliminating the mass transfer between the anode and cathode chambers of an MFC.

Figure 4-12 An MFC with the chambers separated by stainless steel plate (left) and two separate Schott bottles (right).

MFC literature only discusses the importance of a membrane separator in the terms of influence on internal resistance and hydrogen proton transfer to the cathode (Logan, 2008; Lovley, 2006b; Oh and Logan, 2006). Protons are naturally present in water (in the cathode chamber), their concentration depending on pH (Stumm and Morgan, 2013). It was therefore deduced that the two MFC chambers could be physically separated and the

reaction on the cathode would still take place. The performance of an MFC with Nafion membrane was therefore compared with other two systems: MFCs with the membrane replaced by a stainless steel plate, and two Schott bottles which were only connected by the wire (Figure 4-12).

The experiments were set up in duplicate (only CC-MFC and S-MFC due to the lack of MFC devices available) with minimal media in both chambers, and groundwater inoculum (borehole 59, depth 12 mbgl) and 180 mg/l of phenol in the anode chamber. The bacteria were removed from the groundwater (100 ml) by microfiltration through the 0.1 μm sterile filter (Whatman® Cyclopore®, 47 mm, polycarbonate) (Figure 4-16) and this filter then inserted into the anode chamber as an inoculum. Electricity production was measured every day by a voltmeter, samples for HPLC were taken once/twice weekly through a 0.2 μm syringe filter (changed at every time point) and the concentration of dissolved oxygen was checked twice a week.

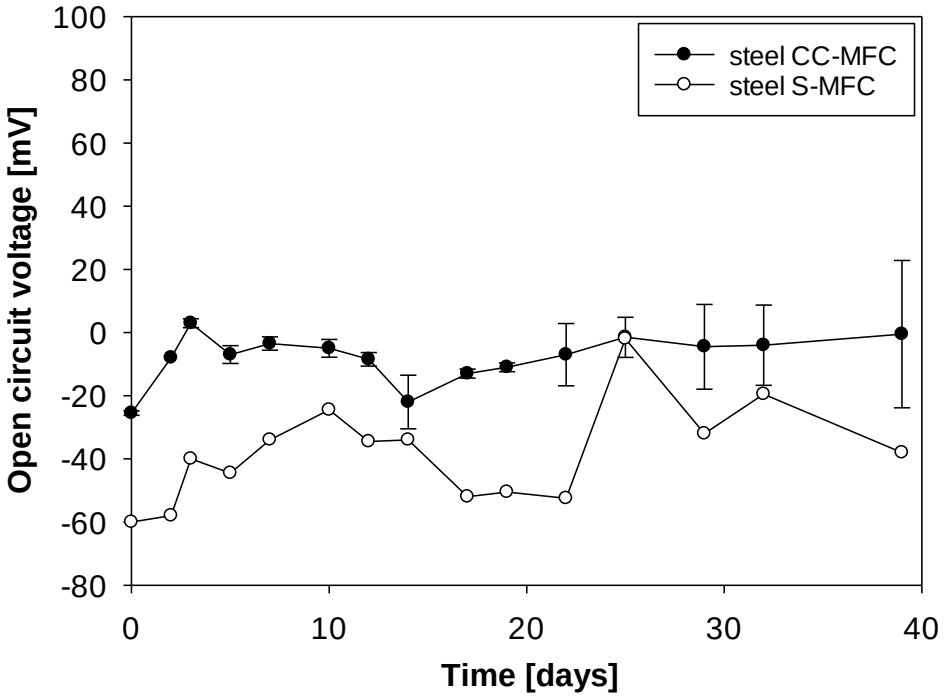

Figure 4-13 Open circuit voltage of MFCs having stainless steel plate as a separator.

As expected, there was no mass transfer between the chambers in an MFC with stainless steel plate and between two separate Schott bottles (data not shown). No electricity was produced by the separate Schott bottles (data not shown). Although protons should be present in the cathode chamber, electricity production was disabled by the infinite internal resistance of the system. This can be seen from Ohm's law (Equation 8)

$$I = \frac{E_{MFC}}{R_{ext}} \quad (8)$$

where I is electrical current and E_{MFC} is the potential of the MFC measured across the resistor R_{ext} (Logan, 2008). The OCV of an MFC with stainless steel plate was negative (Figure 4-13).

The only MFC design capable of electricity production in this experiment was the original H-type dual-chamber MFC with the Nafion membrane as a separator. The CCV measured across the 1 kΩ resistor was not detected (appearing to be zero) during the experiment. The OCV reached only 64 ± 29 mV as its maximum (Figure 4-14). The reason why no significant electricity production in the terms of CCV was measured in this MFC set-up (groundwater bacteria from 12 mbgl, phenol as a sole carbon source in minimal media) becomes apparent in Chapter 5.

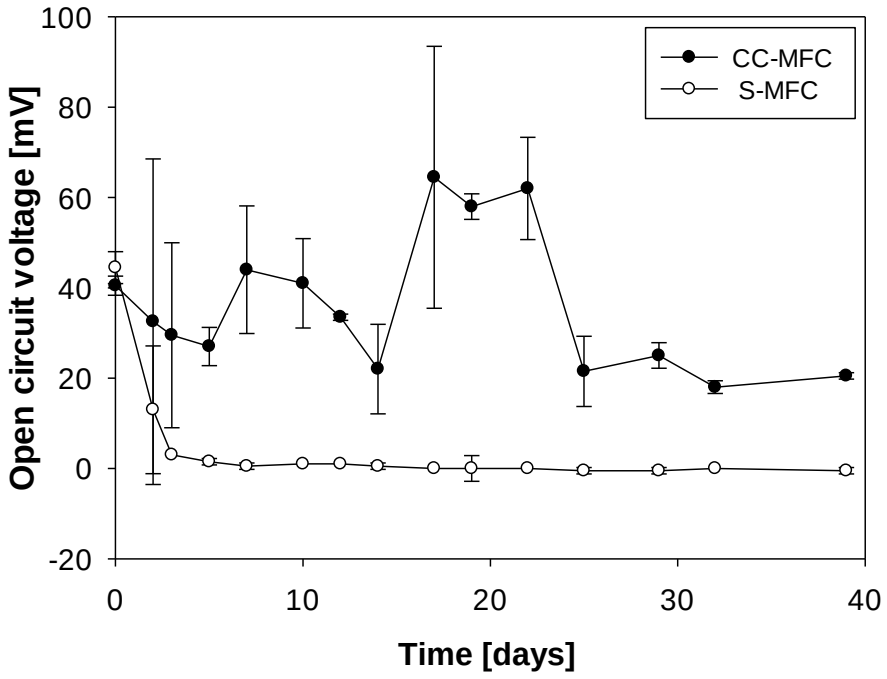

Figure 4-14 Open circuit voltage in MFCs with Nafion membrane as a separator.

Changing the 0.2 μm syringe filters attached to the sampling valves at each time-point helped ensure good quality data collection of the phenol concentration. Phenol diffused from the anode chamber to the cathode chamber as shown by the data from S-MFC (Figure 4-15). Biodegradation of phenol occurred in the anode chamber of CC-MFC. Unfortunately, there was no open circuit control MFC available so it is unclear if the electrode presence had any effect on phenol biodegradation. However, phenol biodegradation should be enhanced only in case the CC-MFC produces electricity. As no

significant electricity production (CCV) was detected in CC-MFCs, it is very unlikely that biodegradation of phenol was enhanced in this case.

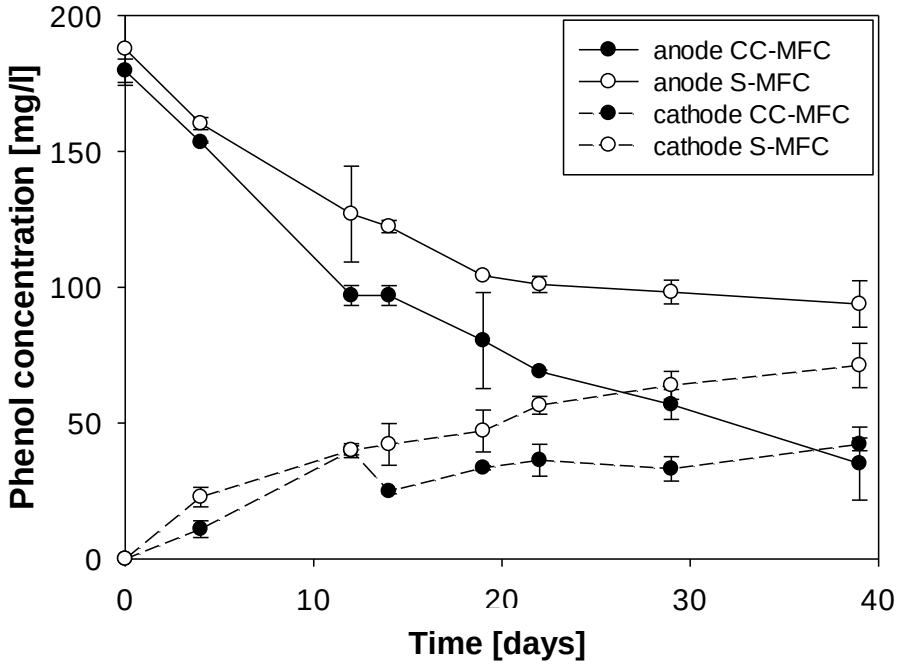

Figure 4-15 Changes in phenol concentration in CC- and S-MFCs with Nafion membrane as a separator.

To summarise,

- mass transfer between the chambers cannot be avoided
- changing 0.2 μm filters on the sampling ports at each sampling points prevents bacterial contamination of phenol samples
- no significant electricity production which could enhance biodegradation of phenol was measured.

4.3.3 Preliminary groundwater MFC

At the start of the previous experiment, microbial community was separated from the groundwater and introduced in the minimal media in the MFCs. The separation step, filtration through 0.1 μm filter, could have had a negative effect on the community viability as a high pressure gradient is required for the filtration. It was suspected that this could have decreased electricity production. Groundwater (borehole 59, depth 12 mbgl) was therefore put in the anode chamber without any alteration as a source of inoculum and also chemical contamination.

To ensure that the microbial community growth was not limited by the availability of nutrients and trace metals, one set of MFCs was filled with a 1:1 mixture of groundwater

and minimal media with phenol (up to the concentration present in groundwater). The cathodes were filled with the same groundwater or groundwater and minimal media mixture to prevent any unwanted mass transfer of contaminants from the anode chamber.

Figure 4-16 Vacuum filtration of groundwater through 0.1 μm filter in anaerobic chamber.

The groundwater in the anode chamber of an S-MFC and in all the cathodes was sterilised by tangential flow filtration (Section 4.1) followed by filtration through the 0.1 μm filter (Figure 4-16). All the sterilising processes were carried out either with the groundwater being continuously bubbled with sterile nitrogen or in the anaerobic chamber filled with nitrogen to ensure no oxygen would enter the groundwater and react with dissolved iron(II). This experiment was set up without any replicates due to the lack of available MFC devices.

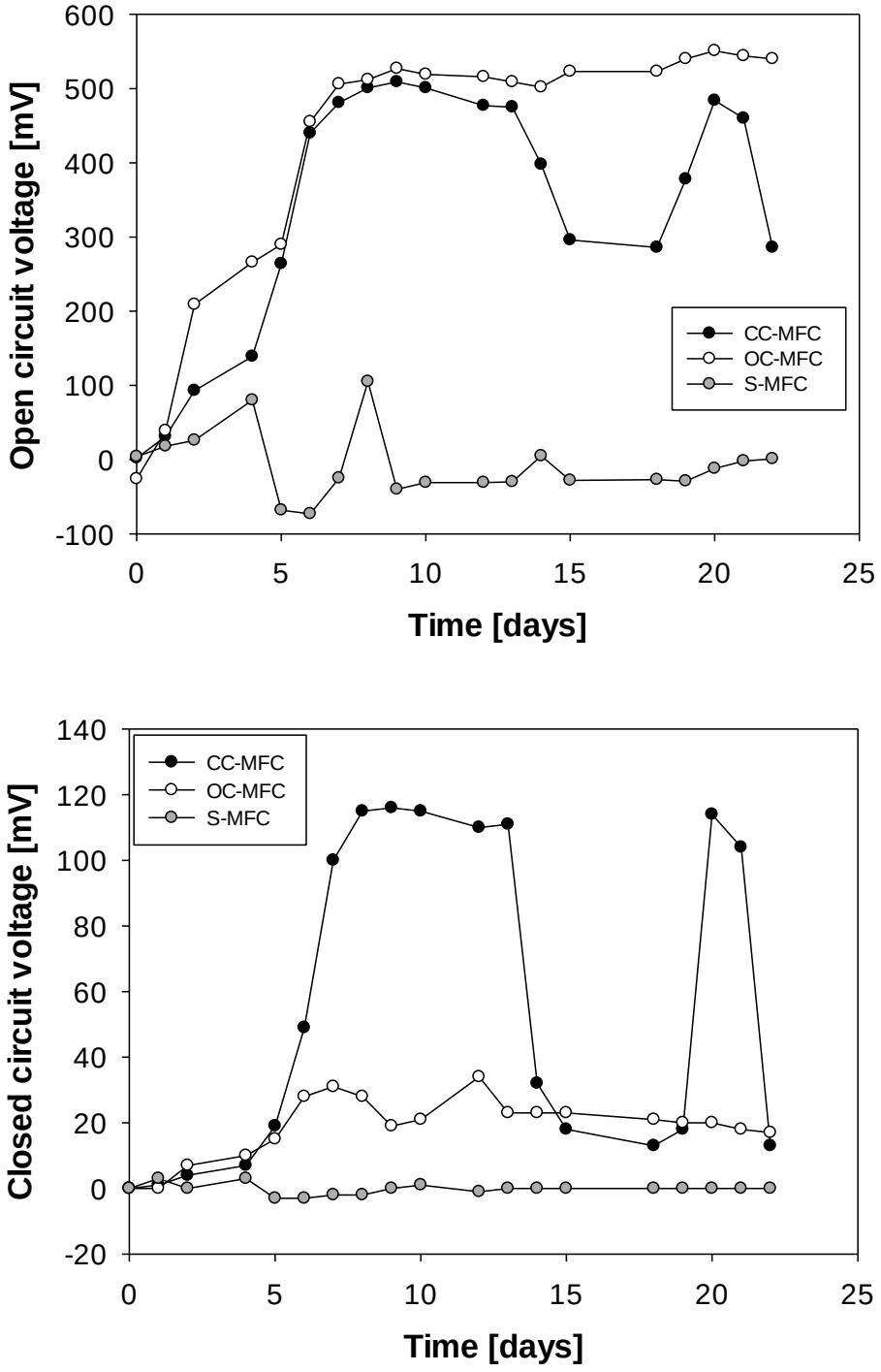

Figure 4-17 Open circuit voltage (top) and closed circuit voltage (bottom) in MFCs containing groundwater contaminated by phenolic compounds.

CCV across 1 kΩ resistor in MFCs filled with a mixture of groundwater and minimal media did not rise above 5 mV (data not shown). Interestingly, the microbial community thrived better in the original groundwater than in the mixture of groundwater and minimal media. Microbiologists used to believe that creating favourable conditions for bacteria by for example nutrient addition or increased temperature would make bacteria thrive. This

principle is used in enrichment cultures (Pepper et al., 2011; Perry and Staley, 1997). However, the results above do not indicate this. When no nutrients were added to groundwater, electricity production was observed.

CCV started exponentially increasing at day 5 in a CC-MFC filled with groundwater without nutrient addition, reaching up to 115 mV. Maximum OCV in both CC- and OC-MFC reached a value higher than 500 mV. S-MFC did not produce significant amount of current (Figure 4-17). As shown by the power density curve measured at day 8 by changing the resistors, the maximum power produced reached 2.8 mW/m^2 of the projected electrode area at 3.3 kΩ internal resistance (Figure 4-18). CC-MFC generated maximum current density of 25.5 mA/m^2 whereas OC-MFC generated only 3.4 mA/m^2, indicating that the microbial community in CC-MFC was adapted to use the electrode as an electron acceptor.

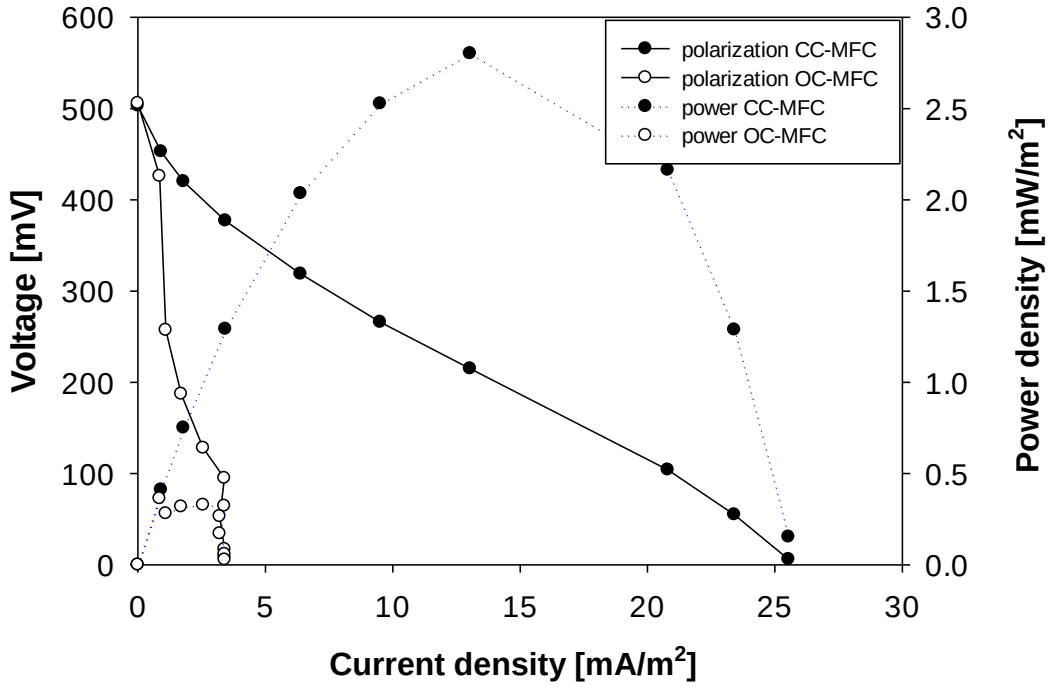

Figure 4-18 Polarisation and power curve measured in CC- and OC-MFC filled with groundwater contaminated by phenolic compounds.

There was again a problem with the concentration data for the phenolic compounds (Figure 4-19). It shows that the groundwater which was put in the cathode chambers and the anode chambers of S-MFC was not sterilised properly. No conclusion could therefore be obtained from the sterile controls and the experiment was terminated.

It was suspected that the source of biological contamination was the funnel holding the 0.1 μm filter. The filter was changed for every 100 ml of groundwater but the funnel stayed

the same. It could have introduced bacteria in the sterile part of the filtration system, the vacuum flask. It was therefore decided that the following experiments would have to use other means of sterilisation.

Interestingly, in the groundwater, where most bacteria were removed and only a few bacterial cells were introduced as biological contamination, the contaminating bacteria were able to grow fast and degrade a carbon source at a fast rate. Without removing the original groundwater population (about 10^7 cells/ml), the contaminating bacteria could not thrive due to competition with the original groundwater microbial community.

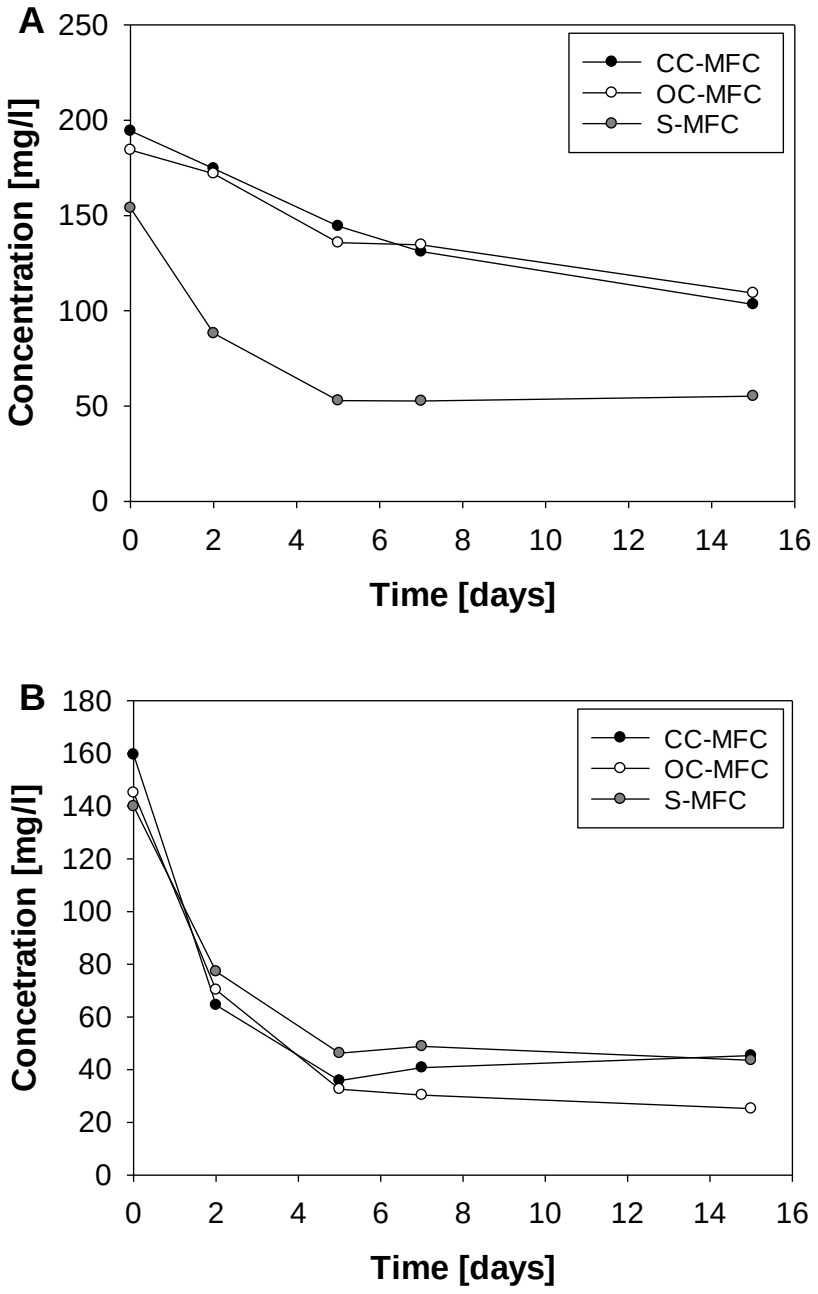

Figure 4-19 Concentration of total phenolics in groundwater MFCs in the anode chamber (A) and the cathode chamber (B).

4.4 First groundwater MFCs

It was proven in the previous experiment (Section 4.3.3) that electricity can be produced in an MFC containing groundwater contaminated by phenolic compounds. It was therefore decided to proceed with these MFCs. The good quality of the data on biodegradation of phenolics had to be ensured by keeping the groundwater in the cathode chambers and the anode chamber of the S-MFC sterile.

The groundwater in the cathode chambers was sterilised by autoclaving. The disadvantage is that this process changes the chemical composition of groundwater. Specifically, phenolic compounds can evaporate at the high temperature and pressure (Chen et al., 2014) and iron(II) can oxidise to iron(III) (Stumm and Morgan, 2013). Sodium azide (2 g/l) is bacteriostatic and used as a preservative (Lichstein and Soule, 1944) so it was added to the TFF sterilised groundwater to prevent bacterial growth in the anode chamber of S-MFCs.

An additional experiment was set up to observe if azide anions are transferred through the Nafion membrane. Sodium azide was added to one of the MFC chambers and its concentration in both chambers was measured by ion chromatography (full description of the method can be found in Section 5.1.3). Azide anion was then detected in both MFC chambers (data not shown) which demonstrates that the azide anion can be transferred via the Nafion membrane. Addition of sodium azide to the cathode chamber to prevent biological contamination was therefore only provisional as the azide transferred to the anode chamber could affect bacterial growth within. A better means of sterilising the cathode groundwater was required, potentially an efficient way of filtration through 0.2 μm filter. This problem was therefore researched while running the MFC experiment.

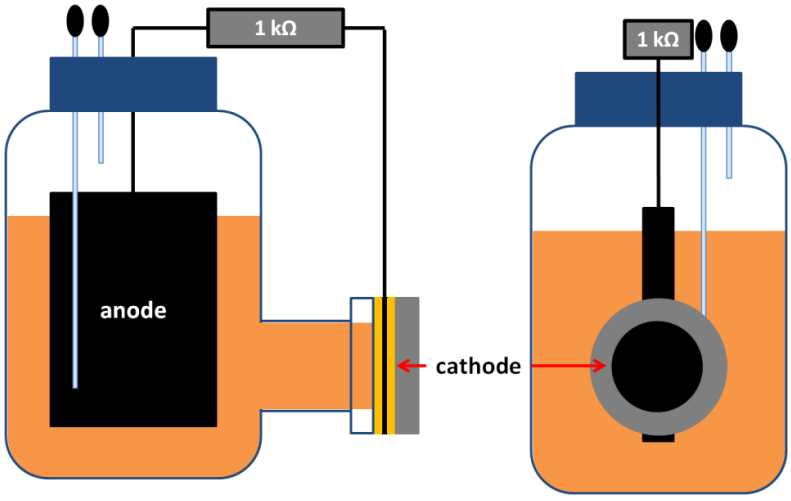

Figure 4-20 Single-chamber MFC from two different angles. The cathode has access to oxygen in the air through the 4 layers of PTFE.

Three different MFC set-ups without replicates were tested in this MFC experiment to explore which experimental design offers the best data interpretation for biodegradation of phenols. Single-chamber MFCs were built from the Schott bottles which were used in H-type MFCs (Figure 4-20). Only one Schott bottle was used for one MFC, with the cathode placed where the Nafion membrane originally was, attached with the pinch clamp. As the cathode was made of highly permeable carbon cloth, risk of leakage from the anode chamber was high. The cathode was therefore on the external facing side coated with 4 layers of PTFE (Cheng et al., 2006) to prevent leakage from the chamber. No Pt or carbon powder was applied to this electrode and Nafion membrane was not installed in this single-chamber MFC.

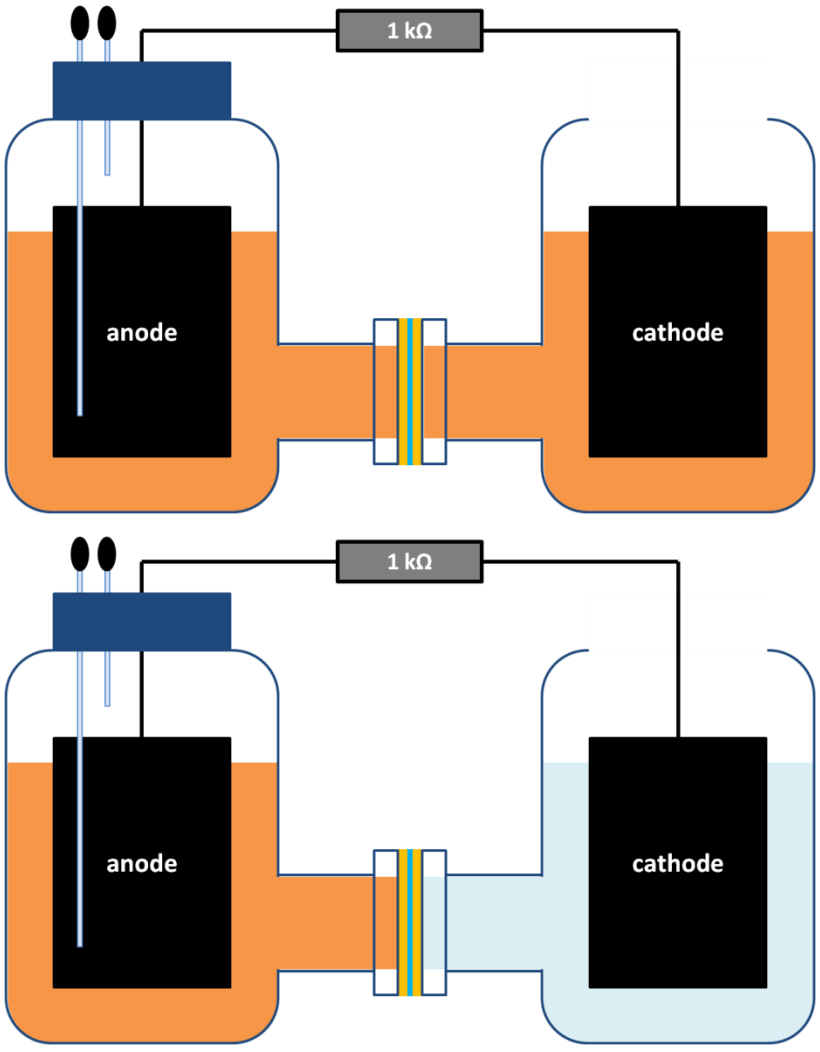

Figure 4-21 Dual chamber MFCs with contaminated groundwater in the cathode chamber (top) and uncontaminated groundwater in the cathode chamber (bottom).

The advantage of this set-up is that no unwanted mass transfer of phenolic compounds would occur in a single-chamber MFC. However, oxygen diffusion into the anode chamber could occur at a higher rate. In a dual-chamber MFC oxygen has to firstly dissolve in water

in the cathode chamber (only up to 9 mg/l) and then be transferred via the membrane. In a single-chamber MFC, it can be transferred through the PTFE directly from air where it is present at high concentration (21%). In theory, oxygen transfer into the anode chamber should be decreased when electricity production starts; at this point oxygen gets depleted on the cathode.

The other two set-ups used dual-chamber MFC as previously described at the beginning of this chapter (Figure 4-21). One of them had contaminated groundwater in the cathode chamber to decrease the mass transfer of contaminants from the anode chamber. As the concentration of phenols would decrease in the anode chamber due to biodegradation, phenols would be transferred from the cathode to the anode chamber. The second set had uncontaminated groundwater (borehole 59, depth 7 mbgl) in the cathode chamber. This MFC is based on the field conceptual model presented in Section 2.2.5.1 (Figure 2-7) where the anode is in contact with the contamination and the cathode is exposed to air in uncontaminated groundwater above the plume. All the MFCs were set up in the anaerobic chamber.

The main data measured in this experiment were the concentration of phenolics and electricity production. Voltage data logger was tested for the first time during this experiment. Polarisation curves were measured at the point of highest voltage generation. Groundwater taken from MFCs during sampling was not replaced immediately but after a longer period of time. 25 ml of autoclaved groundwater (7 mbgl and 12 mbgl depending on MFC set-up) was added on day 24 and 16 ml on day 59. Phenol (100 mg/l concentration) was added to MFCs on day 31. Electricity production of a single-chamber MFC was not monitored after day 59 as the MFC did not seems active. The MFCs were stirred on a shaker at 100 rpm for the duration of the experiment except for sampling and addition of groundwater and phenol. For evaluation of enhanced bioremediation of phenols by MFCs, it is important to compare the biodegradation rate of phenol in CC-MFCs with OC-MFCs, which differ only in the presence of the electrical circuit connection. It is therefore not necessary to compare the phenol biodegradation rate with the aerobic and anaerobic Schott bottle systems which are completely different from an MFC set-up (no membrane transferring oxygen and other chemical compounds, no carbon electrodes to enable biofilm development or adsorption of phenols).

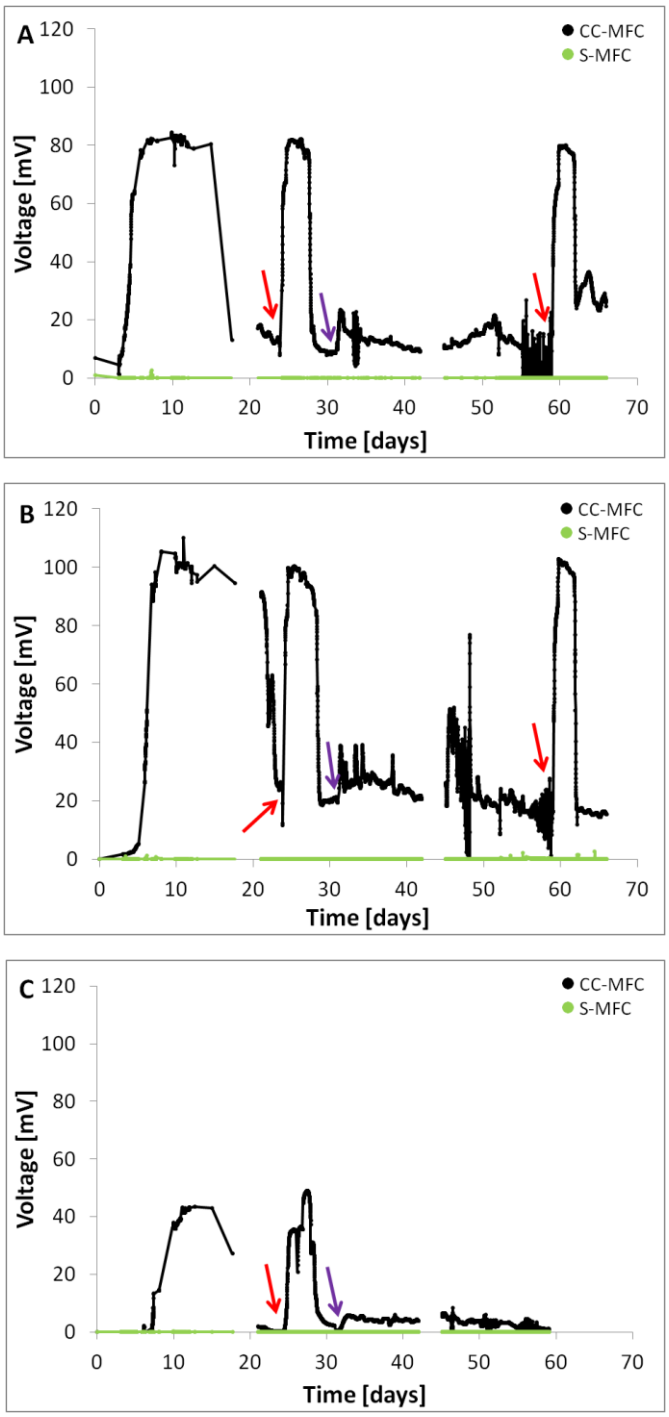

Figure 4-22 Electricity production measured by data logger in (A) dual-chamber MFC with uncontaminated groundwater in the cathode chamber, (B) dual-chamber MFC with contaminated groundwater in the cathode chamber, (C) single-chamber MFC. Red arrow - groundwater addition, purple arrow - phenol addition.

Electricity production in a dual-chamber MFC with uncontaminated (pristine) groundwater (7 mbgl) in the anode chamber (dual-MFC prist) started on day 3 and increased exponentially up to 82 mV over 1 kΩ resistor where it was maintained for 8 days after which rapid decline was observed (Figure 4-22). The other two MFCs followed a similar trend. The start-up time was longer, 5 days for dual-chamber MFC with

contaminated groundwater in the cathode chamber (dual-MFC cont) and 7 days for a single-chamber MFC (single-MFC). Dual-MFC cont reached higher voltage values of up to 110 mV over 1 kΩ resistor, which can be explained by decreased internal resistance caused by the higher conductivity of the contaminated groundwater in the cathode chamber (2.30 mS vs. 0.53 mS) (Logan, 2008). Indeed, internal resistance as acquired from the polarisation curve measurement (not shown) was higher for the dual-MFC prist (~2.9 kΩ) than for dual-MFC cont (~2.1 kΩ). Electricity production also lasted longer in the dual-MFC cont (14 days) than in dual-MFC prist. It could have been caused by the fact that more electron donors were available due to the possible membrane transfer from the cathode chamber (Section 4.3.2, Kim et al. 2007). Single-MFC, on the other hand, reached much lower voltage (43 mV) at its peak of electricity production, lasting only for 3 days. It was deduced that due to the simplicity of the cathode design (no carbon and Pt coating) the oxygen reaction on the cathode was not efficient to sustain a high voltage generation (Logan, 2008).

Electricity generation was rapidly restored to its original value (ca. 80 mV, 100 mV and 40 mV in dual-MFC prist, dual-MFC cont and single-MFC, respectively) in all the MFC systems after sterile groundwater was added on day 24. The groundwater therefore contained electron donors used for electricity production. It was hypothesised that phenol served as an electron donor for electricity production. Phenol was therefore added to MFCs on day 31 after the rapid decrease in electricity production. For easier manipulation of MFCs, stirring was disabled for the addition. After phenol addition when stirring was restored, a small peak in electricity production was observed (Figure 4-22). However, the increase in electricity generation was not as significant as after groundwater addition. This result indicates that some other organic compound in groundwater served as electron donor.

The MFCs were operated in their non-turnover mode at day 31, when electricity generation is limited by low concentration of electron donor and therefore its slow mass transfer to the electrode. The level of stirring in non-turnover mode affects the amount of current generated (Rabaey et al., 2010). Restoring the stirring after the addition of phenol therefore temporarily restored higher electricity production. The main carbon source which serves as an electron donor will be revealed in the following chapter (Chapter 5).

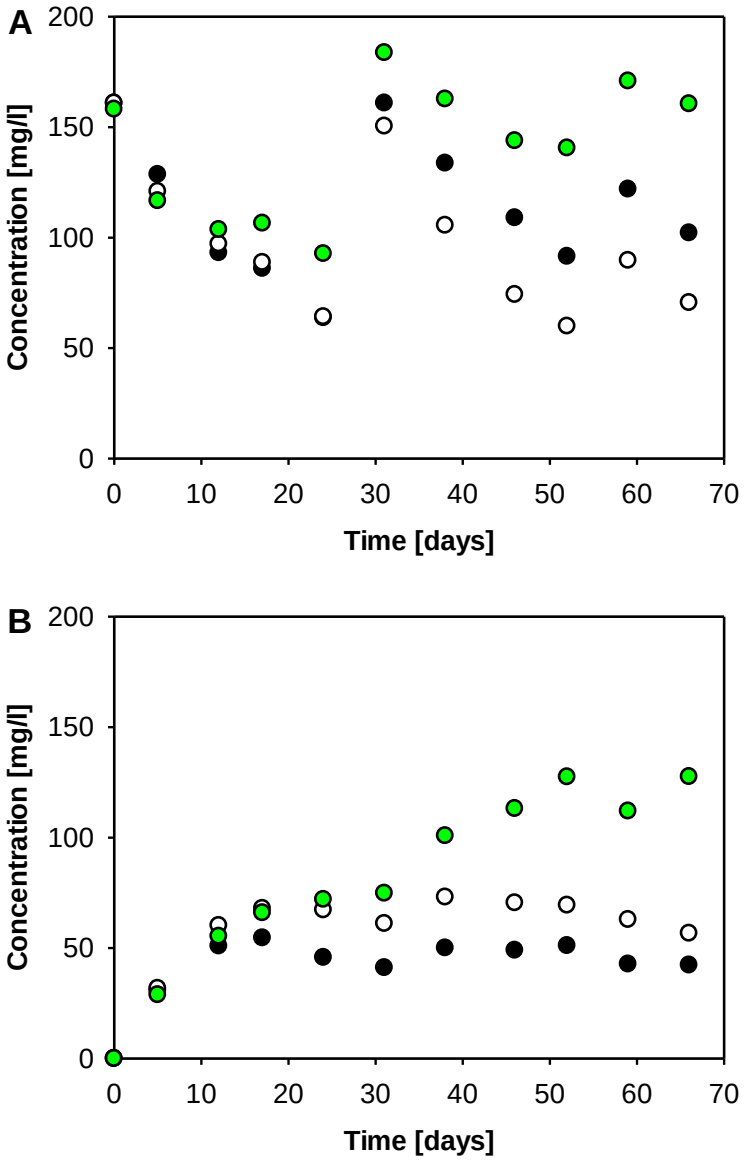

Figure 4-23 Changes in concentrations of total phenols in dual-MFC prist in the anode chamber (A) and cathode chamber (B) of CC-MFC (black), OC-MFC (white), S-MFC (green). Phenol (100 mg/l) was added on day 31.

Phenols diffused through the Nafion membrane from the anode to the cathode chamber in dual-MFC prist which can be seen from data for S-MFC in Figure 4-23. The change in concentration of total phenols is more rapid in CC-MFC and OC-MFC than in S-MFC in dual-MFC prist set-up. This indicates that biodegradation of phenols took place. During the first 24 days of the experiment, there is no significant difference between the CC- and OC-MFC, regarding the concentration of total phenols in the anode chamber. During this period, phenols in the cathode chamber of CC-MFC decrease faster than in the OC-MFC. It is unlikely that phenols would evaporate from the solution in CC-MFC faster than in OC-MFC. Phenols could have been transported back to the anode chamber where they got biodegraded. However, the concentration gradient does not favour the transfer of phenols from the cathode chamber to the anode chamber. As samples were taken from

MFCs and groundwater was added back to the tightly enclosed anode chamber only in larger batches, the pressure in the anode chamber decreased, creating pressure gradient between the chambers. This pressure gradient could have enhanced the transfer of phenols from the cathode chamber to the anode chamber.

The data following on from day 31 show a higher concentration of total phenolic compounds in the anode chamber of CC-MFC than OC-MFC. This contradicts the hypothesis that electricity generation enhanced biodegradation of phenols. The overall concentration (anode + cathode chamber) in CC-MFC is only slightly higher (by 15 mg/l) than in OC-MFC.

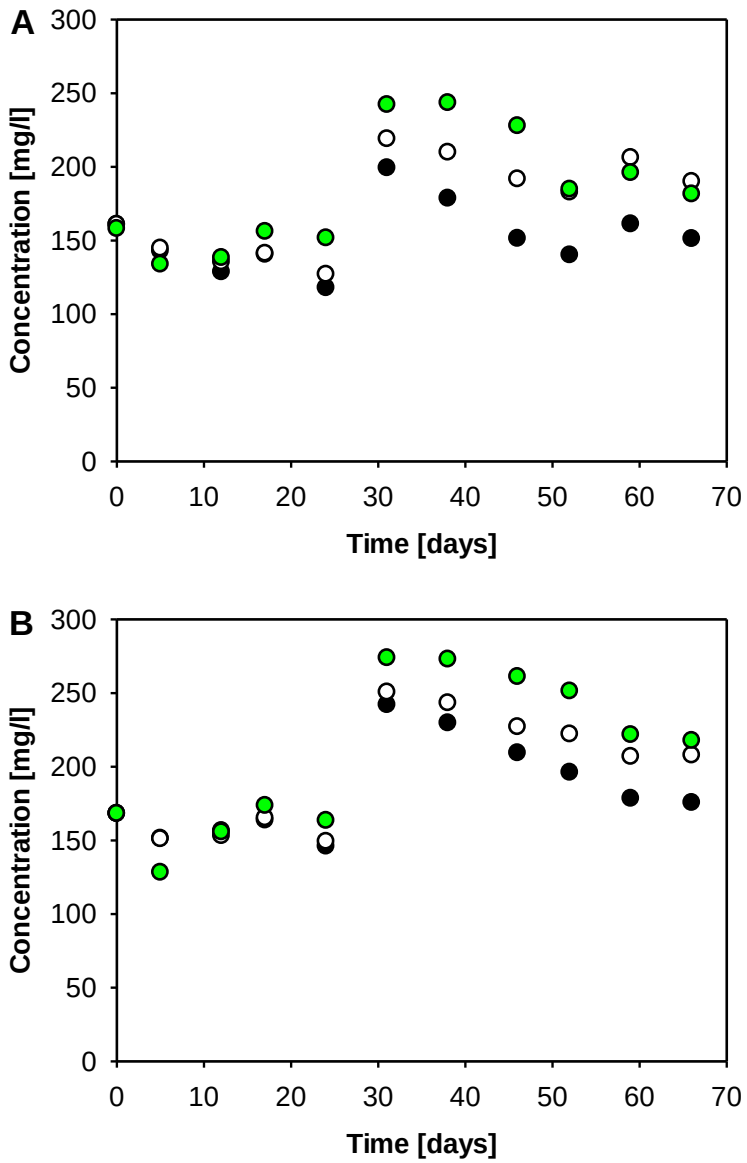

Figure 4-24 Changes in concentrations of total phenols in dual-MFC cont in the anode chamber (A) and cathode chamber (B) of CC-MFC (black), OC-MFC (white), S-MFC (green). Phenol (100 mg/l) was added on day 31.

The data showing the changes of concentration of the phenolic compounds (Appendix F), namely phenol, cresols and xylenols, were not very consistent. The concentration of phenol in the anode chamber of CC-MFC was higher than in OC-MFC, whereas the opposite trend was observed in the cathode chamber. There was no significant difference in concentration of cresols between the anode chambers of CC-MFC and OC-MFC during the first 24 days of the experiment but the CC-MFC had lower cresols concentration in the cathode chamber in comparison with OC-MFC. Later on (after day 31 when phenol was added to the systems), the concentration of cresols in the CC-MFC increased in comparison with OC-MFCs, making it higher in the anode chamber of CC-MFC than in OC-MFC and similar in the cathode chamber. There was no significant difference in the concentration of xylenols in the anode chamber of CC- and OC-MFC and the cathode chamber of CC-MFC in general contained less xylenols than the cathode chamber of OC-MFC. This experiment was set up only in one replicate and therefore it is difficult to exclude any problem with the contamination of the samples or MFCs themselves.

The results from the dual-MFC cont are more consistent. After day 31, there was significant difference in total phenols concentration (Figure 4-24) but also single groups of phenols (Appendix F) between the CC- and OC-MFC. Both, anode chamber and cathode chamber showed similar trend; faster decrease in concentration of phenolic compounds in CC-MFC in comparison with OC-MFC. These results confirm the hypothesis that the electricity production in MFCs can enhance biodegradation of phenols.

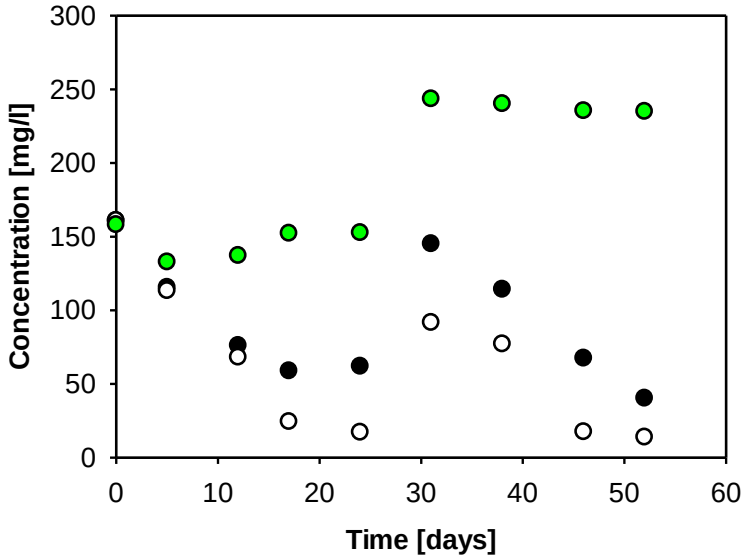

Figure 4-25 Changes in concentrations of total phenols in single-MFC of CC-MFC (black), OC-MFC (white), S-MFC (green). Phenol (100 mg/l) was added on day 31.

Single-MFCs produced significantly lower amount of electricity than dual-MFCs (Figure 4-22) but also the results of phenol biodegradation (Figure 4-25) show no evidence of enhanced phenol removal. Hence, this MFC design was not chosen for the subsequent experiments.

In addition to the measurements of concentration of phenolics by HPLC, two peaks of potential metabolites of phenols were observed on the chromatogram and the changes in the peak sizes were recorded (Appendix G). The metabolites would be identified by mass spectrometry in the future work (Chapter 5).

In summary, the dual-chamber MFCs were more reliable in electricity production from contaminated groundwater than single-MFCs. The phenolic data from the dual-chamber MFC with the contaminated groundwater in the cathode chamber show that providing bacteria with an electrode as electron acceptor may enhance bioremediation of phenols in groundwater. More evidence, especially from replicated MFCs, was needed to confirm this conclusion. It was therefore decided to repeat the experiment in dual-chamber MFCs to gather more evidence about biodegradation of phenols (replicate data and statistical testing).

Although the data from the dual-chamber MFC with the uncontaminated groundwater in the anode chamber did not provide good evidence of enhanced biodegradation of phenols, the experiment was repeated in triplicates using this design (Chapter 5). The main benefit of this set-up should be the potential representation of the field conceptual model (Figure 2-7) and comparability with previously performed studies on enhanced bioremediation of organic compounds in MFCs.[*] A triplicate set-up should eliminate any problem with biological contamination of the samples.

The sampling and groundwater addition were performed simultaneously one after another in subsequent experiments to prevent changes of pressure in the anode chamber. The methodology for MFC set-up is described in the following chapter (Chapter 5) which discusses the results from the triplicate dual-chamber MFCs with the uncontaminated groundwater in the anode chamber.

[*] Most of these studies (Section 2.3) apply the contaminants in one of the BES chambers, anode or cathode depending on the redox potential of the contaminants.

4.5 Effect of sterilisation and sampling on groundwater composition

A new sterilisation method for groundwater was sought. Filtration through 0.2 μm would be preferable. The filtering device would have to enable sterilisation of larger volumes, up to 5 L, of groundwater without getting blocked or changing the groundwater chemistry significantly. Bottle-top filter, size 90 mm with 0.8 μm pre-filter to remove bigger particles and 0.2 μm sterilising filter (VacuCap, Pall) was identified as a potentially good option. The filter is placed on the sterile bottle, with one tube drawing liquid (groundwater) from the reservoir vessel and the other connected to the vacuum pump (Figure 4-26). The vacuum draws the liquid into the sterile bottle. This is potentially easy to set up in the anaerobic chamber.

Figure 4-26 VacuCap filter (Pall) for culture media sterilisation (www.pall.com).

The efficiency of the device was tested prior to experimentation with MFCs and the changes in groundwater composition were compared with autoclaving. Contaminated groundwater was manipulated in an anaerobic chamber during the filtration. The concentration of phenols was measured by HPLC, calcium and magnesium by ion chromatography and soluble iron by induced coupled plasma mass spectrometry. The details of the analytical methods used can be found in Section 5.1.3. Main changes in groundwater composition can be seen in Table 4-3 and Table 4-4 (triplicate samples).

Table 4-3 Changes in composition of phenolic compounds in contaminated groundwater (GW) prior to and after autoclaving and filtration through 0.2 μm filter (VacuCap 90 PF 0.8/0.2 μm, Pall).

Sample	Phenol [mg/L]	Cresols [mg/L]	Xylenols [mg/L]
Non-sterile GW	20.5 ± 0.2	71.4 ± 0.4	85.5 ± 0.8
Autoclaved GW	20.4 ± 0.2	65.3 ± 0.3	71.4 ± 0.3
Filtered GW	19.7 ± 1.1	70.8 ± 0.8	85.1 ± 0.9

Autoclaving, as expected (Chen et al., 2014), affected the composition of phenolics in the groundwater (Table 4-3), decreasing the concentration of cresols and xylenols which

are more volatile than phenol (Dohnal and Fenclova, 1995). Filtration through the VacuCap filter did not change the concentration of phenolics. Autoclaving also significantly changed the concentration of magnesium, calcium and soluble iron (Table 4-4). The concentration of calcium and magnesium in groundwater probably decreased due to precipitation with carbonate ion during boiling (Stumm and Morgan, 2013). The content of calcium and magnesium remains unchanged after VacuCap filtration. Soluble iron, mostly in the form of Fe^{2+}, could have been oxidised by oxygen to iron(III) during autoclaving, forming insoluble precipitates (Stumm and Morgan, 2013), which considerably decreased the concentration of soluble iron in autoclaved groundwater. Filtration also decreased the concentration of soluble iron in the groundwater, possibly due to iron precipitation on the filter itself. However, the decrease in concentration of soluble iron is less significant than in the case of autoclaving. Filtration through the VacuCap 0.8/0.2 μm filter (Pall) was therefore chosen as a groundwater sterilisation method in future experiments (Chapter 5).

Table 4-4 Changes in composition of selected metals in contaminated groundwater (GW) prior to and after autoclaving and filtration through 0.2 μm filter (VacuCap 90 PF 0.8/0.2 μm, Pall).

Sample	Mg^{2+} [mg/L]	Ca^{2+} [mg/L]	Soluble Fe [mg/L]
Non-sterile GW	25.2 ±0.3	63.1 ± 0.9	1.37 ± 0.11
Autoclaved GW	19.4 ± 0.0	23.6 ± 0.4	0.20 ± 0.08
Filtered GW	25.3 ± 0.3	61.7 ± 0.6	0.62 ± 0.01

The concentration of soluble iron in groundwater in the field was significantly higher (10.47 ± 0.57 mg/L) than in the groundwater after storage of the sample in a cold room (1.37 ± 0.11 mg/L) and used in the next experiment (Chapter 5). The 2.5 L sampling bottles were degassed in the laboratory prior to groundwater sampling. However, the bottles were not closed completely during groundwater pumping so some oxygen might have entered the bottle and oxidised iron. The groundwater therefore contained a lower amount of soluble iron and possibly iron(III) oxides (Stumm and Morgan, 2013).

Chapter 5

Biodegradation of phenolic compounds and their metabolites in contaminated groundwater using MFCs

Phenolic compounds (phenol, isomers of cresols and xylenols) can enter groundwater from coal-gasification plants, wood preservation facilities and many other industrial processes (Thornton et al., 2014; Thornton et al., 2001b). Phenols are a group of eco-toxins with potential carcinogenic and mutagenic effects on humans and other living organisms (Michałowicz and Duda, 2007). Hence, the groundwater contaminated by phenols requires treatment (Thornton et al., 2014). In this chapter, potential of BESs to enhance biodegradation of phenols in groundwater is tested in MFCs.

The groundwater was sampled from the upper fringe of a plume of phenolic compounds in a Permo-Triassic sandstone aquifer (Thornton et al., 2001b). The contamination originates from a coal tar distillation plant. The fringe is the most biologically active zone of a contaminant plume (Thornton et al., 2001a; Lerner et al., 2000) and from chemical analysis the groundwater sample collected was characterised as anaerobic and nitrate depleted, with iron(III) in colloid oxide/hydroxide form and sulphate as electron acceptors. It contains phenol, cresols and xylenols with a total concentration of 1.4 mM and acetate (1.9 mM) as a fermentation product of these contaminants (Thornton et al., 2001b). Twenty-five percent of the indigenous planktonic microbial community consists of *Geobacter* sp. (unpublished data), meaning that the community could be electro-active (Logan, 2008; Rabaey et al., 2010).

Geobacter sp. are often dominant in MFCs fed by acetate (Zhu et al., 2014; Kiely et al., 2011) but can also degrade aromatic compounds (Zhang et al., 2010; Bond et al., 2002; Rooney-Varga et al., 1999). Phenolic compounds and/or acetate could therefore serve as electron donors for electricity production. If the phenols were degraded directly by the electro-active bacteria, the enhanced removal of phenols should occur immediately with current generation. However, exoelectrogens might prefer simpler substrates such as acetate (Kiely et al., 2011). In that case, enhanced removal of phenols could occur after acetate depletion and such MFC-aided biodegradation should be enhanced by syntrophic metabolism within the microbial community.

The biological and chemical processes expected to occur in the MFCs include: (i) biodegradation of phenolic compounds to carbon dioxide via organic metabolites; (ii)

attachment of bacteria to the electrode and biofilm development; (iii) bacterial respiration, with the anode and other chemical compounds in the groundwater serving as electron acceptors; (iv) enhanced biodegradation of phenolic compounds in CC-MFC compared with OC-MFC, due to bacterial transfer of electrons to the anode; (v) reduction of oxygen on the cathode by electron transfer from the anode to the cathode, supporting electricity generation; and (vi) diffusion and electromigration of dissolved ions between the chambers.

5.1 Materials and methods

5.1.1 Groundwater

Groundwater was collected from the plume of phenolic contaminants using a multilevel sampler equipped with monitoring points able to sample different depths at 1 m resolution (Thornton et al., 2001b). Uncontaminated water from above the plume was sampled at 7 mbgl (meters below ground level). Contaminated water was taken from the upper plume fringe located at 12 mbgl. The groundwater was collected in sterile, nitrogen-purged 2.5 L amber glass bottles, which were filled completely. Samples were stored at 4 °C prior to use in the experiments.

5.1.2 Microbial fuel cells

H-type dual-chamber MFCs were constructed using two 250 mL Schott bottles, joined by a 7.5 cm glass tube (1.5 cm diameter), with a Nafion^{TM} 117 proton exchange membrane (DuPont) between the chambers. The anode chamber was equipped with a 3-port gas-tight screw cap fitted with two ports for separate gas and liquid sampling and one port to insert the wire. The sampling ports were covered by 0.22 μm sterile PES filters (Millex®, Merck KGaA) and the cathode chamber was closed by a wooden pulp stopper to keep both chambers aseptic. The electrodes were made of carbon cloth (H2315, Freudenberg FCCT SE & Co. KG) with a projected surface area of 50 cm^2.

Three MFCs were created in triplicate in an anaerobic chamber. These comprised a closed circuit MFC (CC-MFC), an open circuit control MFC (OC-MFC) and sterile control MFC (S-MFC). The anode chamber of the CC-MFC and OC-MFC contained 200 ml of contaminated groundwater (12 mbgl). 200 ml of filter-sterilised (bottle-top filter VacuCap 90 PF 0.8/0.2 μm, Pall) contaminated groundwater were added to the anode chamber of the S-MFC. All cathode chambers were filled with 200 mL of filter-sterilised uncontaminated groundwater (7 mbgl). The circuits of the CC-MFC and S-MFC were closed with copper wire connecting a 1 kΩ resistor to the electrodes, whereas the OC-MFC

operated under open circuit conditions. All MFCs were shaken (100 rpm) at 25 °C ± 2 °C for the first 27 days of the 92 day experiment.

Unfortunately, one of the OC-MFCs got biologically contaminated so the results presented from OC-MFCs show duplicate data. As previously discussed in Logan (2012), duplicate results should be sufficient.

The voltage across the resistor was monitored every 10 min with a data logger (NI USB-6251, National Instruments) connected to a computer. Polarization and power curves were generated using a potentiostatic discharge technique when the closed circuit voltage (i.e. electricity production by the MFC) reached a maximum value. The electrical potential of the cathode was measured at the maximum electricity production point against a silver chloride electrode (Ag/AgCl/saturated KCl, 0.197 V vs. SHE at 25 °C) under open and closed circuit conditions.

Individual carbon sources were added to the anode chamber of the MFCs later in the experiment (days 56–80) to evaluate the contribution of potential electron donors in electricity production. 4 mL of liquid were removed from the MFCs and replaced by a pure chemical dissolved in ultra pure water. The concentrations used reflected those in the original groundwater (control: no chemical added, phenol: 213 μmol/L, m- and p-cresol: 185 μmol/L each, 3,4- and 3,5-xylenol: 164 μmol/L each, acetate: 508 μmol/L, 1016 μmol/L and 2033 μmol/L).

The role of the electrode biofilm in electricity production was examined. An electrode from one of the closed circuit MFCs (running for 87 days) was removed and replaced by a sterile electrode from a new sterile MFC (sterile electrode in a mature closed circuit MFC, SE+CC-MFC). The mature electrode was gently washed in filter-sterilised contaminated groundwater (12 mbgl) and put into a new sterile MFC (mature electrode in a sterile MFC, ME+S-MFC).

5.1.3 Chemical analysis

Groundwater (3–13 mL) for chemical analysis was sampled at approximately 1 week intervals and filtered (0.22 μm sterile PES). The filters were changed for each sampling point. Samples for analysis of dissolved metals were acidified (1% (*v*/*v*) ultra pure nitric acid) and stored with samples for analysis of phenols at 4 °C. Samples for major ion and acetate analysis were stored at -20 °C (Shah et al., 2009). A volume of fresh filter-sterilised groundwater equal in volume to the sample removed, with the same composition as the starting sample, was added to MFCs to maintain the total volume during the experiment.

Phenolic compounds (phenol, isomers of cresols and xylenols) were analyzed by reversed-phase high performance liquid chromatography (HPLC) using a PerkinElmer instrument with a UV detector (wavelength 280 nm) and C18 column (Thermo Scientific™ Hypersil™ ODS-2, particle size 5μm, 250 mm x 4.6 mm I.D.) and C18 guard column. The sample injection loop was 10 μL. The eluent was an 80:20 mixture of 1% (*v*/*v*) acetic acid and acetonitrile, with 1.6 mL/min flow rate, changing to 1.0 ml/min between 4.7 and 5.7 min, followed by a 12 min gradient to a 60:40 ratio for another 4 min. The detection limit was 1 mg/L, with an analytical precision of ± 7%.

Organic acid metabolites of phenols were identified using a QStar Elite (AppliedBiosystems) mass spectrometer with ionspray injection. 0.3 ml fractions of HPLC eluent were collected in Eppendorf tubes between 2 and 6 min elution time. Samples were vacuum dried overnight (SpeedVac Plus, Thermo Scientific™) and re-suspended in 100 μl of 50% methanol and 0.1% formic acid in UHQ water. These fractions were then analyzed on the mass spectrometer.

Major ions and acetate were analyzed using an ion chromatograph (Dionex ICS 3000, Thermo Scientific™) with autosampler and eluent regeneration. The anions and acetate were separated using a Dionex IonPac® AS18 column with a AG18 guard column and 31mM sodium hydroxide as eluent, at a flow rate of 0.25 mL/min. The cations were separated by a Dionex IonPac® CS16 column with a CG16 guard column and 48 mM methane sulphonic acid as eluent, at a flow rate of 0.42 mL/min. Sample conductivity and pH were measured prior to ion analysis. Dissolved Fe(II) and Mn(II) were analyzed by ICP-MS (PerkinElmer Elan DRC II, MA, USA) using standard methods (Shah et al., 2009).

The dissolved oxygen concentration in the MFCs was measured weekly, non-invasively, using a fibre-optic probe and oxygen sensor (Fibox, PreSens, Germany) fitted to the inside of MFC chambers. The detection limit was 15 ppb (Shah et al., 2009).

Statistical comparison of CC- and OC-MFC performance (phenolics, metabolite and acetate data) at day 27 and 34 was completed with two-tailed t-test ($\alpha = 0.05$) in SigmaPlot 12.5.

5.1.4 Scanning electron microscopy (SEM)

All carbon cloth anodes were removed from the MFCs at the end of the experiment, drained using a sterile paper tissue, washed gently in filter-sterilised phosphate buffer saline (PBS) and drained again. A 1 cm^2 piece of carbon cloth from the middle of the each electrode was fixed overnight in 0.1 M cacodylate buffer with 3% glutaraldehyde at 4 °C.

The specimens were then washed twice in 0.1 M cacodylate buffer with 15 minute intervals at 4 °C. Secondary fixation was carried out in 2% osmium tetroxide aqueous for 1 hour at room temperature. The washing step was then repeated. All the following steps took place at room temperature. Samples were dehydrated through a graded series of ethanol (75%, 95%, 100% twice), each for 15 minutes. Samples were dried over anhydrous copper sulphate for 15 minutes, removing most of the ethanol. Residual ethanol was then removed by hexamethyldisilazane. Initially, the specimens were placed in a 50/50 mixture of 100% ethanol and 100% hexamethyldisilazane for 30 minutes, followed by 30 minutes in 100% hexamethyldisilazane. They were then allowed to air dry overnight before mounting. After drying, the samples were mounted on 12.5 mm diameter stubs and attached with carbon-sticky tabs and then coated in a sputter coater (Edwards S150B) with approximately 25 nm of gold. The specimens were examined in a Philips XL-20 scanning electron microscope at an accelerating voltage of 20 kV.

5.2 Results and discussion

5.2.1 Biodegradation of phenolic compounds and their metabolites

Phenolic compounds can be biodegraded to carbon dioxide, firstly by fermentation to structurally simpler and more easily biodegradable compounds, with subsequent respiration using different electron acceptors (Watson et al., 2003; Christensen et al., 2000). Fermentation is generally considered rate limiting in the biodegradation of phenols, but is important for the production of acetate in groundwater at the field site under consideration (Watson et al., 2005; Thornton et al., 2001b).

In this experiment, phenolic compounds diffused from the anode chamber to the cathode chamber via the membrane along a concentration gradient, as shown in the S-MFC data (Figure 5-1AB). The concentration of total phenols in the S-MFC decreased from 1440 μM ± 30 μM to 664 μM ± 8 μM at the end of the experiment. The final concentration of phenols in the cathode and anode chamber of the S-MFC should theoretically be equal. The lower than expected (462 μM ± 18 μM) final concentration of phenols in the cathode chamber of the S-MFC can be explained by their aqueous volatility (Chen et al., 2014; Dohnal and Fenclova, 1995). Biodegradation of phenols occurred in the CC- and OC-MFC, shown by the faster decrease in concentration in the anode chamber (Figure 5-1A). At most time points, there was no significant difference in the concentration of phenols between the CC-MFC and OC-MFC. However, the concentration of total

phenols was significantly lower ($P < 0.05$) in the CC-MFC than in the OC-MFC at day 27 and 34.

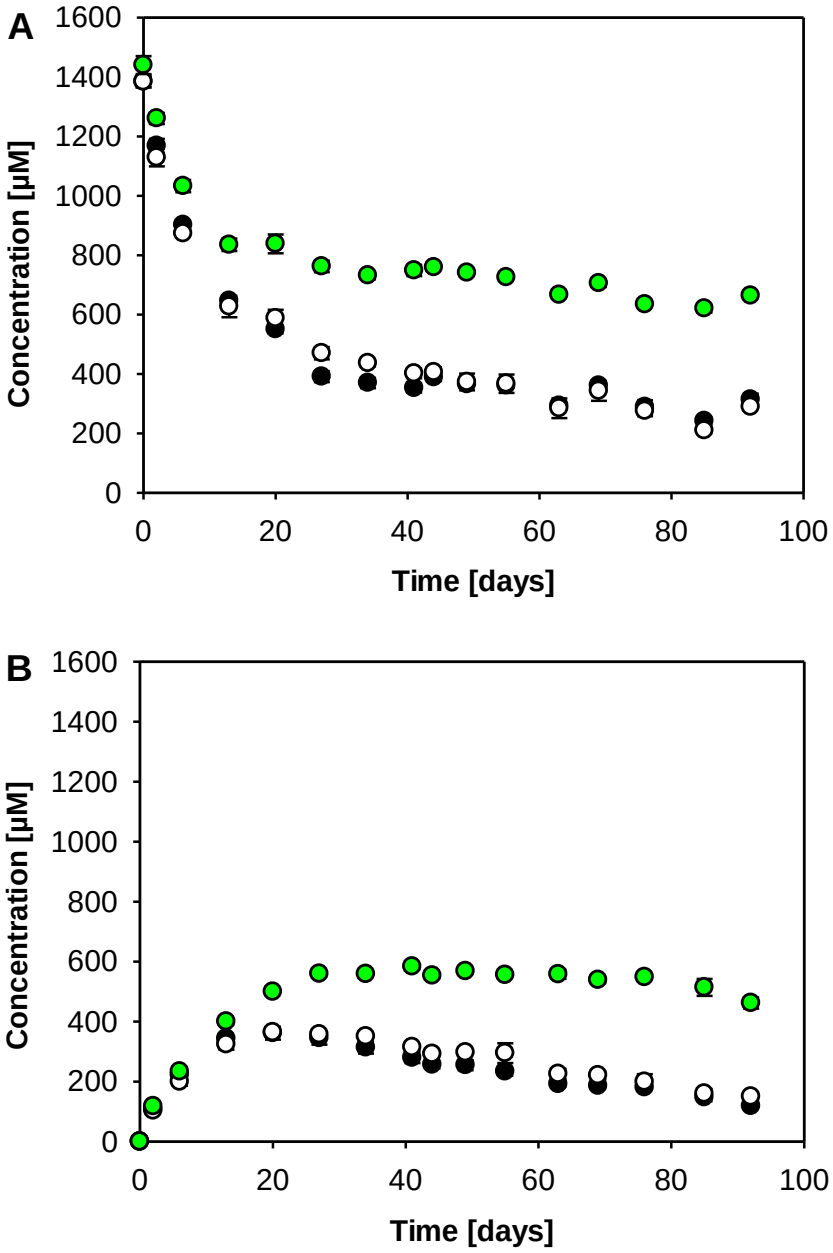

Figure 5-1 Changes in concentrations of total phenols in the anode chamber (A) and cathode chamber (B) of the CC-MFC (black), OC-MFC (white), S-MFC (green). Average data from replicates shown with error bars representing standard deviation.

Two metabolites of phenols, 4-hydroxybenzoic acid (4HB acid) and 4-hydroxy-3-methylbenzoic acid (4H3MB acid), referred to as metabolites hereafter, were identified by mass spectrometry (Appendix H) and a comparison of their elution times on HPLC (Appendix I). Both metabolites were detected at low concentration in the groundwater at the start of the experiment (21 µM ± 7 µM for 4HB acid and 21 µM ± 1 µM for 4H3MB acid). As biodegradation of phenols proceeded, the concentration of metabolites in the

anode chamber of the CC- and OC-MFC increased to the maximum value 108 μM ± 6 μM and 104 μM ± 4 μM for 4HB acid and 4H3MB acid, respectively, after ~30 days (Figure 5-2AB and CD, respectively). There was a significant difference ($P < 0.05$) in concentration of 4HB acid between the CC- and OC-MFC at day 27, and 4H3MB acid at day 27 and 34. After reaching the peak value, the concentration of metabolites decreased, indicating that the rate of the following metabolic reactions had increased and/or the rate of conversion of phenols to hydroxybenzoic acids had decreased. No significant change in metabolite concentration was observed in the S-MFC.

The metabolites also diffused from the anode chamber to the cathode chamber via the membrane. There was a significant difference in the diffusion rate of metabolites through the membrane between the CC-MFC and OC-MFC, which could have been caused by their electromigration to the anode or faster biodegradation in the CC-MFC. As shown in the text below, electromigration is likely to have affected the diffusion of metabolites within the chambers and therefore through the membrane.

The MFC systems were not stirred after day 27. Diffusion was therefore the main mechanism for mass transfer of chemicals within the anode and cathode chambers in all MFCs. The metabolites in the anode chamber were present in ionic form at pH 8 and therefore susceptible not only to diffusion but also to electromigration induced by the electrical current in the CC-MFC. The electromigration flux, J_E (Acar and Alshawabkeh, 1993), and diffusion flux, J_D (Kim et al., 2007), are given by the following equations (Equation 9 and 10), respectively:

$$J_E = D\frac{z \cdot F \cdot c}{R \cdot T}\frac{\Delta E}{\Delta L} \quad (9)$$

$$J_D = -D\frac{\Delta c}{\Delta L} \quad (10)$$

where D is the solute diffusion coefficient, z is the charge of the ion, F is the Faraday constant (96,485 C/mol), R is the universal gas constant (8.314 J/mol·K), c is the solute molar concentration, L is the distance, T is the temperature in Kelvin and ΔE is the voltage.

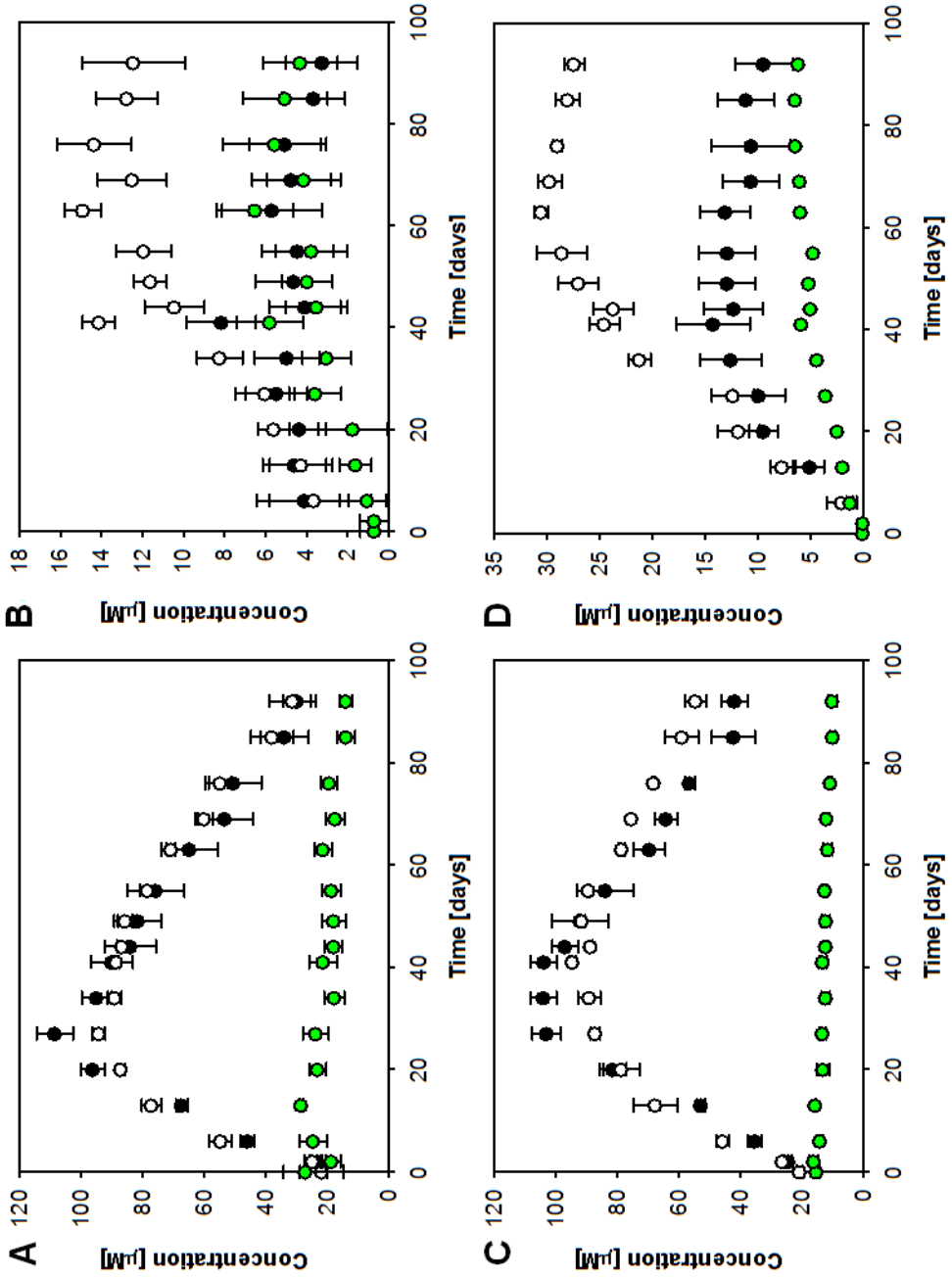

Figure 5-2 Changes in concentrations 4-hydroxybenzoinc acid (A, B), 4-hydroxy-3-methylbenzoinc acid (C, D) in the anode chamber (left) and cathode chamber (right) of CC-MFC (black), OC-MFC (white), S-MFC (green). Average data from replicates shown with error bars representing standard deviation.

The mass transfer of hydroxybenzoic acids between the electrode and membrane over distance ΔL at the overall MFC voltage of 60 mV is considered. It is assumed that the concentration difference Δc in Equation (10) is small compared with the term $(zFc\Delta E)/(RT)$ in Equation (9) at 25 °C for an anion with charge –1 and voltage difference of ~30 mV between the electrode and membrane (Appendix J). In this case, electromigration to the electrode is more significant mass transfer mechanism than diffusion from the electrode. The hydroxybenzoic acids will therefore be attracted to the anode in the CC-MFC, limiting their transfer to and across the membrane. This explains their lower concentration in the cathode chamber in the CC-MFC compared with the OC-MFC. With respect to field application of BES technology, negatively charged metabolites or contaminants could be drawn towards the anode, keeping the biodegrading microorganisms, contaminants, organic metabolites and electron acceptors in close proximity.

Acetate also diffused through the membrane, along the concentration gradient, and was biodegraded in the CC-MFC and OC-MFC (Figure 5-3AB). There was a significant difference between the rate of acetate biodegradation in the CC-MFC and OC-MFC; starting at 1905 μM ± 53 μM at day 0, acetate decreased to 536 μM ± 8 μM, 234 μM ± 30 μM and 256 μM ± 31 μM in the OC-MFC at day 20, 27 and 34, respectively, but was not detected in the CC-MFC. During the next 72 days, a smaller amount of acetate was detected in the CC-MFC (0–6 μM) than in the OC-MFC (0–200 μM).

Acetate was biodegraded faster and eventually depleted in the presence of the electrode (Figure 5-3A). As the acetate concentration decreased in the CC-MFC, the metabolite concentrations increased faster in the CC-MFCs than in the OC-MFC (Figure 5-2AC). Metabolite accumulation was higher in the CC-MFC compared with the OC-MFC after acetate depletion at day 27 and 34. At these time points, the concentration of phenols was significantly lower in the CC-MFC than in the OC-MFC (Figure 5-1A), showing that biodegradation of phenols was enhanced. It is unclear why this trend was not sustained after day 34.

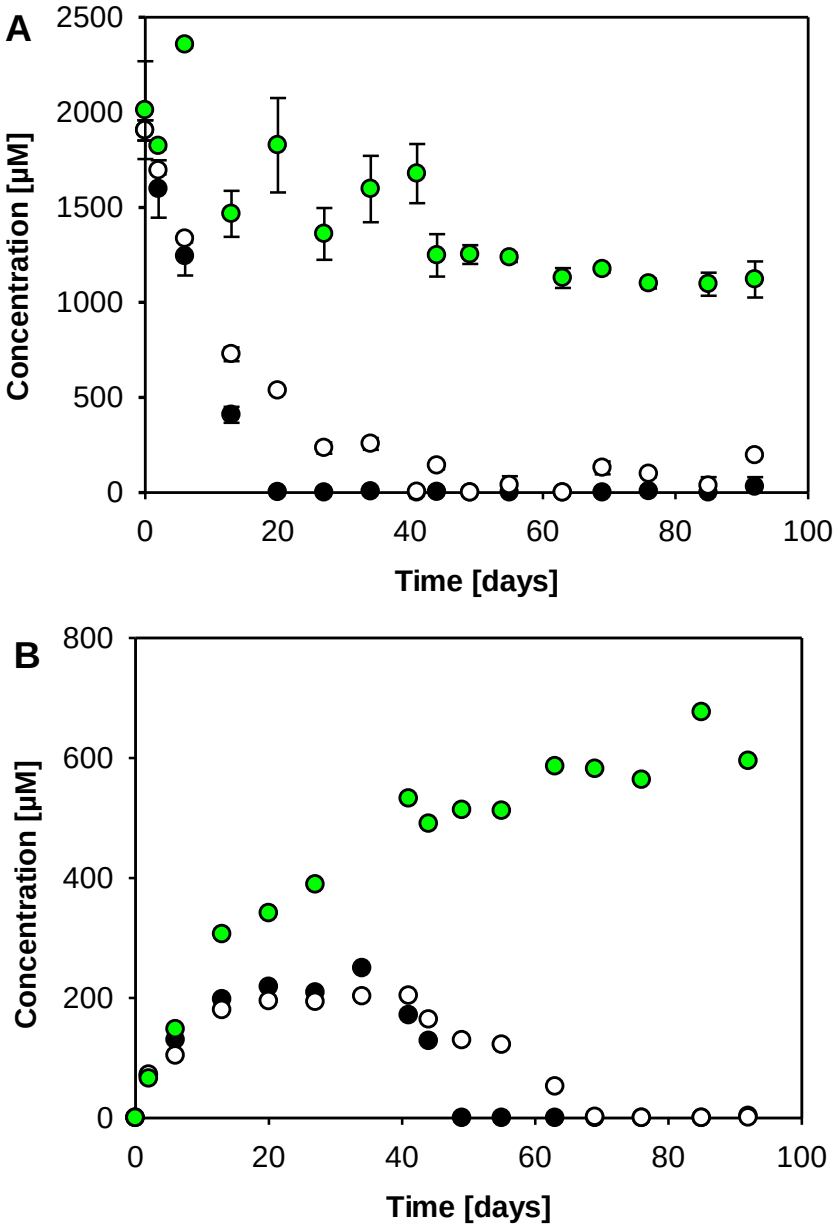

Figure 5-3 Changes in concentrations of acetate in the anode chamber (A) and the cathode chamber (B) of CC-MFC (black), OC-MFC (white), S-MFC (green). Average data from replicates shown with error bars representing standard deviation.

5.2.2 Electricity production

Electricity production in the CC-MFC started 5 days after inoculation with contaminated groundwater. The voltage then increased exponentially, reaching a maximum of 90 mV with a resistance of 1 kΩ (Figure 5-4A), which was maintained for 11 days. Electricity production then fell rapidly to 11 mV, but could be quickly restored to 60-70 mV by the addition of filter-sterilised contaminated groundwater. The S-MFC did not produce any current; the voltage stayed at –0.17 mV ± 0.30 mV (1 kΩ).

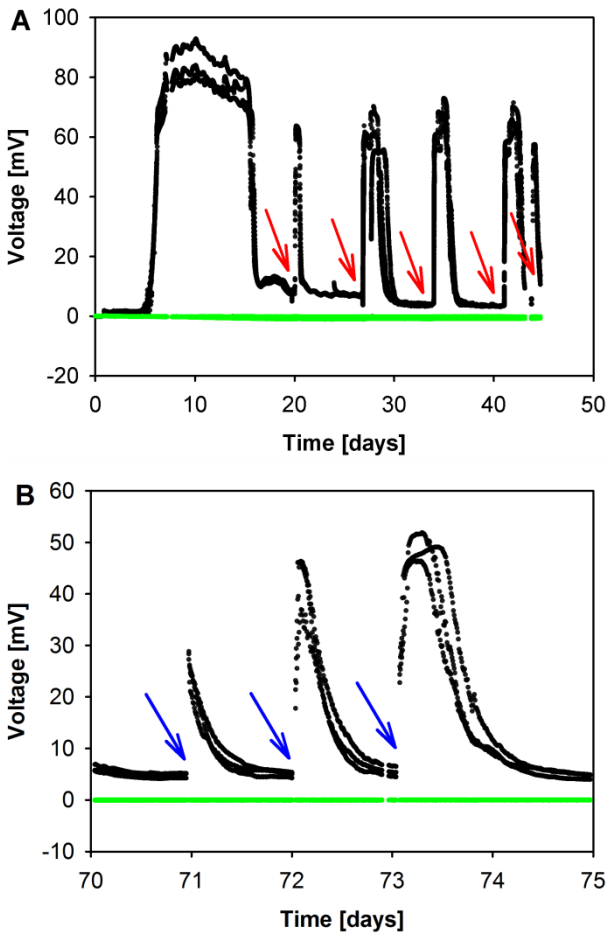

Figure 5-4 Electricity production in the CC-MFCs (black), S-MFCs (green) at the start of the experiment (A) and day 70 to 75 (B). Groundwater addition indicated with red arrows, acetate addition (2.0, 3.4 and 7.7 µmol) with blue arrows. Showing all replicate data.

Polarization curves were measured at the point of the highest voltage; the highest power output of the CC-MFC was ~1.8 mW/m^2 of projected electrode surface area (Figure 5-5), the internal resistance of the systems being 3.9 kΩ, while the OC-MFC produced only ~0.8 mW/m^2. The open circuit voltage in the CC- and OC-MFC reached approximately 550 mV, the potential of the CC-MFC cathode at open circuit being 290 ± 28 mV vs. SHE. Based on the measured cathode potential and cathode material (carbon cloth), the increased concentration of nitrate in the cathode chamber of the CC-MFC (Section 5.2.3) and pH 9, it is likely that an anion of hydrogen peroxide was produced on the cathode as a product of oxygen reduction (Song and Zhang, 2008).

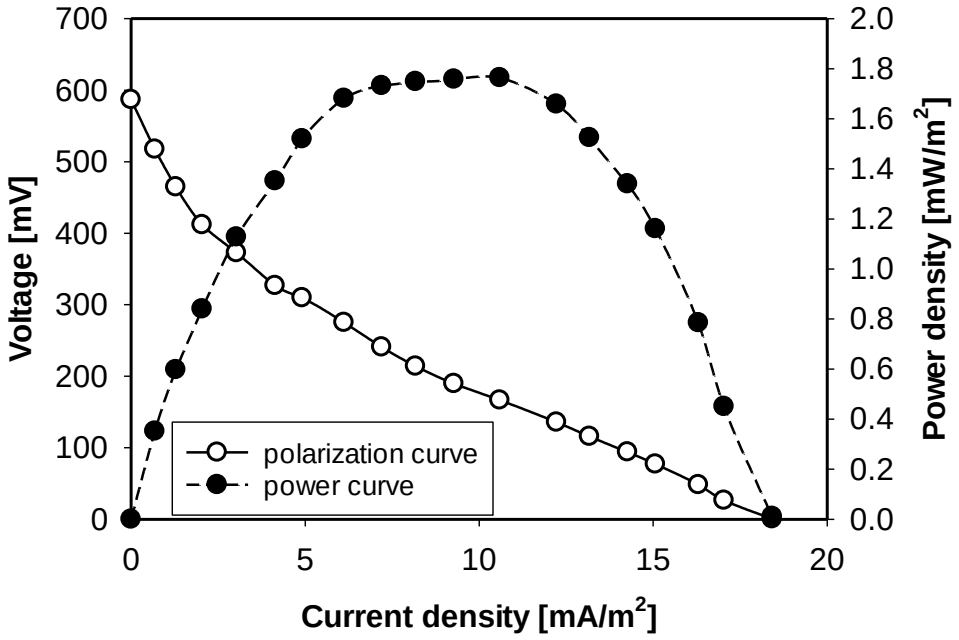

Figure 5-5 Polarization and power curve for CC-MFC. Showing data from one representative replicate.

To explore which carbon source in the groundwater served as an electron donor for electricity production and the Coulombic efficiency of MFCs, 4 ml of selected chemical compounds dissolved in UHQ water at the concentration found in the groundwater were added to all MFCs. Electricity generation in the CC-MFC did not increase when UHQ water (control), phenol, cresols or xylenols were added (data not shown). The addition of acetate to the MFCs induced a rapid voltage increase, in proportion to the acetate added, with a Coulombic efficiency of 54% (Figure 5-4B). This demonstrated that acetate, rather than the contaminants, served as an electron donor for electricity generation.

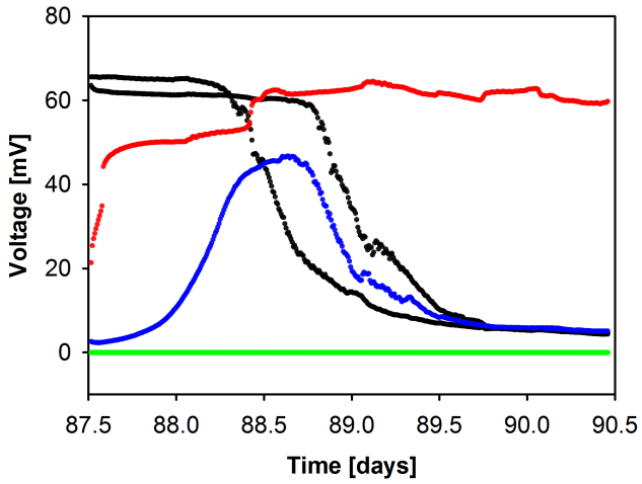

Figure 5-6 Electricity production in CC-MFCs (black), S-MFCs (green), ME+S-MFC (red) and SE+CC-MFC (blue) at days 87 to 91. Showing all replicate data.

As electro-active bacteria typically build a biofilm on the electrode (Franks et al., 2010; Logan, 2008), it was hypothesised that the current generation in the CC-MFC reflected the development of a biofilm on the carbon electrode surface. To test this, a mature electrode (ME) from a working CC-MFC at its highest point of electricity production was removed and put into a sterile MFC (ME+S-MFC), and a sterile electrode (SE) placed in the mature CC-MFC (SE+CC-MFC). Electricity production in ME+S-MFC started to increase immediately (Figure 5-6), indicating that current generation required a biofilm community on the electrode. In contrast, current generation was delayed in the SE+CC-MFC, most likely due to the time required for a new biofilm to form on the electrode. This is supported by SEM images of the electrodes at the end of the experiment (Figure 5-7), 5 days after the electrode exchange. The biofilm on a CC-MFC electrode was mature with a complex 3D structure, whereas only single cells had attached to the electrode fibres in a SE+CC-MFC. The results show that electrogenic biofilm on the electrode produced electricity using acetate derived from fermentation of phenols.

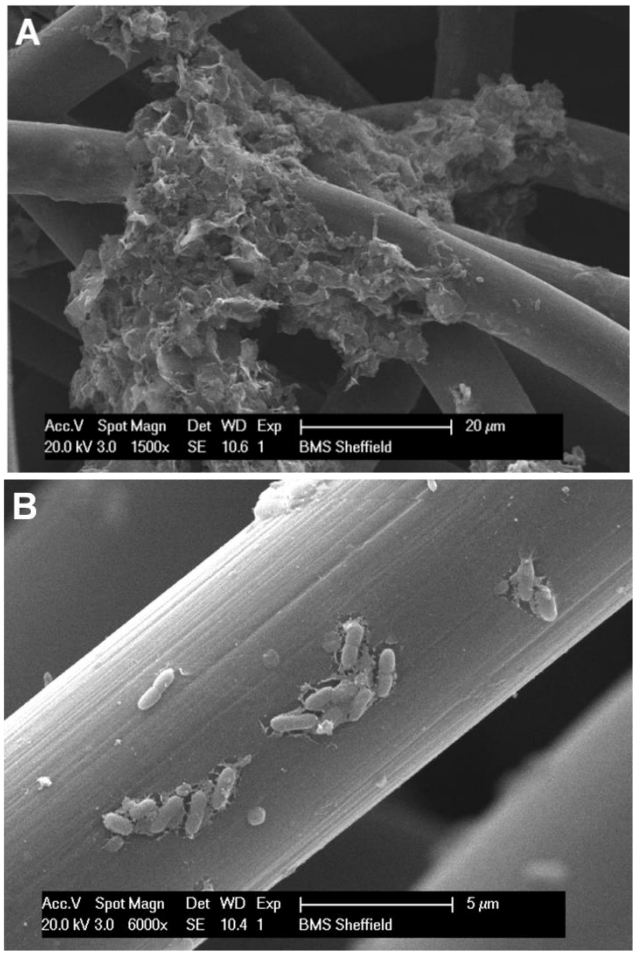

Figure 5-7 SEM images of biofilm on the carbon cloth electrode in (A) CC-MFC and (B) SE+CC-MFC.

5.2.3 Electron acceptors

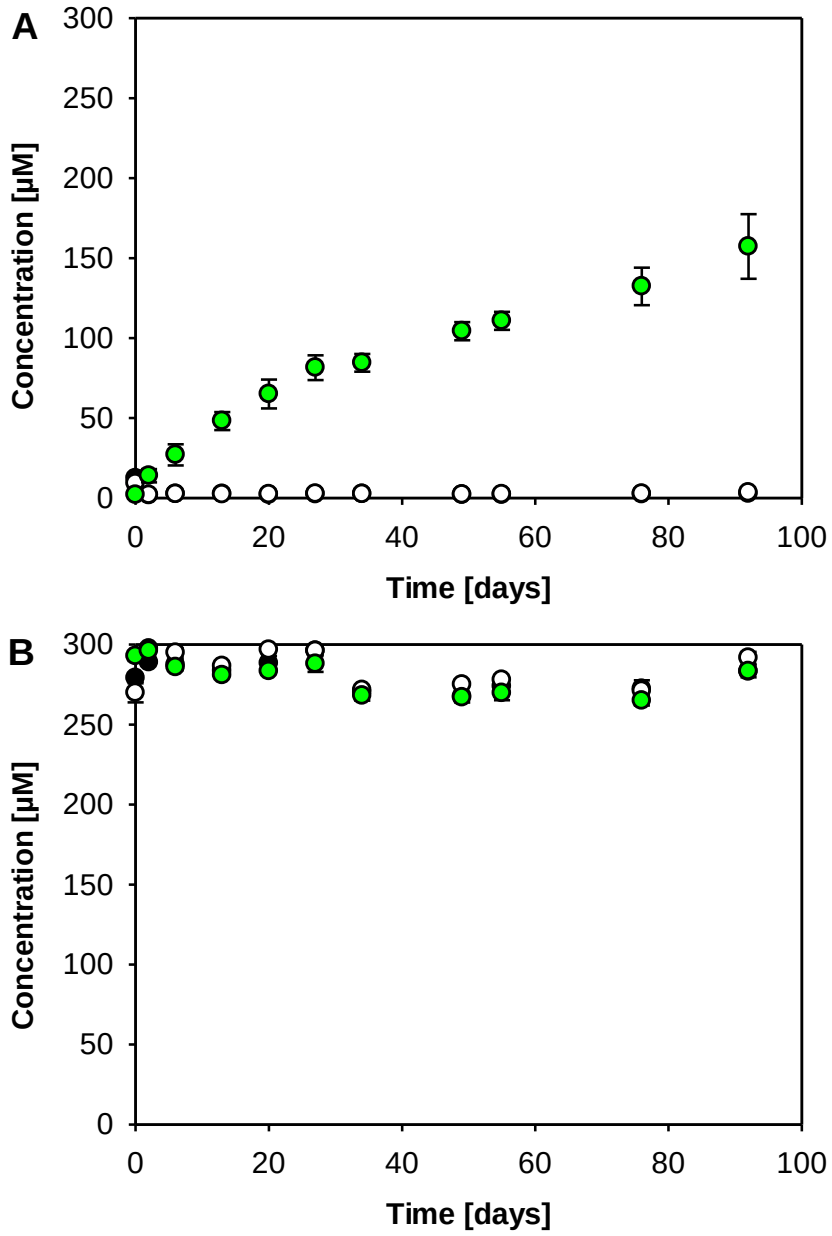

Figure 5-8 Changes in concentrations of oxygen in the anode chamber (A) and the cathode chamber (B) of CC-MFC (black), OC-MFC (white), S-MFC (green). Average data from replicates shown with error bars representing standard deviation.

Various electron acceptors were available in the anode chamber. Oxygen diffused via the membrane from the cathode chamber to the anode chamber, as evident from the S-MFC data in Figure 5-8. Oxygen was not detected in the anode chamber of the CC- or OC-MFC, indicating that it was rapidly consumed by the microbes. The rate of diffusion to the S-MFC containing sterile contaminated groundwater was slower than that reported for pure water (Chapter 4, Section 4.2) (Kim et al., 2007). The chemicals in the groundwater would decrease the oxygen solubility in this water (Stumm and Morgan, 2013), thereby

decreasing the apparent oxygen diffusion rate. For the mass balance (Section 5.2.4), it was assumed that any oxygen entering the anode chamber through the membrane was depleted immediately. Hence, the diffusion coefficient for pure water was used (Kim et al., 2007). The diffusion followed a linear trend as the oxygen concentration in both chambers remained the same, i.e. no oxygen detected in the anode chamber and saturated oxygen concentration in the cathode chamber. The average rate of oxygen transfer into the anode chamber was therefore 4.9 µmol/day.

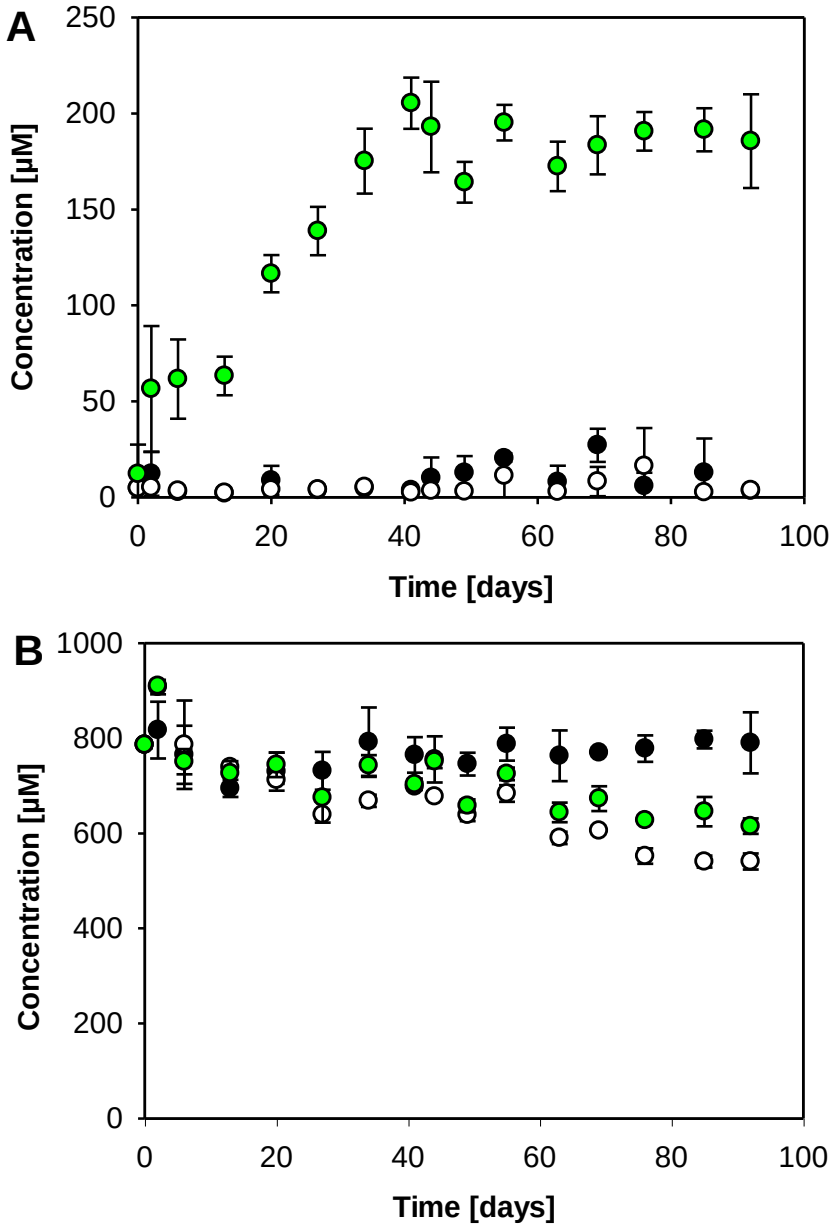

Figure 5-9 Changes in concentrations of nitrate in the anode chamber (A) and the cathode chamber (B) of CC-MFC (black), OC-MFC (white), S-MFC (green).

As with oxygen, nitrate diffused into the anode chamber from the cathode chamber (S-MFC data), where it was used by bacteria (CC- and OC-MFC data) (Figure 5-9). The

calculated nitrate diffusion coefficient was $2.15 \cdot 10^{-7} cm^2/s$, with an average diffusion of 1.2 µmol/day. The higher concentration of nitrate in the cathode chamber of the CC-MFC was likely due to the oxidation of ammonium or nitrous oxides by hydrogen peroxide which developed in the cathode (Section 5.2.2).

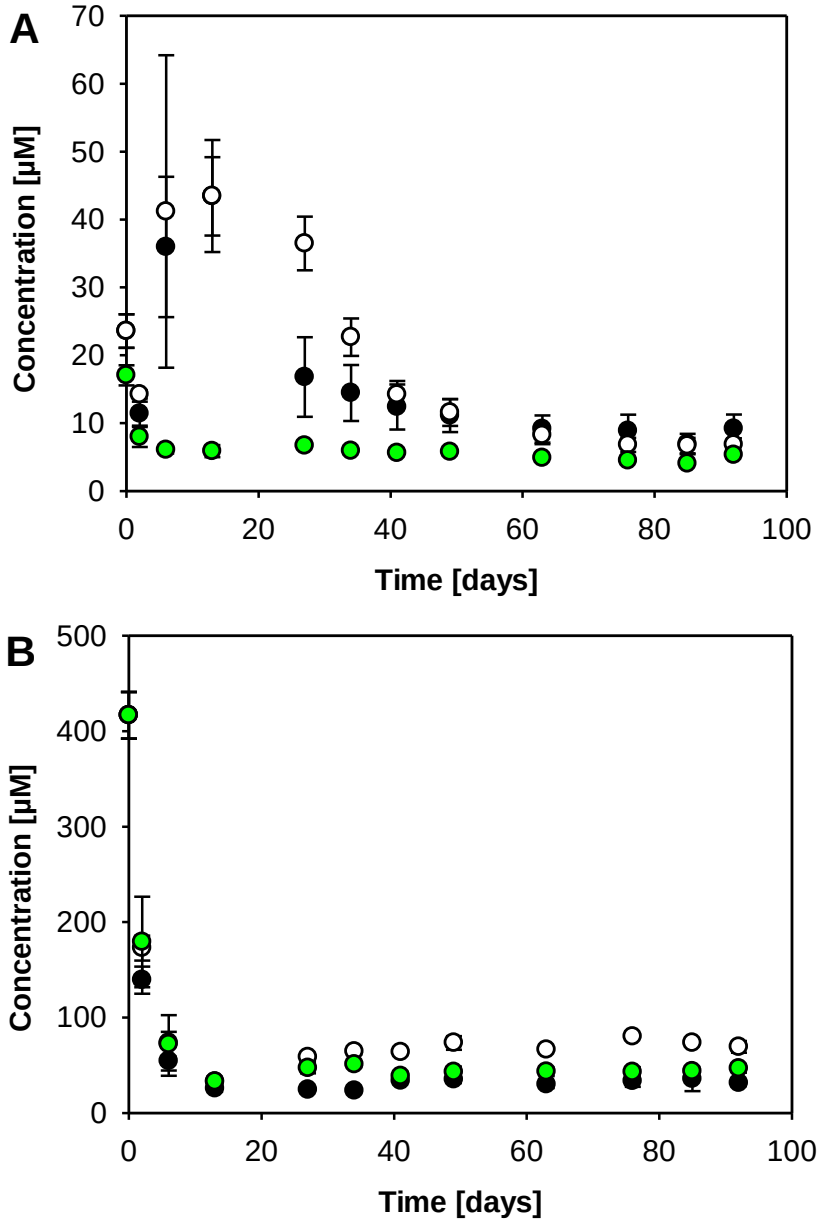

Figure 5-10 Changes in concentrations of soluble iron in the anode (A) and the cathode chamber (B) of CC-MFC (black), OC-MFC (white), S-MFC (green). Average data from replicates shown with error bars representing standard deviation.

Iron(III) reduction occurred between days 2 and 13, causing a rapid increase in the concentration of soluble iron, from 11 µM ± 2 µM and 14 µM ± 1 µM to 43 µM ± 6 µM and 43 µM ± 8 µM in the CC-MFC and OC-MFC, respectively (Figure 5-10). Iron reduction and electricity production started simultaneously (ca. day 5), showing that the anode was an electron acceptor as thermodynamically favourable as iron(III). It is therefore

possible that the electro-active bacteria attached to the electrode belonged iron reducers. *Geobacter* sp., a dominant iron-reducing species in the groundwater studied, could have been the primary exoelectrogenic species using acetate as an electron donor, which is typical for this bacterium (Chae et al., 2009; Logan, 2008). The concentration of soluble iron in the cathode chamber decreased rapidly, probably due to oxidation to iron(III) oxides by oxygen or hydrogen peroxide.

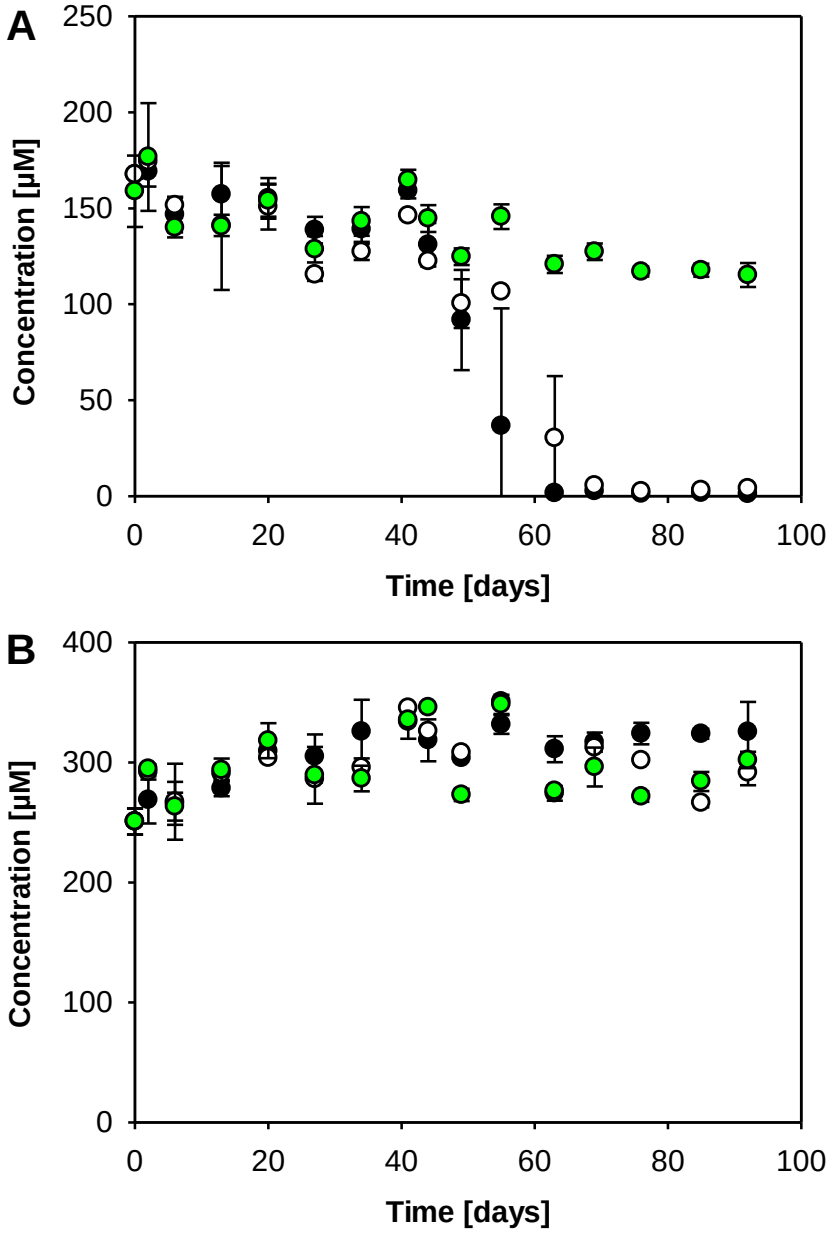

Figure 5-11 Changes in concentrations of sulphate in the anode (A) anode the cathode chamber (B) of CC-MFC (black), OC-MFC (white), S-MFC (green). Average data from replicates shown with error bars representing standard deviation.

Sulphate reduction occurred between days 41 and 63 in both live MFCs , decreasing the sulphate concentration from 9.4 µM ± 1.7 µM and 7.9 µM ± 0.4 µM in the CC-MFC and

OC-MFC, respectively, to 0.8 μM ± 0.2 μM (Figure 5-11). This was accompanied by the formation of a black precipitate (iron sulphide) in the anode chambers of the CC- and OC-MFC (Morris et al., 2009). The respiration processes were sequential and followed theoretical predictions (Stumm and Morgan, 2013).

5.2.4 Conceptual model

A conceptual model of the processes occurring within the CC-MFC can be developed from the observed results (Figure 5-12).

Phenols in the anode chamber are first transformed anaerobically by oxidation or *para*-carboxylation, forming 4HB acid and 4H3MB acid. Both acids can originate from anaerobic biodegradation of phenols. 4HB acid can be produced during *para*-carboxylation of phenol (Boll and Fuchs, 2005) or anaerobic oxidation of *p*-cresol (Bossert and Young, 1986), whereas 4H3MB acid is produced by para-carboxylation of *o*-cresol (Bisaillon et al., 1991) and presumably also from anaerobic oxidation of 2,4-xylenol. The hydroxybenzoic acids can be then biodegraded to acetyl-CoA (Boll and Fuchs, 2005) and then acetate, to complete the fermentation of phenols (Madigan et al., 2011). As previously mentioned, fermentation is an important process for biodegradation of phenols in the contaminant plume (Watson et al., 2005). The decreased concentrations of phenols and increased concentrations of hydroxybenzoic acids are evidence of anaerobic biodegradation of phenols in the MFCs. However, it is unclear whether the biodegradation proceeded to acetyl-CoA and further. The location of fermenting bacteria is also unknown; they could have been present in planktonic or electrode biofilm form.

Acetyl-CoA is a central compound of metabolism. It can be transformed to acetate and also used to build biomass or enter the TCA cycle, followed by the respiratory chain (Madigan et al., 2011). Respiration was a dominant process in the MFCs and resulted in fast removal of acetate after its transfer to acetyl-CoA. Acetate is a more metabolically favourable carbon source for bacteria than phenols (Madigan et al., 2011) and was therefore biodegraded more rapidly in the MFCs.

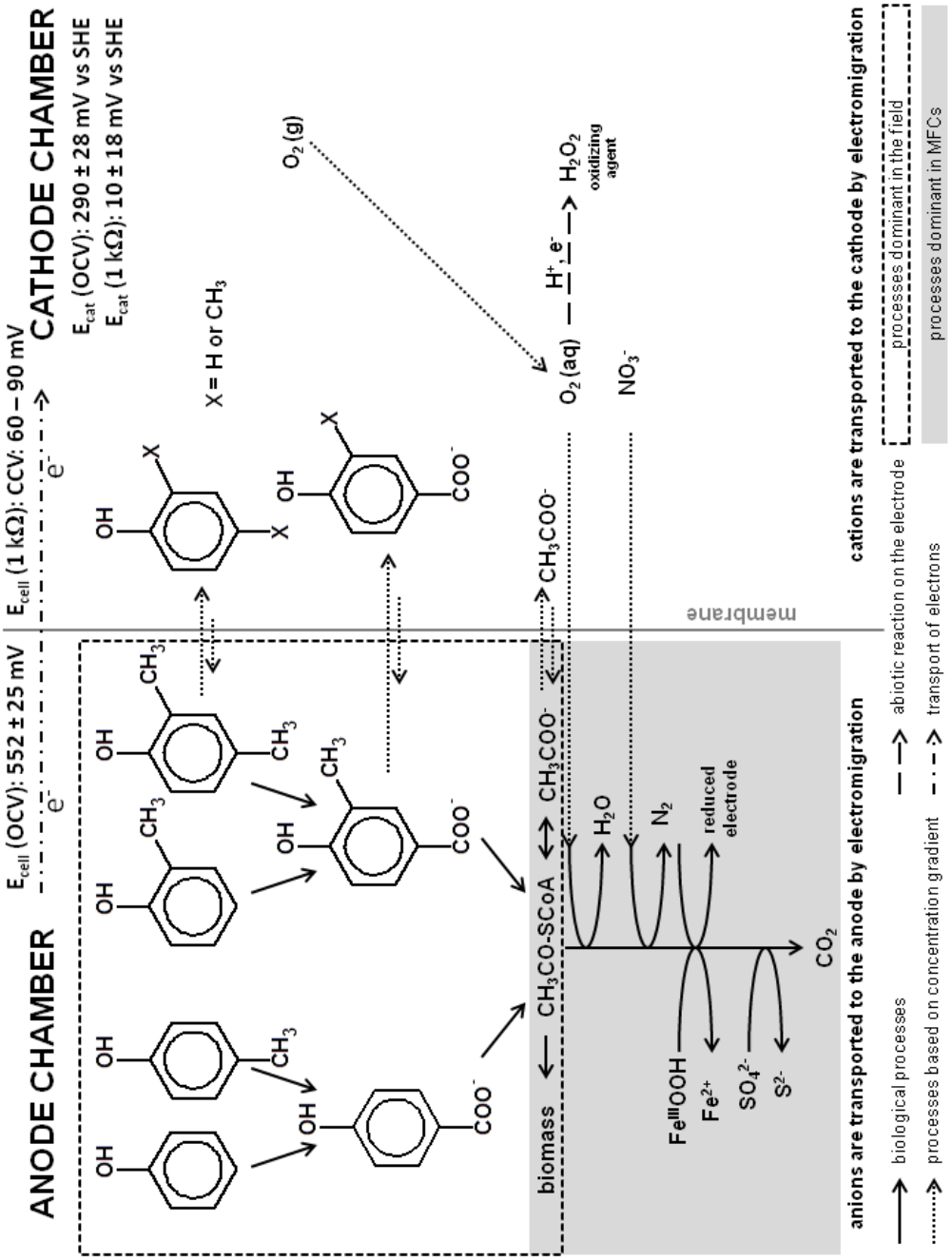

Figure 5-12 Conceptual model of processes occurring in CC-MFCs containing groundwater contaminated by phenolics compounds.

Based on this conceptual model, the mass balance of acetate vs. electron acceptors was calculated and compared with the total amount of acetate available. The measured amount of biodegraded acetate was corrected for diffusion through the membrane, and sampling and additions of groundwater/acetate to the MFCs. If there was more available acetate than electron acceptors, it was assumed that it was used to build biomass. The calculation was done in two parts: the first 20 days of the experiment before acetate depletion and subsequent 72 days when the MFCs were operated under acetate limitation.

Table 5-1 Stoichiometry of phenol fermentation to acetate and acetate respiration using different electron acceptors.

Chemical reaction with acetate	Stoichiometry
Phenol fermentation to acetate	$C_6H_6O + 5\ H_2O \rightarrow 3\ CH_3COOH + 2\ H_2$
Aerobic degradation	$CH_3COOH + 2\ O_2 \rightarrow 2\ CO_2 + 2\ H_2O$
Denitrification	$5\ CH_3COOH + 8\ NO_3^- + 8\ H^+ \rightarrow 4\ N_2 + 10\ CO_2 + 14\ H_2O$
Iron reduction	$CH_3COOH + 8\ FeOOH + 16\ H^+ \rightarrow 8\ Fe^{2+} + 2\ CO_2 + 14\ H_2O$
Electrode reduction	$CH_3COOH + 2\ H_2O \rightarrow 2\ CO_2 + 8\ H^+ + 8\ e^-$
Sulphate reduction	$CH_3COOH + SO_4^{2-} \rightarrow S^{2-} + 2\ CO_2 + 2\ H_2O$

Several electron acceptors were present in the MFCs to support respiration. The amount of acetate biodegraded by oxygen, nitrate, iron and sulphate respiration was the same for the CC- and OC-MFC, as calculated from previously presented data using the stoichiometry in Table 5-1. Data from electricity production were numerically integrated according to Equation 11 to obtain the amount of charge Q and subsequently the amount of electrons released from acetate:

$$Q = \int_{t_0}^{t_i} I\ dt = \int_{t_0}^{t_i} \frac{E}{R}\ dt \qquad (11)$$

where I is the electric current generated between time t_0 and t_i, E is the measured voltage and R is the external resistance (Logan, 2008). Eight moles of electrons are produced from one mole of acetate. The CC-MFC biodegraded 1733 μM ± 30 μM, which is 520 μM ± 30 μM more acetate biodegraded compared with the OC-MFC (1213 μM ± 30 μM) during the first 20 days of the experiment (Table 5-2). This corresponds with the acetate used for electricity production (455 μM ± 30 μM). Hence, the presence of the electrode as an electron acceptor enhanced acetate removal.

The results explain why a peak in electricity production occurred when the removal of phenol reached approximately 90% in a similar study (Luo et al., 2009). Supposedly, phenol was fermented to less complex substrates (e.g. acetate), which were then utilised by exoelectrogens. Similarly, an experiment in Chapter 4 (Section 4.3.2) was set up using the same groundwater as in this chapter as an inoculum with minimal media and phenol as a sole carbon source. No significant increase of closed circuit voltage was observed. Based on the results presented here, it is clear that there was no acetate, electron donor, available for the electro-active bacteria. It is likely that electricity production would start up later on in the experiment as acetate would be produced from phenol fermentation.

Table 5-2 Mass balance of acetate in the MFCs. The total decrease in acetate results from consumption by different electron acceptors (MFC electrode and O_2, NO_3^-, Fe(III), SO_4^{2-}) and biomass synthesis. Difference in acetate decrease between the CC- and OC-MFC due to electricity production. The total amount of acetate biodegraded in the CC-MFC is lower than the amount of electron acceptors available.

	First 20 days			Next 72 days		
Acetate (µM ± 30 µM)	CC-MFC	OC-MFC	Difference (CC-MFC – OC-MFC)	CC-MFC	OC-MFC	difference (CC-MFC – OC-MFC)
Total decrease measured	1733	1213	520	1469	1748	-279
• Electrode	455	0	455	792	0	792
• O_2, NO_3^-, Fe(III), SO_4^{2-}	326	326	0	1306	1306	0
• Biomass	953	888	65	0	442	-442
Theoretically produced from phenols	1516	1402	114	1713	1774	-61

Removing a fermentation product such as acetate reduces potential feedback inhibition effects. This can theoretically accelerate fermentation and increase the biodegradation rate of phenols (Kiely et al., 2011). The concentration of total phenols in the CC-MFC was slightly lower than in the OC-MFC at two time points (day 27 and 34) after acetate depletion (Figure 5-1 and Figure 5-3). However, it is unclear why this trend was not maintained for the duration of the experiment.

The mass of electron acceptors available in the CC-MFC is significantly higher than in the OC-MFC, shown especially in the results for the latter 72 days of the experiment. The equivalent mass of acetate biodegraded in the CC-MFC should theoretically be higher (1306 µM + 792 µM) than the measured value 1468 µM ± 30 µM (Table 5-2). This indicates that more electron acceptors were available than needed for complete acetate removal. These electron acceptors could be used for the biodegradation of phenols. The

CC-MFC could have therefore biodegraded 180 μM ± 10 μM more phenols than the OC-MFC. This difference between the two MFC set-ups was not observed (Figure 5-1); the maximum concentration difference was 80 μM ± 20 μM at day 27. There is potentially a high amount of acetate produced by fermentation of phenols in the MFCs (approximately 1500 μM during the first 20 days and 1700 μM afterwards). As previously stated, it is unclear whether the fermentation of phenols to acetate was complete. Hence, understanding the regulation of fermentation pathways is essential for the future application of BESs for enhanced *in situ* bioremediation of phenols.

5.3 Conclusion

The results presented here demonstrate that it is crucial to identify compound(s) utilised by exoelectrogens as electron donor(s) to implement bioelectrochemically-enhanced remediation of organic contaminants. Two theoretical scenarios are possible. Firstly, the contaminants can serve directly as electron donors for extracellular electron transfer to the electrode. The presence of the electrode as an electron acceptor will therefore directly enhance their biodegradation rate. In this case, exoelectrogens should be able to transfer electrons to the electrode *and* degrade contaminants. In the second scenario, electro-active bacteria cannot directly degrade contaminants but utilise their metabolites. This study suggests that the second scenario is more likely to occur. Hence, knowledge of biodegradation pathways of the parent compound to the electron donating metabolite and their regulation, as well as the cell-cell interactions and carbon flow in the microbial community, is critical for successful application of remediation BESs at the field scale.

Chapter 6

Microbial community structure in an MFC degrading phenolic compounds and their metabolites

Laboratory microcosm studies, such as the one performed in Chapter 5, use indigenous microbial communities under conditions as similar to the field as possible. They provide an initial understanding of different selection pressures on microbial community development and function under specific conditions, in this case MFC-enhanced bioremediation. However, the microbial processes and communities studied in confined microcosm experiments can differ significantly from the ones present in the environment (Hammes et al., 2010; Konopka, 2009).

Microcosm experiments using media, e.g. soil or groundwater, samples directly from the contaminated field are preferable to model laboratory studies. The latter may lack some of the features present in the environment as they use artificial media and/or inoculate the experiments with communities originating from sources other than the contaminated field of interest (Hammes et al., 2010; Konopka, 2009).

Research on bioelectrochemically-enhanced remediation is still in its infancy, with most studies being constructed as model laboratory studies (Section 2.3, Table 2-2D) with inocula from waste water treatment plants or using single strains of bacteria, and mineral media amended with vitamins and single carbon sources. To date, only one study has used contaminated groundwater as an MFC inoculum but this still amended the groundwater with phosphate buffer and surfactants (Morris et al., 2009).

The main interests of microbial ecology are to characterise microbial communities in terms of structure, i.e. identifying the species present and their abundance, and where possible link to function with respect to biochemical processes (Fuhrman, 2009; Osborn and Smith, 2005).

Basic variables which describe any ecological community, not only microbial, are the species richness (the number of species present in a certain environment, also known as alpha diversity) (Whittaker, 1972) and species evenness reflecting the distribution of the species (Morin, 1999). Species evenness can be calculated from Equation 12

$$J = \frac{\sum_{i=1}^{S}[-P_i ln(P_i)]}{\ln(S)} \quad (12)$$

where J is the species evenness, S is the species richness for the samples and P_i is the proportion of the species in the sample. The results are within the range of 0–1, where 0 corresponds with no evenness at all and 1 with complete evenness (Osborn and Smith, 2005; Morin, 1999). The species diversity of a microbial community can be typically described by long-tailed (e.g. lognormal, power law or log Laplace) distribution of species, dominated by just a few species with a long tail of possibly tens of thousands species (Fuhrman, 2009; Bent et al., 2007).

The aim of any microbial community analysis is to capture the diversity as true to reality as possible. Hence, appropriate methods for community characterisation should be chosen and their efficiency in capturing the true nature of the community (coverage) evaluated (Osborn and Smith, 2005). DNA-based methods are replacing cultivation techniques to analyse microbial communities, as only a small percentage of bacteria can be cultured (Wooley et al., 2010; Fuhrman, 2009; Osborn and Smith, 2005). 16S rRNA genes are used as a molecular marker in molecular microbial ecology. However, it should be noted that a single bacterium can possess multiple heterogeneous copies of the 16S rRNA gene within its genome, or two organisms with identical 16S rRNA gene sequences can differ significantly in terms of their protein-encoding genes and hence function (Case et al., 2007).

The polymerase chain reaction (PCR) is used to amplify 16S rRNA genes from DNA isolated from the environment; the primers chosen, the reaction conditions and various biases introduced during the PCR affect the community coverage (Osborn and Smith, 2005). Further steps in the analysis of microbial community structure can involve fingerprinting and/or sequencing techniques. Fingerprinting is appropriate for comparison of temporal changes within the community and captures only the dominant species (Case et al., 2007; Osborn and Smith, 2005).

Percentage similarity threshold (97%) of 16S rRNA gene sequences is typically used to cluster bacteria and archaea in operational taxonomic units (OTUs), a species distinction in microbiology (Kunin et al., 2010; Wooley et al., 2010). The coverage of the community by sequencing is influenced by the depth of sequencing, i.e. how many sequences are read per each sample. The coverage can be evaluated by plotting either a rarefaction or accumulation curve with the number of sequences on the *x*-axis and number of number of OTUs identified on the *y*-axis, or rank-abundance curve with OTU type on *x*-axis and their abundance on *y*-axis (Osborn and Smith, 2005; Gotelli and Colwell, 2001; Hughes et al., 2001).

In this chapter, the microbial community established in an MFC containing phenols-contaminated groundwater without any amendments (Chapter 5) is analysed in the terms of structure and function where possible. The following hypotheses are tested:

- **The microbial community of the electrode biofilm in the CC-MFC is significantly different from the one in the OC-MFC.** The biofilm community in the CC-MFC used the electrode as an additional electron acceptor for acetate degradation, whereas the OC-MFC biofilm only had access to dissolved electron acceptors (Chapter 5). The electrode biofilm community of the CC-MFC was shown to be involved in enhanced acetate degradation in comparison with the OC-MFC. This was due to the extracellular electron transfer from bacteria to the electrode. In case the electro-active species are different from the ones utilising soluble electron acceptors, significant differences between the biofilm community of the CC- and OC-MFCs might be observed. This would indicate that the CC-MFC system put selection pressure on bacteria and significantly altered the community, enriching the electrode biofilm with electro-active species. It is expected that *Geobacter* spp. could be dominant members of the CC-MFC electrode biofilm as hypothesised earlier (Chapter 5).

- **The structure of the planktonic microbial community within the MFCs differs significantly from the electrode biofilm community.** Most microorganisms in the environment live in a biofilm form (Dreeszen, 2003) and the attached community can be significantly different from the planktonic one. This was previously shown in the aquifer at the site examined in this thesis (Rizoulis et al., 2013). Enhanced acetate biodegradation took place on the electrode which had a positive effect on biodegradation of phenols. Bacteria degrading phenols (e.g. *Pseudomonas* sp. previously found in the groundwater used) could be present in both the biofilm and planktonic form. The presence of phenol degraders exclusively on the electrode would indicate a close connection (syntrophy) between the metabolism of phenol and acetate degrading bacteria.

  Syntrophic interactions between the acetate and phenol degraders within the field-scale BESs are likely as discussed in Chapter 5. The successful field-scale application of biodemediation BESs would therefore require the knowledge of

the location of phenol degraders. In case phenol degraders were present in the electrode biofilm community, biodegradation of phenols and acetate would take place at the same place regardless the groundwater flow. However, phenol degraders in the planktonic phase could be moved along with the groundwater flow which could disrupt the interaction between the acetate and phenol degradation. Biodegradation of phenols would be likely to occur behind the acetate degrading zone along the groundwater flow. This would have to be taken into account when designing field-scale *in situ* BESs. It is therefore important to understand the structure and the role of biofilm and planktonic communities within the bioremediation BESs.

- **Microbial communities in the MFCs have undergone significant changes in structure when compared with the starting groundwater microbial community.** The microbes in the MFCs were exposed to selection pressures different from the ones in the groundwater. The original groundwater community is very diverse with ~600 OTUs identified when reading ~44,000 16S rRNA gene sequences (unpublished data). Presumably, only a few dominant species would be involved in the biochemical changes occurring in the MFCs. This should lead to significant changes in the community structure (Fuhrman, 2009; Rabaey and Verstraete, 2005). The MFC dominant species and their function within the system can be identified. Similarly, after the introduction of BES electrodes in the field, the groundwater community should undergo changes in its structure as the community would adapt to electricity generation under present conditions. Different BES set-ups could select different dominant species with different functions. Linking the BES conditions with the selection of different groundwater species would enable engineer the BES system for best bioremediation performance.

6.1 Materials and methods

6.1.1 Total cell counts

The total number of microorganisms in suspension was enumerated using the groundwater samples taken in the field, at the start and end of the experiment and fixed by formaldehyde at final concentration 3% (*v*/*v*). Samples were filtered through 0.2 μm polycarbonate black filter (Whatman®) and stained by SYTO® 9 (Life Technologies) according to the manufacturer's protocol. The stained cells were visualised with a Zeiss

Axioplan 2 fluorescence microscope (Carl Zeiss, Germany) using Zeiss filter cube 10 (FITC/GFP). The duplicate samples were diluted so the number of cells counted in a 2901.05 μm^2 area was between 50 and 150 (Figure 6-1), counting 5 fields for each duplicate. The cells were counted using the image processing software, ImageJ (http://imagej.nih.gov/ij/). Statistical comparison of total cell counts in groundwater and MFC samples was completed with one-way ANOVA ($\alpha = 0.05$) in SigmaPlot 13.0.

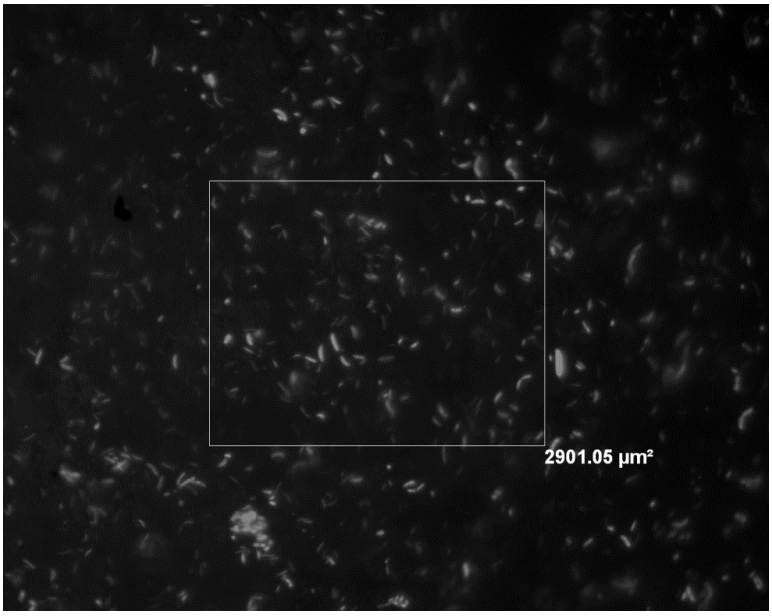

Figure 6-1 An example of an image used for determining the total cell count in the area of 2901.05 μm^2. The bacteria laying on the left and bottom boundary were counted whereas the one on the top and right boundary were not.

All carbon cloth anodes were removed from MFCs at the end of the experiment, drained using a sterile paper tissue, washed gently in filter-sterilised phosphate buffer saline (PBS) and drained again. They were cut into smaller pieces for further microbial analysis (Figure 6-2).

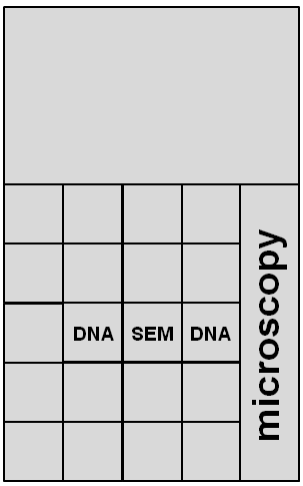

Figure 6-2 The electrodes (5 x 8 cm) were cut into smaller pieces for further analysis. DNA - DNA extraction, SEM - scanning electron microscopy, microscopy - epifluorescence and confocal microscopy.

6.1.2 Biofilm microscopy

Stripe-pieces (5 cm^2) of electrodes (Figure 6-2) were stored at 4°C prior to epifluorescence and confocal microscopy. Samples were stained with SYTO® 9 Green Fluorescent Nucleic Acid Stain (Molecular Probes®, 4μL of stain diluted into 2 mL of 9 g/L sodium chloride) by applying droplets of diluted stain on the electrode and incubating for 5 min. After incubation, the electrodes were gently washed with 9 g/L sodium chloride and viewed by epifluorescence or confocal microscopy.

Maximum projection images were acquired using a BX50 (Olympus Optical Co., Ltd.) microscope under 10x objective, using appropriate fluorescence filter. The images were taken from three places on the electrode (top, middle and bottom), and were processed and analysed in ImageJ. The percentage of the electrode surface area covered was measured as a representation of the level of biofilm development. Three maximum projection images were processed per sample. Statistical comparison of the percentage of the electrode surface area covered by biofilm was completed with one-way ANOVA ($\alpha = 0.05$) in SigmaPlot 13.0.

3D images of the electrode biofilm were acquired by a confocal microscope (Zeiss LSM510 Meta) under a 40x objective with excitation from an argon laser at 488 nm, with a band pass filter 500–550 nm. The images were processed to create a 2D projection image using Axiovision software (Zeiss).

Scanning electron microscopy was performed as described previously in Chapter 5 (Section 5.1.4).

6.1.3 DNA extraction

A 15 ml volume of groundwater from the field (triplicate), groundwater from the start of the experiment (triplicate) and suspensions from all CC-, OC-MFCs and ME+S-MFC (45 mL) at the end of the experiment were filtered immediately through 0.1 μm filter (Whatman® Cyclopore®, 47 mm). The filters and electrode pieces were stored at -80 °C.

DNA was extracted from the filters and electrodes (2 cm^2 from the middle of the electrode, 4 cm^2 piece for SE+CC-MFC) according to the UltraClean® Microbial DNA Isolation Kit (MO-BIO Laboratories, Inc.) protocol as previously performed (Rizoulis et al., 2013), with the following modifications: the MicroBead tubes were replaced by Lysing Matrix E tubes (MP Biomedicals, LLC) and the volume of Microbead solution and solution MD1 was doubled. Filters and electrodes were cut with flame-sterilised scissors into small pieces (~5 mm^2) and put into Lysing tubes. They were then homogenised on FastPrep®-24

machine (MP Biomedicals, LLC) for 2 x 5 seconds at 5.5 m/s and on Vortex Genie® (MO-BIO Laboratories, Inc.) for 5 seconds, centrifuged afterwards at 6100 x g at room temperature for 2 min. The homogenization step was repeated. The Lysing tubes were centrifuged at 10,000 x g for 30 seconds at room temperature and 350 µL of supernatant was removed. The manufacturer's DNA extraction kit protocol was followed from that point onwards.

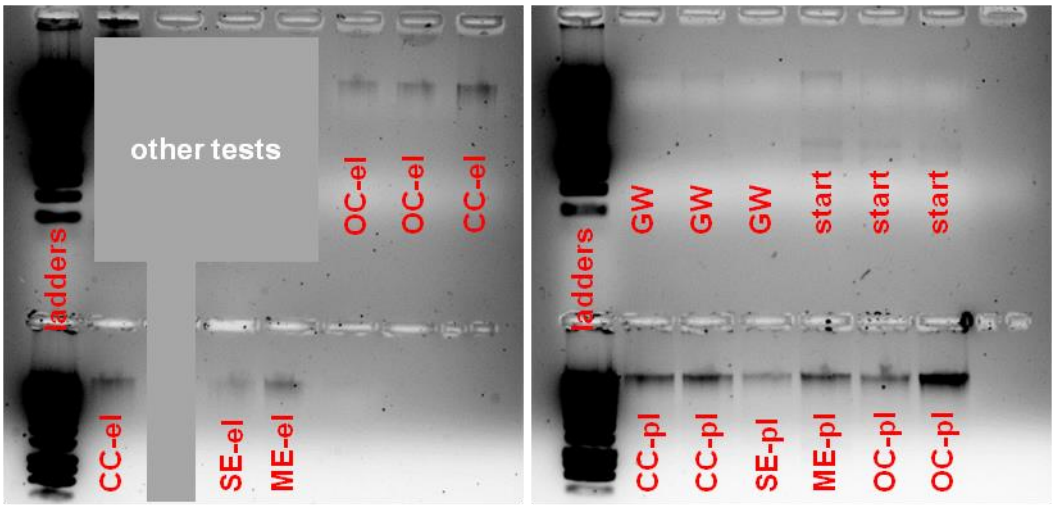

Figure 6-3 Photographs of extracted DNA separated by agarose gel electrophoresis. OC - DNA from OC-MFC, CC - CC-MFC, SE - SE+CC-MFC, ME - ME+S-MFC, GW - groundwater, start - DNA from the start of the experiment, el - electrode biofilm, pl - planktonic phase. SE-el2 for DNA extraction from a 2 cm^2 piece of the electrode, SE-el4 from a 4 cm^2 piece.

The extraction method used provided good quality DNA with a yield of at least 1 ng/µl. Five µl was electrophoresed on a 1% agarose gel and stained by ethidium bromide using HyperLadder I (Bioline, 200 to 10,037 bp) as a molecular weight standard (Figure 6-3). The extracted DNA was used in tests described in Section 6.1.4 and 6.1.5.

6.1.4 Terminal Restriction Fragment Length Polymorphism (T-RFLP)

Bacterial 16S rRNA genes were amplified from the total DNA extracts, using 63F FAM labelled primer (5'-CAGGCCTAACACATGCAAGTC-3') and 806R primer (5'-GGACTACVSGGGTATCTAAT-3'). The PCR mixture contained 1 µL DNA extract, 5 µL 10x KCl reaction buffer (Bioline), 1.5 µL $MgCl_2$ (50mM), 0.2 µL Taq DNA polymerase (5U/µL, Bioline), 5 µL dNTPs (1 mM), 2 µL of each primer (10 pmoL/µL) and 33.3 µL of sdH_2O. The reaction mixture was incubated at 94 °C for 2 min followed by 35 cycles of 95 °C for 30 seconds, 55 °C for 1 min and 72 °C for 75 seconds. The final extension step was 5 min at 72 °C. The PCR product was then purified using QIAquick PCR Purification Kit (QIAGEN) according to manufacturer's instructions. The purified PCR product was digested by CfoI restriction enzyme (Promega UK) for 3 hours at 37 °C, using 6.5 µL

sdH_2O, 1.5 µL 10x restriction buffer, 2 µL CfoI, 5 µL DNA sample, giving a total volume of 15 µL. 5 µL of the enzyme digest was desalted by precipitation, using 0.25 µL 20 mg/mL glycogen (ThermoScientific), 0.53 µL 3M sodium acetate and 14.5 µL ethanol. The solution was mixed gently and incubated for 2 hours on ice. It was centrifuged at 4°C for 15 min at 17,700 x g and washed twice with 70% ethanol and centrifuged at 4 °C for 2 min between each wash. Ethanol was removed and the sample allowed to air dry. The samples were stored at -20 °C prior to further analysis.

The DNA digest was then diluted into 5 µL of Tris-EDTA (10mM Tris, 0.1mM EDTA pH 8.0). 5 µL of ROX 500 size standard (Applied Biosystems) was diluted in 1 mL of HiDi formamide (Applied Biosystems). 1 µL of DNA digest was mixed with 9.5 µL of ROX and formamide mixture in a 96-well plate (Applied Biosystems) and the plate was spun on a salad spinner. The DNA was denatured at 94 °C for 3 min and cooled down quickly on ice-water. The plate was then analysed on ABI 3730 capillary sequencer (Applied Biosystems).

The raw data were processed in PeakScanner 2.0 (Applied Biosystems) and analysed further using T-REX software (Culman et al., 2009) which is available online and based on T-align (Abdo et al., 2006; Smith et al., 2005) and Additive Main Effects and Multiplicative Interaction (AMMI) model (Culman et al., 2008). The parameters used in T-REX were as follows: peaks of sizes between 50 and 500 bp labelled with blue fluorophore (FAM) were analysed, the noise was filtered applying 1x standard deviation multiplier, the peaks were aligned with clustering threshold of 0.7 bp, TRFs were automatically recalculated each time the set of active peaks changed, peak areas were relativised and samples were omitted if they contained less than 20 peaks to ensure good data quality.

Statistical comparison of the data generated (OTU richness and evenness) was completed with one-way ANOVA ($\alpha = 0.05$) in SigmaPlot 13.0.

6.1.5 16S rRNA gene sequencing

16S rRNA genes were amplified from the samples and sequenced using MiSeq Illumina 250 bp paired sequencing. As the 63F and 806R primers used for T-RFLP analysis amplify *in silico* only 11.5% (28.44% with 1 bp mismatch) when compared with SILVA database (Quast et al., 2013), Bakt_341F and Bakt_805R primers were chosen instead. They match 86.3% of bacterial sequences in the SILVA database and when 1 bp mismatch is allowed, they amplify 94.7% of Bacteria and 68.1% of Archaea. The comparison with the SILVA database was performed by Dr. Anne Cotton from the Department of Animal and Plant

Sciences. The Bakt primers are also Illumina recommended primers for MiSeq sequencing based on a study performed by Klindworth et al. (2013).

The V3/V4 region of 16S rRNA genes was amplified using the Bakt_341F (CCTACGGGNGGCWGCAG) and Bakt_805R (GACTACHVGGGTATCTAATCC) primers (Herlemann et al., 2011; Klindworth et al., 2013). The PCR mixture contained 2 μL DNA extract, 4 μL KAPA HiFi Fidelity Buffer (x5) (KAPA Biosystems), 0.4 μL $MgCl_2$ (25 mM), 0.6 μL KAPA dNTP Mix (10 mM each), 0.4 μL of each, forward and reverse primer (10 μM), 0.4 μL KAPA HiFi HotStart DNA Polymerase (1U/μl) and 11.8 μL sdH_2O. The reaction mixture was incubated at 95 °C for 3 min followed by 25 cycles of 95 °C for 30 seconds, 55 °C for 30 seconds and 72 °C for 30 seconds. The final extension step was 5 min at 72 °C, with hold at 4 °C. This first set of PCR amplifications was done in triplicate to avoid PCR biases. Prior to purification, equal volumes of all three replicates were mixed together. The PCR product was purified using Agencourt® AMPure® XP kit (Beckman Coulter) according to the manufacturer's instructions. The kit utilises solid-phase paramagnetic beads which bind to DNA and can be separated by magnetic field. The quality of the samples was checked using 1% agarose gel stained by ethidium bromide.

The cleaned-up PCR products were then bar-coded in a second PCR reaction (http://www.illumina.com/documents/products/datasheets/datasheet_sequencing_multiplex.pdf). The PCR mixture contained 5.0 or 2.5 μL DNA from the first set of PCRs and clean up, 10 μL KAPA HiFi Fidelity Buffer (x5) (KAPA Biosystems), 1.0 μL $MgCl_2$ (25 mM), 1.5 μL KAPA dNTP Mix (10mM each), 5.0 μL of each, forward and reverse, indexed Nextera XT (N7XX and S5XX) from the Nextera XT Index kit (Illumina, Essex, UK), 1.0 μL KAPA HiFi HotStart DNA Polymerase (1U/μl) and 21.5 μL or 24 μL sdH_2O. The samples were cleaned up using Agencourt® AMPure® XP kit as above. The quality of the samples was checked using a 1% agarose gel stained by ethidium bromide.

The cleaned-up bar-coded amplicons were quantified using a PicoGreen Assay (Invitrogen™). PicoGreen dye was 200x diluted in filter-sterilised (0.2 μm, polyethersulfone, Nalge Nunc International, Rochester) tris-EDTA buffer (10 mM Tris-HCl, 1 mM EDTA, pH 7.5). 100 μL of the tris-EDTA buffer without any dye was pipetted in a black 96-well micro plate (BMG LABTECH, Ltd). 0.5–2.0 μL of DNA samples or 2.0 μL standard and 100 μL of diluted PicoGreen dye was added in the well. The concentration of the herring sperm DNA standards ranged from 0 to 20 ng/μL. After 5 min incubation, the fluorescence in the wells was measured on a FluoStar Optima (BMG LABTECH, Ltd) spectrofluorimeter (excitation at 485 nm, fluorescence emission

measured at 545 nm). The concentration of the DNA in the samples was calculated from the calibration curve.

The barcoded samples (18 in total) were then diluted to 15 nM concentration by pipetting 2 μL of DNA sample into calculated volume of 10 mM Tris buffer (pH 8.5). 5 μL of each diluted DNA sample was mixed in a single sample to obtain approx. 100,000 sequences per sample. Sequencing was performed using the Illumina MiSeq Sequencing kit v2 (500 cycles) to produce 250 bp paired end reads (TGAC - The Genome Analysis Centre, Norfolk, UK).

6.1.6 Data processing for 16S rRNA sequencing

The demultiplexed data (without indexes) was separated into single files for each sample by TGAC. The data quality, i.e. length of the reads vs sequencing errors, was first checked using FastQC v0.11.4 (Babraham Bioinformatics). The displayed plot (Figure 6-4) shows the quality of the base pair reads as it depends on the position in the read for one of the groundwater field samples for forward and reverse primer sequences. The data quality decreased as the position in the read increased. This effect was more pronounced for the reverse primer sequencing and this data was of limited use for further analysis. Similar results were observed for all the groundwater and MFC samples. The forward primer sequences were therefore used in the data-processing pipeline. (Preliminary analyses demonstrated that using both forward and reverse primer sequences led to few sequences passing quality controls and introducing the possibility of biasing sequence count data.)

The data was processed in QIIME 1.9.1 64-bit (Caporaso et al., 2010) in combination with USEARCH v8.1.1861 and USEARCH v6.1.544 for Linux (Edgar, 2010). The more up-to-date version of USEARCH was used for initial data processing but the older version was necessary later to integrate with QIIME analysis pipelines. Symbolic links were set to each version (usearch81 and usearch61, respectively).

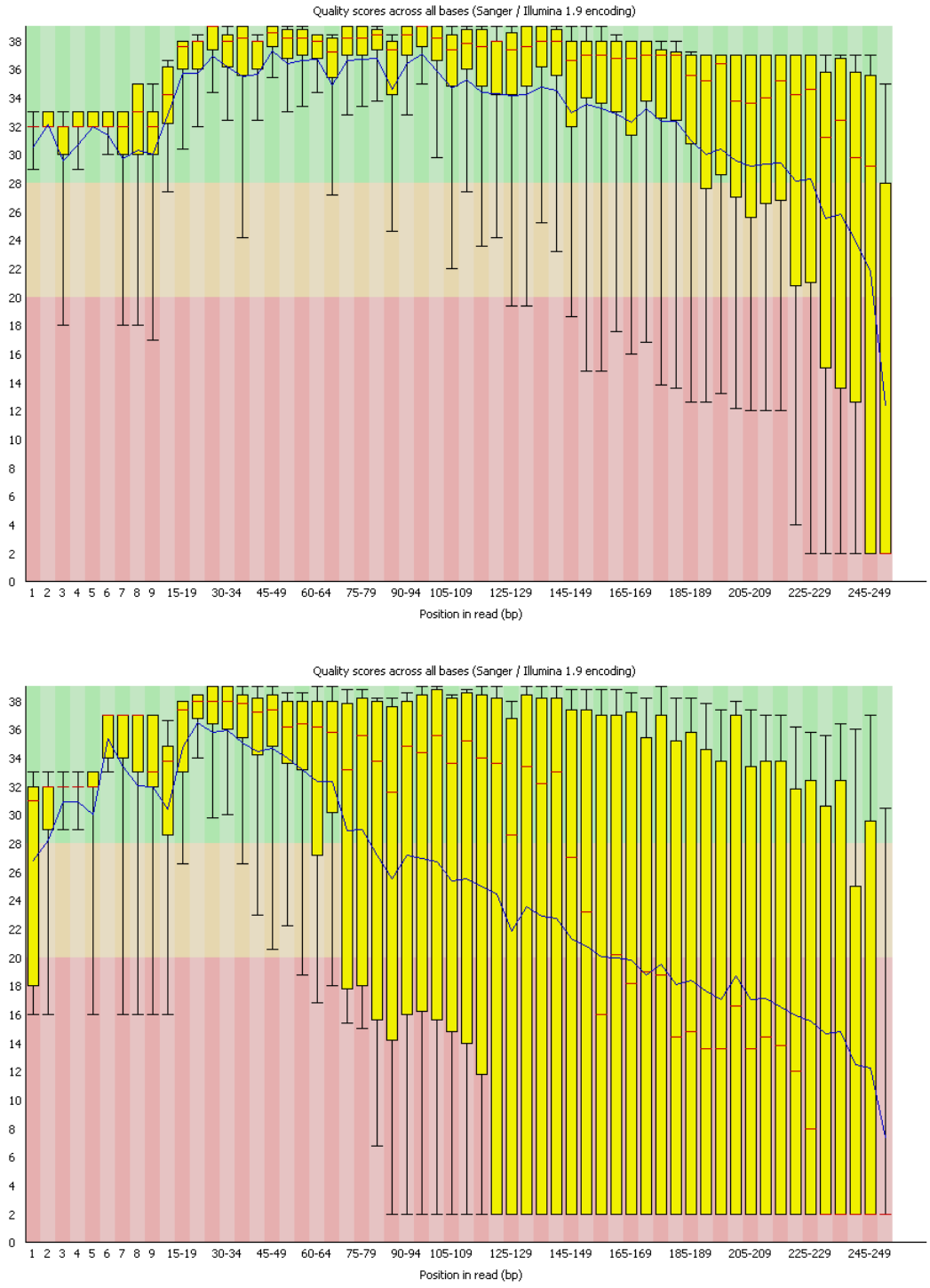

Figure 6-4 Output from FastQC for the groundwater field sample GW1 for the forward primer (top) and the reverse primer (bottom). Median value (red line), interquartile range (yellow box), mean value (blue line) and 10/90% (upper/lower whiskers). Good quality scores (green background), reasonable quality (orange background) and poor quality (red background).

The steps involved in the data processing pipeline were as follows, including the `QIIME code using Consolas font`.

- The data quality of each sample was displayed enabling filtering criteria for the next step to be chosen.

```
usearch81 -fastq_eestats2 GW1F.fastq -output GW1F.txt
```

output:

```
39404 reads, max len 251, avg 251.0
Length         MaxEE 0.50         MaxEE 1.00         MaxEE 2.00
------   ----------------   ----------------   ----------------
    50      38548( 97.8%)      39367( 99.9%)      39396(100.0%)
   100      35126( 89.1%)      38438( 97.5%)      39307( 99.8%)
   150      29937( 76.0%)      34924( 88.6%)      37963( 96.3%)
   200      24699( 62.7%)      30434( 77.2%)      35326( 89.7%)
   250      10728( 27.2%)      16453( 41.8%)      23245( 59.0%)
```

The result table for sample GW1F shows that 39404 reads are available for this sample each of length of 251 bp. Allowing for a MaxEE of 1.00 (maximum expected error of 1 bp per 1000 bp sequence) at 250 bp length would keep 41.8% of the reads. By reducing the read length somewhat many more sequences can be retained. The filtering criteria for the next step can be chosen using the produced table to balance the quality of the reads and their length for good phylogenetic resolution.

- The sequences were filtered on quality and length.

```
usearch81 -fastq_filter GW1F.fastq -fastaout fasta/GW1F.fasta
-fastq_maxee 1 -fastq_minlen 230
```

output:

```
00:01  32Mb  100.0% Filtering, 31.1% passed
     39404  FASTQ recs (39.4k)
     27157  Low qual recs discarded (expected errs > 1.00)
     12247  Converted (12.2k, 31.1%)
```

The maximum length of reads was kept for good phylogenetic analysis, discarding 69.9% of low quality sequences for sample GW1F.

- A mapping tab-delimited file (Table 6-1) was created for combining all the sample files into one file.

Table 6-1 An example of the mapping .txt file. BarcodeSequence was unknown.

#SampleID	BarcodeSequence	LinkerPrimerSequence	InputFilename	Description	Deskription1	Deskription2
GW1		CCTACGGGAGGCAGCAG	GW1F.fasta	groundwater_field	groundwater	field
S1		CCTACGGGAGGCAGCAG	S1F.fasta	groundwater_start	groundwater	start
1AE		CCTACGGGAGGCAGCAG	1AEF.fasta	CCMFC_electrode	CCMFC	electrode

- All the sample files were combined in one file "combined_seqs.fna" using the mapping map.txt file. This format is required for further processing in QIIME.

```
add_qiime_labels.py -m map.txt -i fasta/ -c InputFilename -o fout/
```

- The primers were removed.

```
usearch81 -fastx_truncate fout/combined_seqs.fna -stripleft 18 -fastaout fout/combined_np.fna
```

- During the amplification process, chimeric sequences can be generated (Osborn and Smith, 2005). Chimeras were identified by *de novo* methods and by comparison with the "rdp_gold.fa" database (available at http://drive5.com/usearch/manual/cmd_uchime_ref.html) and removed.

```
identify_chimeric_seqs.py -i fout/combined_np.fna -m usearch61 -o chimeras/ -r rdp_gold.fa
filter_fasta.py -f fout/combined_np.fna -o comb_nc_np.fna -s chimeras/chimeras.txt -n
mv comb_nc_np.fna comb_nc_np.fasta
```

- Sequences were clustered using 97% similarity threshold by USEARCH v6.1.544 (Edgar, 2010) and matched against "rdp_gold.fa" database to assign taxonomy.

```
pick_open_reference_otus.py -i $PWD/comb_nc_np.fasta -r $PWD/rdp_gold.fa -o $PWD/usearch/ -m usearch61
```

A minimum of 2 sequences was required to assign an OTU. Single sequences were removed as these might be present due to sequencing errors. Any sequences which failed to align were omitted. OTU table "otu_table_mc2_w_tax_no_pynast_failures.biom" was therefore used for further analysis. Summarising the data in the table

```
biom summarize-table -i
usearch/otu_table_mc2_w_tax_no_pynast_failures.biom
```

gives the number of observed OTUs in 18 samples of 1100 with a minimum of 11830 total counts/sample and a maximum of 54371 total counts/sample.

- The OTU table produced in a previous step was copied and renamed and then rarefied based on the minimum number of total counts/sample. The rarefied OTU table contained the same number of sequences for each sample.

```
cp usearch/otu_table_mc2_w_tax_no_pynast_failures.biom
otu_table_usearch.biom
single_rarefaction.py -i otu_table_usearch.biom -o
otu_table_usearch_rare.biom -d 11830
```

- Alpha diversity of all the samples was evaluated by plotting rarefaction curves.

```
alpha_rarefaction.py -i otu_table_usearch.biom -m map.txt --
min_rare_depth 1000 --max_rare_depth 11000 -o alpha_usearch/ -t
usearch/rep_set.tre
```

- Beta diversity of all the samples and MFC samples only was analysed by principal coordinates analysis (PCoA).

```
jackknifed_beta_diversity.py -i otu_table_usearch_ rare.biom
-o beta_usearch / -m map.txt -t usearch/rep_set.tre -e 3000
```

```
jackknifed_beta_diversity.py -i
otu_table_usearch_MFCs_rare.biom -o beta_usearch_MFCs/ -m
map.txt -t usearch_MFCs/rep_set.tre -e 3000
```

- Non-replicate samples (SE+CC-MFC and ME+S-MFC) and OTUs with less than 30 counts were removed from the OTU table and after rarefaction, the OTUs which differed significantly ($P < 0.05$) between the samples were identified.

```
filter_samples_from_otu_table.py -i
otu_table_usearch_rare.biom -o
otu_table_usearch_rare_replicate.biom --sample_id_fp remove.txt
--negate_sample_id_fp
```

```
filter_otus_from_otu_table.py -i otu_table_usearch_rare_replicate.biom -o otu_table_usearch_rare_replicate_min30.biom -n 30
single_rarefaction.py -i otu_table_usearch_rare_replicate_min30.biom -o otu_table_usearch_rare_min30.biom -d 10648
group_significance.py -i otu_table_usearch_rare_min30.biom -m map_replicate.txt -c Description -o sig_test.txt -s g_test
```

- Dominant, significantly different ($P < 0.05$) OTUs were plotted in Microsoft Excel using the transferred rarefied BIOM table and taxonomic assignment file (rep_set_tax_assignments.txt).

```
biom convert -i otu_table_usearch_rare.biom -o otu_table_usearch_rare.txt --to-tsv
```

- Dominant *Geobacter* sp. and *Desulfuromonas* sp. sequences were of special interest and were therefore clustered at 99% similarity threshold. Sequences, which were firstly clustered at 97% and identified as dominant *Geobacter* sp. and *Desulfuromonas* sp. OTUs, were listed in Geobacter_Desulfuromonas.txt. These sequences were isolated from the comb_nc_np.fasta and then clustered at 99% similarity threshold.

```
filter_fasta.py -f comb_nc_np.fasta -o comb_Geobacter_Desulfuromonas.fasta -s Geobacter_Desulfuromonas.txt
pick_de_novo_otus.py -i comb_Geobacter_Desulfuromonas.fasta -o uclust99/ -p param.txt
```

param.txt content as follows:

```
pick_otus:otu_picking_method uclust
pick_otus:similarity 0.99
```

example of sequences:

```
SS_15153
S3_6065
1BE_65021
1BE_77646
2AE_106529
```

6.2 Results and discussion

The parameters and techniques used to describe the structure of the microbial community developed in the MFCs (Chapter 5) are:

- the total cell count,
- the percentage of the electrode covered and the morphology of the colonies as an indicator of biofilm development,
- T-RFLP (terminal restriction fragment length polymorphism) fingerprint in combination with the calculations of OTU richness and evenness, and AMMI (additive main effects and multiplicative interaction) analysis,
- 16S rRNA gene sequencing followed by alpha and beta diversity analysis, including the OTU richness and evenness and estimation of true OTU richness. Dominant OTUs were identified and their potential function within groundwater and MFCs discussed.

6.2.1 Total cell counts

The suspended cells in the groundwater samples and MFCs were enumerated as a first indicator of changes within the microbial community. In groundwater samples collected from the field and after 6 weeks of storage, similar planktonic cell numbers (~3 x 10^6 cells/ml) were present (Figure 6-5). After incubation in the CC- and OC-MFCs, the cell numbers had increased significantly ($P < 0.05$) to ~100 x 10^6 cells/ml.

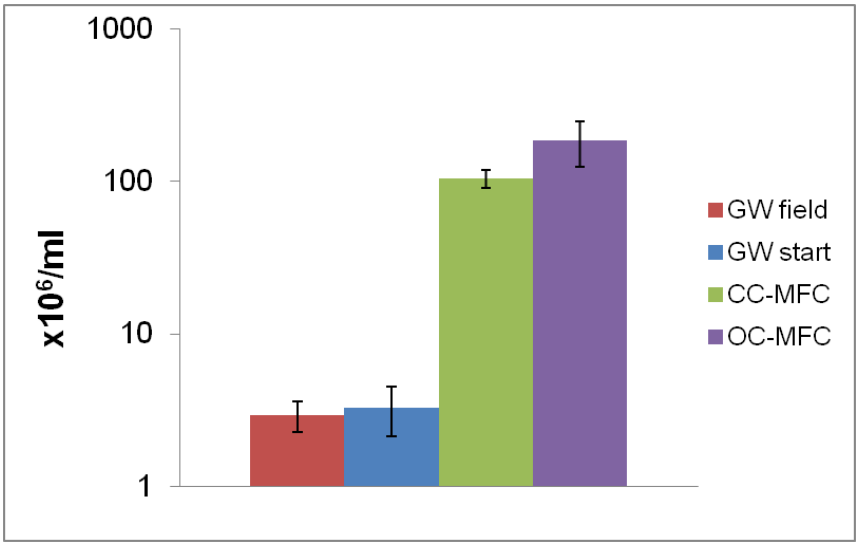

Figure 6-5 Total cell counts in groundwater in the field (GW field) and at the start of the experiment (GW start), CC-MFC and OC-MFC.

6.2.2 Biofilm microscopy

The biofilm development on the electrode was monitored using maximum projection images which were further processed and analysed in ImageJ. The percentage of the area covered by biofilm was acquired as a simple measure of cell adhesion level (Schreiberová et al., 2012). It does not provide any information about the biofilm structure and its complexity. For those purposes, scanning electron microscopy or confocal microscopy are more appropriate.

Maximum projection image is an image of a single plane within a 3D structure. Only part of the image is in focus. A sequence of such images taken from different planes along the Z-axis can be used to build a single sharp image, capturing the 3D structure in a 2D image. An example of a maximum projection image of an electrode biofilm can be seen in Figure 6-6A. For practicality, the colours in the fluorescence microscopy images were inverted (Figure 6-6B) prior to creating a binary image (Figure 6-6C). Colour inversion enables easier definition of the binary threshold. The area covered with biofilm was overestimated (Figure 6-6B and Figure 6-6C) due to high background fluorescence. More sophisticated image processing method would have to be used to create a more accurate binary image. The structure of the carbon cloth with the fibres crossing each other is complex and is difficult to capture in a 2D image.

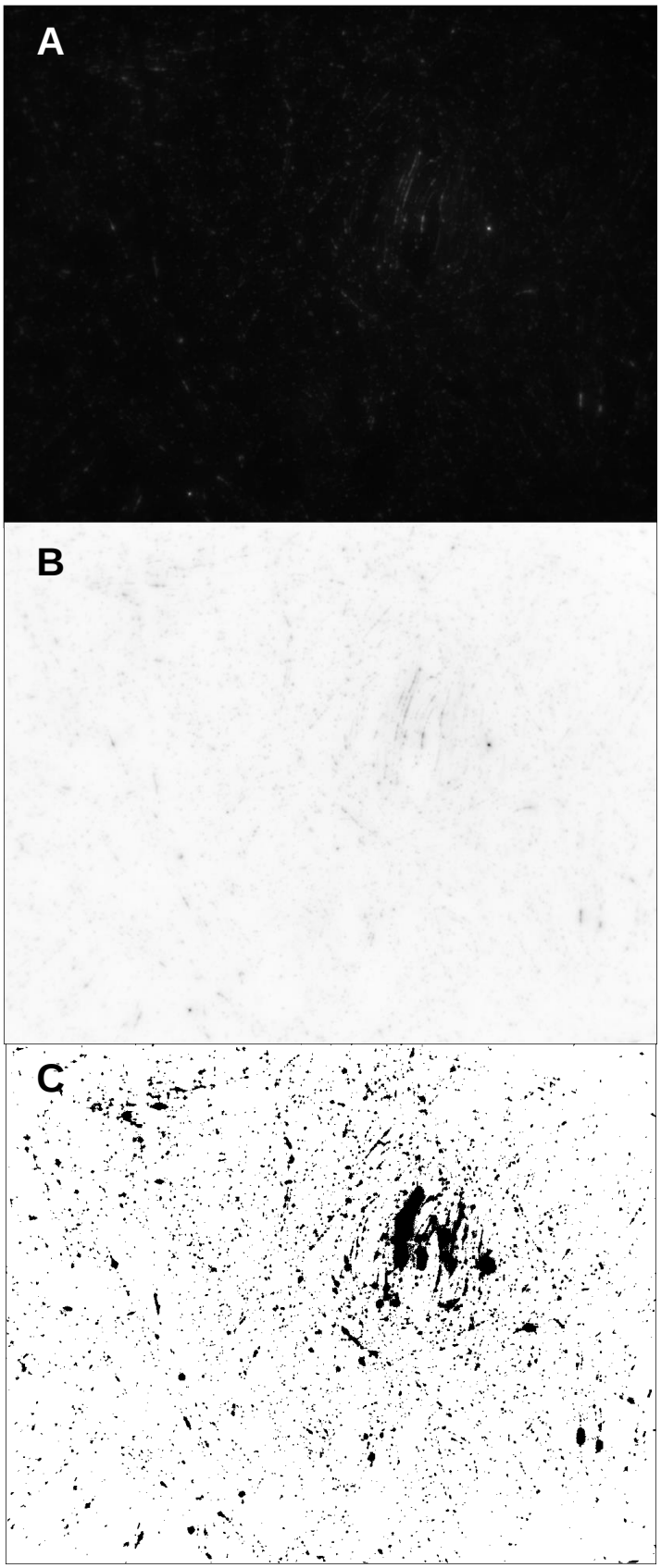

Figure 6-6 Maximum projection image of electrode biofilm in SE+CC-MFC at the end of the experiment (A), its colour-inverted version (B) and a binary image (C).

The biofilm covered ~2% of the electrode surface area in the CC- and OC-MFC (Figure 6-7). When electrodes were moved (SE+CC-MFC and ME+S-MFC) then biofilm coverage was significantly ($P < 0.05$) greater at ~4%. Examples of different biofilm coverage are shown in Figure 6-8.

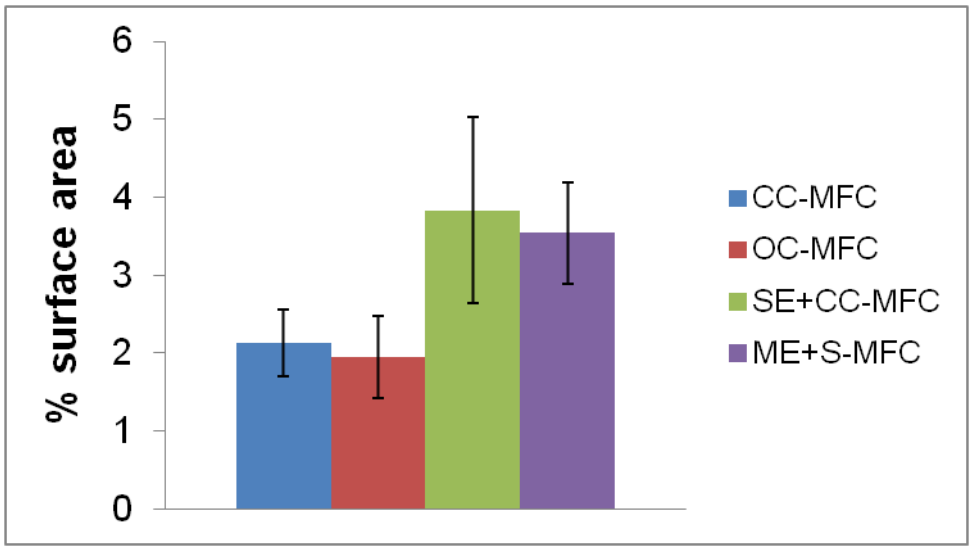

Figure 6-7 Percentage of the electrode area covered by biofilm in the CC-MFC, OC-MFC, SE+CC-MFC and ME+S-MFC at the end of the experiment.

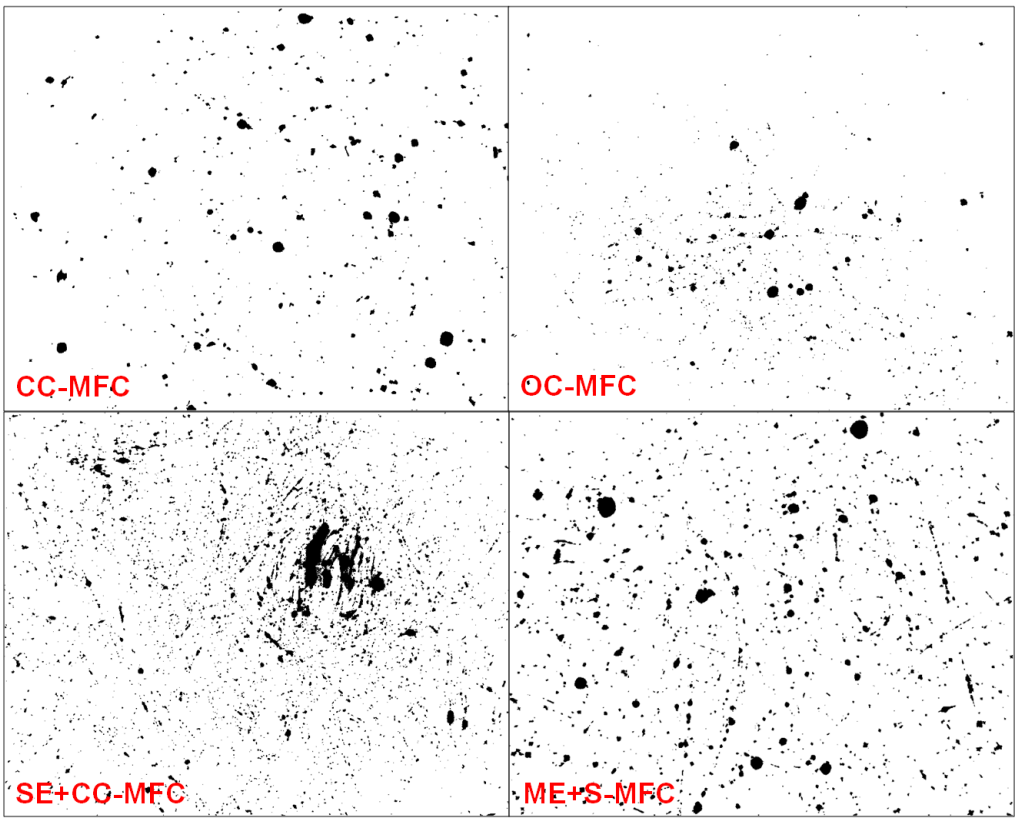

Figure 6-8 Examples of biofilm images from different MFC set-ups.

Confocal microscopy revealed cell clusters along the carbon fibres in both, CC- and OC-MFC (Figure 6-9 and Figure 6-10). SE+CC-MFC and ME+MFC were not imaged under confocal microscope.

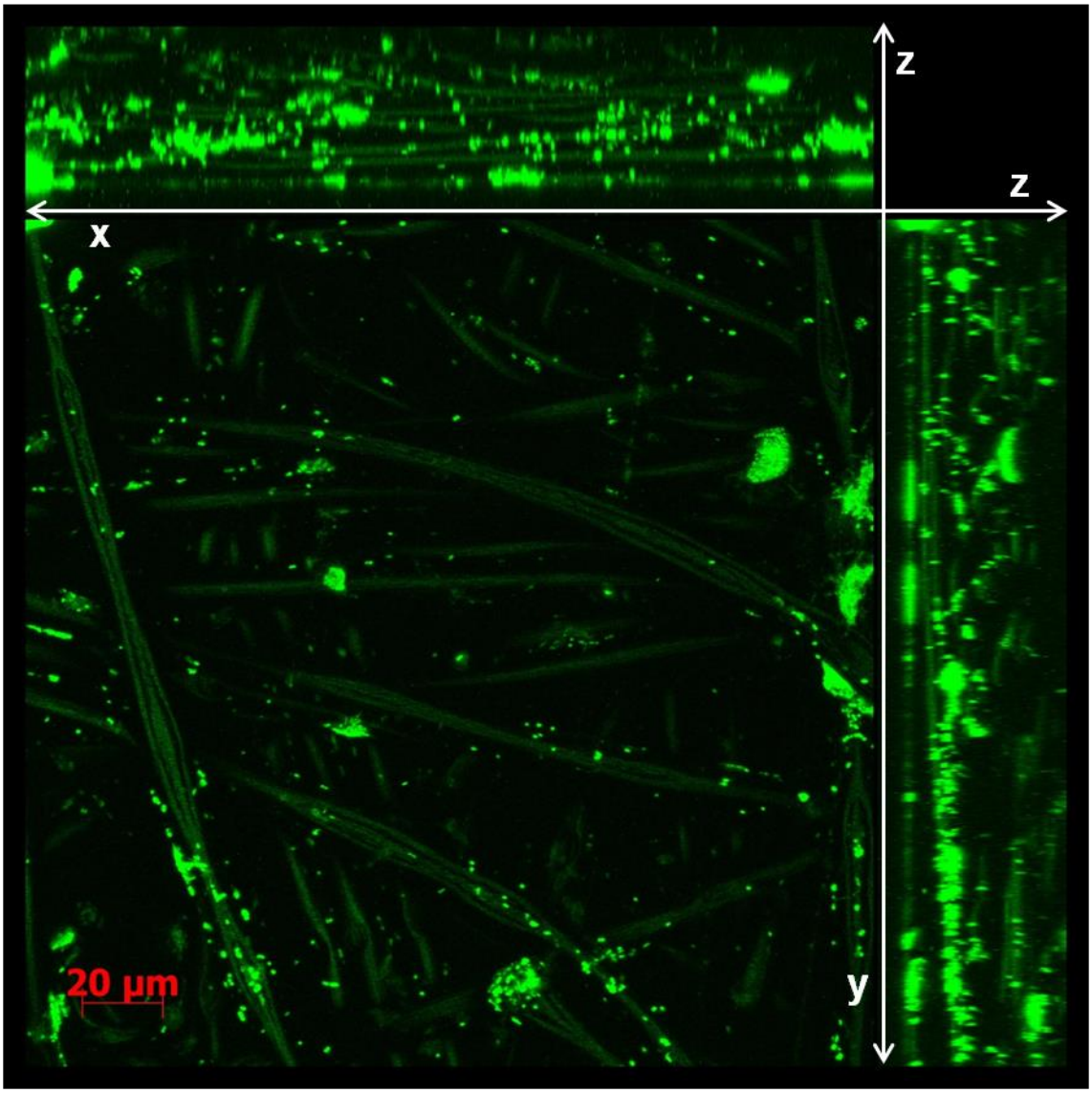

Figure 6-9 Biofilm on the electrode of CC-MFC at the end of the experiment (40x, confocal microscope).

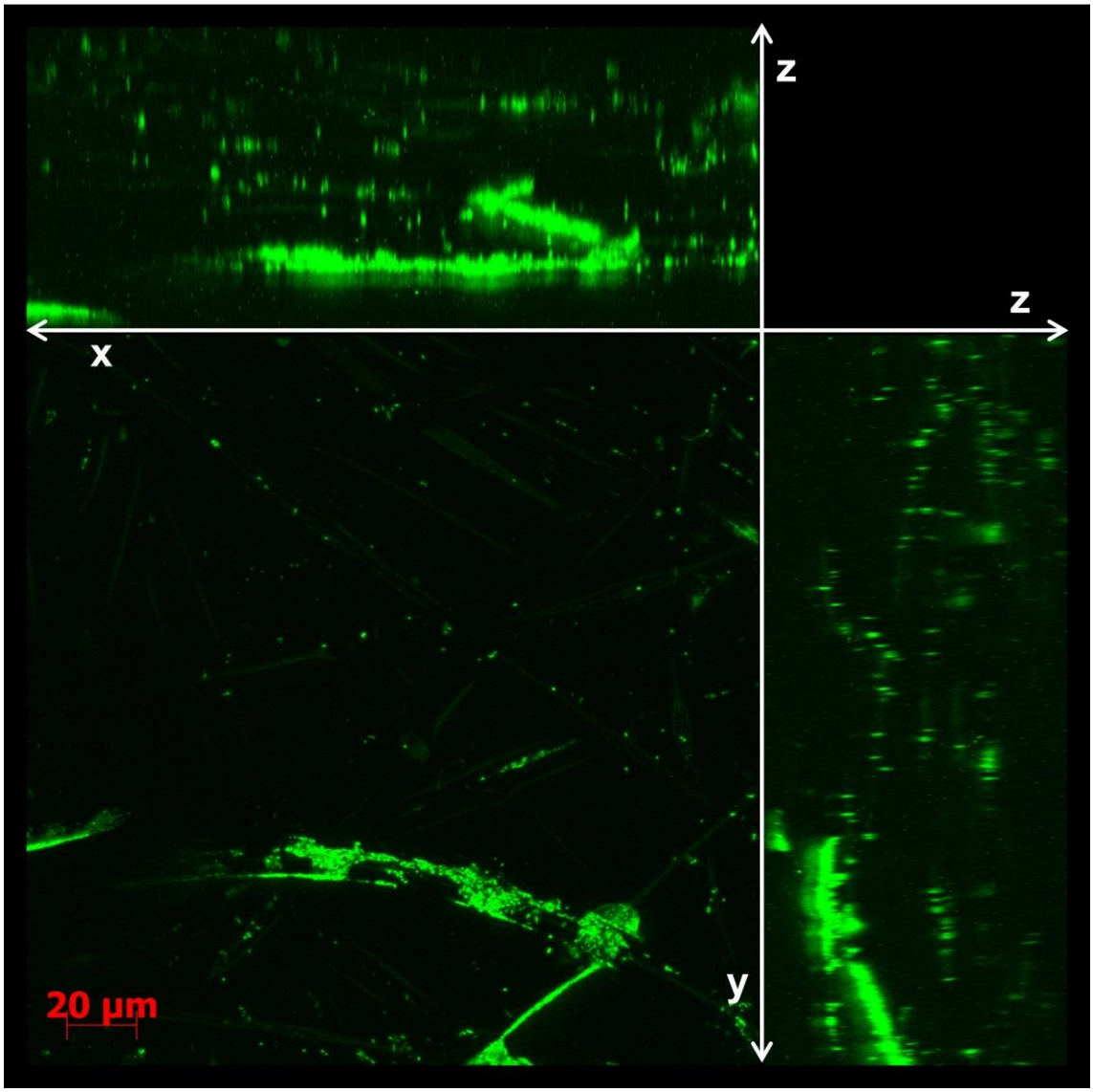

Figure 6-10 Biofilm on the electrode of OC-MFC at the end of the experiment (40x, confocal microscope).

Electron microscopy (SEM) provided more information regarding the structure of the cell clusters present in all the MFCs, showing the morphological difference of colonies in different MFC set-ups. Larger clusters of cells (~30–40 µm) surrounded by extracellular polymeric substances (EPS) as well as single cells attached to the electrode fibres were observed in the CC-MFC (Figure 6-11). The large colonies bridged the gap between the neighbouring fibres, which potentially provided the colony with higher surface area of the electrode for (direct) electron transfer. The mechanism, if any, of electron transfer within the colony is not clear. Bacteria (e.g. *Geobacter* sp.), could have built nanowires to reach the electrode from within the centre of the colony (Reguera et al., 2006). However, no visible *pilus*-like structures were observed on the surface of the colonies. Iron colloids present in the groundwater (Chapter 5) did not seem to have played a role in the electron transfer

within the colony (Nakamura et al., 2009) as no colloid particles were detected by SEM and were likely to have precipitated on the bottom of the MFC. A rust-coloured precipitate was observed in the anode chamber.

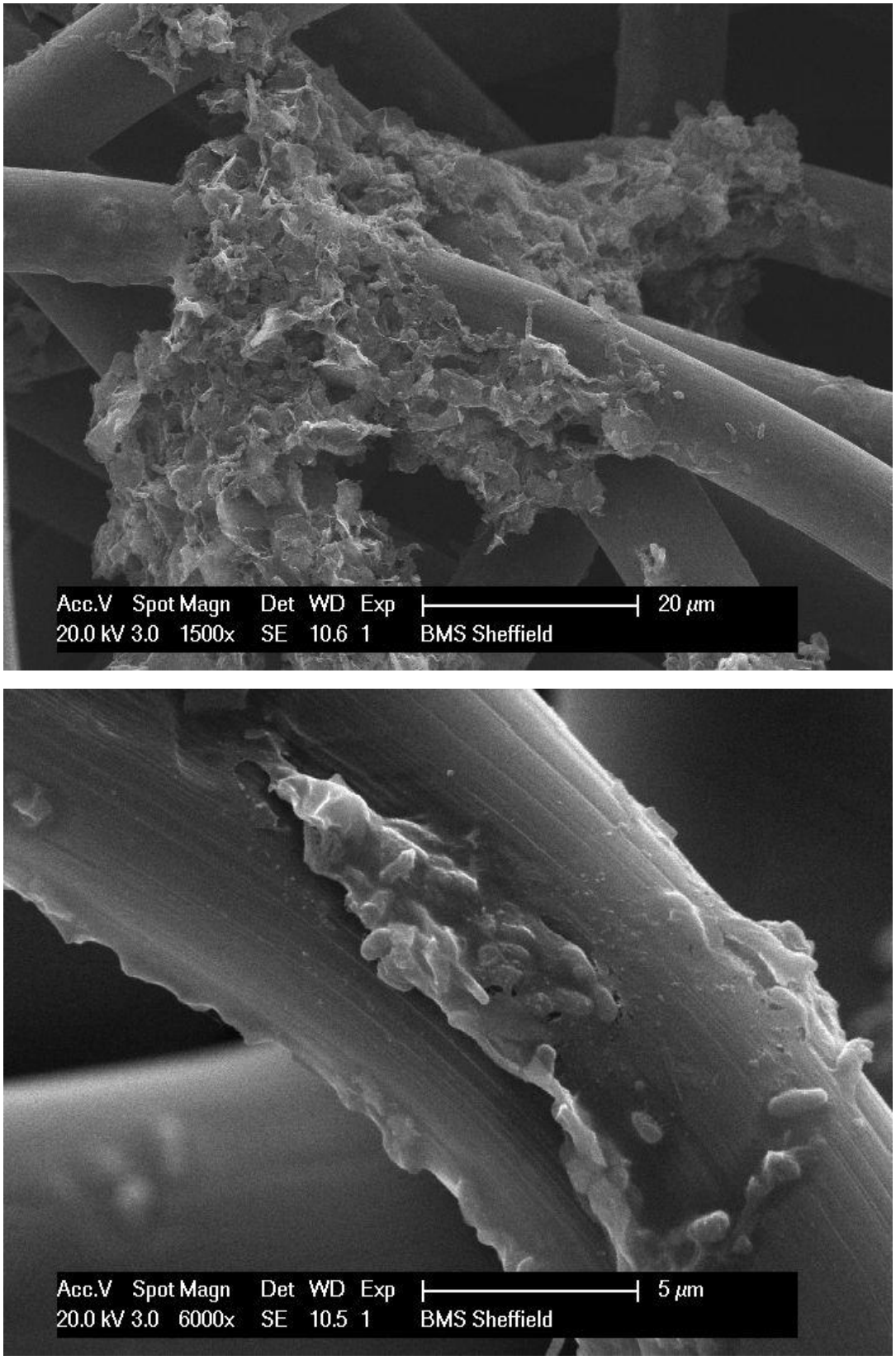

Figure 6-11 SEM images of electrode biofilm in CC-MFC after 92 days of incubation.

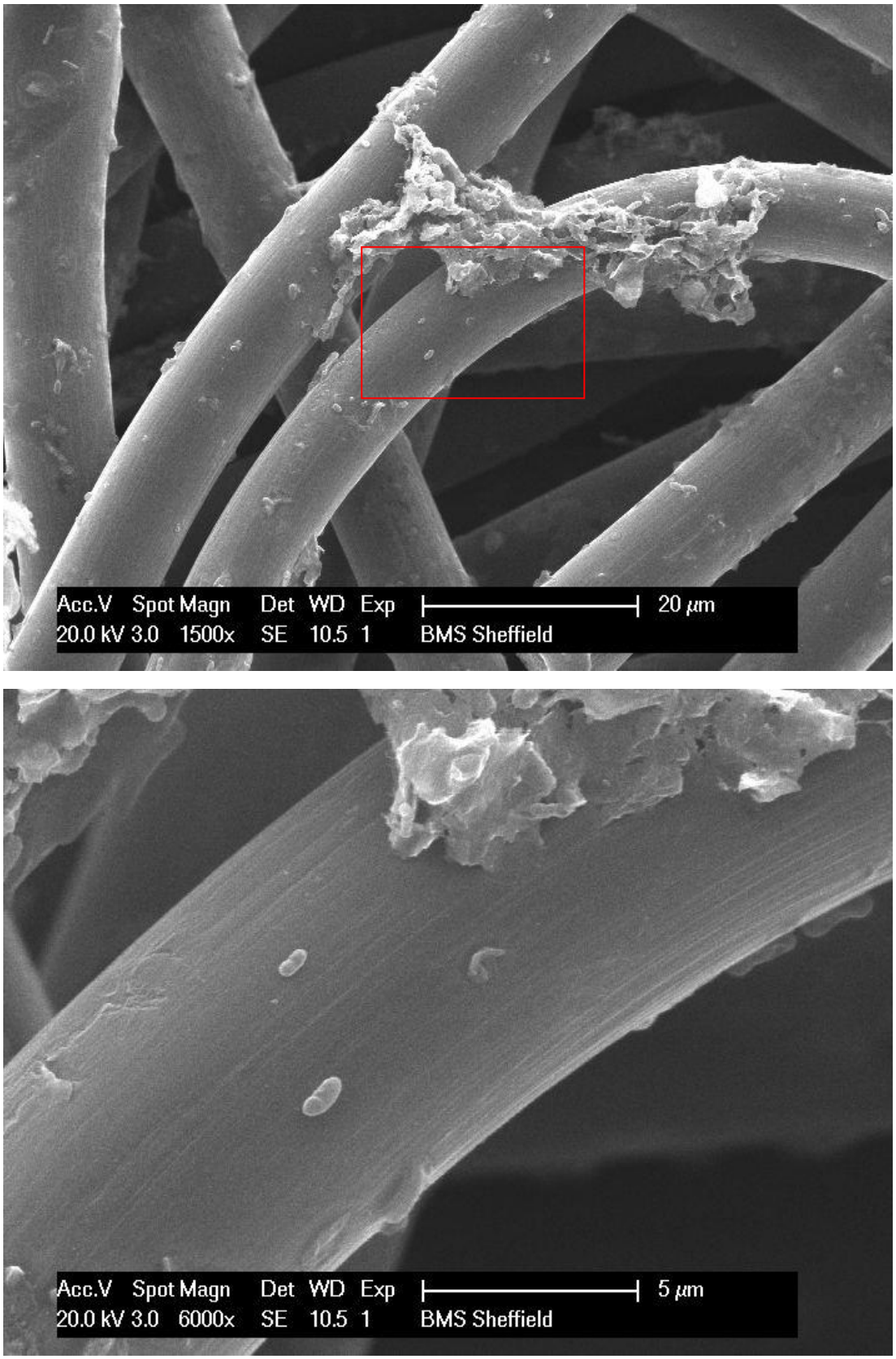

Figure 6-11 SEM images of electrode biofilm in CC-MFC after 92 days of incubation.

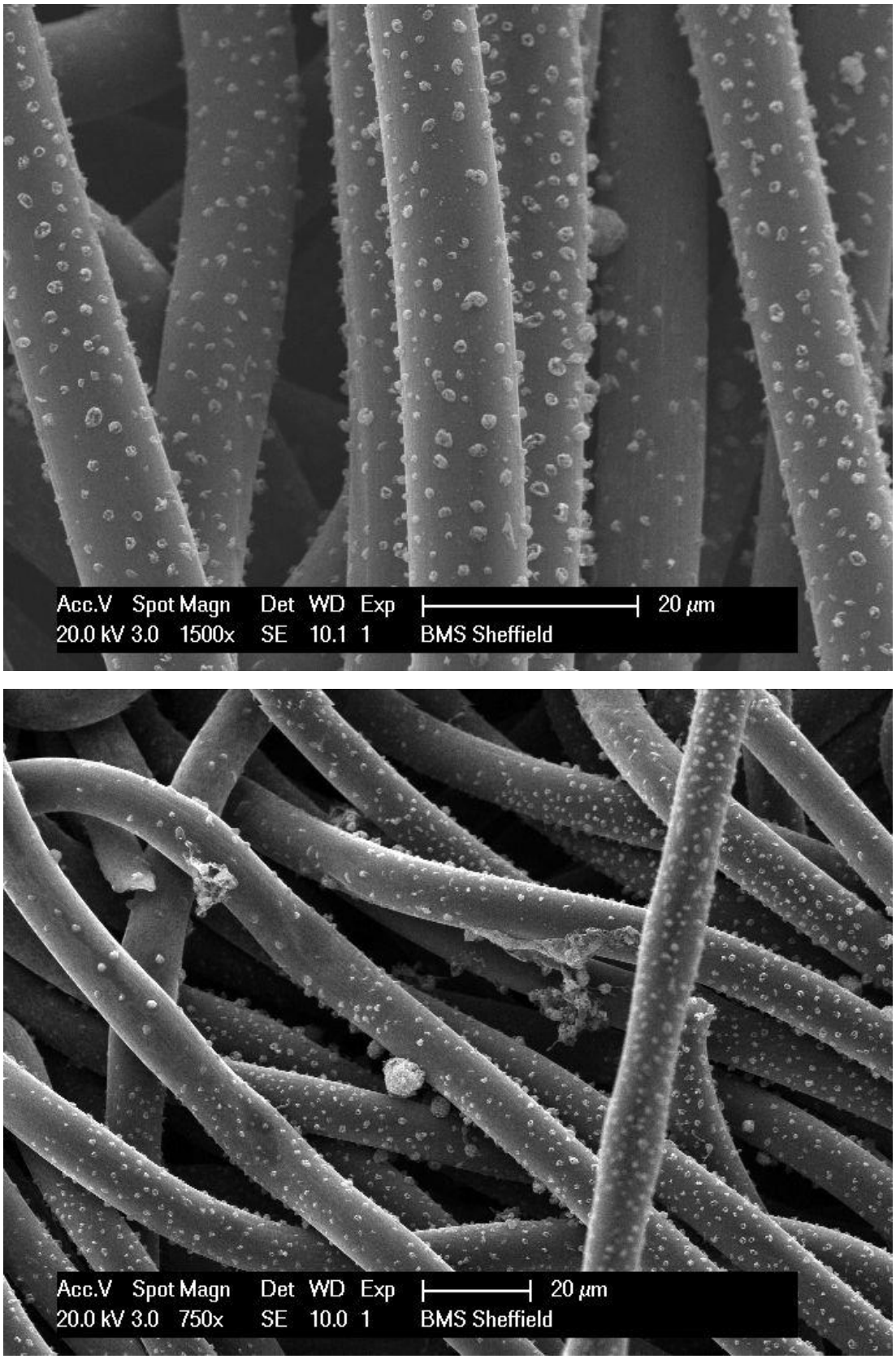

Figure 6-12 SEM images of electrode biofilm in OC-MFC after 92 days of incubation.

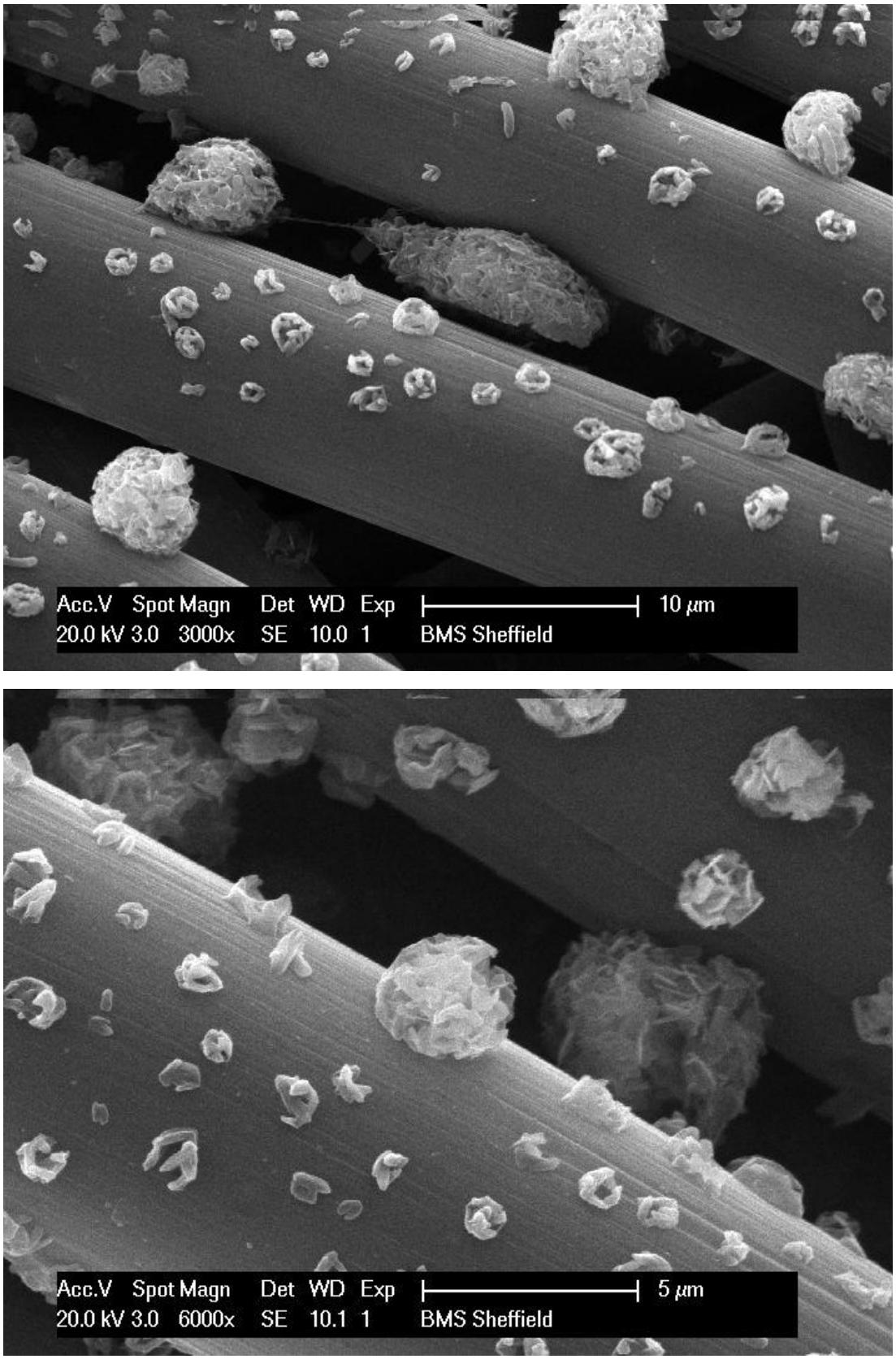

Figure 6-12 SEM images of electrode biofilm in OC-MFC after 92 days of incubation.

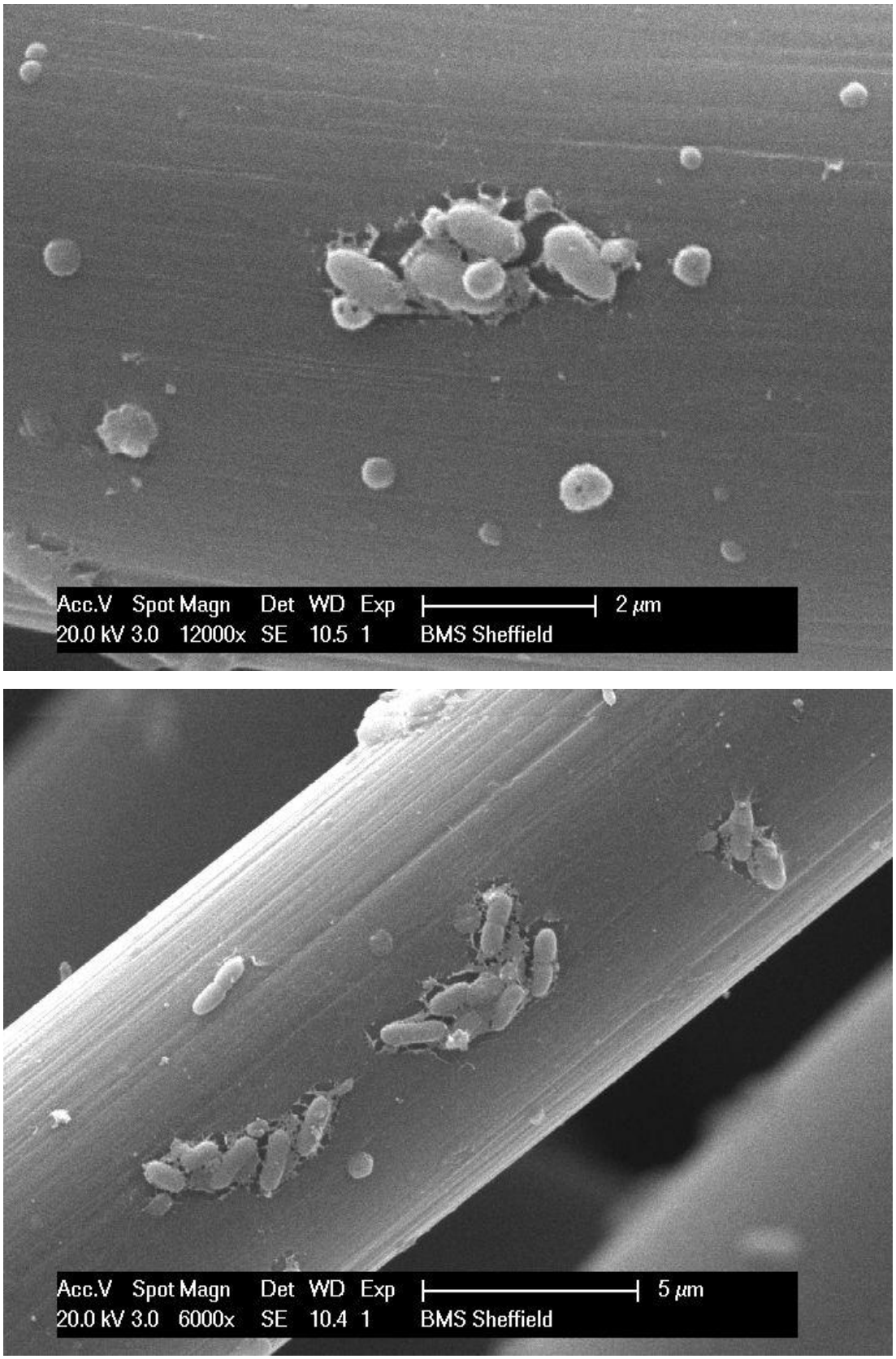

Figure 6-13 SEM images of electrode biofilm in SE+CC-MFC after 5 days of incubation of a sterile electrode in mature CC-MFC.

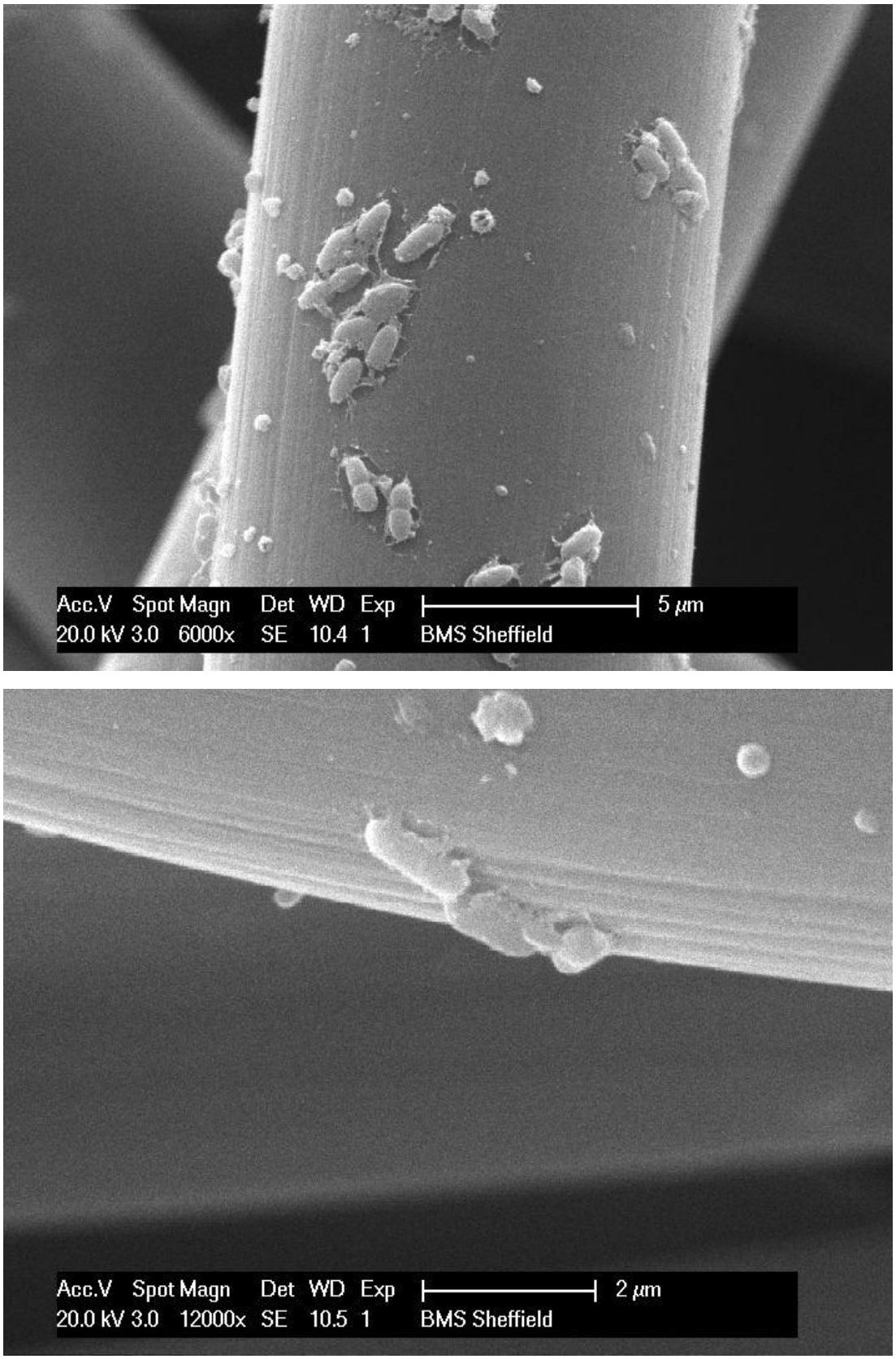

Figure 6-13 SEM images of electrode biofilm in SE+CC-MFC after 5 days of incubation of a sterile electrode in mature CC-MFC.

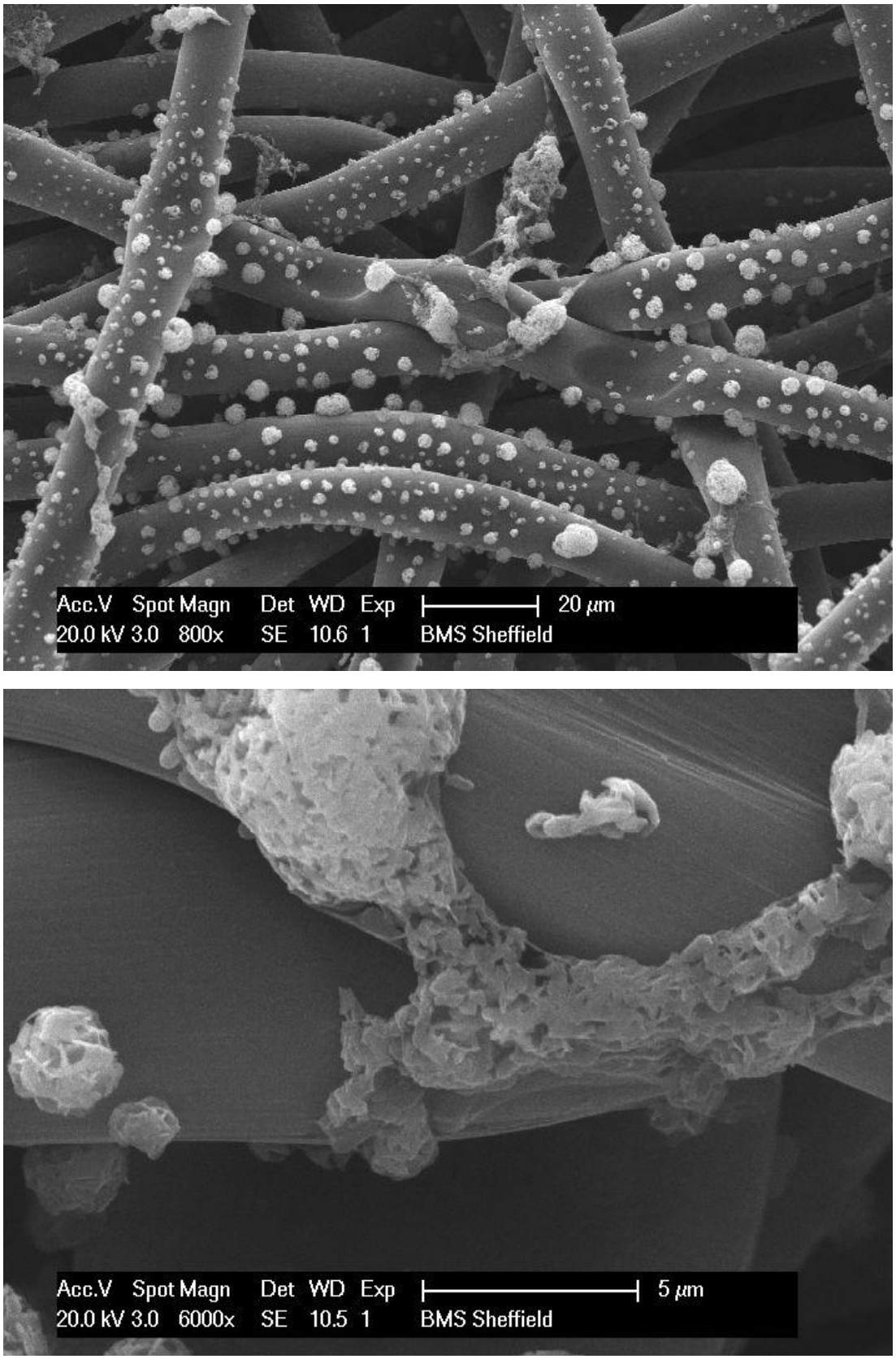

Figure 6-14 SEM images of electrode biofilm in ME+S-MFC after 87 days incubation in the CC-MFC and the following 5 days in a sterile MFC.

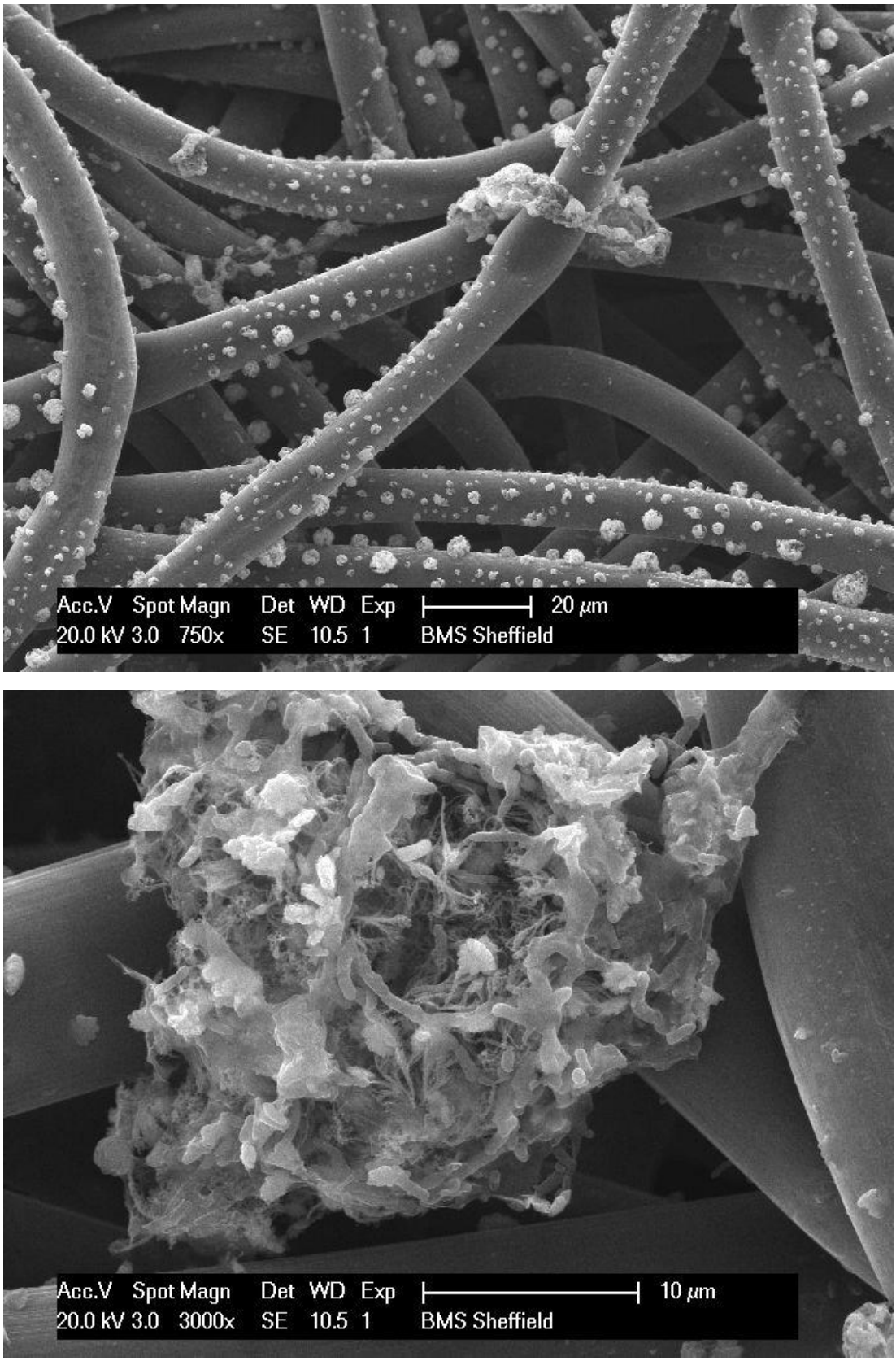

Figure 6-14 SEM images of electrode biofilm in ME+S-MFC after 87 days incubation in the CC-MFC and the following 5 days in a sterile MFC.

The morphology of the colonies in the OC-MFC was significantly different from the one observed in the CC-MFC (Figure 6-12). The colonies had a rounded shape, size of up to 10 μm and did not bridge the gap between the electrode fibres. Bacteria attached to this electrode were not involved in the electron transfer to the electrode and therefore did not need to maximise the contact with it. These bacteria probably utilised the electron acceptors dissolved in water for which the round-shape colonies seem to be optimised. Some individual cells attached were observed but most had a capsule around them.

Individual cells initiating the biofilm development were attached to the electrode of SE+CC-MFC after 5 days of sterile electrode introduction in the CC-MFC (Figure 6-13) (Chapter 5). The cells started the cell division process and EPS development. Interestingly, the ME+S-MFC electrode biofilm consisted of cell clusters structurally similar to both, CC- and OC-MFC (Figure 6-14). Round-shape colonies were present as well as the colonies bridging the gap between the single electrode fibres. Single and encapsulated cells were detected, too.

6.2.3 Terminal restriction fragment length polymorphism

T-RFLP is a fingerprinting technique for microbial community characterisation. Amplified 16S rRNA genes are labelled with a fluorophore and digested by restriction enzyme(s) cutting DNA at a specific palindromic sequence. In this way, terminal restriction fragments (TRFs) of different length are created. TRFs do not characterise single bacterial species as two or more different species can share the same TRF. Each sample than has a characteristic TRF fingerprint (Osborn and Smith, 2005; Clement et al., 1998). The raw TRF data obtained by a sequencer is processed into either a binary matrix indicating TRF presence or absence (unweighted), or a matrix showing the TRF abundance data by using peak area or relativised peak area (weighted).[*] The matrix is then analysed by multivariate statistical ordination analyses, for example principal component analysis (PCA) or additive main effects and multiplicative interaction (AMMI) and others (Culman et al., 2008).

[*] For the purposes of this thesis section, weighted analysis proved to be more appropriate as unweighted did not show any significant differences between the sample treatments (groundwater vs MFCs).

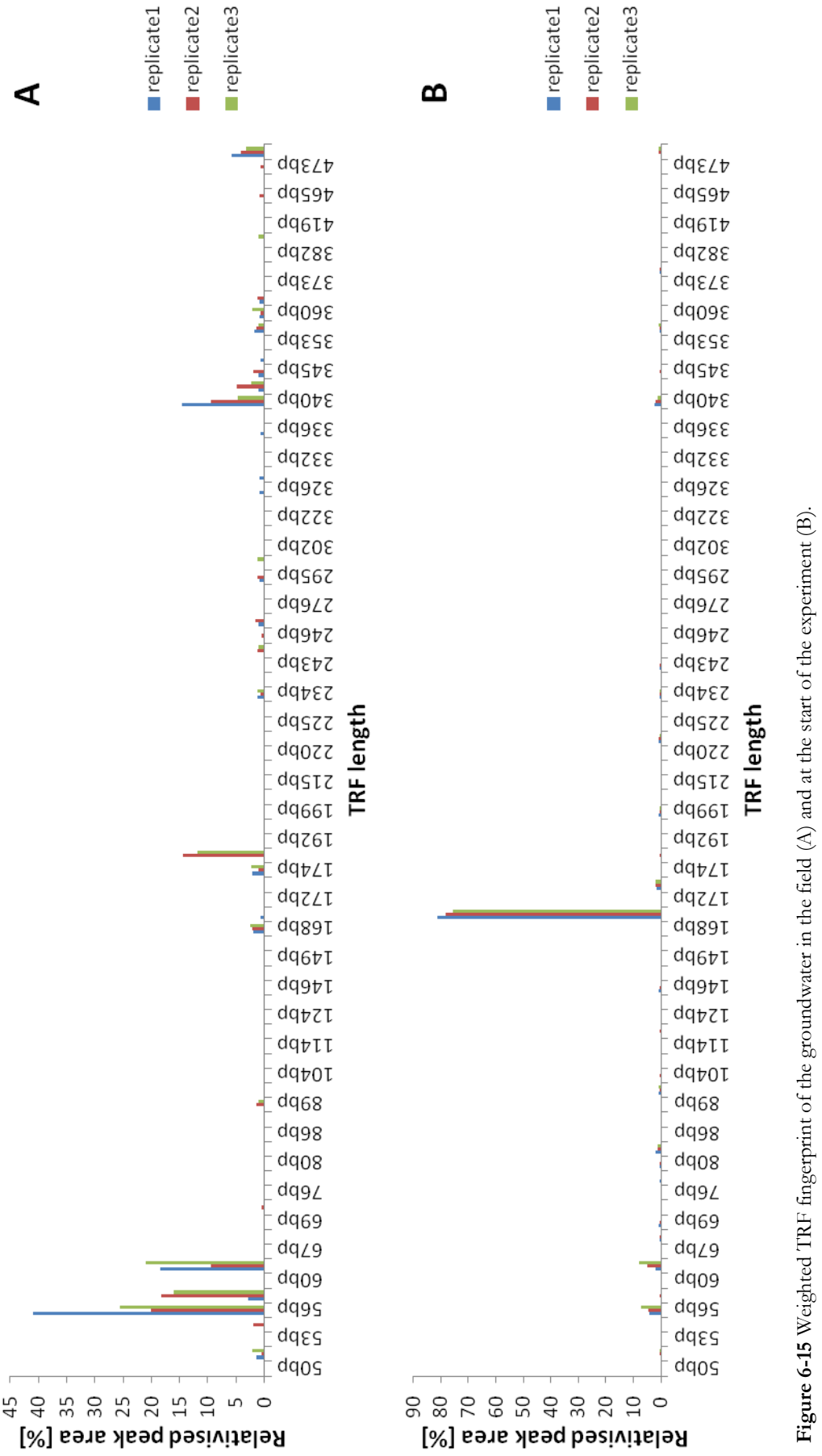

Figure 6-15 Weighted TRF fingerprint of the groundwater in the field (A) and at the start of the experiment (B).

Relativised (Culman et al., 2009) peak area was used to create TRF fingerprints for each sample analysed. Relativising the peak area eliminated the difference in TRF signal intensity caused by the difference in amount of DNA analysed on the sequencer. This enabled the sample fingerprints to be compared with each other as if the same amount of DNA was analysed for each sample (Culman et al., 2008). The fingerprints of replicate samples were very similar to each other as can be seen from two examples in Figure 6-15.

Table 6-2 OTU richness for different groundwater and MFC samples.

Microbial community	OTU richness	Microbial community	OTU richness
Groundwater field	21 ± 3		
Groundwater start	18 ± 4		
CC-MFC planktonic	33 ± 3	CC-MFC biofilm	30 ± 8
SE+CC-MFC planktonic	31	SE+CC-MFC biofilm	23
ME+S-MFC planktonic	15	ME+S-MFC biofilm	17
OC-MFC planktonic	22 ± 8	OC-MFC biofilm	21 ± 3

Species richness describes the number of the species present in a certain habitat (Morin, 1999). In T-RFLP analysis, OTU richness reflects the number of TRFs present in each sample (Osborn and Smith, 2005). Generally, there was no significant difference in OTU richness between the samples analysed (Table 6-2). However, OTU richness in the CC-MFC planktonic community was significantly ($P < 0.05$) higher than in the initial groundwater communities. It should be noted that the T-RFLP analysis significantly underestimates the real species richness in the samples due to the exclusion of rare taxa in the fingerprint (Bent et al., 2007; Osborn and Smith, 2005). The species richness detected by 16S rRNA Illumina sequencing is therefore likely to be higher.

Table 6-3 OTU evenness for different groundwater and MFC samples.

Microbial community	OTU evenness	Microbial community	OTU evenness
Groundwater field	0.74 ± 0.06		
Groundwater start	0.36 ± 0.03		
CC-MFC planktonic	0.63 ± 0.02	CC-MFC biofilm	0.72 ± 0.02
SE+CC-MFC planktonic	0.61	SE+CC-MFC biofilm	0.57
ME+S-MFC planktonic	0.73	ME+S-MFC biofilm	0.72
OC-MFC planktonic	0.64 ± 0.05	OC-MFC biofilm	0.71 ± 0.03

Although the OTU richness of the groundwater in the field and at the start of the experiment is the same (Table 6-2), the TRF fingerprint changed significantly during the 6 weeks of storage (Figure 6-15). OTU evenness was therefore calculated from Equation 12 as a measure of distribution of OTUs within different samples.

The groundwater was stored at 4 °C prior to experimentation (6 weeks). The OTU evenness of the groundwater species decreased significantly ($P < 0.05$) during the groundwater storage from 0.74 to 0.36. The groundwater microbial community at the start of the experiment was largely (~78%) represented by the 171 bp TRF. However, the OTU evenness was restored back to the value similar in the field groundwater (~0.7) during the incubation in the MFCs. OTU evenness was similar between the CC- and OC-MFC as well as between the electrode biofilm and planktonic MFC communities. The T-RFLP data was further processed by AMMI.

AMMI, also called doubly-centred PCA, firstly performs analysis of variance (ANOVA) to partition the variation into main effects and interactions, and then applies PCA to these interactions, creating interaction principal components (IPCs). The variation in samples can originate from main effects, i.e. TRFs and environments (ENV), or their interaction TRFs x ENV (Culman et al., 2008).

The variation in TRFs depends on their abundance in different samples, which means how rarely or commonly they occur. The ENV variation originates from the number of peaks present in the sample and the overall signal strength. From the microbial ecology point of view, it is important to understand the TRFs x ENV interaction, describing how the microbial community (TRFs) responds to different treatments (ENV) (Culman et al., 2008). As research conducted by Culman et al. (2008) shows, the ENV variation can be eliminated by peak relativisation but the percentage of TRF variation in the given data set is always significant (40–90%) and can affect the understanding of the data. Statistical methods which eliminate the TRF variation are therefore appropriate, e.g. TRF-centred PCA or AMMI. AMMI applies PCA to the TRFs x ENV interaction and provides useful inside into microbial community structure as it depends on different treatments. It is an especially useful statistical method for processing the data in which the percentage of TRFs x ENV variation is low.

Table 6-4 Percentage of variation for TRFs, ENV and their interaction for all groundwater and MFC samples.

Source	Percentage of Variation
TRFs	52.42%
ENV	0%
TRFs x ENV	47.58%

The AMMI analysis of all the T-RFLP data, from the groundwater and MFCs including biofilm and planktonic communities, revealed important features. ANOVA showed that 52.42% of variation between the samples originated from TRFs (Table 6-4). The first two ICPs (interaction principal components) created by AMMI captured most of the variation (84.79%) in the data (Table 6-5). The biplot created therefore represents the variation in the community sufficiently.

Table 6-5 Percentage of variation for TRFs x ENV interaction represented by the individual ICPs for all groundwater and MFC samples.

Source	Percent Variation	Cumulative Percent
ICP1	62.21%	62.21%
ICP2	22.59%	84.79%
ICP3	8.19%	92.98%
ICP4	3.88%	96.86%

The replicate samples clustered together on the biplot (Figure 6-16) which reflects the fact that the fingerprints of replicate samples were similar (Figure 6-15). The samples from the electrode biofilm and planktonic MFC communities also cluster together (Figure 6-16), indicating that the biofilm communities differ significantly from the planktonic communities. The microbial fuel cells communities appear to be different from the ones initially present in the groundwater. The groundwater community as it was present in the field (GW field) went through a significant shift in composition before the start of the experiment (GW start) which is due to the containment in the bottle and manipulation (Hammes et al., 2010; Konopka, 2009). The community composition then shifts again as it goes through changes in the MFCs. The main TRFs driving the microbial community changes, as determined by AMMI analysis, were 53, 56, 171 and 172 bp long, with other significant TRFs being 58, 62, 176, 339, 340 and 499 bp long. This could also be seen from the relativised peak area matrix (data not shown).

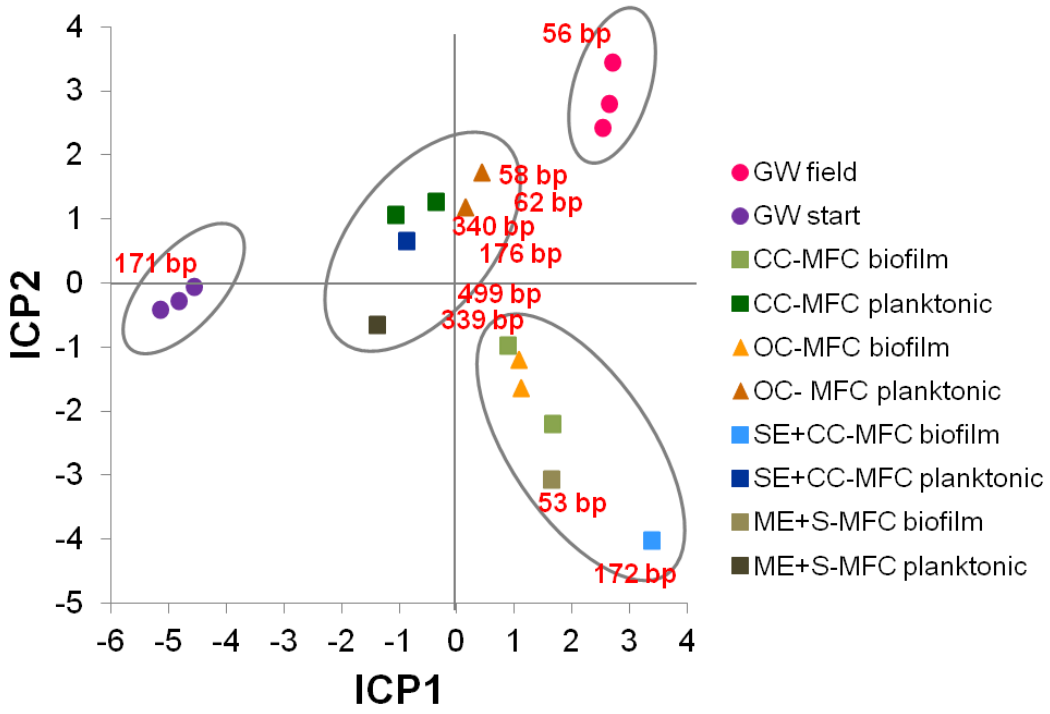

Figure 6-16 Principal component analysis of TRFs x ENV interactions for all groundwater and MFC samples. The red text highlights the main TRFs driving the changes within the different communities. The further from the [0, 0] point, the more pronounced the effect of a certain TRF is.

For better understanding of microbial community interactions within the MFCs, the MFC communities, attached in the electrode biofilm and planktonic communities as well, were compared in a separate AMMI analysis. This time, percentage of variation originating from TRFs was higher (66.71%) (Table 6-6). Cumulative percentage of variation captured by biplot was 88.73% (Table 6-7).

Table 6-6 Percentage of variation for TRFs, ENV and their interaction for all MFC samples.

Source	Percentage of Variation
TRFs	66.71%
ENV	0%
TRFs x ENV	33.29%

Table 6-7 Percentage of variation for TRFs x ENV interaction represented by the individual ICPs for all MFC samples.

Source	Percent Variation	Cumulative Percent
ICP1	65. 58%	65.58%
ICP2	23.14%	88.73%
ICP3	7.25%	95.97%
ICP4	1.9%	97.87%

The replicate samples clustered together as they did in the previous AMMI biplot (Figure 6-17). There was a significant difference between the communities present in the electrode biofilm and planktonic communities, with this difference represented by ICP1 covering 65.58% of the TRFs x ENV variation. The communities present in the OC-MFC were significantly different from the ones in the CC-MFC, the OC-MFC samples clustering on top of the biplot and the CC-MFC samples in the lower part of the graph. The difference between the CC- and OC-MFC communities was less pronounced than the difference between the biofilm and planktonic communities as the ICP2 captured less variation (23.14%) than the ICP1. The main drivers of the AMMI differences were TRFs 53, 171 and 172 bp long, with TRFs 62, 174, 192, 225 339 and 499 bp long contributing somewhat.

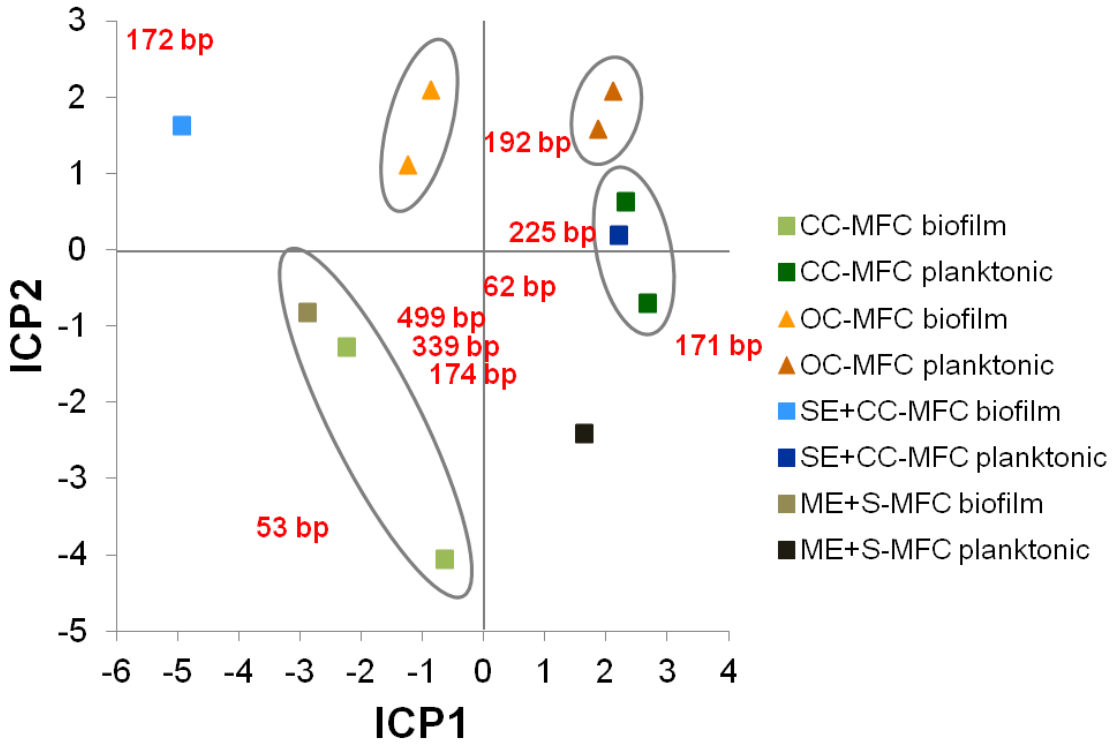

Figure 6-17 Principal component analysis of TRFs x ENV interactions for all MFC samples. The red text highlights the main TRFs driving the changes within the different communities. The further from the [0, 0] point, the more pronounced the effect of certain TRF is.

A sterile electrode was introduced in the CC-MFC (SE+CC-MFC) and mature electrode from the CC-MFC was inserted in the sterile MFC (ME+S-MFC). In theory, the planktonic cells present in the CC-MFC, preferably the electro-active bacteria, would start attaching to the sterile electrode in SE+CC-MFC. Similarly, some cells could detach,

actively or passively, from the mature electrode biofilm in ME+S-MFC (Dreeszen, 2003; Nadell et al., 2009; Stoodley et al., 2002).

The results in Figure 6-17 show that the planktonic community of the SE+CC-MFC was similar to the planktonic communities of other CC-MFCs. This means that the planktonic community remained similar to the CC-MFC community prior to the electrode swap. However, the community which attached to the electrode in SE+CC-MFC differed from other CC-MFC electrode biofilm communities. The SE+CC-MFC electrode community was after 5 days in the initial stages of biofilm development as confirmed by SEM (Section 6.2.2). Based on the electricity data (Chapter 5, Section 5.2.2), it is very likely that the electro-active bacteria attached preferably to the electrode. The community did not have time to develop a complicated biofilm structure.

The electrode of ME+S-MFC was removed from the CC-MFC 5 days prior to the experiment termination. The biofilm electrode community in the ME+S-MFC was confirmed to be similar to other CC-MFC electrode biofilm communities, clustering with the CC-MFC biofilm samples on the biplot (Figure 6-17). This result could be expected as the community did not have much time to undergo changes in the new environment. The bacteria which detached from this electrode biofilm into planktonic phase seem to be significantly different from other CC-MFC planktonic communities.

6.2.4 16S rRNA gene sequencing

Alpha diversity of the samples was analysed after the sequences were clustered and assigned to OTUs. When taking 11,000 sequences per sample (as used for further analysis), ~480 OTUs were identified in the groundwater as sampled in the field (Figure 6-18). The alpha diversity of the community decreased to ~330 OTUs after storing the groundwater in the fridge prior to the MFC experiment. This could be expected due to the confinement in the bottle and significant change of conditions in comparison with the field (Hammes et al., 2010). The conditions in the MFCs are likely to favour a few dominant species which are performing the observed biochemical changes (Rabaey and Verstraete, 2005), resulting in a decrease in alpha diversity of the MFC communities (~140 observed OTUs). A selection of these OTUs would detach from ME+S-MFC biofilm into the planktonic phase and also attach to the electrode in SE+CC-MFC from the planktonic phase as discussed above (Section 6.2.3). This is reflected in the observed alpha diversity of these samples (~80 OTUs). OTU richness determined by 16S rRNA gene sequencing is indeed significantly higher than estimated by T-RFLP analysis (Section 6.2.3).

The shape of the rarefaction curves in Figure 6-18 suggests that the number of sequences analysed was sufficient for capturing the diversity of the MFC communities. More sequences would be needed to identify all the OTUs in the groundwater samples (Osborn and Smith, 2005; Hughes et al., 2001). Previous studies of this groundwater have shown that up to 10 million sequences were required to capture the rare OTUs (unpublished data). However, the main focus of this study are the dominant OTUs in the relation to their function in MFCs. Sequencing effort was therefore adequate for the purposes of this thesis (Hamady and Knight, 2009).

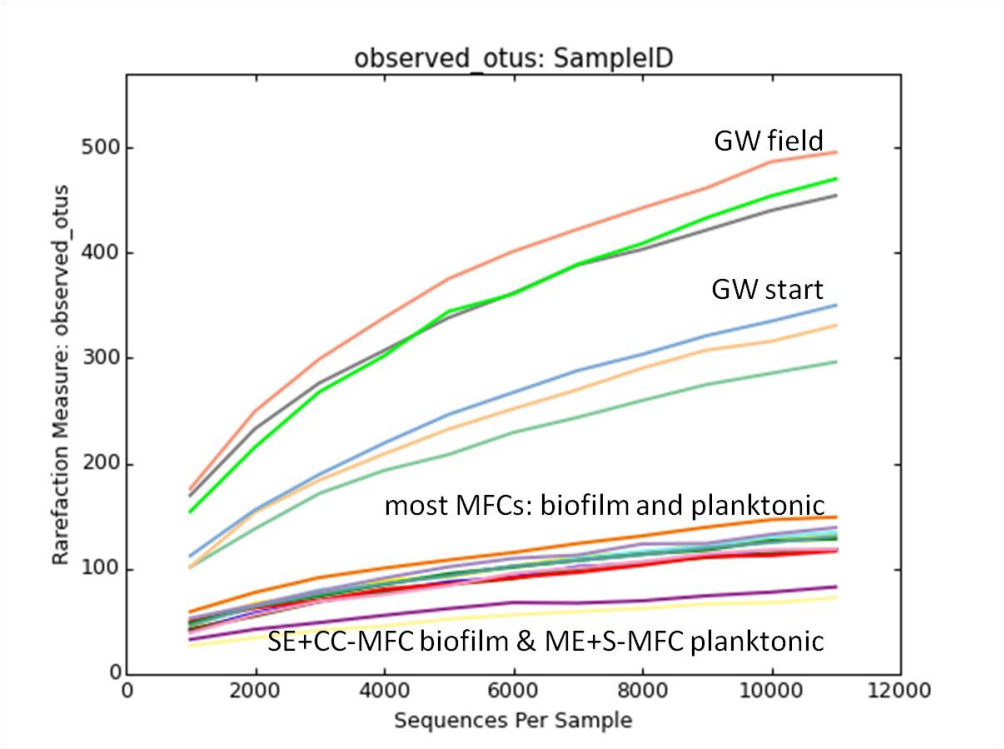

Figure 6-18 Captured alpha diversity of the groundwater and MFC samples. Groundwater as sampled in the field (GW field), groundwater at the start of the experiment (GW start), CC-MFC biofilm and planktonic & OC-MFC biofilm and planktonic & SE+CC-MFC planktonic & ME+S-MFC biofilm (most MFCs: biofilm and planktonic, SE+CC-MFC biofilm & ME+S-MFC planktonic (SE+CC-MFC biofilm & ME+S-MFC planktonic).

Chao1 index is an estimator of richness and can be used to estimate the true number of OTUs present in the samples. It can be calculated from Equation 13 (Hamady and Knight, 2009; Hughes et al., 2001)

$$Chao1 = S_{obs} + \frac{n_1^2}{2n_2} \quad (13)$$

where *Chao1* is the Chao1 index, S_{obs} is the number of observed OTUs, n_1 is the number of singletons (OTUs captured once) and n_2 is the number of doubletons (OTUs captured

twice).* It was estimated that the real number of OTUs present in the groundwater sample as present in the field was ~650, which decreased to ~500 during the storage (Figure 6-19). The estimated number of OTUs present in MFCs is also higher in comparison with the observed value, reaching ~220 OTUs for most MFCs and ~120 OTUs in the ME+S-MFC planktonic phase and the electrode in the SE+CC-MFC.

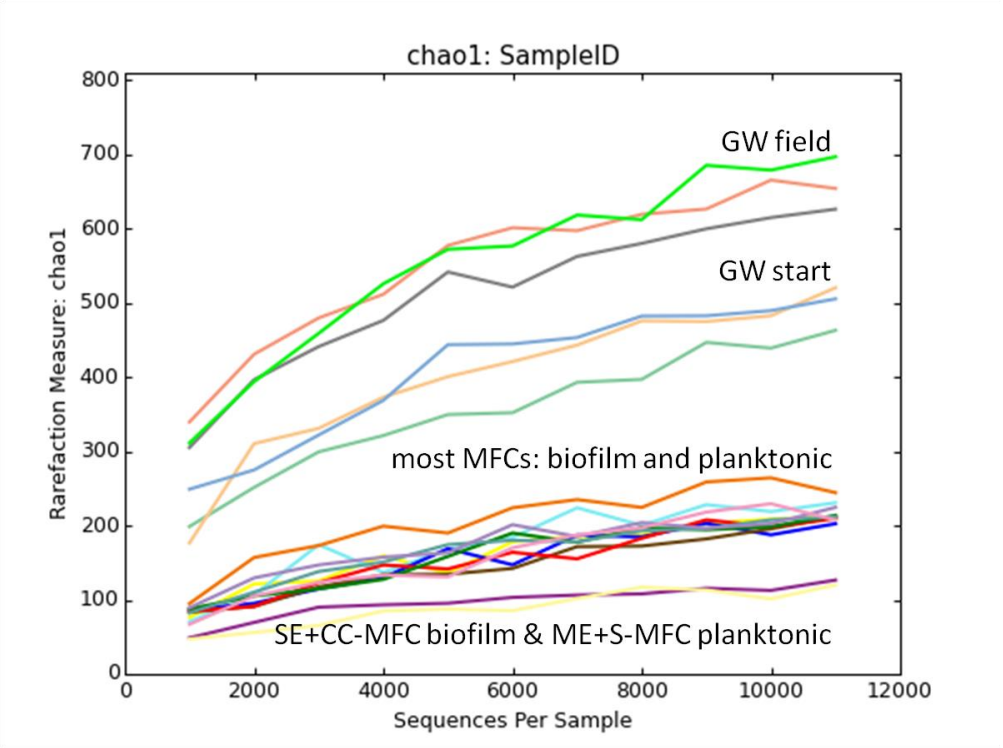

Figure 6-19 Estimated alpha diversity of the groundwater and MFC samples using the chao1 index. Groundwater as sampled in the field (GW field), groundwater at the start of the experiment (GW start), CC-MFC biofilm and planktonic & OC-MFC biofilm and planktonic & SE+CC-MFC planktonic & ME+S-MFC biofilm (most MFCs: biofilm and planktonic, SE+CC-MFC biofilm & ME+S-MFC planktonic (SE+CC-MFC biofilm & ME+S-MFC planktonic). Calculations are shown at different rarefaction depths up to a maximum of 11,000 - the fewest sequences obtained from a sample.

The OTU evenness calculated from Equation 12 was equal to 0.67 for groundwater field samples, 0.43 for starting groundwater and ~0.51 for MFC electrode biofilm and ~0.45 for MFC planktonic samples. This means that the OTUs were more evenly distributed in the groundwater field samples than after manipulation and incubation in the MFCs, indicating that a few OTUs became dominant in the starting groundwater and MFC samples (Morin, 1999; Osborn and Smith, 2005). These OTU evenness values are different from the ones obtained by T-RFLP analysis (Section 6.2.3). Due to the significantly higher coverage of 16S rRNA gene sequencing, these evenness values are more likely to reflect the true structure of the microbial communities.

* Single sequences were removed from the analysis in QIIME as these might be present due to sequencing errors. QIIME then subtracts one from the OTU counts for the calculation of Chao1.

Beta diversity, i.e. the difference between the samples, was explored via UniFrac. It uses the phylogenetic information from the phylogenetic tree and principle coordinates analysis (PCoA) of the unweighted or weighted data (Lozupone et al., 2011). Unweighted analysis provides qualitative view of the data as it only considers the presence or absence of OTUs, whereas the weighted analysis is a quantitative approach as it takes the OTU abundance (percentage) into account (Hamady and Knight, 2009).

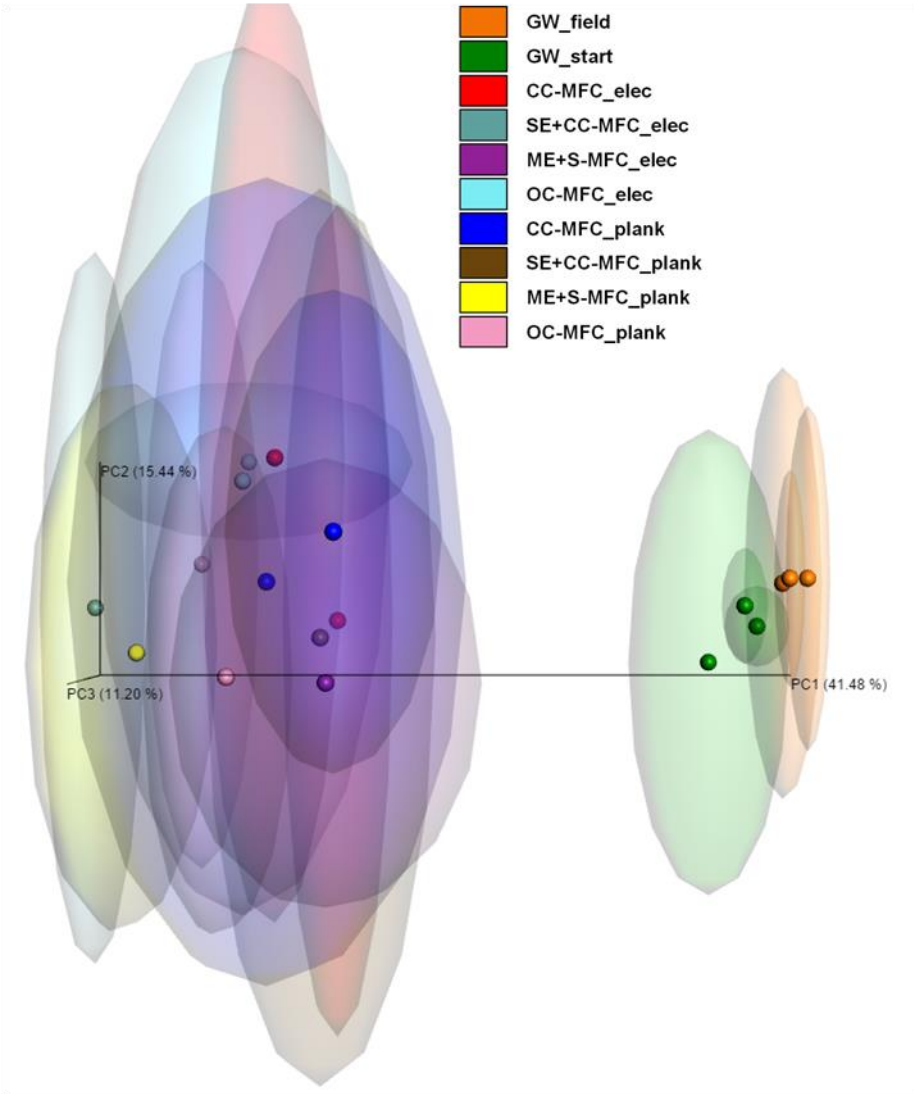

Figure 6-20 UniFrac principal coordinates analysis of unweighted OTU data for all the samples (groundwater and MFCs). The transparent area around the sample point shows the confidence interval for each sample.

The unweighted beta diversity analysis of OTU data shows significant difference between the groundwater samples (field and start) and the MFCs samples (PC1 41.48%) (Figure 6-20). When performing this qualitative analysis, the confidence intervals around the samples were wide. No significant difference could be therefore observed between the

MFC samples. This indicates that the same OTUs were present in all MFC samples but their abundance might vary.

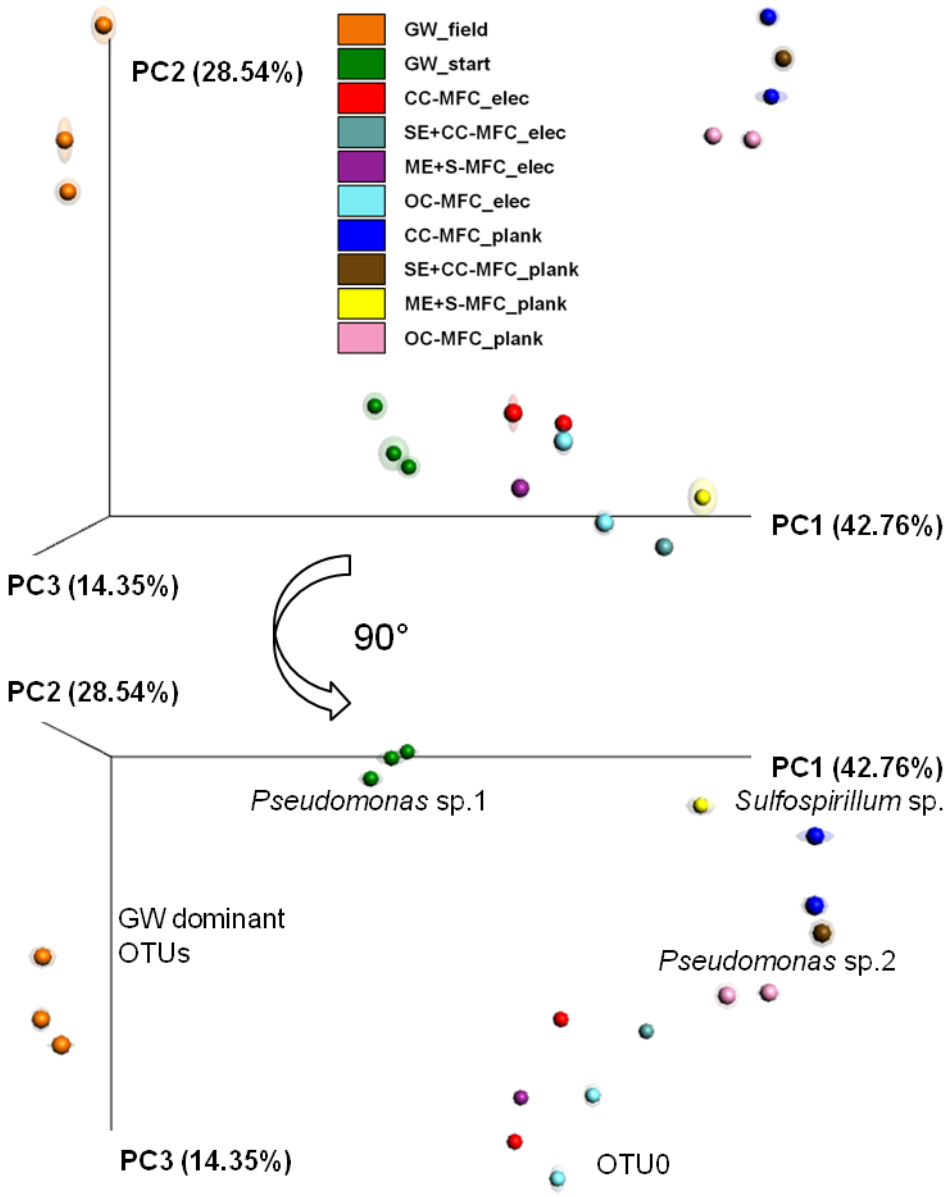

Figure 6-21 UniFrac principal coordinates analysis of weighted OTU data for all the samples (groundwater and MFCs) under two different angles. The transparent area around the sample point shows the confidence interval for each sample. OTUs key to different types of samples are overlaid. GW dominant OTUs: OTU11 Anaerolinaceae, OTU16 Bacteroidales, OTU2 *Geobacter* sp., OTU3 Synergistaceae, OTU31 Peptococaceae, OTU4 Desulfobacteraceae, unassigned OTU45, OTU6 *Desulfobacter* sp. OTU9 Gammaproteobacteria, *Georgfuchsia* sp.

Weighed beta diversity analysis plotted for both, all samples and MFC samples only (Figure 6-21, Figure 6-22), provides better insight into the differences between the groundwater and MFC samples as the confidence intervals decrease. Similarly as with T-RFLP, groundwater field and groundwater start samples separated in the plot clearly

(Figure 6-21). Various OTUs contributed to the separation of the groundwater samples in the plot, namely OTU11 Anaerolinaceae, OTU16 Bacteroidales, OTU2 *Geobacter* sp., OTU3 Synergistaceae, OTU31 Peptococaceae, OTU4 Desulfobacteraceae, unassigned OTU45, OTU6 *Desulfobacter* sp. OTU9 Gammaproteobacteria, *Georgfuchsia* sp. One *Pseudomonas* sp. OTU dominated the starting groundwater sample (Figure 6-21, Figure 6-24, Table 6-8).

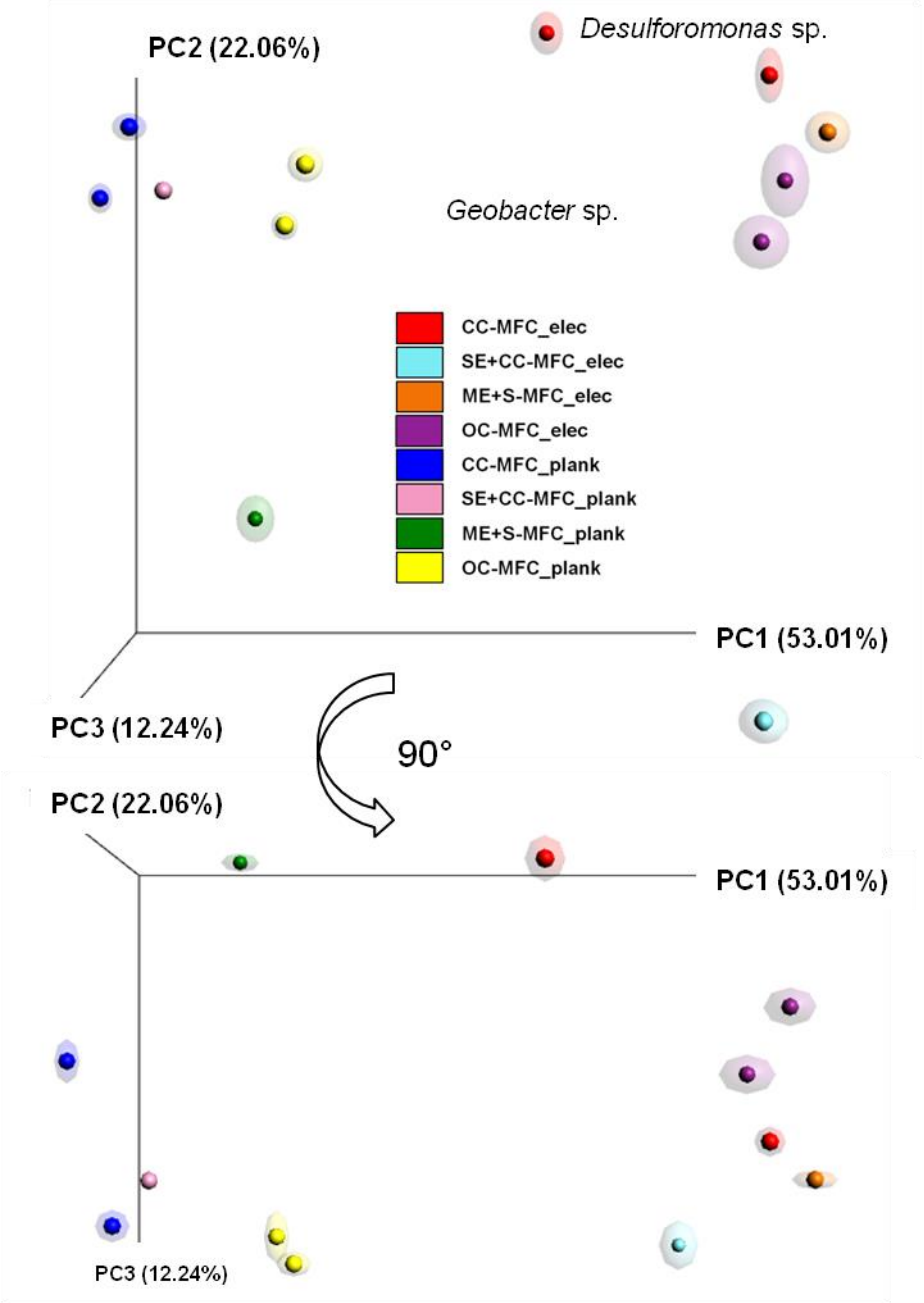

Figure 6-22 UniFrac principal coordinates analysis of weighted OTU data for all the MFC samples under two different angles. The transparent area around the sample point shows the confidence interval for each sample. OTUs key to different types of samples are overlaid.

There was a significant difference between the electrode biofilm and planktonic MFC communities (Figure 6-22, PC1 53.01%) as these clustered closely together. OTU0 Rhofocyclaceae was a dominant member of electrode biofilm communities in all the MFCs (Figure 6-24, Table 6-8). Similarly, *Sulfospirillum* sp. was dominant in the planktonic communities. *Pseudomonas* sp., different to the one dominant in the starting groundwater, occurred in the electrode biofilm and planktonic communities. However, it was more dominant in the planktonic phase. The difference between the CC- and OC-MFC communities was less pronounced but still significant. *Desulfuromonas* sp. dominated the electrode biofilm communities in all the electricity-generating MFCs (CC-MFCs, SE+CC-MFC, ME+S-MFC). *Geobacter* sp. on the other hand occurred mainly in the OC-MFCs, in the biofilm and planktonic phase. The planktonic community of the ME+S-MFC which detached from the electrode, and the electrode community of the SE+CC-MFC which attached to the electrode, were different from other planktonic/electrode biofilm communities, respectively (Figure 6-22, PC2 22.06%).

171 OTUs were found to differ significantly (corrected Bonferroni $P < 0.05$) between the different treatments (groundwater and MFCs). Figure 6-24 and Table 6-8 show the dominant OTUs[*] (above 4% relative abundance in at least one sample, which corresponds to ~500 sequences) which differ significantly for all the samples analysed. P value in the following text represents the corrected Bonferroni P value. Possible function of dominant OTUs based on current literature is discussed below.

As predicted based on previously acquired unpublished data, *Geobacter* spp. were present in the field groundwater. However, their abundance was not as high as 25%, but ranged between 5.1 and 11.9% (data not shown). One of the most dominant *Geobacter* OTUs (uncultured OTU2, sequences clustered at 99% similarity) reached the value of 9.2% in one of the groundwater samples. This OTU was not as abundant in the MFCs (max 0.5% in one of the CC-MFC electrode biofilms) (Figure 6-24 and Table 6-8). Another *Geobacter* sp. OTU (AF223382, sequences clustered at 99% similarity), not as abundant in the groundwater (up to 0.2%), became more dominant in the MFCs, with higher abundance in the OC-MFCs (up to 24%) than CC-MFCs (up to 10%) ($P < 0.05$) in both electrode biofilm and planktonic communities (Figure 6-23). This differs from previous findings where *Geobacter* sp. is the dominant member of the CC-MFC anode community (Chae et al., 2009; Jung and Regan, 2007; Lovley, 2006a; Bond et al., 2002). *Geobacter* sp.,

[*] The sequences assigned to the dominants OTUs can be found in Appendix K.

especially in the OC-MFCs, could have been involved in acetate oxidation using nitrate, Fe(III) or elemental sulphur as electron acceptors (Chae et al., 2009; Sung et al., 2006; De Wever et al., 2000). *Geobacter* sp. could have also contributed to biodegradation of phenols as *Geobacter* sp. were previously shown to degrade aromatic compounds (Zhang et al., 2010; Rooney-Varga et al., 1999; Tender et al., 2002). Some interaction with the electrode is theoretically possible. However, due to lower abundance of this OTU in the CC-MFC electrode biofilm than in the OC-MFC, it is unlikely that this OTU contributed to the electron transfer to the anode significantly.

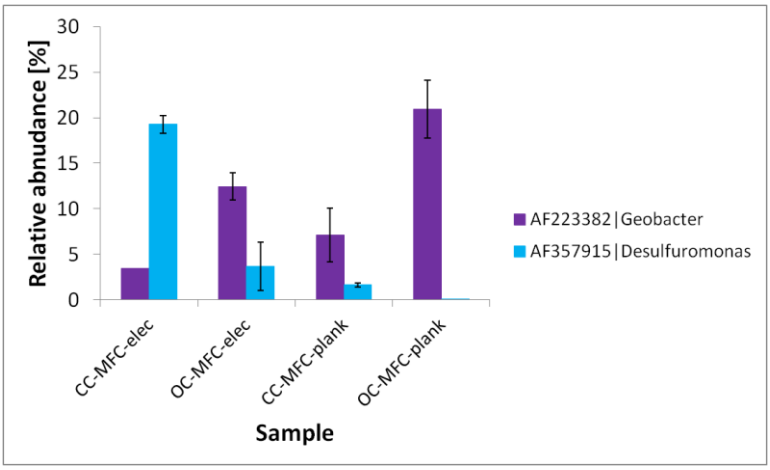

Figure 6-23 Relative abundance of *Geobacter* sp. and *Desulfuromonas* sp. OTUs in the CC- and OC-MFCs. The error bars represent the range of relative abundance in the samples.

Desulfuromonas sp. (AF357915, sequences clustered at 99% similarity), a member of the Geobacteraceae family, was significantly ($P < 0.05$) enriched (18.2–20.7%) on the CC-MFC, SE+CC-MFC and ME+S-MFC electrodes (Figure 6-23, Figure 6-24 and Table 6-8). *Desulforomonas* sp. can, similarly as its close relative *Geobacter* sp., anaerobically oxidise acetate and utilise Fe(III) as an electron acceptor. Extracellular electron transfer (EET) of *Desulforomonas* sp. is performed using c-type cytochromes (Butler et al., 2009; Coates et al., 1996; Lonergan et al., 1996). No evidence of *Desulforomonas* EET via nanowires was found in the up-to-date literature (Web of Science, 14/03/2016, search for Desulfuromonas and nanowires). This is with agreement with the shape of the biofilm colonies in the closed circuit MFCs. Bacteria bridged the gaps between the fibres of the carbon cloth electrode, thereby increasing the surface area for electron transfer to the electrode. *Desulforomonas* sp. have also been previously shown to be the dominant species on the sediment-MFC anodes with acetate serving as an electron donor (Lowy et al., 2006; Holmes et al., 2004; Bond et al., 2002). It is therefore plausible that *Desulforomonas* sp. was responsible for electricity generation in the CC-MFCs while utilising acetate as an electron donor.

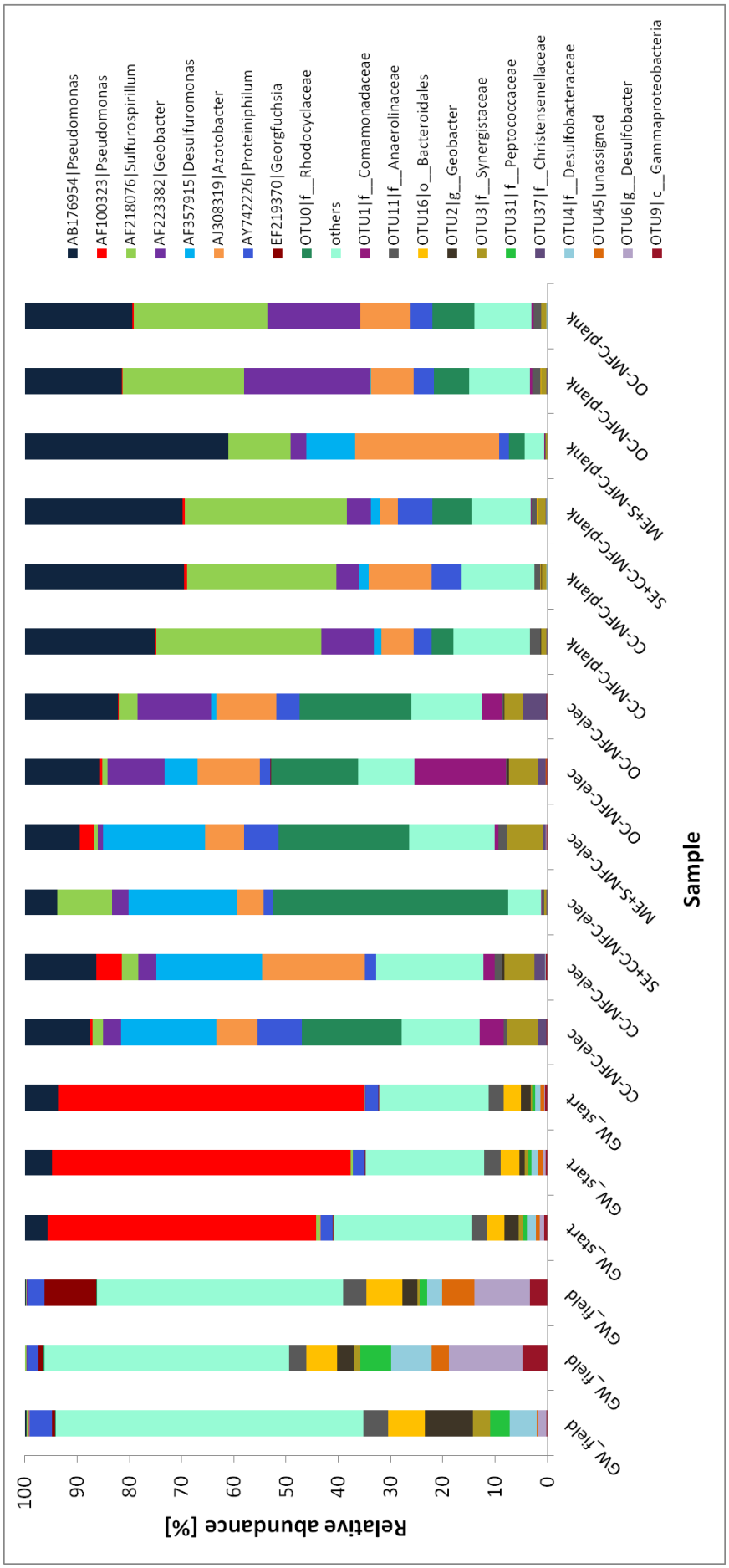

Figure 6-24 Dominant OTUs (above 4% relative abundance, ~500 sequences) in the groundwater (GW) and MFC electrode biofilm (elec) and planktonic (plank) samples.

Table 6-8 Dominant OTUs, their affiliation and abundance range in the groundwater and MFC samples. Percentage of abundance reflects the graph in Figure 6-24, CC-MFC values include SE+CC-MFC and ME+S-MFC, ND - not detected.

Taxonomic affiliation + RDP Gold database match	Highest BLAST hit accession number (sequence identity)	Environment + reference	Groundwater field/ groundwater start abundance (%)	CC-MFC electrode/ planktonic abundance (%)	OC-MFC electrode/ planktonic abundance (%)
Pseudomonadaceae, *Pseudomonas* sp. AB176954	-	-	~0.1/4.4–6.3	6.2–13.6/ 25.0–38.9	14.3–17.7/ 18.6–20.6
Pseudomonadaceae, *Pseudomonas* sp. AF100323	-	-	0.0/51.4–58.6	0.0–4.9/ 0.1–0.5	0.3–0.5/ 0.1–0.3
Campylobacteraceae, *Sulfurospirillum* sp. AF218076	-	-	~0.3/0.2–0.7	0.8–10.3/ 12.0–31.6	1.0–3.6/ 23.3–25.6
Geobacteraceae, *Geobacter* sp. AF223382	-	-	0.1–0.2/~0.1	1.0–3.5/ 3.0–10.0	11.0–14.0/ 17.8–24.1
Geobacteraceae, *Desulfuromonas* sp. AF357915	-	-	0.0/ND	18.2–20.7/ 1.4–9.2	1.0–6.4/ ~0.1
Pseudomonadaceae, *Azotobacter* sp. AJ308319	-	-	0.0/ND–0.0	5.1–19.7/ 3.5–27.6	~11.7/ 8.2–9.5
Porphyromonadaceae, *Proteiniphilum* sp. AY742226	-	-	2.2–4.3/~2.3	1.8–8.5/ 1.9–6.6	2.0–4.4/ ~4.1
Rhodocyclaceae, *Georgfuchsia* sp. EF219370	-	Degradation of aromatic compounds using Fe(III), Mn(IV) and nitrate as electron acceptors (Weelink et al., 2009)	0.5–9.9/~0.2	0.0/0.0	0.0/0.0

Table 6-VIII continued Dominant OTUs, their affiliation and abundance range in the groundwater and MFC samples. Percentage of abundance reflects the graph in Figure 6-24, CC-MFC values include SE+CC-MFC and ME+S-MFC, ND - not detected.

Taxonomic affiliation + RDP Gold database match	Highest BLAST hit accession number (sequence identity)	Environment + reference	Groundwater field/ groundwater start abundance (%)	CC-MFC electrode/ planktonic abundance (%)	OC-MFC electrode/ planktonic abundance (%)
Uncultured bacterium, OTU0 Rhodocyclaceae, *Azovibrio* sp.	JN651989 (100%) KM269364 (100%)	Uncultured bacterium in alkane-dependent methanogenic community (Mbadinga et al., 2012) and biodegradation of alkanes under methanogenic conditions (Abu Laban et al., 2015)	~0.2/0.0	ND–45.1/ ND–7.4	16.7–21.3/ 6.7–8.1
Uncultured bacterium, OTU1 Comamonadaceae	AB731939 (100%)	Organic waste MFC (Yamamoto et al., 2014)	0.0/ND	0.1–4.7/ ~0.1	3.8–17.6/ ~0.4
Uncultured bacterium, OTU11 Anaerolinaceae	EU266919 (100%)	Tar oil contaminated aquifer (Winderl et al., 2008)	3.3–4.7/~3.1	0.4–1.5/ 0.1–2.0	~0.2/~1.5
Uncultured bacterium, OTU16 Bacteroidales	JX307534 (99%) JX307534 (99%)	Toluene contaminated aquifer (Larentis et al., 2013)	5.9–7.0/~3.4	ND–0.0/ ND–0.2	0.0/~0.1
Uncultured bacterium, OTU2 Geobacteraceae, *Geobacter* sp.	EU266833 (99%) EU266825 (99%)	Tar oil contaminated aquifer (Winderl et al., 2008)	2.8–9.2/1.1–2.6	0.0–0.5/ ND–0.1	~0.3/0.0
Uncultured bacterium, OTU3 Synergistaceae	JQ087154 (99%) KF443374 (99%)	BTEX contaminated aquifer - enrichment (Kuppardt et al., 2014)	0.5–3.4/0.4–0.9	0.5–6.8/ 0.4–1.4	3.5–5.5/ ~0.9

Table 6-VIII continued Dominant OTUs, their affiliation and abundance range in the groundwater and MFC samples. Percentage of abundance reflects the graph in Figure 6-24, CC-MFC values include SE+CC-MFC and ME+S-MFC, ND - not detected.

Taxonomic affiliation + RDP Gold database match	Highest BLAST hit accession number (sequence identity)	Environment + reference	Groundwater field/ groundwater start abundance (%)	CC-MFC electrode/ planktonic abundance (%)	OC-MFC electrode/ planktonic abundance (%)
Uncultured bacterium, OTU31 Peptococcaceae, *Desulfosporosinus meridiei*	HM217323 (99%)	BTEX contaminated aquifer (Bombach et al., 2010), isolate - groundwater contaminated by petroleum hydrocarbons (Robertson et al., 2001)	1.5–5.9/~0.6	ND–0.0/ ND	ND/ND
Uncultured bacterium, OTU37 Christensenellaceae	KC853588 (100%)	Contaminated soil (Wiegert et al., 2013)	ND–0.1/ ND–0.0	0.1–2.1/ 0.0–0.1	1.5–4.5/ ~0.1
Uncultured bacterium, OTU4 Desulfobacteraceae	AB754182 (100%) KM410819 (100%)	Sulphur oxidisers (Kojima et al., 2014), biofilm from a sulphidic cave (Hamilton et al., 2015)	2.9–7.7/1.0–1.8	ND–0.1/ ND–0.1	ND–0.0/ ~0.1
Uncultured bacterium, OTU45 unassigned	JQ379757 (97%)	Soil with elevated CO_2 content (Dunbar et al., 2012)	0.1–6.2/~0.7	ND–0.0/ ND–0.0	0.0/0.0
Uncultured bacterium, OTU6 Desulfobacteraceae, *Desulfobacter* sp.	JQ267726 (99%)	Sulphate reducer in petroleum reservoir (Guan et al., 2013)	1.7–14.0/0.2-0.8	ND–0.0/ ND	ND/0.0
Uncultured bacterium, OTU9 Gammaproteobacteria	Not a good cover	-	0.1–4.8/0.3-0.6	0.0–0.3/ ND–0.0	~0.2/ ND–0.0

Two different *Pseudomonas* sp. OTUs were identified in the field groundwater (Figure 6-24, Table 6-8). One of them (AF100323) became significantly ($P < 0.05$) dominant (55.7%) in the groundwater stored at 4 °C. This *Pseudomonas* strain could therefore be psychrophilic (D'Amico et al., 2006). After introduction in the MFCs, the abundance of this strain decreased significantly ($P < 0.05$). Due to high abundance of this *Pseudomonas* OTU (55.7%) in starting groundwater, it is very likely that this OTU corresponds to the 171 bp TRF in the TRF fingerprint (~78% relativised peak area) (Section 6.2.3). However, the percentage of their abundance in the starting groundwater differs significantly between the two techniques. This discrepancy can be explained by the fact that T-RFLP can only capture the dominant OTUs (Bent et al., 2007; Osborn and Smith, 2005).

The second *Pseudomonas* sp. OTU (AB176954) became dominant in the MFCs, especially in the CC-MFC planktonic phase. It is also one of the OTUs which primarily detached from the electrode in the ME+S-MFC. As discussed in section 2.2.3, *Pseudomonas* spp. belong to denitrifying bacteria (Morris et al., 2009), can metabolise various hydrocarbons (Hamme et al., 2003; Samanta et al., 2002; Margesin and Schinner, 2001; Allard and Neilson, 1997) and also produce electricity via electron shuttles (Franks et al., 2010; Pham et al., 2008). This *Pseudomonas* sp. OTU could therefore have contributed to biodegradation of phenols within MFCs while utilising nitrate as an electron acceptor or even possibly contributing to electricity generation due to its presence on the electrode.

Azotobacter sp. (AJ308319) was dominant in the MFCs on the electrodes (5.0–19.7%) and also in the planktonic phase (3.5–27.6%) (Figure 6-24 and Table 6-8). It detached from the electrode in the ME+S-MFC. *Azotobacter* sp. belongs to the Pseudomonaceae family and is best known as an aerobic nitrogen fixer, producing ammonium as a final product of nitrogen reduction. Growth under micro-aerophilic conditions has also been reported (Tilak et al., 2010). Nitrates can serve as an alternative source of nitrogen (Garrity, 2005). *Azotobacter* sp. can degrade various organic substrates, including phenol and acetate (Wong and Maier, 1985). *Azotobacter* sp. OTU was therefore likely to contribute to degradation of phenols and acetate in the MFCs while utilising nitrate as nitrogen source and oxygen entering the anode chamber through the membrane as an electron acceptor.

Proteiniphilum sp. (AY742226) was a dominant species in both groundwater and MFCs (Figure 6-24 and Table 6-8). It belongs to obligate anaerobic chemotrophic bacteria. It was previously found to produce acetic acid from pyruvate (Chen, 2005). *Proteiniphilum* sp. could have therefore produced acetate in the groundwater and MFCs. Uncultured bacterium, OTU0 Rhodocyclaceae, *Azovibrio* sp. was enriched in electrode biofilm communities (ND–

45.1%) which indicates that this bacterium preferably grows in biofilm. It was previously found in alkane-dependent methanogenic community (Mbadinga et al., 2012) and during biodegradation of alkanes under methanogenic conditions (Abu Laban et al., 2015). Its function within the MFCs is unclear. Uncultured bacterium OTU1 Comamonadaceae was dominant in the electrode biofilm communities of the CC- and OC-MFCs. Yamamoto et al. (2014) found the sequence of this bacterium in the anode community of an MFC degrading organic waste. OTU3 Synergistaceae and OTU37 Christensenellaceae were significantly enriched in the MFC communities. The sequences of these OTUs were previously detected in BTEX contaminated aquifer enrichment study (Kuppardt et al., 2014) and contaminated soil (Wiegert et al., 2013), respectively.

OTUs potentially involved in the sulphur cycle include *Sulfurospirillum* sp., OTU31 Peptococcaceae *Desulfosporosinus meridiei*, OTU4 Desulfobacteraceae and OTU6 Desulfobacteraceae *Desulfobacter* sp. (Figure 6-24 and Table 6-8). *Sulfurospirillum* sp. (AF218076) occurred preferably in the planktonic phase of the MFCs ($P < 0.05$). It was previously isolated from anaerobic contaminated soil and was found to be able to utilise various electron acceptors, including nitrate and elemental sulphur, with acetate serving as a carbon source (Luijten, 2003). *Sulfurospirillum* sp. could have therefore contributed to acetate degradation and sulphur reduction in the MFCs. However, it is unclear whether it was capable of sulphate reduction or whether it reduced elemental sulphur after other species performed sulphate reduction to sulphur. Other sulphate reducing OTUs (OTU 31 *Desulfosporosinus meridiei*, OTU4 Desulfobacteraceae and OTU6 *Desulfobacter* sp.) were detected in the field groundwater but were not detected or very few sequences were found in the MFCs. Their previous occurrence is summarised in Table 6-8.

Other OTUs dominant in the groundwater field samples but not in the MFCs include *Georgfuchsia* sp. (EF219370), OTU11 Anaerolinaceae, OTU16 Bacteroidales, unassigned OTU45 and OTU9 Gammaproteobacteria. Their previous occurrence is also summarised in Table 6-8.

In summary, the number of cells in the groundwater incubated in the MFCs increased 10 times in comparison with the groundwater at the start of the experiment. A small percentage of electrode surface (2–4%) was colonised by bacteria. The morphology of the electrode biofilm colonies differed significantly between the different MFC set-ups tested. This was the first indication confirming the hypothesis that the CC- and OC-MFC biofilm communities were significantly different.

Although the primers used for the T-RFLP analysis amplified only small fraction of present bacterial 16S rRNA (Section 6.1.5), T-RFLP provided good insight into temporal changes within the microbial community in the groundwater and MFCs. The 16S rRNA gene sequencing then aided the analysis in the terms of phylogenetic identification of dominants OTUs. OTU richness calculated from T-RFLP data strongly underestimated the true nature of the samples. 16S rRNA sequencing is therefore more appropriate technique to determine the species richness of the sample.

It was hypothesised that the groundwater microbial community will undergo significant changes when incubated in the laboratory MFCs. The number of cells in the planktonic phase increased tenfold when compared with the original groundwater. The MFC and groundwater samples separated clearly on both, the T-RFLP AMMI biplots and PCoA plots created from 16S rRNA gene sequencing. Groundwater field samples were dominated by various OTUs with highest abundance of 14% for *Desulfobacter* sp. and up to 11% *Geobacter* sp. This groundwater contained the highest number of OTUs, ~650 OTUs as calculated from Chao1 index, and the OTUs were more evenly distributed than in the other samples (OTU evenness ~0.7). The groundwater has undergone significant changes when introduced in the MFCs. Only a few OTUs strongly dominated the MFC microbial communities as a result of the MFC selection pressure. This led to lower number of OTUs (~220 or ~120 in some MFCs) and lower OTU evenness (~0.5). The *Geobacter* sp. OTU, which was most dominant in the groundwater (up to 9%), did not become dominant in the MFCs and its abundance decreased significantly. However, another *Geobacter* sp. OTU dominated in the MFCs (up to 24% in the OC-MFC). Similarly, the sulphur reducers dominant in the groundwater were not detected after MFC incubation and *Sulfurospirillum* sp. (~0.3 in the field groundwater) was significantly enriched in the MFCs (up to 31%). *Desulfuromonas* sp. became dominant on the CC-MFC electrodes and was therefore likely to contribute to acetate degradation and electricity generation.

These results demonstrate that the introduction of BES electrodes in the groundwater contaminated by phenolic compounds is likely to generate a distinct microbial community on its surface with enrichment for community members involved in acetate consumption and electro-genesis.

T-RFLP and 16S rRNA gene sequencing revealed significant differences between the electrode biofilm and planktonic MFC microbial communities as hypothesised. Some microbes, namely uncultured bacteria from the families Rhodocyclaceae, Comamonadaceae and Synergistaceae, preferentially attached to the electrode irrespective of whether the

electrode could serve as an electron acceptor or not. Sulphur reducing *Sulfurospirillum* sp. was significantly enriched in the planktonic phase of both the CC- and OC-MFCs. On the other hand, *Pseudomonas* sp. and *Azotobacter* sp. which were likely to have degraded phenols, were present in both electrode biofilm and planktonic communities. Bearing the field-scale BES application or a laboratory-scale BES-PRB in mind, the flow of groundwater through the BESs could remove part of the phenol-degrading community which is not attached to the anode. Some phenol biodegradation could therefore occur on the BES electrode and in the zone behind it.

The hypothesis, that there is significant difference between the CC- and OC-MFC electrode biofilm communities, was also confirmed by the T-RFLP analysis and 16S rRNA gene sequencing. This difference was less pronounced than the difference between the biofilm and planktonic communities as could be seen from the AMMI and PCoA plots. This result is in agreement with the fact that there were not many differences in the biochemical processes occurring in the CC- and OC-MFCs (Chapter 5). The most significant difference between the two MFC systems is in the biodegradation of acetate with acetate removal enhanced by the presence of the electrode. The electrode biofilm communities therefore differed in the terms of the presence of acetate-degrading OTUs. *Desulforomonas* sp., a potential electro-active bacterium and acetate degrader, was significantly enriched on the electrode in all the electricity producing MFCs, whereas *Geobacter* sp. was more dominant in the OC-MFC biofilm. *Geobacter* sp. originally dominant in the groundwater was not shown to be the main exoelectrogen in the CC-MFCs. The difference between the CC- and OC-MFC electrode biofilm community shows that the current generation in the CC-MFC selectively enriched electro-active species. However, it is difficult to predict which exoelectrogen will be dominating the biofilm community.

Desulforomonas sp. was identified as the bacterium potentially responsible for electricity generation in the CC-MFCs, while utilising acetate as an electron donor. *Pseudomonas* sp. and *Azotobacter* sp. were likely to be involved in biodegradation of phenols, using nitrate and oxygen as electron acceptors, respectively. *Sulfurospirillum* sp. was likely to be a key player in sulphur reduction within the MFCs. *Geobacter* sp. was one of the dominant species in the MFCs, possibly contributing to acetate degradation and Fe(III) reduction. *Proteiniphilum* sp. could have been one of the acetate producers. The function of these bacteria within the MFCs would have to be confirmed by further analysis. Various methods for further studies of the microbial community and the function of different bacteria within the MFCs are discussed below.

Understanding the microbial community development in the terms of structure and function generally requires answering the following scientific questions:

- Who is there i.e. what bacteria are present?
- What are they capable of doing?
- What are they doing?

The first question was answered in this thesis by the 16S rRNA gene sequencing. The presence of different functional genes within the microbial community's DNA is the evidence of phylogenetic potential of the community, i.e. what they are capable of. The gene expression in the form of mRNA is linked to the biochemical function performed by the community at a time (Osborn and Smith, 2005; Sharpton, 2014). Various methods of molecular microbial ecology highlighted below can be used to detect the presence of different functional (protein-encoding) genes and their expression.

Metagenome is a collection of all the genes (including the 16S rRNA and functional genes) from all the bacteria present in a sample. Physiological capacity of the community as a whole can be therefore estimated from it (Osborn and Smith, 2005). PICRUSt (phylogenetic investigation of communities by reconstruction of unobserved states) (Langille et al., 2013) is a computational method for predicting metagenome based on the 16S rRNA gene sequences. Its accuracy in the terms of its metagenome predictive power is good for e.g. Human Microbiome Project (Huttenhower et al., 2012) where >700 reference genomes are available. However, environmental samples contain bacteria which have not been cultured and fully sequenced before. The accuracy of PICRUSt predicted metagenome decreases accordingly (Langille et al., 2013). PICRUSt was tested on the MFC samples by Dr. Stephen Rolfe. Although 16S rRNA gene sequencing revealed significant differences between the groundwater and the MFC communities in terms of the abundance of dominant OTUs, there was no significant difference between the groundwater and MFC samples when analysed by PICRUSt. PICRUSt's accuracy was probably not sufficient enough for this analysis for the reasons stated above. It could be used for estimation of the groundwater and MFC metagonomes in the future when more of the complete genomes of environmental bacteria are available.

Shotgun metagenomic sequencing would be preferable for obtaining metagenomic data from the groundwater and MFC microbial communities although the data processing of the raw sequencing data might be challenging and computationally demanding (Sharpton, 2014). It could reveal the differences between the abundance of functional genes between

the groundwater and different MFC samples. The advantage of this method is the fact, that the MFC experiment would not have to be repeated and the DNA extracted from it (Chapter 5 and 6) could be used. Obtaining this data would be useful in the terms of overall capabilities of the different MFC communities. Whole genomes could also be put together during the analysis, thereby linking particular OTUs with their potential function within the microbial community (Sharpton, 2014). However, this could be limited in case the sequenced fragments do not contain a robust phylogenetic marker (e.g. 16S rRNA gene) (Osborn and Smith, 2005).

Linking the OTUs with their potential function within the MFC community would be of main interest of any further studies. Whole-genome sequencing of the dominant OTUs could therefore be performed. The dominant OTUs would have to be isolated, i.e. cultured, from another MFC experiment and then sequenced ("Introduction to Whole-Genome Sequencing," n.d.; Kameshwar and Qin, 2016). *Desulfuromonas* sp., *Geobacter* sp., *Pseudomonas* sp. and *Azotobacter* sp. which are potentially of main interest have been cultured before (for example Venkataraman et al., 2011; Butler et al., 2009; Wong and Maier, 1985). However, other dominant OTUs might prove to be difficult to be cultured under laboratory conditions.

The metagenomic data and whole-genome sequencing provide information about the OTUs present in a sample and potential functional capabilities of the microbial community, i.e. who is there and what are they capable of doing (Sharpton, 2014). This data cannot give evidence of the biochemical processes actually occurring within the community. Reverse transcription PCR (RT-PCR) is a useful technique for investigation of gene expression within the community. RNA is extracted from the samples and protein-encoding mRNA is subjected to reverse transcription to complementary DNA. For example, genes involved in biodegradation of specific pollutants known from metagenomic sequencing can be targeted and quantified in quantitative RT-PCR (q-RT-PCR). Great care has to be taken during the sample preparation as mRNA is an unstable molecule with a short half-life (Osborn and Smith, 2005). q-RT-PCR gives evidence of which genes are expressed and in what quantity and therefore what function is the microbial community performing at a specific time. It can be useful for linking the biochemical processes occurring with the functional genes. The disadvantage of this technique is the need for the choice of specific primers for targeting the specific mRNA molecules.

Stable isotope probing (SIP) is a useful technique for linking specific bacteria with their function within the microbial community. During SIP chemicals labelled with heavy

isotopes of carbon ^{13}C or other elements (^{15}N, ^{2}H, ^{18}O) can be added to the samples to identify the bacteria capable of degrading these chemicals as they would incorporate the heavy isotopes in their DNA. Heavy DNA fraction can then be separated from the light DNA fraction by centrifugation and sequenced (Osborn and Smith, 2005). In this case, ^{13}C-labelled phenol could be added to the MFCs to identify the phenol degraders. It could be confirmed that *Geobacter* sp., *Pseudomonas* sp. or *Azotobacter* sp. are the main phenol degraders. The experiment with ^{13}C-labelled phenol could be performed for a longer period of time, potentially identifying syntrophic interactions within the community. ^{13}C-labelled metabolites of phenol (e.g. acetate) could be utilised by bacteria which are not capable of phenol degradation. Similarly, ^{13}C-labelled acetate could be added in a parallel experiment to identify acetate-degrading bacteria, likely to be *Desulfuromonas* sp., *Geobacter* sp. and *Sulfurospirillum* sp. The MFC experiment would have to be repeated and the DNA samples extracted throughout the duration of the experiment.

Fluorescence in situ hybridisation (FISH) is a hybridisation technique useful for localisation of bacteria within the community, especially in biofilm (Osborn and Smith, 2005; Wolf et al., 2002). The data from 16S rRNA sequencing could be used to create fluorescent-labelled oligonucleotide probes for FISH. In FISH, the fluorescent labelled probes are hybridised with the microbial community's DNA *in situ* and the fluorescence of the hybridised probes is detected. *Desulfuromonas* sp. and other bacteria could be localised within the electrode biofilm using FISH in combination with confocal microscopy. It could be shown whether *Desulfuromonas* sp. is attached directly to the electrode surface as mentioned above and surrounded by other symbiotic bacteria.

Last but not least technique of molecular microbial ecology discussed in this thesis is GeoChip (He et al., 2007). It is a microarray based hybridisation method focused on environmental application enabling identification of >10,000 genes in >150 functional groups. These include genes involved in nitrogen, carbon, sulphur and phosphorus cycles, metal reduction and resistance, and also organic contaminant degradation. It can be used to link the microbial community function to the biochemical processes occurring in the system. Light and heavy DNA fractions as well as mRNA can be applied to GeoChip to inform of the potential function of the community, the function of the SIP-labelled bacteria and also the gene expression linked to the function of the community at a time. As such, it is a powerful tool in molecular microbial ecology.

GeoChip was successfully used for identification and quantification of functional genes involved in uranium bioremediation. Fe(III) and sulphate reducers such as *Geobacter* spp.

and *Desulfovibrio* spp., respectively, are involved in uranium(VI) reduction. The abundance of their genes (c-type cytochrome genes) increased as uranium(VI) reduction increased. It could be used to quantify the abundance of phenol-degrading, TCA cycle, electricity related (c-type cytochrome) and many more genes in the groundwater and MFC samples. The abundance and expression of c-type cytochrome genes in the CC- and OC-MFC would be of special interest as both *Desulfuromonas* sp. dominant in the CC-MFC biofilm and *Geobacter* sp. dominant in the OC-MFC biofilm possess c-type cytochrome genes (Butler et al., 2009). Theoretically, as the CC-MFCs produce electricity, more c-type cytochrome genes should be expressed in the CC-MFC than in the OC-MFC.

Considering all the molecular microbial ecology techniques, GeoChip in combination with SIP and FISH would provide best insight into the MFC microbial community function. The key phenol-degrading and electro-active bacteria including their potential syntrophic interactions within the MFC microbial community could be identified. The dominant bacteria could also be localised within the electrode biofilm and groundwater. This information would be useful for the design of the laboratory BES-PRB reactor and its testing. These techniques could be also used to analyse the microbial communities developed in pilot-scale BESs which are likely to be different from the ones developed in the laboratory BESs. The design of the field-scale BESs could be improved based on the pilot-scale testing and microbial community analysis.

6.3 Conclusion

This is the first study of microbial community development in a microbial fuel cell inoculated with contaminated groundwater without any addition of nutrients. Three hypotheses predicting the microbial community development were set based on the biochemical processes occurring in an MFC degrading phenolic compounds and in a control MFC system. All these hypotheses were confirmed using the microscopic techniques, T-RFLP and 16S rRNA sequencing. The fact that the development of the microbial community within BESs can be forecasted, although in a limited way, is encouraging in the terms of the technology development to the field-scale application. The knowledge of the changes in the microbial community structure (electrode biofilm, sediment and surrounding groundwater) depending on different conditions within BESs can be used to engineer the field-scale systems towards better bioremediation performance. However, more research into microbial response to different BES environments, especially at the field scale, is needed.

Chapter 7

Groundwater microbial fuel cell: *in situ* experiment

Results in Chapter 4 and 5 show that electricity can be produced in a laboratory-scale MFC containing groundwater contaminated by phenolic compounds. Electro-active bacteria use acetate, a product of fermentation of phenols, as an electron donor for electricity generation. The presence of an electrode acting as an electron acceptor enhances biodegradation of acetate even though alternative electron acceptors are present. Enhanced removal of acetate can reduce the feedback inhibition of fermentation of phenols, resulting in their faster removal. Electricity production is an indicator of activity of exoelectrogens and potential for enhanced biodegradation of phenols. The possibility to generate electricity was therefore tested in an *in situ* pilot-scale MFC.

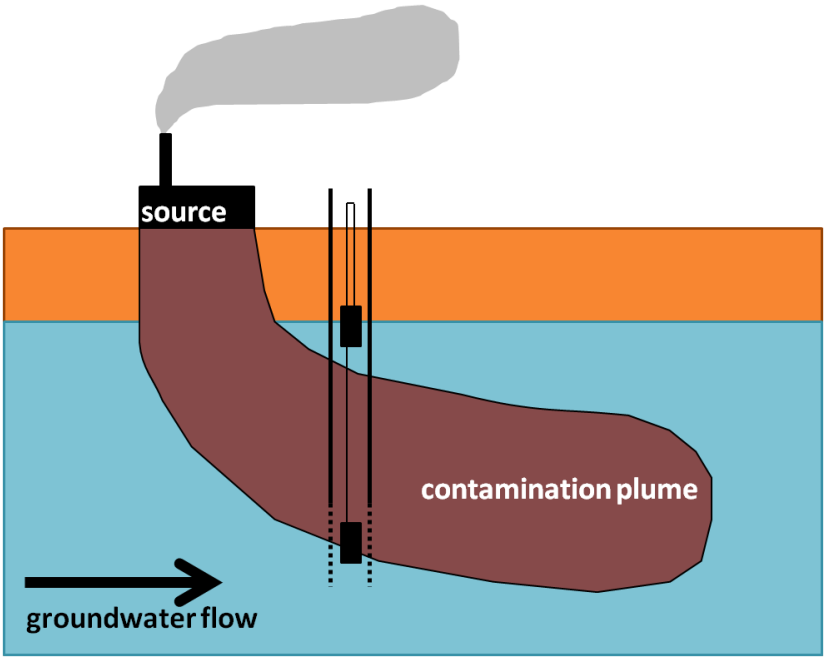

Figure 7-1 Pilot-scale MFC with the anode placed in the borehole screen and floating cathode.

The MFC was installed in borehole 59 at the field site previously used to extract groundwater for MFC experiments (Chapter 4 and 5) (Thornton et al., 2001b). Unfortunately, the borehole did not enable access to groundwater at 12 mbgl which was studied in laboratory-scale MFCs. The anode was therefore placed in the borehole screen at the lower plume fringe at 30 mbgl, the cathode was constructed as a floating cathode, placed at the water table (~5 mbgl) (Thornton et al., 2001b). The electrodes were connected via copper wire and 1 kΩ resistor (Figure 7-1).

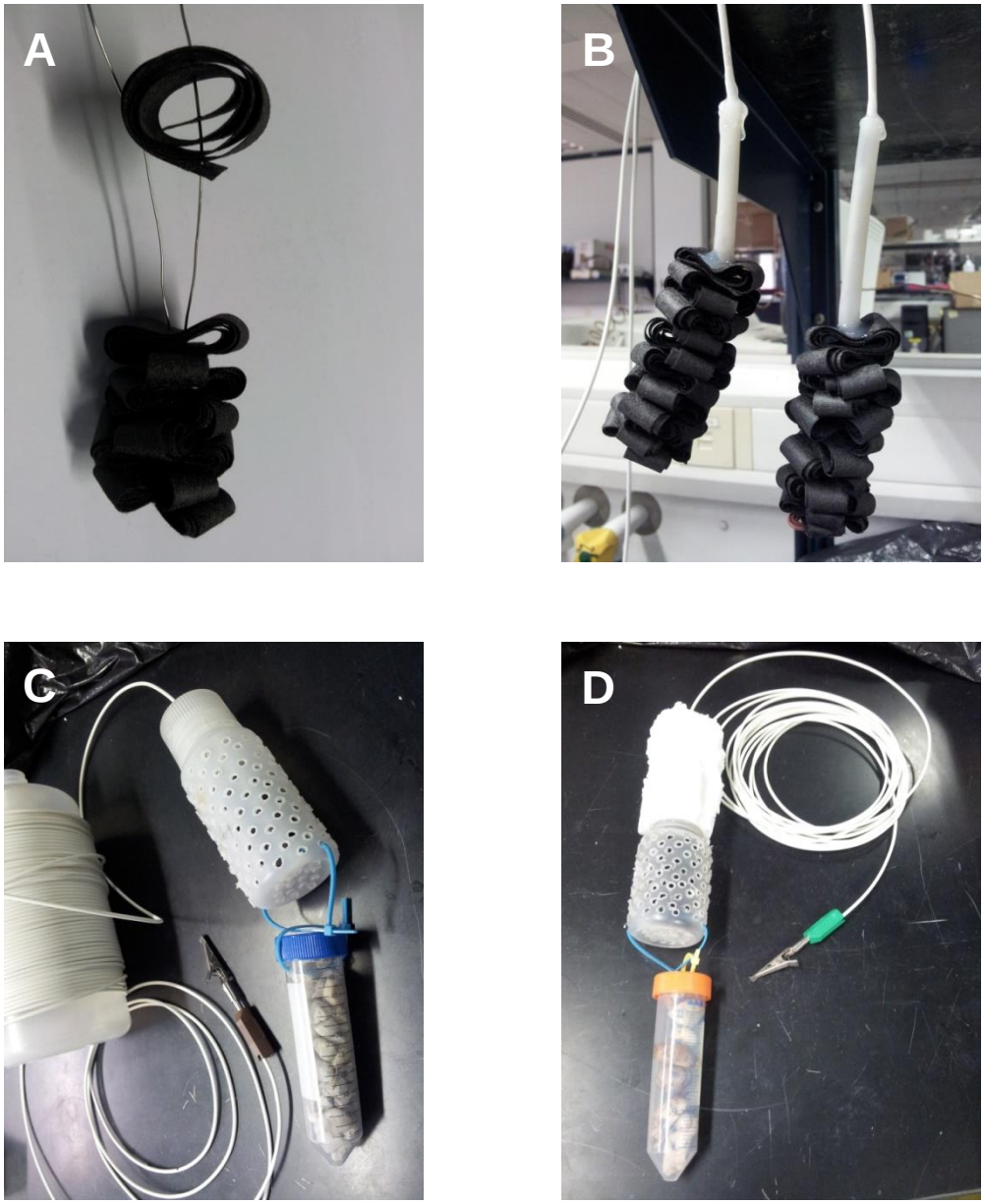

Figure 7-2 Construction of field-scale MFC electrodes. Connection of the carbon cloth strips to the copper wire (A), insulation of the connection between the electrodes and the wire (B), anode inserted in the PTFE bottle with the weight (C) and the floating cathode with the weight (D).

The electrodes were constructed in the laboratory prior to installation in the field (Figure 7-2). Carbon cloth was cut into thin strips which were then pierced by a copper wire functioning as a current collector. The strips were folded so the surface area of the electrode was as large as possible, increasing the space for attachment of electro-active bacteria and providing large area for oxygen reduction on the cathode. Both electrodes were then connected to the wire which would lead up to the surface and attach to the resistor via crocodile clips. The anode wire was 31 metres and the cathode wire 8 metres long. The connection between the electrodes and the wire was insulated by PTFE tubes and silicon glue to prevent the corrosion of the connections which could decrease MFC

efficiency. Both electrodes were then inserted in a perforated PTFE bottle with weight (a cuvette filled with stones and water) attached to it. Polystyrene block was glued to the cathode to make the cathode float at the water table in order to provide good access to oxygen. The MFC was installed in the field at the end of May 2014 and was incubated the first week as an open circuit MFC. After this, 1 kΩ resistor was connected and the OCV and CCV were monitored regularly by a voltmeter. There was 30 min incubation period between the CCV and OCV measurement. The measurement and MFC installation in the field performed by Dr. Steven F. Thornton and Juan Mujica who were collecting other data.

Table 7-1 Voltage measurement results for *in situ* pilot-scale MFC.

Time [days]	OCV [mV]	CCV [mV]
0	234	2
7	125	2
14	34	1
29	86	1
127	4	193

At the day of MFC installation, the OCV reached 234 mV (Table 7-I) which indicates that there was significant difference in redox conditions between the anode and cathode. CCV was low at this point (2 mV) as could be expected because exoelectrogenic bacteria had no time to attach to the electrode. The measured OCV decreased to 34 mV and 86 mV during the first two and four weeks of the experiment, respectively. However, it is questionable whether the OCV value reached steady state during the 30 min incubation. The CCV stayed low during this initial period of the experiment. The next voltage measurement was taken after 4 months of incubation. Confusingly, the OCV is significantly lower (4 mV) than the CCV (193 mV). It seems that there was a mistake made during the voltage measurement and the values were switched and assigned to wrong voltages. The OCV of 193 mV and CCV 4 mV could be expected instead.

To conclude, the pilot-scale MFC did not produce significant amount of electricity (CCV) during the observed period of 4 months. The amount of electricity produced from the pilot-scale MFC could have potentially been limited by high internal resistance of the system (Clauwaert et al., 2008). The distance between the electrodes was 25 m which is approx. 10x more than in the tested laboratory-scale MFC. However, the size of the electrodes could not be increased proportionally. The composition of microbial community

at this depth (30 mbgl) is significantly different from the groundwater present at 12 mbgl tested in laboratory MFCs.

In the ideal case, the future pilot-scale MFC would be set up with the anode at 12 mbgl to provide comparable data with the laboratory study (Chapter 5). The distance between the electrodes would be decreased to 7 metres which would significantly decrease the internal resistance. This could also be reduced by increasing the surface area of the electrodes (Table 2-1). The data quality could be improved by continuous monitoring of the CCV as it was achieved in the laboratory. However, this field-scale set-up would require drilling/digging at the field site to install the electrodes and weather insulation of the data logger. Significant financial support would be needed to conduct this experiment.

Chapter 8

Thesis synthesis, future research and conclusion

8.1 Synthesis

In this thesis, the potential for bioelectrochemically-enhanced remediation as an *in situ* groundwater remediation technique was evaluated. The literature review on the topic revealed numerous knowledge gaps. Most studies performed to date have used bioelectrochemical systems inoculated with microbial communities which did not originate from contaminated field sites (Section 2.3, Table 2-2). The experiments were typically carried out in mineral media often enriched with vitamins, with single carbon sources. Such systems are far away from practical BES *in situ* applications where the naturally occurring microbial community would be involved in biodegradation of contaminants in mixtures. Preferably, no nutrients would be added. In this study, laboratory BESs (H-type MFCs) were used to evaluate the effect of electrode presence on the biodegradation rate of phenolic compounds in contaminated groundwater. The microbial community developed in these MFCs from the groundwater inoculum was studied subsequently.

8.1.1 Initial tests

The MFC device and methodology of operating it were improved in order to obtain good quality electrical, chemical and microbiological data (Chapter 4). Filtration of groundwater through the bottle-top filter (90 mm with 0.8 μm pre-filter and 0.2 μm sterilising filter VacuCap, Pall), was identified to be the best means of groundwater sterilisation prior to MFC experimentation, with a minimum impact on its chemical composition (Section 4.5).

In the first tests (Chapter 4, Section 4.4), the dual-chamber MFCs were operated either with contaminated groundwater in both chambers or with contaminated groundwater in the anode chamber and uncontaminated in the cathode chamber. Both of these MFCs generated electricity. The MFC with contaminated groundwater in both chambers was able to reach higher voltage value than the MFC with uncontaminated groundwater in the cathode chamber. This was due to the higher electrical conductivity of the contaminated groundwater and therefore decreased internal resistance. These MFCs provide the first evidence that biodegradation of phenols can be enhanced by the presence of the electrode. Phenols did not serve as electron donors for electricity production.

8.1.2 Processes occurring in an MFC inoculated with groundwater contaminated by phenolic compounds

The main experiment, studied in the terms of biochemical changes (Chapter 5) and microbial community development (Chapter 6), used the MFC set-up with the contaminated groundwater in the anode chamber and uncontaminated groundwater in the cathode chamber as this resembles the field-scale BES design (Section 2.2.5). These MFCs produced electricity of ~1.8 mW/m^2 of projected electrode surface area, with the internal resistance of the systems being 3.9 kΩ (Chapter 5, Section 5.2.2).

Syntrophic interactions within the groundwater microbial community were shown to be important for enhanced biodegradation of the phenolic compounds and for extracellular electron transfer in BESs (Chapter 5). Phenols were fermented to acetate in the field studied and this acetate then served as an electron donor for electricity generation by the electrode biofilm community in an MFC. Biodegradation of all phenols (phenol, isomers of cresols and xylenols) was enhanced in the MFCs after acetate depletion. 4-hydroxybenzoic acid and 4-hydroxy-3-methylbenzoic acid were identified as key metabolites of phenols which indicates that phenolic compounds were degraded via anaerobic metabolic pathways. However, the end product of this degradation was not identified. Phenols could have therefore been fermented to acetate, thereby supporting further electricity generation, or directly to carbon dioxide. This would have to be evaluated in further experiments (Section 8.2).

Syntrophic interactions within the microbial community are likely to be important during the BES-enhanced biodegradation of organic contaminants other than phenols. Contaminants such as alkanes and aromatic hydrocarbons (BTEX and phenols) are after initial activation of the molecule anaerobically biodegraded in β-oxidation process. This results in the production of acetyl-CoA and potentially acetate (Bian et al., 2015; Heider and Fuchs, 1997). As stated earlier, bacteria in the Geobacteraceae family prefer simple substrates such as acetate (Chae et al., 2009), although biodegradation of toluene and benzoate by *Geobacter metallireducens* in a BES has been reported (Zhang et al., 2010; Tender et al., 2002). Biodegradation of more complex organic compounds therefore requires syntrophy between the fermentative bacteria and exoelectrogens (Chae et al., 2009).

Bioelectrochemically-enhanced biodegradation of chlorinated solvents such as TCE and PCE is likely to be different in terms of syntrophy. When fermentable substrates are added for successful biodegradation of chlorinated solvents, syntrophic interactions between the fermenters and chlorinated-solvents reducers have been observed. Complex

carbohydrates were fermented to acetate and hydrogen. These metabolites were then utilised by chlorinated-solvents reducing bacteria as electron donors for reductive dehalogenation (David et al., 2015). Theoretically, the BES electrodes provide chlorinated-solvents reducers with electrons directly without any need for syntrophy. Indeed, most studies on biodegradation of chlorinated solvents in BESs used pure cultures of bacteria (Section 2.3). This hypothesis should be tested in experiments where BES-enhanced biodegradation of chlorinated solvents is observed using microbial communities originating from contaminated sites.

The bacterium likely to be responsible for acetate degradation while producing electricity was identified using 16S rRNA gene sequencing as *Desulfuromonas* sp. It comprised ~20% of the electrode biofilm community in the MFCs which were generating electricity (Chapter 6). *Desulfuromonas* spp. are capable of direct extracellular electron transfer via c-type cytochromes (Butler et al., 2009) and no evidence of *Desulfuromonas* sp. producing nanowires has been reported to date (Web of Science, 14/03/2016, search for Desulfuromonas and nanowires).

Desulfuromonas sp. was not as abundant in the groundwater at the field site (0.02%) as *Geobacter* spp. (11%), which was originally hypothesised to be the main electro-active bacteria in the laboratory MFCs. These results demonstrate that it is difficult to predict which exoelectrogen will become dominant in the electrode biofilm community based on the composition of the original groundwater microbial community. As previously reported by Ishii et al. (2008), different exoelectrogens can be enriched under different conditions (external resistance or anode potential). *Geobacter* sp. could therefore become dominant under different BES conditions.

The Coulombic efficiency of acetate degradation in MFCs reached 54%. This indicates that bacteria other than the electricity-generating *Desulfuromonas* sp. were utilising acetate as a carbon source. Bacteria which could have degraded acetate in the MFCs include *Geobacter* sp. (mainly in the OC-MFCs) and planktonic *Sulfurospirillum* sp. These bacteria might not be the only acetate degraders as acetate is easily degradable and many bacteria are known to possess the genes for acetate metabolism (Madigan et al., 2011).

The presence of the electrode as an electron acceptor enhanced acetate removal, which had a positive effect on biodegradation of phenolic compounds (Chapter 4 and 5). *Geobacter* sp., *Pseudomonas* sp. and *Azotobacter* sp., present in both biofilm and planktonic communities, were identified as candidate phenolics-degrading bacteria. When the water level in the MFCs was maintained by the addition of fresh sterile groundwater (containing

acetate) after each sampling, the maximum difference in phenol concentration between the electricity-producing MFC and its open-circuit control was 80 μM ± 20 μM (Chapter 5). This corresponded to an 8% enhancement in phenol biodegradation. Enhanced removal of phenols was observed only for a short period of time. When MFCs were operated with contaminated groundwater in both chambers, and no fresh sterilised contaminated groundwater or acetate solution was added to maintain the water level in the chambers, the evidence of enhanced phenol biodegradation was clearer (Chapter 4, Section 4.4). Without groundwater addition, the MFCs operated in non-turnover mode, generating lower voltages (20-30 mV) for more than 30 days. During this period, the concentration of total phenols in the electricity-producing MFC decreased 45% faster compared with the open-circuit control. Operating the MFCs with no acetate supply, and therefore limited electricity generation, enhanced the biodegradation of phenols much more significantly (Chapter 4, Section 4.4) than when acetate was provided throughout the experiment (Chapter 5).

These results show that the presence of the electrode can enhance removal of acetate and when acetate is removed completely and limited amount of electricity is generated in non-turnover mode, biodegradation of phenols is enhanced significantly. In field-scale BESs constructed as BES-PRB (Section 2.2.5.1), different zones could be developed to support different stages of biodegradation of phenols and presence of different dominant bacterial species in relation to the groundwater flow. The contaminated groundwater containing the mixture of phenols and acetate would firstly enter the electrode section of the PRB. It would be the main area suitable for enhanced acetate removal with acetate degraders mostly attached in the electrode biofilm community. The following section would receive the contaminated groundwater depleted of acetate. In this zone, enhanced phenol removal would occur. Phenol degraders would be likely present in sediment biofilm and groundwater planktonic phase (Chapters 5 and 6).

Electron acceptors other than the electrode were present in the anode chamber of the laboratory MFC (Chapter 5). Oxygen and nitrogen could enter the anode chamber via the Nafion membrane whereas Fe(III) and sulphate were already present in the contaminated groundwater. The evidence presented in Chapter 5 shows that all these electron acceptors were utilised by bacteria in an order consistent with thermodynamic predictions and the redox ladder concept. The dominant OTUs, identified in the MFCs by the 16S rRNA gene sequencing, included oxygen, nitrate, Fe(III) and sulphate (sulphur) reducers (Chapter 6) which is in agreement with the biochemical processes observed. Obligate aerobic,

facultative and also strictly anaerobic bacteria were present. Obligate aerobes could have theoretically been present near the membrane where oxygen was entering the anode chamber. These bacteria would deplete oxygen, preventing it from reaching further into the anode chamber. Strictly anaerobic bacteria could have therefore coexisted in the MFC system with strict aerobes. The presence of oxygen in a field-scale BES is probably very limited due to fast oxygen depletion by biodegradation in the contaminant plume, relative to supply by diffusion and dispersion (Atlas and Philp, 2005). Strictly aerobic bacteria might not therefore be enriched in an *in situ* BES, such that biodegradation of phenols would occur under anaerobic conditions.

8.1.3 Pilot-scale test

A pilot-scale groundwater MFC (Chapter 7) was installed in a monitoring well within the contaminant plume at the field site used in the study in Chapter 5. The anode was placed at a depth of 30 mbgl, which significantly increased the internal resistance of the system (Clauwaert et al., 2008; Logan et al., 2006). The groundwater in contact with the anode at the field site was a different composition from that (12 mbgl) successfully tested in Chapter 5 with a different microbial community (unpublished data). The experiment did not provide good quality data. It would have to be repeated and the set-up improved. Ideally, the anode would be placed in the groundwater from 12 mbgl which was tested in Chapter 5. This should decrease the internal resistance of the MFCs and provide a microbial community which was shown to produce electricity and enhance biodegradation of phenols in laboratory experiments. However, this comparison could not be made at the field scale due to the design of the monitoring well, which sampled groundwater from a different part of the contaminants plume.

8.2 Future research

After performing experiments in this thesis, new scientific questions have arisen. The biodegradation of phenolic compounds was enhanced after depletion of acetate in the substrate mixture (Chapter 4, Section 4.4 and Chapter 5). The regulation of the metabolic pathways for biodegradation of phenols and the final products of this biodegradation remain unknown. The dominant bacterial species in the MFCs were identified using 16S rRNA gene sequencing and linked with their function within the MFCs using the information available in the literature. However, two organisms which share the 16S rRNA sequences do not have to possess the same protein encoding genes and therefore do not display the same function within the community (Case et al., 2007). Horizontal gene

transfer between bacteria can also occur, potentially providing distant relatives with genes needed for biodegradation of contaminants they would not be able to utilise otherwise (Walker, 2010). The function of the dominant bacteria within the phenol degrading MFCs should be therefore evaluated by further experiments.

The regulation of pathways involved in biodegradation of phenols in MFCs could be studied using chemostat (Novick and Szilard, 1950), in combination with numerical modelling. Kinetics of the biochemical reactions involved in biodegradation of phenols, mass transfer processes and other non-biological processes could be quantified. This information would be useful when designing a laboratory-scale BES-PRB similar to the one developed by Lai et al. (2014) and Majone et al. (2013). Metabolic rate of electro-active and phenol-degrading bacteria could be regulated by varying the concentration of acetate in the feed and effluent as evident from the results presented in Chapters 4 and 5 as discussed in Section 8.1.2.

The results observed in Chapter 5 in combination with Section 4.4 suggest that the groundwater community growing under limitation by acetate would degrade phenols at a faster rate than in the system where acetate was not a limiting substrate. By definition of a chemostat, the amount of acetate in the effluent should be kept below detection limit. However, this could still provide enough acetate for the community to use as a main carbon source and electron donor for electricity generation. The acetate concentration in the feed should therefore be regulated to approach a near zero concentration in the influent, leaving the community with phenolic compounds as the main carbon source. Based on the results from this thesis (Chapter 4 Section 4.4 and Chapter 5), the MFCs without acetate supply would operate in non-turnover mode and biodegradation of phenols could be enhanced significantly.

The information gained from the chemostat studies could be enhanced by using the stable isotope probing (SIP) technique, either directly in chemostat or batch MFC experiments. SIP is useful for studying biodegradation pathways and also for microbial community analysis as discussed in Chapter 6 (Osborn and Smith, 2005). C^{13}-labelled phenol could be added to the chemostat feed or to the batch experiment. Heavy isotopes of all the metabolites of phenol (4-hydroxybenzoic acid, 4-hydroxy-3-methylbenzoic acid, acetate and carbon dioxide) could be quantified using mass spectrometry. This would help quantify the rates of biochemical reactions and identify the final products of phenol metabolism, as the final product of phenol degradation in the MFCs was unclear (Chapter

5). Moreover, phenol-degrading bacteria would incorporate C^{13} into their DNA, enabling their identification by 16S rRNA sequencing. The presence/absence of C^{13} DNA in the cells of electro-active bacteria would show whether they utilise acetate produced by phenol degraders, thereby confirming or refusing the syntrophic interactions within the MFC microbial community. Electro-active bacteria and phenol-degraders could be localised within the electrode biofilm community by FISH in combination with confocal microscopy.

The above mentioned microbial community analyses would have to be performed within a new BES experiment. However, functional genes present in the groundwater and MFCs could be identified by GeoChip or metagenomic sequencing prior to any further BES experiments. GeoChip would also be a useful technique to apply to the microbial community analysis after a new BES experiment, to examine the functional genes of light and heavy DNA fractions and gene expression. The combination of SIP, FISH and GeoChip data would provide information about the microbial community function within the MFCs and link the biochemical processes occurring with the bacterial species performing them. This information could then be used when designing further BES experiments.

The research on biodegradation of phenols in BESs could be expanded from using the MFCs in the initial experiments to BESs with a controlled anode potential, as this set-up is more likely to be feasible for *in situ* application (Section 2.2.5). The optimum anode potential supporting the fastest biodegradation rate of phenols could be found.

Biodegradation of contaminants other than phenols should be explored, including the biodegradation pathways and microbial community development and function. Understanding the regulation of the pathways of different contaminants and the knowledge of the optimum anode potential could lead to the development and first testing of the PRB-BES reactor on a laboratory scale. Pilot-scale test in the field would be the next step for bioelectrochemically-enhanced remediation of contaminated groundwater. Pilot-scale field tests would be necessary to evaluate the feasibility of this technology in the field-scale application as the laboratory-scale tests fail to represent the environmental conditions discussed in Chapter 2. The knowledge of microbial community development and function under different BES conditions would lead to a tailored BES field design for best bioremediation performance.

Every contaminated field setting is different in terms of the contaminants present, microbial community and environmental conditions. Bioelectrochemically-enhanced bioremediation will have to be adapted to the conditions specific to a given field setting (Chabert et al., 2015; Li and Yu, 2015). A framework for field-scale BES application could be created to firstly evaluate the suitability of the technology for the specific contamination scenarios and microbial communities. The BESs are likely to be designed specifically for each contaminated field after initial testing.

8.3 Thesis conclusion

The biodegradation of organic contaminants with a low redox potential can be enhanced by providing the indigenous groundwater microbial community with an electrode serving as an electron acceptor. This was shown in the thesis in a laboratory-scale microbial fuel cell inoculated with groundwater contaminated by phenolic compounds. Biodegradation of organic contaminants in the bioelectrochemical systems is likely to be a two-step process, where the contaminants are firstly fermented to simpler compounds such as acetate, which are further utilised by electro-active bacteria. Syntrophic interactions within the microbial community are therefore important for successfully enhancing the biodegradation of these contaminants. Electro-active bacteria build biofilm on the electron-accepting electrode which enhances the overall electron transfer. Electron acceptors dissolved in groundwater can be used by other bacteria as usual. Bacteria degrading the organic contaminants can be present in both a biofilm and plantkonic phase. This potential functional distribution should be considered when designing bioelectrochemical systems for enhanced bioremediation of groundwater. More research on the regulation of metabolic pathways involved in contaminant biodegradation and microbial community function is needed for successful future development of bioelectrochemically-enhanced remediation. Other research areas identified for the development of bioelectrochemical systems for *in situ* application in remediation of organic contaminants include (i) the development of novel materials and BES designs, (ii) the effect of various environmental conditions, (iii) the role of the microbial community present and (iv) the effect of the electrode potential on the contaminant biodegradation rate.

9 References

Abdo, Z., Schüette, U.M.E., Bent, S.J., Williams, C.J., Forney, L.J., Joyce, P., 2006. Statistical methods for characterizing diversity of microbial communities by analysis of terminal restriction fragment length polymorphisms of 16S rRNA genes. Environ. Microbiol. 8, 929–38. doi:10.1111/j.1462-2920.2005.00959.x

Abu Laban, N., Dao, A., Semple, K., Foght, J., 2015. Biodegradation of C 7 and C 8 iso -alkanes under methanogenic conditions. Environ. Microbiol. 17, 4898–4915. doi:10.1111/1462-2920.12643

Acar, Y.B., Alshawabkeh, A.N., 1993. Principles of electrokinetic remediation. Environ. Sci. Technol. 27, 2638–2647. doi:10.1021/es00049a002

Aelterman, P., Freguia, S., Keller, J., Verstraete, W., Rabaey, K., 2008. The anode potential regulates bacterial activity in microbial fuel cells. Appl. Microbiol. Biotechnol. 78, 409–418. doi:10.1007/s00253-007-1327-8

Ahn, Y., Logan, B.E., 2010. Effectiveness of domestic wastewater treatment using microbial fuel cells at ambient and mesophilic temperatures. Bioresour. Technol. 101, 469–475. doi:10.1016/j.biortech.2009.07.039

Allard, A.-S., Neilson, A.H., 1997. Bioremediation of organic waste sites: A critical review of microbiological aspects. Int. Biodeterior. Biodegradation 39, 253–285. doi:10.1016/S0964-8305(97)00021-8

Alvarez, P.J.J., Illman, W.A., 2006. Bioremediation and natural attenuation: Process fundamentals and mathematical models, 1st ed. John Wiley & Sons, Inc., New Jersey.

An, J., Kim, B., Nam, J., Ng, H.Y., Chang, I.S., 2013. Comparison in performance of sediment microbial fuel cells according to depth of embedded anode. Bioresour. Technol. 127, 138–42. doi:10.1016/j.biortech.2012.09.095

Andrews, J.E., Brimblecombe, P., Jickells, T.D., Liss, P.S., Reid, B.J., 2004. An introduction to environmental chemistry, 2nd ed. Blackwell Science, Ltd., Oxford.

Arends, J.B.A., Blondeel, E., Tennison, S.R., Boon, N., Verstraete, W., 2012. Suitability of granular carbon as an anode material for sediment microbial fuel cells. J. Soils Sediments 12, 1197–1206. doi:10.1007/s11368-012-0537-6

Atlas, R.M., Philp, J., 2005. Bioremediation: applied microbial solutions for real-world, 1st ed. ASM Press, Washington, DC.

Aulenta, F., Canosa, A., Reale, P., Rossetti, S., Panero, S., Majone, M., 2009. Microbial reductive dechlorination of trichloroethene to ethene with electrodes serving as electron donors without the external addition of redox mediators. Biotechnol. Bioeng. 103, 85–91. doi:10.1002/bit.22234

Aulenta, F., Majone, M., 2010. Bioelectrochemical systems for subsurface remediation, in: Rabaey, K., Angenent, L.T., Schröder, U., Keller, J. (Eds.), Bioelectrochemical Systems: From Extracellular Electron Transfer to Biotechnological Application. London, New York, pp. 305–326.

Aulenta, F., Reale, P., Canosa, A., Rossetti, S., Panero, S., Majone, M., 2010. Characterization of an electro-active biocathode capable of dechlorinating trichloroethene and cis-dichloroethene to ethene. Biosens. Bioelectron. 25, 1796–1802. doi:10.1016/j.bios.2009.12.033

Aulenta, F., Tocca, L., Verdini, R., Reale, P., Majone, M., 2011. Dechlorination of trichloroethene in a continuous-flow bioelectrochemical reactor: effect of cathode potential on rate, selectivity, and electron transfer mechanisms. Environ. Sci. Technol. 45, 8444–51. doi:10.1021/es202262y

Aulenta, F., Verdini, R., Zeppilli, M., Zanaroli, G., Fava, F., Rossetti, S., Majone, M., 2013. Electrochemical stimulation of microbial cis-dichloroethene (cis-DCE) oxidation by an ethene-assimilating culture. N. Biotechnol. 30, 749–55. doi:10.1016/j.nbt.2013.04.003

Behera, M., Murthy, S.S.R., Ghangrekar, M.M., 2011. Effect of operating temperature on performance of microbial fuel cell. Water Sci. Technol. 64, 917–922. doi:10.2166/wst.2011.704

Bent, S.J., Pierson, J.D., Forney, L.J., 2007. Measuring Species Richness Based on Microbial Community Fingerprints : the Emperor Has No Clothes 73, 2399–2401. doi:10.1128/AEM.02383-06

Bian, X.-Y., Maurice Mbadinga, S., Liu, Y.-F., Yang, S.-Z., Liu, J.-F., Ye, R.-Q., Gu, J.-D., Mu, B.-Z., 2015. Insights into the Anaerobic Biodegradation Pathway of n-Alkanes in Oil Reservoirs by Detection of Signature Metabolites. Sci. Rep. 5, 9801. doi:10.1038/srep09801

Bisaillon, J.G., Lepine, F., Beaudet, R., Sylvestre, M., 1991. Carboxylation of o-cresol by an anaerobic consortium under methanogenic conditions. Appl. Environ. Microbiol. 57, 2131–2134.

Boll, M., Fuchs, G., 2005. Unusual reactions involved in anaerobic metabolism of phenolic compounds. Biol. Chem. 386, 989–97. doi:10.1515/BC.2005.115

Bombach, P., Hubschmann, T., Fetzer, I., Kleinsteuber, S., Geyer, R., Harms, H., Muller, S., 2010. Resolving composition and structure of natural microbial communities in contaminated aquifers using community fingerprinting and flow cytometry.

Bond, D.R., Holmes, D.E., Tender, L.M., Lovley, D.R., 2002. Electrode-reducing microorganisms that harvest energy from marine sediments. Science 295, 483–485. doi:10.1126/science.1066771

Bosch, J., Fritzsche, A., Totsche, K.U., Meckenstock, R.U., 2010a. Nanosized Ferrihydrite Colloids Facilitate Microbial Iron Reduction under Flow Conditions. Geomicrobiol. J. 27, 123–129. doi:10.1080/01490450903456707

Bosch, J., Heister, K., Hofmann, T., Meckenstock, R.U., 2010b. Nanosized iron oxide colloids strongly enhance microbial iron reduction. Appl. Environ. Microbiol. 76, 184–189. doi:10.1128/AEM.00417-09

Bossert, I.D., Young, L.Y., 1986. Anaerobic oxidation of p-cresol by a denitrifying bacterium. Appl. Environ. Microbiol. 52, 1117–1122.

Bullen, R.A., Arnot, T.C., Lakeman, J.B., Walsh, F.C., 2006. Biofuel cells and their development. Biosens. Bioelectron. 21, 2015–2045. doi:10.1016/j.bios.2006.01.030

Butler, J.E., Young, N.D., Lovley, D.R., 2009. Evolution from a respiratory ancestor to fill syntrophic and fermentative niches: comparative fenomics of six Geobacteraceae species. BMC Genomics 10, 103. doi:10.1186/1471-2164-10-103

Cameotra, S.S., Makkar, R.S., 2010. Biosurfactant-enhanced bioremediation of hydrophobic pollutants. Pure Appl. Chem. 82, 97–116. doi:10.1351/PAC-CON-09-02-10

Caporaso, J.G., Kuczynski, J., Stombaugh, J., Bittinger, K., Bushman, F.D., Costello, E.K., Fierer, N., Peña, A.G., Goodrich, J.K., Gordon, J.I., Huttley, G.A., Kelley, S.T., Knights, D., Koenig, J.E., Ley, R.E., Lozupone, C.A., McDonald, D., Muegge, B.D., Pirrung, M., Reeder, J., Sevinsky, J.R., Turnbaugh, P.J., Walters, W.A., Widmann, J., Yatsunenko, T., Zaneveld, J., Knight, R., 2010. QIIME allows analysis of high-throughput community sequencing data. Nat. Methods 7, 335–336. doi:10.1038/nmeth.f.303

Case, R.J., Boucher, Y., Dahllof, I., Holmstrom, C., Doolittle, W.F., Kjelleberg, S., 2007. Use of 16S rRNA and rpoB Genes as Molecular Markers for Microbial Ecology Studies. Appl. Environ. Microbiol. 73, 278–288. doi:10.1128/AEM.01177-06

Chabert, N., Amin Ali, O., Achouak, W., 2015. All ecosystems potentially host electrogenic bacteria. Bioelectrochemistry 106, 88–96. doi:10.1016/j.bioelechem.2015.07.004

Chae, K., Choi, M., Verstraete, W., 2008. Microbial fuel cells: Recent advances, bacterial communities and application beyond electricity generation. Environ. Eng. Res. 13, 10–15.

Chae, K.-J., Choi, M.-J., Lee, J.-W., Kim, K.-Y., Kim, I.S., 2009. Effect of different substrates on the performance, bacterial diversity, and bacterial viability in microbial fuel cells. Bioresour. Technol. 100, 3518–3525. doi:10.1016/j.biortech.2009.02.065

Chapelle, F., 2001. Groundwater microbiology and geochemistry, 2nd ed. John Wiley & Sons, Inc., New Jersey.

Chen, S., 2005. Proteiniphilum acetatigenes gen. nov., sp. nov., from a UASB reactor treating brewery wastewater. Int. J. Syst. Evol. Microbiol. 55, 2257–2261. doi:10.1099/ijs.0.63807-0

Chen, Z., Zhao, Y., Bai, J., Li, H., Zhou, R., Hong, M., 2014. Migration and transformation behavior of volatile phenol in the vadose zone. Water Sci. Technol. 70, 685. doi:10.2166/wst.2014.279

Cheng, S., Liu, H., Logan, B.E., 2006. Increased performance of single-chamber microbial fuel cells using an improved cathode structure. Electrochem. commun. 8, 489–494. doi:10.1016/j.elecom.2006.01.010

Christensen, T.H., Bjerg, P.L., Banwart, S.A., Jakobsen, R., Heron, G., Albrechtsen, H.-J., 2000. Characterization of redox conditions in groundwater contaminant plumes. J. Contam. Hydrol. 45, 165–241. doi:10.1016/S0169-7722(00)00109-1

Clauwaert, P., Aelterman, P., Pham, T.H., De Schamphelaire, L., Carballa, M., Rabaey, K., Verstraete, W., 2008. Minimizing losses in bio-electrochemical systems: the road to applications. Appl. Microbiol. Biotechnol. 79, 901–913. doi:10.1007/s00253-008-1522-2

Clement, B.G., Kehl, L.E., DeBord, K.L., Kitts, C.L., 1998. Terminal restriction fragment patterns (TRFPs), a rapid, PCR-based method for the comparison of complex bacterial communities. J. Microbiol. Methods 31, 135–142. doi:10.1016/S0167-7012(97)00105-X

Coates, J.D., Phillips, E.J., Lonergan, D.J., Jenter, H., Lovley, D.R., 1996. Isolation of Geobacter species from diverse sedimentary environments. Appl. Environ. Microbiol. 62, 1531–6.

Commission, E., 2008. Groundwater Protection in Europe. Luxembourg.

Cruz Viggi, C., Bellagamba, M., Matturro, B., Rosseti, S., Aulenta, F., 2014. An innovative bioelectorchemical approach to accelerate hydrocarbons biodegradation in anoxic contaminated marine sediments: the "Oil-Spill Snorkel," in: EU-ISMET 2014. Alcala, Spain.

Culman, S.W., Bukowski, R., Gauch, H.G., Cadillo-Quiroz, H., Buckley, D.H., 2009. T-REX: software for the processing and analysis of T-RFLP data. BMC Bioinformatics 10, 171. doi:10.1186/1471-2105-10-171

Culman, S.W., Gauch, H.G., Blackwood, C.B., Thies, J.E., 2008. Analysis of T-RFLP data using analysis of variance and ordination methods: a comparative study. J. Microbiol. Methods 75, 55–63. doi:10.1016/j.mimet.2008.04.011

D'Amico, S., Collins, T., Marx, J.-C., Feller, G., Gerday, C., 2006. Psychrophilic microorganisms: challenges for life. EMBO Rep. 7, 385–389. doi:10.1038/sj.embor.7400662

David, M.M., Cecillon, S., Warne, B.M., Prestat, E., Jansson, J.K., Vogel, T.M., 2015. Microbial ecology of chlorinated solvent biodegradation. Environ. Microbiol. 17, 4835–4850. doi:10.1111/1462-2920.12413

De Wever, H., Cole, J.R., Fettig, M.R., Hogan, D.A., Tiedje, J.M., 2000. Reductive Dehalogenation of Trichloroacetic Acid by Trichlorobacter thiogenes gen. nov., sp. nov. Appl. Environ. Microbiol. 66, 2297–2301. doi:10.1128/AEM.66.6.2297-2301.2000

Dohnal, V., Fenclova, D., 1995. Air-Water Partitioning and Aqueous Solubility of Phenols. J. Chem. Eng. Data 40, 478–483. doi:10.1021/je00018a027

Dreeszen, P.H., 2003. Biofilm: The key to understanding and controlling bacterial growth in automated animal drinking water systems.

Du, Z., Li, H., Gu, T., 2007. A state of the art review on microbial fuel cells: A promising technology for wastewater treatment and bioenergy. Biotechnol. Adv. 25, 464–482. doi:10.1016/j.biotechadv.2007.05.004

Dunbar, J., Eichorst, S.A., Gallegos-Graves, L.V., Silva, S., Xie, G., Hengartner, N.W., Evans, R.D., Hungate, B.A., Jackson, R.B., Megonigal, J.P., Schadt, C.W., Vilgalys, R., Zak, D.R., Kuske, C.R., 2012. Common bacterial responses in six ecosystems exposed to 10 years of elevated atmospheric carbon dioxide. Environ. Microbiol. 14, 1145–1158. doi:10.1111/j.1462-2920.2011.02695.x

Edgar, R.C., 2010. Search and clustering orders of magnitude faster than BLAST. Bioinformatics 26, 2460–2461. doi:10.1093/bioinformatics/btq461

Eweis, J.B., Ergas, S.J., Chang, D.P.Y., Schroeder, E.D., 1998. Bioremediation Principles, 1st ed. WCB/McGraw-Hil.

Franks, A.E., Malvankar, N., Nevin, K.P., 2010. Bacterial biofilms: the powerhouse of a microbial fuel cell. Biofuels 1, 589–604. doi:10.4155/bfs.10.25

Franks, A.E., Nevin, K.P., 2010. Microbial Fuel Cells, A Current Review. Energies 3, 899–919. doi:10.3390/en3050899

Friman, H., Schechter, A., Nitzan, Y., Cahan, R., 2013. Phenol degradation in bio-electrochemical cells. Int. Biodeterior. Biodegradation 84, 155–160. doi:10.1016/j.ibiod.2012.04.019

Fuhrman, J. a, 2009. Microbial community structure and its functional implications. Nature 459, 193–199. doi:10.1038/nature08058

Garrity, G.M. (Ed.), 2005. Bergey's Manual of Systematic Bacteriology, Volume 2: Proteobacteria. Springer, New York.

Gorby, Y. a, Yanina, S., McLean, J.S., Rosso, K.M., Moyles, D., Dohnalkova, A., Beveridge, T.J., Chang, I.S., Kim, B.H., Kim, K.S., Culley, D.E., Reed, S.B., Romine, M.F., Saffarini, D. a, Hill, E. a, Shi, L., Elias, D. a, Kennedy, D.W., Pinchuk, G., Watanabe, K., Ishii, S., Logan, B., Nealson, K.H., Fredrickson, J.K., 2006. Electrically conductive bacterial nanowires produced by Shewanella oneidensis strain MR-1 and other microorganisms. Proc. Natl. Acad. Sci. U. S. A. 103, 11358–11363. doi:10.1073/pnas.0604517103

Görke, B., Stülke, J., 2008. Carbon catabolite repression in bacteria: many ways to make the most out of nutrients. Nat. Rev. Microbiol. 6, 613–624. doi:10.1038/nrmicro1932

Gotelli, N.J., Colwell, R.K., 2001. Quantifying biodiversity: procedures and pitfalls in the measurement and comparison of species richness. Ecol. Lett. 4, 379–391. doi:10.1046/j.1461-0248.2001.00230.x

Grindstaff, M., 1998. Bioremediation of chlorinated solvent contaminated groundwater.

Guan, J., Xia, L.-P., Wang, L.-Y., Liu, J.-F., Gu, J.-D., Mu, B.-Z., 2013. Diversity and distribution of sulfate-reducing bacteria in four petroleum reservoirs detected by using 16S rRNA and dsrAB genes. Int. Biodeterior. Biodegradation 76, 58–66. doi:10.1016/j.ibiod.2012.06.021

Hamady, M., Knight, R., 2009. Microbial community profiling for human microbiome projects: Tools, techniques, and challenges. Genome Res. 19, 1141–1152. doi:10.1101/gr.085464.108

Hamilton, T.L., Jones, D.S., Schaperdoth, I., Macalady, J.L., 2015. Metagenomic insights into S(0) precipitation in a terrestrial subsurface lithoautotrophic ecosystem. Front. Microbiol. 5. doi:10.3389/fmicb.2014.00756

Hamme, J.D. Van, Singh, A., Ward, O.P., 2003. Recent Advances in Petroleum Microbiology Recent Advances in Petroleum Microbiology. Microbiol. Mol. Biol. Rev. 67, 503–549. doi:10.1128/MMBR.67.4.503–549.2003

Hammes, F., Vital, M., Egli, T., 2010. Critical Evaluation of the Volumetric "Bottle Effect" on Microbial Batch Growth. Appl. Environ. Microbiol. 76, 1278–1281. doi:10.1128/AEM.01914-09

Hau, H.H., Gralnick, J.A., 2007. Ecology and biotechnology of the genus Shewanella. Annu. Rev. Microbiol. 61, 237–58. doi:10.1146/annurev.micro.61.080706.093257

He, Z., Angenent, L.T., 2006. Application of bacterial biocathodes in microbial fuel cells. Electroanalysis 18, 2009–2015. doi:10.1002/elan.200603628

He, Z., Gentry, T.J., Schadt, C.W., Wu, L., Liebich, J., Chong, S.C., Huang, Z., Wu, W., Gu, B., Jardine, P., Criddle, C., Zhou, J., 2007. GeoChip: a comprehensive microarray for investigating biogeochemical, ecological and environmental processes. ISME J. 1, 67–77. doi:10.1038/ismej.2007.2

He, Z., Huang, Y., Manohar, A.K., Mansfeld, F., 2008. Effect of electrolyte pH on the rate of the anodic and cathodic reactions in an air-cathode microbial fuel cell. Bioelectrochemistry 74, 78–82. doi:10.1016/j.bioelechem.2008.07.007

Heider, J., Fuchs, G., 1997. Anaerobic Metabolism of Aromatic Compounds. Eur. J. Biochem. 243, 577–596. doi:10.1111/j.1432-1033.1997.00577.x

Herlemann, D.P.R., Labrenz, M., Jurgens, K., Bertilsson, S., Waniek, J.J., Andersson, A.F., 2011. Transitions in bacterial communities along the 2000 km salinity gradient of the Baltic Sea. ISME J 5, 1571–1579.

Holmes, D.E., Bond, D.R., O'Neil, R. a, Reimers, C.E., Tender, L.R., Lovley, D.R., 2004. Microbial communities associated with electrodes harvesting electricity from a variety of aquatic sediments. Microb. Ecol. 48, 178–90. doi:10.1007/s00248-003-0004-4

Huang, D.-Y., Zhou, S.-G., Chen, Q., Zhao, B., Yuan, Y., Zhuang, L., 2011. Enhanced anaerobic degradation of organic pollutants in a soil microbial fuel cell. Chem. Eng. J. 172, 647–653. doi:10.1016/j.cej.2011.06.024

Huang, L., Chai, X., Quan, X., Logan, B.E., Chen, G., 2012a. Reductive dechlorination and mineralization of pentachlorophenol in biocathode microbial fuel cells. Bioresour. Technol. 111, 167–174. doi:10.1016/j.biortech.2012.01.171

Huang, L., Gan, L., Wang, N., Quan, X., Logan, B.E., Chen, G., 2012b. Mineralization of pentachlorophenol with enhanced degradation and power generation from air cathode microbial fuel cells. Biotechnol. Bioeng. 109, 2211–21. doi:10.1002/bit.24489

Huang, L., Gan, L., Zhao, Q., Logan, B.E., Lu, H., Chen, G., 2011a. Degradation of pentachlorophenol with the presence of fermentable and non-fermentable co-substrates in a microbial fuel cell. Bioresour. Technol. 102, 8762–8768. doi:10.1016/j.biortech.2011.07.063

Huang, L., Regan, J.M., Quan, X., 2011b. Electron transfer mechanisms, new applications, and performance of biocathode microbial fuel cells. Bioresour. Technol. 102, 316–323. doi:10.1016/j.biortech.2010.06.096

Huang, L., Wang, Q., Quan, X., Liu, Y., Chen, G., 2013. Bioanodes/biocathodes formed at optimal potentials enhance subsequent pentachlorophenol degradation and power generation from microbial fuel cells. Bioelectrochemistry 94, 13–22. doi:10.1016/j.bioelechem.2013.05.001

Huang, W.S., 2011. Electricity generation from biochemical energy transformation of microbial fuel cell (MFC) utilizing PAHs as carbon sources. University of Sheffield.

Hughes, J.B., Hellmann, J.J., Ricketts, T.H., Bohannan, B.J.M., 2001. Counting the Uncountable: Statistical Approaches to Estimating Microbial Diversity. Appl. Environ. Microbiol. 67, 4399–4406. doi:10.1128/AEM.67.10.4399-4406.2001

Huttenhower, C., Gevers, D., Knight, R., Abubucker, S., Badger, J.H., Chinwalla, A.T., Creasy, H.H., Earl, A.M., FitzGerald, M.G., Fulton, R.S., Giglio, M.G., Hallsworth-Pepin, K., Lobos, E.A., Madupu, R., Magrini, V., Martin, J.C., Mitreva, M., Muzny, D.M., Sodergren, E.J., Versalovic, J., Wollam, A.M., Worley, K.C., Wortman, J.R., Young, S.K., Zeng, Q., Aagaard, K.M., Abolude, O.O., Allen-Vercoe, E., Alm, E.J., Alvarado, L., Andersen, G.L., Anderson, S., Appelbaum, E., Arachchi, H.M., Armitage, G., Arze, C.A., Ayvaz, T., Baker, C.C., Begg, L., Belachew, T., Bhonagiri, V., Bihan, M., Blaser, M.J., Bloom, T., Bonazzi, V., Paul Brooks, J., Buck, G.A., Buhay, C.J., Busam, D.A., Campbell, J.L., Canon, S.R., Cantarel, B.L., Chain, P.S.G., Chen, I.-M.A., Chen, L., Chhibba, S., Chu, K., Ciulla, D.M., Clemente, J.C., Clifton, S.W., Conlan, S., Crabtree, J., Cutting, M.A., Davidovics, N.J., Davis, C.C., DeSantis, T.Z., Deal, C., Delehaunty, K.D., Dewhirst, F.E., Deych, E., Ding, Y., Dooling, D.J., Dugan, S.P., Michael Dunne, W., Scott Durkin, A., Edgar, R.C., Erlich, R.L., Farmer, C.N., Farrell, R.M., Faust, K., Feldgarden, M., Felix, V.M., Fisher, S., Fodor, A.A., Forney, L.J., Foster, L., Di Francesco, V., Friedman, J., Friedrich, D.C., Fronick, C.C., Fulton, L.L., Gao, H., Garcia, N., Giannoukos, G., Giblin, C., Giovanni, M.Y., Goldberg, J.M., Goll, J., Gonzalez, A., Griggs, A., Gujja, S., Kinder Haake, S., Haas, B.J., Hamilton, H.A., Harris, E.L., Hepburn, T.A., Herter, B., Hoffmann, D.E., Holder, M.E., Howarth, C., Huang, K.H., Huse, S.M., Izard, J., Jansson, J.K., Jiang, H., Jordan, C., Joshi, V., Katancik, J.A., Keitel, W.A., Kelley, S.T., Kells, C., King, N.B., Knights, D., Kong, H.H., Koren, O., Koren, S., Kota, K.C., Kovar, C.L., Kyrpides, N.C., La Rosa, P.S., Lee, S.L., Lemon, K.P., Lennon, N., Lewis, C.M., Lewis, L., Ley, R.E., Li, K., Liolios, K., Liu, B., Liu, Y., Lo, C.-C., Lozupone, C.A., Dwayne Lunsford, R., Madden, T., Mahurkar, A.A., Mannon, P.J., Mardis, E.R., Markowitz, V.M., Mavromatis, K., McCorrison, J.M., McDonald, D., McEwen, J., McGuire, A.L., McInnes, P., Mehta, T., Mihindukulasuriya, K.A., Miller, J.R., Minx, P.J., Newsham, I., Nusbaum, C., O'Laughlin, M., Orvis, J., Pagani, I., Palaniappan, K., Patel, S.M., Pearson, M., Peterson, J., Podar, M., Pohl, C., Pollard, K.S., Pop, M., Priest, M.E., Proctor, L.M., Qin, X., Raes, J., Ravel, J., Reid, J.G., Rho, M., Rhodes, R., Riehle, K.P., Rivera, M.C., Rodriguez-Mueller, B., Rogers, Y.-H., Ross, M.C., Russ, C., Sanka, R.K., Sankar, P., Fah Sathirapongsasuti, J., Schloss, J.A., Schloss, P.D., Schmidt, T.M., Scholz, M., Schriml, L., Schubert, A.M., Segata, N., Segre, J.A., Shannon, W.D., Sharp, R.R., Sharpton, T.J., Shenoy, N., Sheth, N.U., Simone, G.A., Singh, I., Smillie, C.S., Sobel, J.D., Sommer, D.D., Spicer, P., Sutton, G.G., Sykes, S.M., Tabbaa, D.G., Thiagarajan, M., Tomlinson, C.M., Torralba, M., Treangen, T.J., Truty, R.M., Vishnivetskaya, T.A., Walker, J., Wang, L., Wang, Z., Ward, D. V., Warren, W., Watson, M.A., Wellington, C., Wetterstrand, K.A., White, J.R., Wilczek-Boney, K., Wu, Y., Wylie, K.M., Wylie, T., Yandava, C., Ye, L., Ye, Y., Yooseph, S., Youmans, B.P., Zhang, L., Zhou, Y., Zhu, Y., Zoloth, L., Zucker, J.D., Birren, B.W., Gibbs, R.A., Highlander, S.K., Methé, B.A., Nelson, K.E., Petrosino, J.F., Weinstock, G.M., Wilson, R.K., White, O., 2012. Structure, function and diversity of the healthy human microbiome. Nature 486, 207–214. doi:10.1038/nature11234

Introduction to Whole-Genome Sequencing [WWW Document], n.d. URL http://www.illumina.com/areas-of-interest/microbiology/microbial-sequencing-methods/microbial-whole-genome-sequencing.html (accessed 3.20.16).

Ishii, S., Watanabe, K., Yabuki, S., Logan, B.E., Sekiguchi, Y., 2008. Comparison of electrode reduction activities of Geobacter sulfurreducens and an enriched consortium in an air-cathode microbial fuel cell. Appl. Environ. Microbiol. 74, 7348–55. doi:10.1128/AEM.01639-08

Jung, S., Regan, J.M., 2007. Comparison of anode bacterial communities and performance in microbial fuel cells with different electron

donors. Appl. Microbiol. Biotechnol. 77, 393–402. doi:10.1007/s00253-007-1162-y

Kameshwar, A. kumar S., Qin, W., 2016. Recent Developments in Using Advanced Sequencing Technologies for the Genomic Studies of Lignin and Cellulose Degrading Microorganisms. Int. J. Biol. Sci. 12, 156–171. doi:10.7150/ijbs.13537

Kasenow, M., 2001. Applied Ground-water hydrology and well hydraulics, 2nd ed. Water Resources Publications, LLC, Colorado.

Kato, S., Hashimoto, K., Watanabe, K., 2012. Microbial interspecies electron transfer via electric currents through conductive minerals. Proc. Natl. Acad. Sci. U. S. A. 109, 10042–10046. doi:10.1073/pnas.1117592109

Katuri, K.P., Scott, K., Head, I.M., Picioreanu, C., Curtis, T.P., 2011. Microbial fuel cells meet with external resistance. Bioresour. Technol. 102, 2758–2766. doi:10.1016/j.biortech.2010.10.147

Kiely, P.D., Regan, J.M., Logan, B.E., 2011. The electric picnic: synergistic requirements for exoelectrogenic microbial communities. Curr. Opin. Biotechnol. 22, 378–385. doi:10.1016/j.copbio.2011.03.003

Killham, K., 1994. Soil Ecology, 1st ed. Cambridge University Press, Cambridge.

Kim, J.R., Cheng, S., Oh, S.-E., Logan, B.E., 2007. Power Generation Using Different Cation, Anion, and Ultrafiltration Membranes in Microbial Fuel Cells. Environ. Sci. Technol. 41, 1004–1009. doi:10.1021/es062202m

Klindworth, A., Pruesse, E., Schweer, T., Peplies, J., Quast, C., Horn, M., Glöckner, F.O., 2013. Evaluation of general 16S ribosomal RNA gene PCR primers for classical and next-generation sequencing-based diversity studies. Nucleic Acids Res. 41, 1–11. doi:10.1093/nar/gks808

Kojima, H., Watanabe, T., Iwata, T., Fukui, M., 2014. Identification of Major Planktonic Sulfur Oxidizers in Stratified Freshwater Lake. PLoS One 9, e93877. doi:10.1371/journal.pone.0093877

Konopka, A., 2009. Microbial Ecology, in: Encyclopedia of Microbiology. Academic Press, pp. 91–107.

Kunin, V., Engelbrektson, A., Ochman, H., Hugenholtz, P., 2010. Wrinkles in the rare biosphere: Pyrosequencing errors can lead to artificial inflation of diversity estimates. Environ. Microbiol. 12, 118–123. doi:10.1111/j.1462-2920.2009.02051.x

Kuppardt, A., Kleinsteuber, S., Vogt, C., Lüders, T., Harms, H., Chatzinotas, A., 2014. Phylogenetic and Functional Diversity Within Toluene-Degrading, Sulphate-Reducing Consortia Enriched from a Contaminated Aquifer. Microb. Ecol. 68, 222–234. doi:10.1007/s00248-014-0403-8

Lai, A., Verdini, R., Aulenta, F., Majone, M., 2014. Reductive dechlorination in a pilot-scale membraneless bioelectorchemical reactor and effect of competing reactions, in: EU-ISMET 2014. Alcala, Spain.

Langille, M.G.I., Zaneveld, J., Caporaso, J.G., McDonald, D., Knights, D., Reyes, J. a, Clemente, J.C., Burkepile, D.E., Vega Thurber, R.L., Knight, R., Beiko, R.G., Huttenhower, C., 2013. Predictive functional profiling of microbial communities using 16S rRNA marker gene sequences. Nat. Biotechnol. 31, 814–21. doi:10.1038/nbt.2676

Larentis, M., Hoermann, K., Lueders, T., 2013. Fine-scale degrader community profiling over an aerobic/anaerobic redox gradient in a toluene-contaminated aquifer. Environ. Microbiol. Rep. 5, 225–234. doi:10.1111/1758-2229.12004

Larrosa-Guerrero, A., Scott, K., Head, I.M., Mateo, F., Ginesta, A., Godinez, C., 2010. Effect of temperature on the performance of microbial fuel cells. Fuel 89, 3985–3994. doi:10.1016/j.fuel.2010.06.025

Lerner, D.N., Thornton, S.F., Spence, M.J., Banwart, S.A., Bottrell, S.H., Higgo, J.J., Mallinson, H.E.H., Pickup, R.W., Williams, G.M., 2000. Ineffective Natural Attenuation of Degradable Organic Compounds in a Phenol-Contaminated Aquifer. Ground Water 38, 922–928. doi:10.1111/j.1745-6584.2000.tb00692.x

Li, J., Liu, G., Zhang, R., Luo, Y., Zhang, C., Li, M., 2010. Electricity generation by two types of microbial fuel cells using nitrobenzene as the anodic or cathodic reactants. Bioresour. Technol. 101, 4013–4020. doi:10.1016/j.biortech.2009.12.135

Li, W.-W., Sheng, G.-P., Liu, X.-W., Yu, H.-Q., 2011. Recent advances in the separators for microbial fuel cells. Bioresour. Technol. 102, 244–252. doi:10.1016/j.biortech.2010.03.090

Li, W.-W., Yu, H.-Q., 2015. Electro-assisted groundwater bioremediation: Fundamentals, challenges and future perspectives. Bioresour. Technol. 196, 677–684. doi:10.1016/j.biortech.2015.07.074

Lichstein, H.C., Soule, M.H., 1944. Studies of the Effect of Sodium Azide on Microbic Growth and Respiration: I. The Action of Sodium Azide on Microbic Growth. J. Bacteriol. 47, 221–230.

Liu, H., Logan, B.E., 2004. Electricity generation using an air-cathode single chamber microbial fuel cell in the presence and absence of a proton exchange membrane. Environ. Sci. Technol. 38, 4040–4046.

Liu, Y., Climent, V., Berná, A., Feliu, J.M., 2011. Effect of Temperature on the Catalytic Ability of Electrochemically Active Biofilm as Anode Catalyst in Microbial Fuel Cells. Electroanalysis 23, 387–394. doi:10.1002/elan.201000499

Logan, B.E., 2012. Essential data and techniques for conducting microbial fuel cell and other types of bioelectrochemical system experiments. ChemSusChem 5, 988–94. doi:10.1002/cssc.201100604

Logan, B.E., 2010. Scaling up microbial fuel cells and other bioelectrochemical systems. Appl. Microbiol. Biotechnol. 85, 1665–1671. doi:10.1007/s00253-009-2378-9

Logan, B.E., 2008. Microbial fuel cells, 1st ed. John Wiley & Sons, Inc., New Jersey.

Logan, B.E., Hamelers, B., Rozendal, R., Schröder, U., Keller, J., Freguia, S., Aelterman, P., Verstraete, W., Rabaey, K., 2006. Microbial Fuel Cells: Methodology and Technology. Environ. Sci. Technol. 40, 5181–5192. doi:10.1021/es0605016

Logan, B.E., Regan, J.M., 2006. Microbial Fuel Cells—Challenges and Applications. Environ. Sci. Technol. 40, 5172–5180. doi:10.1021/es0627592

Logan, B.E., Regan, J.M., 2006. Electricity-producing bacterial communities in microbial fuel cells. Trends Microbiol. 14, 512–518. doi:10.1016/j.tim.2006.10.003

Lonergan, D.J., Jenter, H.L., Coates, J.D., Phillips, E.J., Schmidt, T.M., Lovley, D.R., 1996. Phylogenetic analysis of dissimilatory Fe(III)-reducing bacteria. J. Bacteriol. 178, 2402–2408.

Lovley, D.R., 2012. Electromicrobiology. Annu. Rev. Microbiol. 66, 391–409. doi:10.1146/annurev-micro-092611-150104

Lovley, D.R., 2011. Live wires: direct extracellular electron exchange for bioenergy and the bioremediation of energy-related contamination. Energy Environ. Sci. 4, 4896. doi:10.1039/c1ee02229f

Lovley, D.R., 2006a. Bug juice: harvesting electricity with microorganisms. Nat. Rev. Microbiol. 4, 497–508. doi:10.1038/nrmicro1442

Lovley, D.R., 2006b. Microbial fuel cells: novel microbial physiologies and engineering approaches. Curr. Opin. Biotechnol. 17, 327–332. doi:10.1016/j.copbio.2006.04.006

Lovley, D.R., Nevin, K.P., 2011. A shift in the current: New applications and concepts for microbe-electrode electron exchange. Curr. Opin. Biotechnol. 22, 441–448. doi:10.1016/j.copbio.2011.01.009

Lovley, D.R., Ueki, T., Zhang, T., Malvankar, N.S., Shrestha, P.M., Flanagan, K.A., Aklujkar, M., Butler, J.E., Giloteaux, L., Rotaru, A.-E., Holmes, D.E., Franks, A.E., Orellana, R., Risso, C., Nevin, K.P., 2011. Geobacter: the microbe electric's physiology, ecology, and practical applications. Adv. Microb. Physiol. 59, 1–100. doi:10.1016/B978-0-12-387661-4.00004-5

Lowy, D. a, Tender, L.M., Zeikus, J.G., Park, D.H., Lovley, D.R., 2006. Harvesting energy from the marine sediment-water interface II. Kinetic activity of anode materials. Biosens. Bioelectron. 21, 2058–63. doi:10.1016/j.bios.2006.01.033

Lozupone, C., Lladser, M.E., Knights, D., Stombaugh, J., Knight, R., 2011. UniFrac: an effective distance metric for microbial community comparison. ISME J. 5, 169–172. doi:10.1038/ismej.2010.133

Luijten, M.L.G.C., 2003. Description of Sulfurospirillum halorespirans sp. nov., an anaerobic, tetrachloroethene-respiring bacterium, and transfer of Dehalospirillum multivorans to the genus Sulfurospirillum as Sulfurospirillum multivorans comb. nov. Int. J. Syst. Evol. Microbiol. 53, 787–793. doi:10.1099/ijs.0.02417-0

Luo, H., Liu, G., Zhang, R., Jin, S., 2009. Phenol degradation in microbial fuel cells. Chem. Eng. J. 147, 259–264. doi:10.1016/j.cej.2008.07.011

Madigan, M.T., Martinko, John, M., Stahl, D.A., Clark, D.P., 2011. Brock biology of microorganisms, 13th ed. Benjamin Cummings, San Francisco.

Majone, M., Verdini, R., Uccelletti, D., Palleschi, C., Aulenta, F., Rossetti, S., Zanaroli, G., Fava, F., Beck, H., Mueller, J.A., Kästner, M., 2013. Electrochemically-assisted biodegradation of chlorinated solvents with electrodes serving as electron donors/acceptors, in: Proceedings of the 2nd European Symposium, Water Technology & Management. Leuven, Belgium, p. 170.

Margesin, R., Schinner, F., 2001. Biodegradation and bioremediation of hydrocarbons in extreme environments. Appl. Microbiol. Biotechnol. 56, 650–663. doi:10.1007/s002530100701

Mbadinga, S.M., Li, K.-P., Zhou, L., Wang, L.-Y., Yang, S.-Z., Liu, J.-F., Gu, J.-D., Mu, B.-Z., 2012. Analysis of alkane-dependent methanogenic community derived from production water of a high-temperature petroleum reservoir. Appl. Microbiol. Biotechnol. 96, 531–542. doi:10.1007/s00253-011-3828-8

Mehta, T., Coppi, M. V, Childers, S.E., Lovley, D.R., 2005. Outer Membrane c -Type Cytochromes Required for Fe (III) and Mn (IV) Oxide Reduction in Geobacter sulfurreducens Outer Membrane c-Type Cytochromes Required for Fe (III) and Mn (IV) Oxide Reduction in Geobacter sulfurreducens. Appl. Environ. Microbiol. 71, 8634–8641. doi:10.1128/AEM.71.12.8634

Michałowicz, J., Duda, W., 2007. Phenols - Sources and toxicity. Polish J. Environ. Stud.

Michie, I.S., Kim, J.R., Dinsdale, R.M., Guwy, A.J., Premier, G.C., 2011. Operational temperature regulates anodic biofilm growth and the development of electrogenic activity. Appl. Microbiol. Biotechnol. 92, 419–430. doi:10.1007/s00253-011-3531-9

Mohan, S.V., Chandrasekhar, K., 2011. Self-induced bio-potential and graphite electron accepting conditions enhances petroleum sludge degradation in bio-electrochemical system with simultaneous power generation. Bioresour. Technol. 102, 9532–9541. doi:10.1016/j.biortech.2011.07.038

Morin, P.J., 1999. Community Ecology. Blackwell Science, Inc., Oxford.

Morris, J.M., Jin, S., 2012. Enhanced biodegradation of hydrocarbon-contaminated sediments using microbial fuel cells. J. Hazard. Mater. 213-214, 474–477. doi:10.1016/j.jhazmat.2012.02.029

Morris, J.M., Jin, S., 2008. Feasibility of using microbial fuel cell technology for bioremediation of hydrocarbons in groundwater. J. Environ. Sci. Health. A. Tox. Hazard. Subst. Environ. Eng. 43, 18–23. doi:10.1080/10934520701750389

Morris, J.M., Jin, S., Crimi, B., Pruden, A., 2009. Microbial fuel cell in enhancing anaerobic biodegradation of diesel. Chem. Eng. J. 146, 161–167. doi:10.1016/j.cej.2008.05.028

Nadell, C.D., Xavier, J.B., Foster, K.R., 2009. The sociobiology of biofilms. FEMS Microbiol. Rev. 33, 206–224. doi:10.1111/j.1574-6976.2008.00150.x

Nakamura, R., Kai, F., Okamoto, A., Newton, G.J., Hashimoto, K., 2009. Self-constructed electrically conductive bacterial networks. Angew. Chem. Int. Ed. Engl. 48, 508–511. doi:10.1002/anie.200804750

Neu, T.R., 1996. Significance of bacterial surface-active compounds in interaction of bacteria with Significance of Bacterial Surface-Active Compounds in Interaction of Bacteria with Interfaces. Microbiol. Mol. Biol. Rev. 60, 151–166.

Nevin, K.P., Richter, H., Covalla, S.F., Johnson, J.P., Woodard, T.L., Orloff, a L., Jia, H., Zhang, M., Lovley, D.R., 2008. Power output and columbic efficiencies from biofilms of Geobacter sulfurreducens comparable to mixed community microbial fuel cells. Environ. Microbiol. 10, 2505–2514. doi:10.1111/j.1462-2920.2008.01675.x

Nielsen, L.P., Risgaard-Petersen, N., Fossing, H., Christensen, P.B., Sayama, M., 2010. Electric currents couple spatially separated biogeochemical processes in marine sediment. Nature 463, 1071–1074. doi:10.1038/nature08790

Novick, A., Szilard, L., 1950. Description of the Chemostat. Science (80-.). 112, 715–716. doi:10.1126/science.112.2920.715

Oh, S.-E., Logan, B.E., 2006. Proton exchange membrane and electrode surface areas as factors that affect power generation in microbial fuel cells. Appl. Microbiol. Biotechnol. 70, 162–9. doi:10.1007/s00253-005-0066-y

Oh, S.T., Kim, J.R., Premier, G.C., Lee, T.H., Kim, C., Sloan, W.T., 2010. Sustainable wastewater treatment: how might microbial fuel cells contribute. Biotechnol. Adv. 28, 871–881. doi:10.1016/j.biotechadv.2010.07.008

Osborn, M., Smith, C. (Eds.), 2005. Molecular Microbial Ecology (Advanced Methods). Taylor & Francis.

Panagos, P., Van Liedekerke, M., Yigini, Y., Montanarella, L., 2013. Contaminated Sites in Europe: Review of the Current Situation Based on Data Collected through a European Network. J. Environ. Public Health 2013, 1–11. doi:10.1155/2013/158764

Pant, D., Van Bogaert, G., Diels, L., Vanbroekhoven, K., 2010. A review of the substrates used in microbial fuel cells (MFCs) for sustainable energy production. Bioresour. Technol. 101, 1533–1543. doi:10.1016/j.biortech.2009.10.017

Pepper, I.L., Gerba, C.P., Gentry, T.J., Maier, R.M. (Eds.), 2011. Environmental Microbiology, Second. ed. Academic Press.

Perry, J.J., Staley, J.T., 1997. Microbiology: Dynamics and Diversity. Saunders College Publishing, Orlando, Florida.

Pfeffer, C., Larsen, S., Song, J., Dong, M., Besenbacher, F., Meyer, R.L., Kjeldsen, K.U., Schreiber, L., Gorby, Y.A., El-Naggar, M.Y., Leung, K.M., Schramm, A., Risgaard-Petersen, N., Nielsen, L.P., 2012. Filamentous bacteria transport electrons over centimetre distances. Nature advance on. doi:10.1038/nature11586

Pham, H., Boon, N., Marzorati, M., Verstraete, W., 2009. Enhanced removal of 1,2-dichloroethane by anodophilic microbial consortia. Water Res. 43, 2936–2946. doi:10.1016/j.watres.2009.04.004

Pham, T.H., Boon, N., Aelterman, P., Clauwaert, P., De Schamphelaire, L., Vanhaecke, L., De Maeyer, K., Höfte, M., Verstraete, W., Rabaey, K., 2008. Metabolites produced by Pseudomonas sp. enable a Gram-positive bacterium to achieve extracellular electron transfer. Appl. Microbiol. Biotechnol. 77, 1119–1129. doi:10.1007/s00253-007-1248-6

Puig, S., Serra, M., Coma, M., Cabré, M., Balaguer, M.D., Colprim, J., 2010. Effect of pH on nutrient dynamics and electricity production

using microbial fuel cells. Bioresour. Technol. 101, 9594–9599. doi:10.1016/j.biortech.2010.07.082

Quast, C., Pruesse, E., Yilmaz, P., Gerken, J., Schweer, T., Yarza, P., Peplies, J., Glöckner, F.O., 2013. The SILVA ribosomal RNA gene database project: Improved data processing and web-based tools. Nucleic Acids Res. 41, 590–596. doi:10.1093/nar/gks1219

Rabaey, K., Angenent, L., Schroeder, U., Keller, J. (Eds.), 2010. Bioelectrochemical Systems: From Extracellular Electron Transfer to Biotechnological Application, 1st ed. London.

Rabaey, K., Rodríguez, J., Blackall, L.L., Keller, J., Gross, P., Batstone, D., Verstraete, W., Nealson, K.H., 2007. Microbial ecology meets electrochemistry: electricity-driven and driving communities. ISME J. 1, 9–18. doi:10.1038/ismej.2007.4

Rabaey, K., Verstraete, W., 2005. Microbial fuel cells: novel biotechnology for energy generation. Trends Biotechnol. 23, 291–298. doi:10.1016/j.tibtech.2005.04.008

Reguera, G., McCarthy, K.D., Mehta, T., Nicoll, J.S., Tuominen, M.T., Lovley, D.R., 2005. Extracellular electron transfer via microbial nanowires. Nature 435, 1098–1101. doi:10.1038/nature03661

Reguera, G., Nevin, K.P., Nicoll, J.S., Covalla, S.F., Woodard, T.L., Lovley, D.R., 2006. Biofilm and nanowire production leads to increased current in Geobacter sulfurreducens fuel cells. Appl. Environ. Microbiol. 72, 7345–7348. doi:10.1128/AEM.01444-06

Reimers, C.E., Tender, L.M., Fertig, S., Wang, W., 2001. Harvesting energy from the marine sediment--water interface. Environ. Sci. Technol. 35, 192–5.

Ren, Z., Ward, T.E., Regan, J.M., 2007. Electricity production from cellulose in a microbial fuel cell using a defined binary culture. Environ. Sci. Technol. 41, 4781–4786.

Revil, a., Mendonça, C. a., Atekwana, E. a., Kulessa, B., Hubbard, S.S., Bohlen, K.J., 2010. Understanding biogeobatteries: Where geophysics meets microbiology. J. Geophys. Res. 115, 1–22. doi:10.1029/2009JG001065

Rinaldi, A., Mecheri, B., Garavaglia, V., Licoccia, S., Di Nardo, P., Traversa, E., 2008. Engineering materials and biology to boost performance of microbial fuel cells: a critical review. Energy Environ. Sci. 1, 417–429. doi:10.1039/b806498a

Rismani-Yazdi, H., Carver, S.M., Christy, A.D., Tuovinen, O.H., 2008. Cathodic limitations in microbial fuel cells: An overview. J. Power Sources 180, 683–694. doi:10.1016/j.jpowsour.2008.02.074

Rizoulis, A., Elliott, D.R., Rolfe, S.A., Thornton, S.F., Banwart, S.A., Pickup, R.W., Scholes, J.D., 2013. Diversity of Planktonic and Attached Bacterial Communities in a Phenol-Contaminated Sandstone Aquifer. Microb. Ecol. doi:10.1007/s00248-013-0233-0

Robertson, W.J., Bowman, J.P., Mee, B.J., Franzmann, P.D., 2001. Desulfosporosinus meridiei sp. nov., a spore-forming sulfate-reducing bacterium isolated from gasolene-contaminated groundwater. Int. J. Syst. Evol. Microbiol. 51, 133–140. doi:10.1099/00207713-51-1-133

Rooney-Varga, J.N., Anderson, R.T., Fraga, J.L., Ringelberg, D., Lovley, D.R., 1999. Microbial communities associated with anaerobic benzene degradation in a petroleum-contaminated aquifer. Appl. Environ. Microbiol. 65, 3056–3063.

Rosenbaum, M., Aulenta, F., Villano, M., Angenent, L.T., 2011. Cathodes as electron donors for microbial metabolism: Which extracellular electron transfer mechanisms are involved? Bioresour. Technol. 102, 324–333. doi:10.1016/j.biortech.2010.07.008

Roundtable, F.R.T., n.d. Remediation Technologies Screening Matrix and Reference Guide 4.0 [WWW Document]. URL https://frtr.gov/matrix2/top_page.html (accessed 3.26.16).

Samanta, S.K., Singh, O. V, Jain, R.K., 2002. Polycyclic aromatic hydrocarbons: environmental pollution and bioremediation. Trends Biotechnol. 20, 243–248.

Schaetzle, O., Barrière, F., Baronian, K., 2008. Bacteria and yeasts as catalysts in microbial fuel cells: electron transfer from micro-organisms to electrodes for green electricity. Energy Environ. Sci. 1, 607–620. doi:10.1039/b810642h

Schreiberová, O., Hedbávná, P., Čejková, A., Jirků, V., Masák, J., 2012. Effect of surfactants on the biofilm of Rhodococcus erythropolis, a potent degrader of aromatic pollutants. N. Biotechnol. 30, 62–68. doi:10.1016/j.nbt.2012.04.005

Schröder, U., Harnisch, F., Angenent, L.T., 2015. Microbial electrochemistry and technology: terminology and classification. Energy Environ. Sci. 8, 513–519. doi:10.1039/C4EE03359K

Scow, K.M., Hicks, K. a, 2005. Natural attenuation and enhanced bioremediation of organic contaminants in groundwater. Curr. Opin. Biotechnol. 16, 246–253. doi:10.1016/j.copbio.2005.03.009

Shah, N.W., Thornton, S.F., Bottrell, S.H., Spence, M.J., 2009. Biodegradation potential of MTBE in a fractured chalk aquifer under aerobic conditions in long-term uncontaminated and contaminated aquifer microcosms. J. Contam. Hydrol. 103, 119–33. doi:10.1016/j.jconhyd.2008.09.022

Sharpton, T.J., 2014. An introduction to the analysis of shotgun metagenomic data. Front. Plant Sci. 5. doi:10.3389/fpls.2014.00209

Smith, C.J., Danilowicz, B.S., Clear, A.K., Costello, F.J., Wilson, B., Meijer, W.G., 2005. T-Align , a web-based tool for comparison of multiple terminal restriction fragment length polymorphism profiles 54, 375–380. doi:10.1016/j.femsec.2005.05.002

Song, C., Zhang, J., 2008. Electrocatalytic Oxygen Reduction Reaction. PEM Feul Cell Electrocatal. Catal. Layers. Fundam. Appl.

Spence, M.J., Bottrell, S.H., Thornton, S.F., Lerner, D.N., 2001. Isotopic modelling of the significance of bacterial sulphate reduction for phenol attenuation in a contaminated aquifer. J. Contam. Hydrol. 53, 285–304. doi:10.1016/S0169-7722(01)00170-X

Stoodley, P., Sauer, K., Davies, D.G., Costerton, J.W., 2002. Biofilms as complex differentiated communities. Annu. Rev. Microbiol. 56, 187–209. doi:10.1146/annurev.micro.56.012302.160705

Strycharz, S.M., Gannon, S.M., Boles, A.R., Franks, A.E., Nevin, K.P., Lovley, D.R., 2010. Reductive dechlorination of 2-chlorophenol by Anaeromyxobacter dehalogenans with an electrode serving as the electron donor. Environ. Microbiol. Rep. 2, 289–294. doi:10.1111/j.1758-2229.2009.00118.x

Strycharz, S.M., Woodard, T.L., Johnson, J.P., Nevin, K.P., Sanford, R. a, Löffler, F.E., Lovley, D.R., 2008. Graphite electrode as a sole electron donor for reductive dechlorination of tetrachlorethene by Geobacter lovleyi. Appl. Environ. Microbiol. 74, 5943–5947. doi:10.1128/AEM.00961-08

Stumm, W., Morgan, J.J., 2013. Aquatic chemistry: chemical equilibria and rates in natural waters. John Wiley & Sons, Inc.

Sung, Y., Fletcher, K.E., Ritalahti, K.M., Apkarian, R.P., Ramos-Hernandez, N., Sanford, R.A., Mesbah, N.M., Loffler, F.E., 2006. Geobacter lovleyi sp. nov. Strain SZ, a Novel Metal-Reducing and Tetrachloroethene-Dechlorinating Bacterium. Appl. Environ. Microbiol. 72, 2775–2782. doi:10.1128/AEM.72.4.2775-2782.2006

Tender, L.M., Gray, S. a., Groveman, E., Lowy, D. a., Kauffman, P., Melhado, J., Tyce, R.C., Flynn, D., Petrecca, R., Dobarro, J., 2008. The first demonstration of a microbial fuel cell as a viable power supply: Powering a meteorological buoy. J. Power Sources 179, 571–575. doi:10.1016/j.jpowsour.2007.12.123

Tender, L.M., Reimers, C.E., Stecher, H. a, Holmes, D.E., Bond, D.R., Lowy, D. a, Pilobello, K., Fertig, S.J., Lovley, D.R., 2002. Harnessing microbially generated power on the seafloor. Nat. Biotechnol. 20, 821–825. doi:10.1038/nbt716

Thornton, S.F., Baker, K.M., Bottrell, S.H., Rolfe, S. a., McNamee, P., Forrest, F., Duffield, P., Wilson, R.D., Fairburn, A.W., Cieslak, L. a., 2014. Enhancement of in situ biodegradation of organic compounds in groundwater by targeted pump and treat intervention. Appl. Geochemistry 48, 28–40. doi:10.1016/j.apgeochem.2014.06.023

Thornton, S.F., Lerner, D.N., Banwart, S. a., 2001a. Assessing the natural attenuation of organic contaminants in aquifers using plume-scale electron and carbon balances: Model development with analysis of uncertainty and parameter sensitivity. J. Contam. Hydrol. 53, 199–232. doi:10.1016/S0169-7722(01)00167-X

Thornton, S.F., Quigley, S., Spence, M.J., Banwart, S.A., Bottrell, S., Lerner, D.N., 2001b. Processes controlling the distribution and natural attenuation of dissolved phenolic compounds in a deep sandstone aquifer. J. Contam. Hydrol. 53, 233–67.

Tilak, K.V.B.R., Pal, K.K., Dey, R., 2010. Microbes for Sustainable Agriculture. I. K. International Publishing House Pvt. Ltd., New Delhi, India.

Torres, C.I., Marcus, A.K., Lee, H.-S., Parameswaran, P., Krajmalnik-Brown, R., Rittmann, B.E., 2010. A kinetic perspective on extracellular electron transfer by anode-respiring bacteria. FEMS Microbiol. Rev. 34, 3–17. doi:10.1111/j.1574-6976.2009.00191.x

Venkataraman, A., Rosenbaum, M. a., Perkins, S.D., Werner, J.J., Angenent, L.T., 2011. Metabolite-based mutualism between Pseudomonas aeruginosa PA14 and Enterobacter aerogenes enhances current generation in bioelectrochemical systems. Energy Environ. Sci. 4, 4550–4559. doi:10.1039/c1ee01377g

Wagner, R.C., Call, D.F., Logan, B.E., 2010. Optimal set anode potentials vary in bioelectrochemical systems. Environ. Sci. Technol. 44, 6036–41. doi:10.1021/es101013e

Walker, J.M., 2010. Bioremediation, Methods in Molecular Biology. Humana Press, Totowa, NJ. doi:10.1007/978-1-60761-439-5

Wang, X., Cai, Z., Zhou, Q., Zhang, Z., Chen, C., 2012. Bioelectrochemical stimulation of petroleum hydrocarbon degradation in saline soil using U-tube microbial fuel cells. Biotechnol. Bioeng. 109, 426–433. doi:10.1002/bit.23351

Watson, I. a, Oswald, S.E., Banwart, S. a, Crouch, R.S., Thornton, S.F., 2005. Modeling the dynamics of fermentation and respiratory processes in a groundwater plume of phenolic contaminants interpreted from laboratory- to field-scale. Environ. Sci. Technol. 39, 8829–39.

Watson, I. a, Oswald, S.E., Mayer, K.U., Wu, Y., Banwart, S. a, 2003. Modeling kinetic processes controlling hydrogen and acetate concentrations in an aquifer-derived microcosm. Environ. Sci. Technol. 37, 3910–9.

Weelink, S.A.B., van Doesburg, W., Saia, F.T., Rijpstra, W.I.C., Röling, W.F.M., Smidt, H., Stams, A.J.M., 2009. A strictly anaerobic betaproteobacterium Georgfuchsia toluolica gen. nov., sp. nov. degrades aromatic compounds with Fe(III), Mn(IV) or nitrate as an electron acceptor. FEMS Microbiol. Ecol. 70, 575–585. doi:10.1111/j.1574-6941.2009.00778.x

Whittaker, R.H., 1972. Evolution and Measurement of Species Diversity. Taxon 21, 213. doi:10.2307/1218190

Wiedemeier, T. H., Rifai, H. S., Newell, C. J., Wilson, J.T., 1999. Natural Attenuation of Fuels and Chlorinated Solvents in the Subsurface. John Wiley & Sons, Inc. doi:10.1002/9780470172964

Wiegert, C., Mandalakis, M., Knowles, T., Hovorkova, I., Polymenakou, P., Aeppli, C., Holmstrand, H., Evershed, R., Pancost, R., Klanova, J., Gustafsson, O., 2013. Carbon and Chlorine Stable Isotope Fractionation during Microbial Degradation of a- and ss-Hexachlorocyclohexanes.

Williams, K.H., Nevin, K.P., Franks, A., Englert, A., Long, P.E., Lovley, D.R., 2010. Electrode-based approach for monitoring in situ microbial activity during subsurface bioremediation. Environ. Ecience Technol. 44, 47–54. doi:10.1021/es9017464

Winderl, C., Anneser, B., Griebler, C., Meckenstock, R.U., Lueders, T., 2008. Depth-Resolved Quantification of Anaerobic Toluene Degraders and Aquifer Microbial Community Patterns in Distinct Redox Zones of a Tar Oil Contaminant Plume. Appl. Environ. Microbiol. 74, 792–801. doi:10.1128/AEM.01951-07

Wolf, G., Crespo, J.G., Reis, M.A.M., 2002. Optical and spectroscopic methods for biofilm examination and monitoring. Rev. Environ. Sci. Bio/Technology 1, 227–251. doi:10.1023/A:1021238630092

Wong, T.-Y., Maier, R.J., 1985. H2-Dependent Mixotrophic Growth of N2-Fixing Azotobacter vinelandii. J. Bacteriol. 163, 528–533.

Wooley, J.C., Godzik, A., Friedberg, I., 2010. A primer on metagenomics. PLoS Comput. Biol. 6. doi:10.1371/journal.pcbi.1000667

Woolston, C., 2015. Career advancement: Insider knowledge. Nature 523, 491–493. doi:10.1038/nj7561-491a

Yamamoto, S., Suzuki, K., Araki, Y., Mochihara, H., Hosokawa, T., Kubota, H., Chiba, Y., Rubaba, O., Tashiro, Y., Futamata, H., 2014. Dynamics of Different Bacterial Communities Are Capable of Generating Sustainable Electricity from Microbial Fuel Cells with Organic Waste. Microbes Environ. 29, 145–153. doi:10.1264/jsme2.ME13140

Yan, Z., Song, N., Cai, H., Tay, J.-H., Jiang, H., 2012. Enhanced degradation of phenanthrene and pyrene in freshwater sediments by combined employment of sediment microbial fuel cell and amorphous ferric hydroxide. J. Hazard. Mater. 199-200, 217–225. doi:10.1016/j.jhazmat.2011.10.087

Yuan, Y., Zhao, B., Zhou, S., Zhong, S., Zhuang, L., 2011. Electrocatalytic activity of anodic biofilm responses to pH changes in microbial fuel cells. Bioresour. Technol. 102, 6887–6891. doi:10.1016/j.biortech.2011.04.008

Zhang, G., Zhao, Q., Jiao, Y., Zhang, J., Jiang, J., Ren, N., Kim, B.H., 2011. Improved performance of microbial fuel cell using combination biocathode of graphite fiber brush and graphite granules. J. Power Sources 196, 6036–6041. doi:10.1016/j.jpowsour.2011.03.096

Zhang, T., Gannon, S.M., Nevin, K.P., Franks, A.E., Lovley, D.R., 2010. Stimulating the anaerobic degradation of aromatic hydrocarbons in contaminated sediments by providing an electrode as the electron acceptor. Environ. Microbiol. 12, 1011–20. doi:10.1111/j.1462-2920.2009.02145.x

Zhao, F., Slade, R.C.T., Varcoe, J.R., 2009. Techniques for the study and development of microbial fuel cells: an electrochemical perspective. Chem. Soc. Rev. 38, 1926–1939. doi:10.1039/b819866g

Zhou, M., Chi, M., Luo, J., He, H., Jin, T., 2011. An overview of electrode materials in microbial fuel cells. J. Power Sources 196, 4427–4435. doi:10.1016/j.jpowsour.2011.01.012

Zhu, X., Ni, J., 2009. Simultaneous processes of electricity generation and p-nitrophenol degradation in a microbial fuel cell. Electrochem. commun. 11, 274–277. doi:10.1016/j.elecom.2008.11.023

Zhu, X., Yates, M.D., Hatzell, M.C., Ananda Rao, H., Saikaly, P.E., Logan, B.E., 2014. Microbial community composition is unaffected by anode potential. Environ. Sci. Technol. 48, 1352–8. doi:10.1021/es404690q

10 Appendices

Appendix A

ADVOCATE bulletin

CL:AIRE

AB 3
(October 2014)

ADVOCATE bulletin

CL:AIRE's ADVOCATE bulletins describe practical aspects of research which have direct application to the characterisation, monitoring or remediation of contaminated soil or groundwater. This bulletin describes laboratory experiments using bioelectrochemical systems to enhance the bioremediation of contaminated groundwater.

Enhancing bioremediation of groundwater by microbial interaction with a solid state electrode: proof-of-concept

1. Introduction

Plumes of organic chemicals in groundwater are frequently anaerobic due to limitations in the availability and aqueous solubility of oxygen. As biodegradation rates for anaerobic processes, which use electron acceptors such as nitrate or sulphate for respiration, are usually slower than for aerobic processes, plumes of organic contaminants may persist in groundwater (Atlas and Philp, 2005). A novel, but under-developed, approach to enhance the anaerobic bioremediation of organic compounds in groundwater is to couple the exchange of electrons between bacteria and solid state electrodes. In this case, electrodes inserted into the subsurface serve as an inexhaustible electron acceptor for microbial metabolism of organic compounds (Zhang *et al.*, 2010). Bioelectrochemical systems (BES) with one electrode in contact with the organic contaminant can be constructed to enhance the bioremediation of groundwater while generating small amounts of electrical energy. This technology, if developed for *in situ* application, could offer an environmentally sustainable option to manage groundwater contaminated with organic compounds.

In principle, an electrode installed in the subsurface can be constructed as a permeable reactive barrier (PRB) made of conductive graphite granules (Figure 1) (Aulenta and Majone, 2010). Groundwater bacteria, which naturally attach to the graphite, degrade contaminants as they pass through and transfer the electrons to the graphite, which functions as an anode. The electrons are then transported to a cathode placed in nearby uncontaminated oxygenated groundwater.

The energy that bacteria gain from the biodegradation of organic compounds is proportional to the electrochemical potential of the final electron acceptor. Oxygen is the most favourable electron acceptor in terms of energy gain for microorganisms. There are two possible ways to regulate the potential of the anode. Firstly, it can develop naturally, according to the metabolic properties of the microbial community and electrical resistance of the load. The second possibility is to use a small amount of electrical energy to fix the anode potential and control the microbial metabolism and biodegradation rate (Logan, 2008; Wagner *et al.*, 2010).

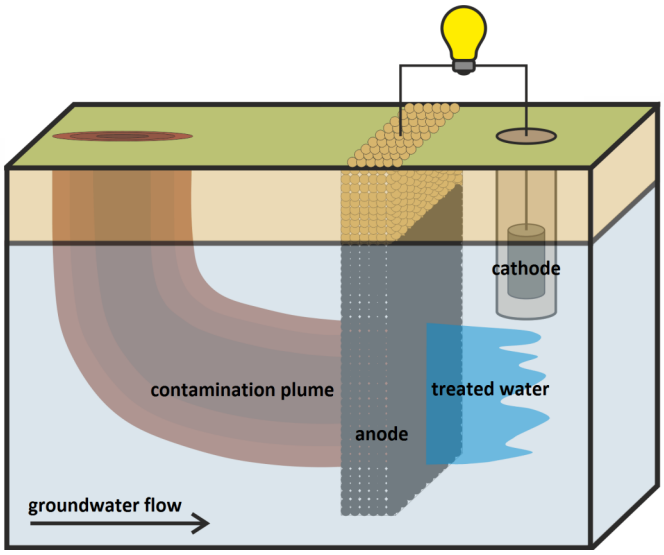

Figure 1: Conceptual model of a bioelectrochemical system (BES) with the anode constructed as permeable reactive barrier.

2. Proof-of-concept Experiment

Recent laboratory studies report that bioremediation of organic pollutants such as petroleum hydrocarbons, phenol, benzene, naphthalene, phenanthrene and pyrene can be enhanced by the electron transfer to an electrode in BES (Luo *et al.*, 2009; Morris *et al.*, 2009; Zhang *et al.*, 2010; Huang *et al.*, 2011; Mohan and Chandrasekhar, 2011; Morris and Jin, 2012; Wang *et al.*, 2012; Yan *et al.*, 2012). However, research on this technology has to date been undertaken in BES reactors at the laboratory level and its application at the field-scale is still under-developed.

Laboratory experiments to date have used groundwater amended with nutrients (Morris and Jin, 2008; Morris *et al.*, 2009), but this fails to represent the *in situ* conditions in most aquifers. This technology has also not been examined in detail for the bioremediation of phenols, which may be released to groundwater as

This bulletin was written by Petra Hedbavna, Steven F. Thornton, Wei E. Huang, Groundwater Protection and Restoration Group, Kroto Research Institute, University of Sheffield, Broad Lane, Sheffield, S3 7HQ, United Kingdom. For further information please email petra.hedbavna@sheffield.ac.uk or Tel +44 114 222 5786.

complex organic mixtures from manufactured gas plants, coking works, wood treatment facilities and other industrial sites. However, previous BES research has only evaluated phenol biodegradation (Luo *et al.*, 2009; Huang *et al.*, 2011).

In this study, the feasibility of using BES to enhance the bioremediation of coal tar-contaminated groundwater, containing a mixture of phenolic compounds, was examined without any addition of nutrients. This laboratory experiment serves as a proof-of-concept analysis for potential field-scale application in subsequent phases.

3. Experimental Design

The laboratory experiment was run in an H-type BES with 1 kΩ resistor (Figure 2). The electrodes made of carbon cloth were placed in different chambers separated by a semi-permeable membrane (Nafion 117), to simulate conditions in the aquifer, i.e the anode and cathode in the contaminated and uncontaminated groundwater, respectively (Figure 1).

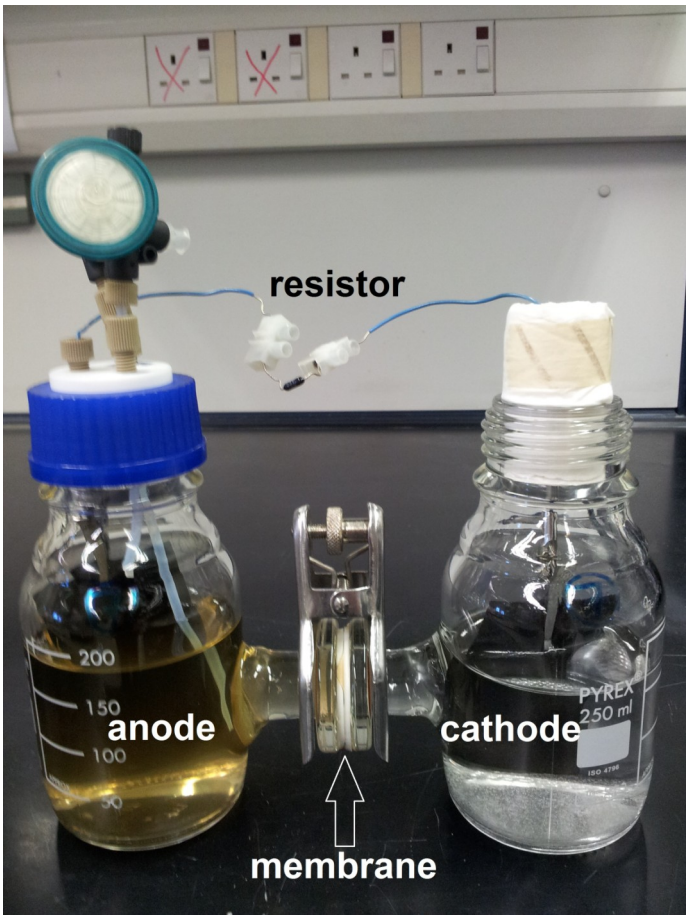

Figure 2: H-type BES used in the experiment.

Groundwater containing a mixture of phenolic compounds was used in the experiments. Three different BES reactors were set up, a closed circuit BES (CC-BES), an open circuit control BES (OC-BES) and a biologically inactive control BES ("sterile"-BES, S-BES) (Table 1). The biodegradation rate should be enhanced in the CC-BES, where the closed circuit enables the transfer of electrons from the anode to the cathode. The system with the open circuit, OC-BES, corrects for background biodegradation rates without an operational BES. The S-BES systems identifies any changes in chemistry or electricity production caused by abiotic processes in the system.

Table 1: Experimental set up.

Type of BES	Resistor	Anode chamber	Cathode chamber
CC-BES	1 kΩ	Contaminated groundwater	Uncontaminated groundwater autoclaved
OC-BES	None	Contaminated groundwater	Uncontaminated groundwater autoclaved
S-BES	1 kΩ	Contaminated groundwater with sodium azide	Uncontaminated groundwater autoclaved

All BES were operated for 24 days, only in one replicate. The closed circuit voltage (across the resistor) was monitored daily. The resistor was mounted on the OC-BES only for the purposes of measuring the closed circuit voltage. The maximum power produced by the BES was measured when the closed circuit voltage, i.e. electricity production by BES, reached its maximum value.

Samples for chemical analysis were taken every 5-7 days from the anode and cathode chamber and filter-sterilized. The concentration of the phenolic compounds was determined by high-performance liquid chromatography (HPLC). The detection limit was 1 mg/l and the precision of this analysis was ±7%.

4. Electricity Production

The closed circuit voltage (Figure 3) started increasing in biologically active BES after 3 days of operation, reaching a maximum value of 82 mV in the CC-BES and 29 mV in the OC-BES. Electricity production decreased to 14 mV in the CC-BES after 16 days (Fig. 3).

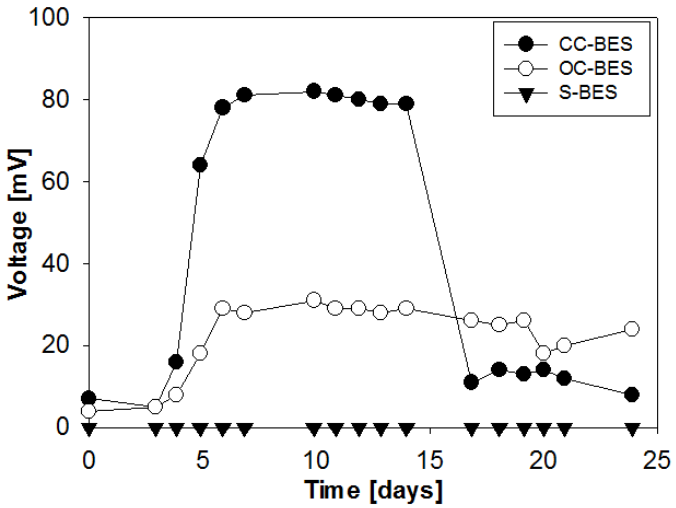

Figure 3: Voltage production for different BES systems used in the experiment.

The measured voltage of the control sample S-BES remained at 0 mV. The maximum power produced by the CC-BES reached 2.0 mW/m^2 of the anode surface area, while the OC-BES produced only 1.2 mW/m^2.

The results demonstrate that no electricity can be produced in the absence of bacterial activity. In this study, the closed circuit voltage production and maximum power show that the CC-BES can produce more electricity than the OC-BES. This is likely due to the adaptation of bacteria in the CC-BES for electricity generation. The closed circuit creates a selection pressure in the CC-BES microbial community, which can lead to a community adapted to the transfer of electrons to the anode (Yang *et al.*, 2013).

5. Biodegradation of Phenolic Compounds

Phenolic compounds diffused from the anode chamber to the cathode chamber through the semi-permeable membrane (Figure 4). This decreased the concentration of total phenols in the anode chamber from 158 mg/l to 93 mg/l at the end of the experiment. The concentration of phenolic compounds in the cathode chamber of the abiotic system, S-BES, increased to 72 mg/l. The diffusion coefficient for the total phenols was calculated from these results to be (1.280±0.017)·10^{-6} cm^2/s.

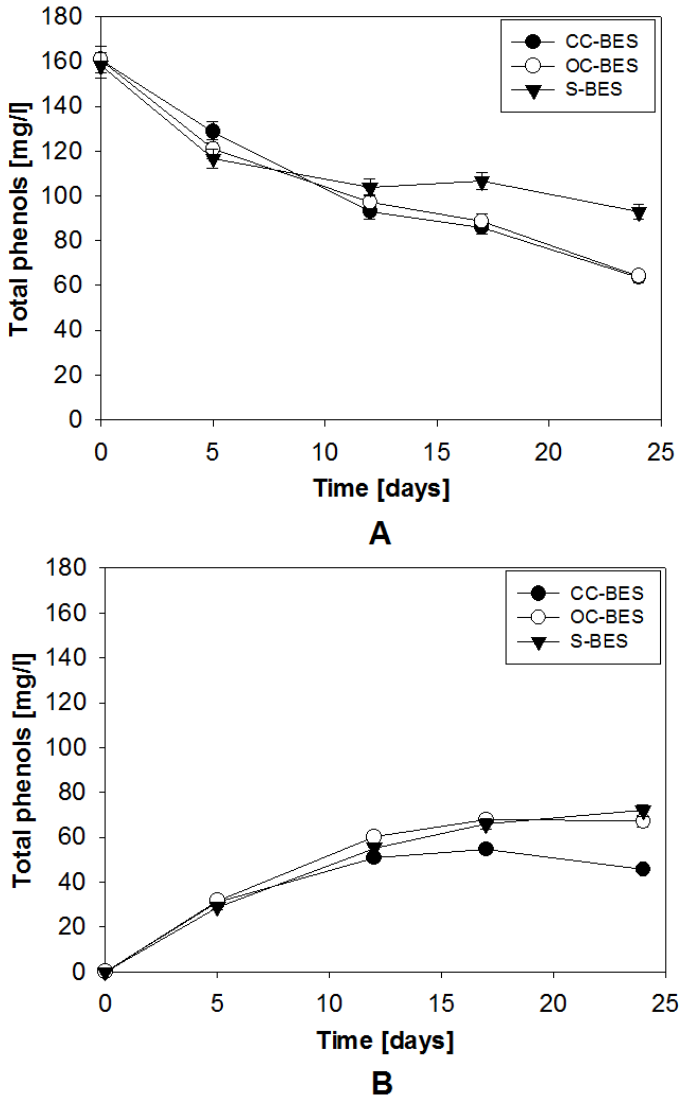

Figure 4: Concentration of total phenols in the anode (A) and cathode (B) chamber. The error bars show the precision of the HPLC analysis.

The concentration of phenolic compounds in the anode chamber of the OC-BES decreased from 161 mg/l to 64 mg/l, due to diffusion into the cathode chamber and biodegradation. The final concentration of total phenols in the cathode chamber is similar to the abiotic system, S-BES (67 mg/l). It was previously reported that oxygen can be transported from the cathode chamber via the Nafion membrane to the anode chamber (Kim *et al.*, 2007). It is likely that oxygen served as the main electron acceptor for biodegradation of the phenolic compounds in the OC-BES. Total phenols in the anode chamber of the CC-BES decreased from 161 mg/l to 64 mg/l. This change was also caused by diffusion and biodegradation. Considering the concentration of phenolic compounds in the anode chamber, there is no significant difference between the CC-BES and OC-BES. However, the concentration of total phenols in the cathode chamber of the CC-BES starts decreasing after 16 days of operation and reaches 46 mg/l at the end of the experiment. It is likely that the phenols were transported back to the anode chamber and then biodegraded, supporting further electricity production.

The microbial community in the CC-BES used two types of electron acceptors: oxygen transported to the anode chamber and the anode electrode. The presence of the anode electrode as an electron acceptor enhanced the biodegradation of the phenolic compounds by 17% compared with the OC-BES.

6. Conclusions

Bioremediation of groundwater contaminated by phenolic compounds was enhanced by the presence of a solid state electrode, which served as an electron acceptor for microbial metabolism. In this case, the biodegradation of total phenols was enhanced by 17%. The results presented in this bulletin are preliminary, only from one replicate and more measurements are needed to confirm this conclusion. Phenolic compounds diffused through the membrane separating the two chambers, which must be considered when interpreting the biodegradation rate and performance of the BES design. The power generated by the BES in this experiment was only 2 mW/m^2 of the anode surface area and is unlikely to be sufficient for practical use. However, when compared with traditional *in situ* bioremediation technologies such as biosparging, BES provide an opportunity to save energy.

Future research will explore the mass transfer processes, electron acceptors and microbial community present in the system in more detail. Further experimentation should involve development of a continuous-flow BES reactor with a PRB electrode that simulates field conditions, including the regulation of the anode potential for better bioremediation performance.

7. Acknowledgements

The research leading to these results has received funding from the European Community's Seventh Framework Programme (FP7/2007-2013 under grant agreement n°265063). We would like to thank Dr. Paul Bentley for building the potentiostat, and Helen Emma Mallinson and Dr. Douglas F. Call for advice with the experimental set up.

8. References

- Atlas, R.M., Philp, J., 2005. Bioremediation: applied microbial solutions for real-world, 1st ed. ASM Press, Washington, DC.
- Aulenta, F., Majone, M., 2010. Bioelectrochemical systems for subsurface remediation, in: Rabaey, K., Angenent, L.T., Schröder, U., Keller, J. (Eds.), Bioelectrochemical Systems: From Extracellular Electron Transfer to Biotechnological Application. London, New York, pp. 305–326.
- Huang, D.-Y., Zhou, S.-G., Chen, Q., Zhao, B., Yuan, Y., Zhuang, L., 2011. Enhanced anaerobic degradation of organic pollutants in a soil microbial fuel cell. Chem. Eng. J. 172, 647–653.
- Kim, J.R., Cheng, S., Oh, S.-E., Logan, B.E., 2007. Power Generation Using Different Cation, Anion, and Ultrafiltration Membranes in Microbial Fuel Cells. Environ. Sci. Technol. 41, 1004–1009.
- Logan, B.E., 2008. Microbial fuel cells, 1st ed. John Wiley & Sons, Inc., New Jersey.
- Luo, H., Liu, G., Zhang, R., Jin, S., 2009. Phenol degradation in microbial fuel cells. Chem. Eng. J. 147, 259–264.
- Mohan, S.V., Chandrasekhar, K., 2011. Self-induced bio-potential and graphite electron accepting conditions enhances petroleum sludge degradation in bio-electrochemical system with simultaneous power generation. Bioresour. Technol. 102, 9532–9541.
- Morris, J.M., Jin, S., 2008. Feasibility of using microbial fuel cell technology for bioremediation of hydrocarbons in groundwater. J. Environ. Sci. Health. A. Tox. Hazard. Subst. Environ. Eng. 43, 18–23.
- Morris, J.M., Jin, S., 2012. Enhanced biodegradation of hydrocarbon-contaminated sediments using microbial fuel cells. J. Hazard. Mater. 213-214, 474–477.
- Morris, J.M., Jin, S., Crimi, B., Pruden, A., 2009. Microbial fuel cell in enhancing anaerobic biodegradation of diesel. Chem. Eng. J. 146, 161–167.
- Wagner, R.C., Call, D.F., Logan, B.E., 2010. Optimal set anode potentials vary in bioelectrochemical systems. Environ. Sci. Technol. 44, 6036–41.
- Wang, X., Cai, Z., Zhou, Q., Zhang, Z., Chen, C., 2012. Bioelectrochemical stimulation of petroleum hydrocarbon degradation in saline soil using U-tube microbial fuel cells. Biotechnol. Bioeng. 109, 426–433.
- Yan, Z., Song, N., Cai, H., Tay, J.-H., Jiang, H., 2012. Enhanced degradation of phenanthrene and pyrene in freshwater sediments by combined employment of sediment microbial fuel cell and amorphous ferric hydroxide. J. Hazard. Mater. 199-200, 217–225.
- Yang, Y., Xu, M., He, Z., Guo, J., Sun, G., Zhou, J., 2013. Microbial Electricity Generation Enhances Decabromodiphenyl Ether (BDE-209) Degradation. PLoS One 8, e70686.
- Zhang, T., Gannon, S.M., Nevin, K.P., Franks, A.E., Lovley, D.R., 2010. Stimulating the anaerobic degradation of aromatic hydrocarbons in contaminated sediments by providing an electrode as the electron acceptor. Environ. Microbiol. 12, 1011–1120.

For more information on the ADVOCATE Project, please visit:
www.theadvocateproject.eu

If you have any questions about this bulletin or would like further information about other CL:AIRE publications please contact us at:
Email: enquiries@claire.co.uk Website: www.claire.co.uk

Appendix B

Hedbavna P., Thornton S.F., Huang W. (2013) Enhanced groundwater bioremediation using microbial fuel cell concepts. Proceedings of the 2nd European Symposium, Water Technology & Management, Belgium.

Enhanced groundwater bioremediation using microbial fuel cell concepts

Hedbavna P.[1], Thornton S.F.[1] and Huang W.E.[1]

1 Groundwater Protection and Restoration Group, Kroto Research Institute, North Campus, University of Sheffield, Broad Lane, Sheffield, S3 7HQ, United Kingdom, p.hedbavna@sheffield.ac.uk, +44 114 222 5786

ABSTRACT: The *in situ* biodegradation of organic contaminants in groundwater is often limited by a lack of electron acceptors for microbial metabolism. Laboratory studies show that microbial fuel cells (MFCs) can enhance biodegradation of organic contaminants by providing electrodes as electron acceptors. This study focused on bioremediation of groundwater contaminated by phenolic compounds (phenol, cresols, xylenols) using MFCs. The MFCs were operated for 24 days. Electricity up to 2.0 mW/m^2 of electrode surface area was produced in an H-type dual-chamber MFC treating contaminated groundwater. The microbial community present in the groundwater used the electrode as an electron acceptor; thus enhancing the degradation of total phenols by 17% in comparison with open circuit control. The electrodes of MFCs installed in the ground have a potential to serve as an inexhaustible electron acceptor for enhanced *in situ* groundwater bioremediation.

INTRODUCTION

Organic contaminants in groundwater can be biodegraded by bacteria when electron donors, electron acceptors and nutrients are available. Natural attenuation of organic compounds (electron donors) under anaerobic conditions is often limited by a lack of readily available electron acceptors, such as oxygen and nitrate for bacterial metabolism (Lovley, 2006). Engineered *in situ* bioremediation technologies e.g. biosparging or nitrate addition, which supply bacteria with electron acceptors, may not be cost-effective, energy efficient or may even cause more environmental pollution (Zhang et al., 2010).

Recent laboratory studies report that bioremediation of petroleum hydrocarbons (Mohan and Chandrasekhar, 2011; Morris et al., 2009; Morris and Jin, 2012; Wang et al., 2012); phenol (Huang et al., 2011; Luo et al., 2009); benzene, toluene, naphthalene, phenanthrene and pyrene (Yan et al., 2012; Zhang et al., 2010) can be enhanced by microbial fuel cells (MFCs). The electrodes of MFCs provide bacteria with a long-term continuous electron acceptor.

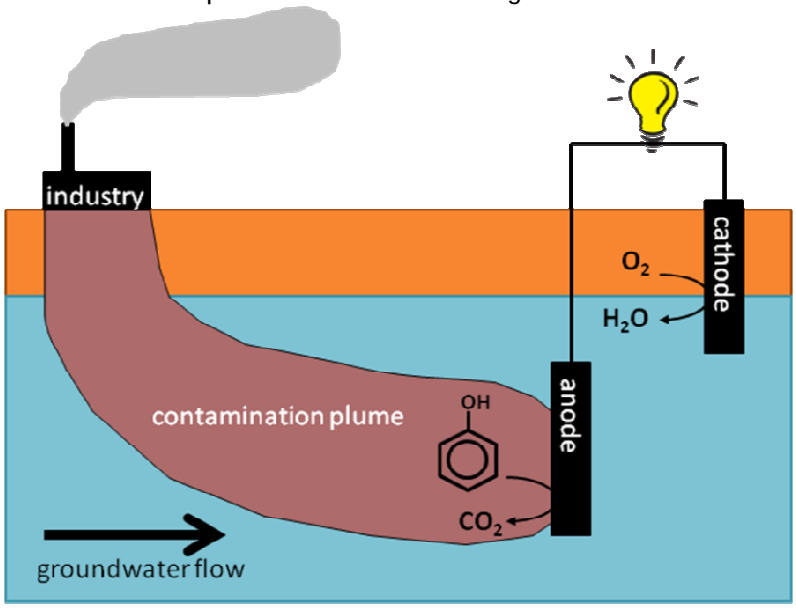

Figure 1: Conceptual model of enhanced in situ groundwater bioremediation using a microbial fuel cell.

Figure 1 shows a conceptual model of an MFC used for enhanced bioremediation in groundwater (bioremediation-MFC). The anode is inserted within the contaminated, oxygen-depleted groundwater and serves as an electron acceptor for biodegradation of organic compounds; phenol is used as an example here. The anode is connected via the wire to the cathode, which is placed in oxygenated uncontaminated groundwater. Electrons released by bacteria at the anode are transported to the cathode and reduce oxygen to water. Electricity is produced during this process, which makes this technology potentially sustainable, considering power consumption. The anode and cathode in the laboratory MFCs can be placed in different chambers separated by a semi-permeable membrane, to simulate the conditions in the aquifer; anode and cathode in the contaminated and uncontaminated groundwater, respectively.

To our knowledge, laboratory experiments, which explored groundwater bioremediation by MFCs, have to date used groundwater amended with nutrients (Morris and Jin, 2008; Morris et al., 2009). Phenolic compounds (e.g. phenol, cresols, xylenols) mainly occur as mixtures in contaminted groundwater (Thornton et al., 2001). However, current research focused on the bioremediation of phenolic compounds using MFCs has only evaluated phenol biodegradation (Huang et al., 2011a; Luo et al., 2009). The aim of this research is to explore the potential of MFCs to enhance bioremediation of groundwater contaminated by coal tar, which contains a mixture of phenol, cresols and xylenols, without any addition of nutrients.

MATERIALS AND METHODS

Groundwater

Groundwater was collected in July 2013 from a multilevel sampler installed within a plume of mixed phenolic contaminants at a site in the UK, using methods described in Thornton et al. (2001). Uncontaminated groundwater was sampled at a depth of 7 meters below ground level (mbgl), whereas contaminated groundwater was sampled from 12 mbgl. This is within a zone defined as the upper plume fringe where dissolved oxygen is below detection, total dissolved phenolic compounds are ca. 200 mg/l, total cell count is 10^7 (Rizoulis et al., 2013; Thornton et al., 2001) and 25% of the microbial population consists of *Goebacter* sp. (unpublished data), a well-known exoelectrogen. Groundwater samples were collected in 2.5-l sterilized bottles filled with nitrogen until all the headspace was removed and then sealed. Samples were stored at 4℃ prior t o experimentation.

MFC set up

H-type dual-chamber MFCs were constructed using two 250-ml Schott bottles joined by a 7.5 cm long glass tube (1.5 cm diameter), which enables a proton exchange membrane, Nafion^{TM} 117 (DuPont), to be inserted between the chambers. Both electrodes were made of carbon cloth (H2315, Freudenberg FCCT SE & Co. KG), with a working surface area of 50 cm^2 and connected to each other using a copper wire and 1 kΩ resistor. The anode chamber was equipped with sampling ports to maintain anaerobic conditions in the anode chamber. The ports were covered by 0.22 µm sterile filters to keep the anode chamber aseptic. All equipment was sterilized by autoclaving (121℃, 0.1 MPa, 20 min.) prior to experimentation.

Three different MFCs were set up, a closed circuit MFC (CC-MFC), an open circuit control MFC (OC-MFC) and a sterile control MFC (S-MFC). The anode chamber of the CC-MFC and the OC-MFC contained 200 ml of contaminated groundwater (12 mbgl). In the S-MFC, 200 ml of filtered (tangential flow filtration unit, 0.1 µm, Pall) contaminated groundwater (12 mbgl) with 2 g/l of sodium azide was added into the anode chamber. All three cathode chambers were filled with 200 ml of uncontaminated groundwater (7 mbgl) sterilized by autoclaving and covered by wooden pulp stopper to allow aeration and prevent contamination by airborne bacteria. The circuits of CC-MFC and S-MFC were closed with a 1 kΩ resistor, whereas the OC-MFC operated under open circuit conditions. All MFCs were placed on a shaker (85 rpm) to support mixing within the chambers and operated for 24 days. The open circuit and closed circuit voltage (across the resistor) were monitored daily. Polarization and power curve measurements were made using a potentiostatic discharge technique when the closed circuit voltage, i.e. electricity production by MFCs, reached its maximum value.

Chemical analysis

Samples for chemical analysis were taken every 5-7 days from the anode and cathode chamber and filter-sterilized through a 0.22 µm filter. Samples were stored at -20℃ prior to analysis. The concentration of total phenols (phenol, isomers of cresols and xylenols) in the anode and cathode chamber was determined by high performance liquid chromatography (HPLC) using a Perkin Elmer instrument and UV detector. The detection limit was 1 mg/l and precision of this analysis was ±7% (Thornton et al., 2001).

RESULTS AND DISCUSSION

Electricity production

The open circuit voltage (OCV) of CC-MFC, OC-MFC and S-MFC reached 137 mV, 165 mV and 76 mV, respectively, at the beginning of the experiment (Figure 2A). Similarly, as in sediment-MFCs (Reimers et al., 2001), the non-zero OCV at time zero was caused by the natural difference in redox potential between contaminated and uncontaminated groundwater. The OCV value of biologically active MFCs increased up to 550 mV and 590 mV in CC-MFC and OC-MFC, respectively, while OCV of S-MFC decreased to -18 mV. The OCV of CC-MFC decreased after 16 days of operation to 330 mV (Fig. 2A). The closed circuit voltage (CCV) (Figure 2B) started increasing in biologically active MFCs after 3 days of operation, reaching a maximum value 82 mV in the CC-MFC and 29 mV in the OC-MFC. The CCV of the CC-MFC decreased to 14 mV after 16 days (Fig. 2B). The CCV of control sample S-MFC remained at 0 mV, suggesting that the electricity production was due to biological activity in the CC-MFC and OC-MFC.

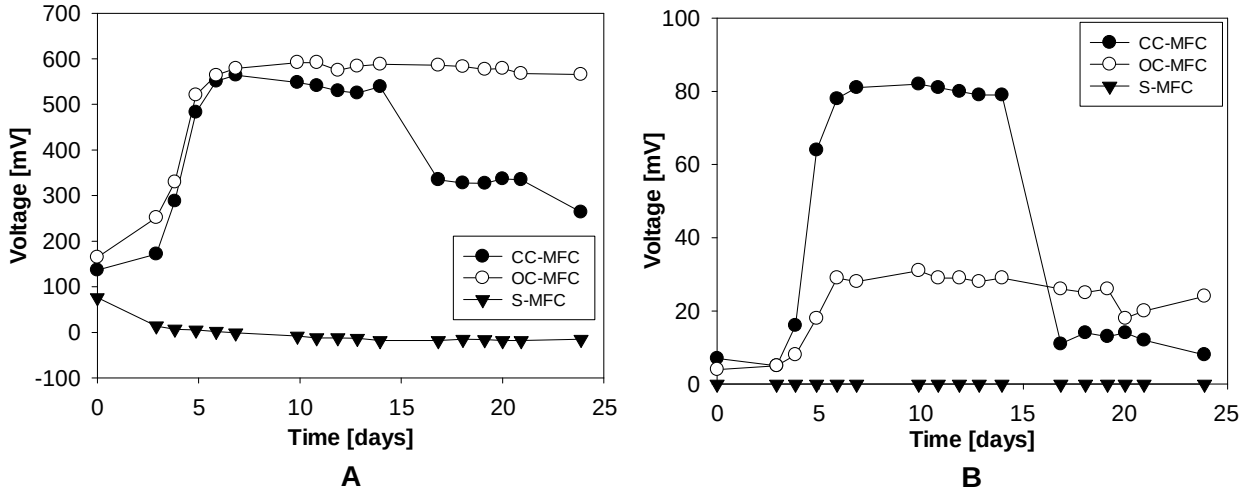

Figure 2: Open circuit voltage (A) and closed circuit voltage (B).

Figure 3 shows the results of polarization and power curve measurement for the CC-MFC and OC-MFC. The OC-MFC voltage decreased more rapidly with increasing current density than for the CC-MFC, resulting in a lower power density (1.2 mW/m^2 in the OC-MFC, 2.0 mW/m^2 in the CC-MFC). The OC-MFC generates a lower maximum current density (10.3 mA/m^2) than the CC-MFC (20.8 mA/m^2). The internal resistance of the CC-MFC was calculated using Ohm's law at the highest power production point, resulting in 2270 Ω. The measured values of electrical efficiency correspond with the values of power density and internal resistance for H-type dual-chamber MFC published previously (Logan, 2008).

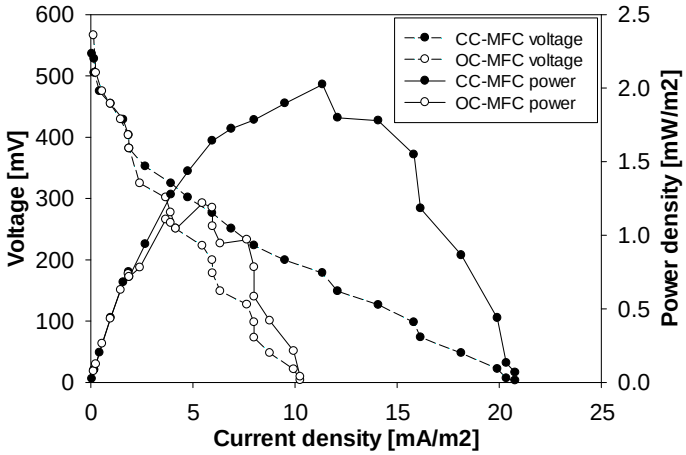

Figure 3: Polarization and power curve for the CC-MFC and OC-MFC.

The results demonstrate that no electricity can be produced in the absence of bacteria (S-MFC), indicating that microbial activity contributed to the electricity generation. In this study, although there is no significant difference in the OCV between the CC-MFC and OC-MFC, the CCV produced and the maximum power density show that the CC-MFC can produce more electricity than the OC-MFC (2.0 mW/m^2 and 1.2 mW/m^2, respectively). This is likely due to the adaptation of bacteria in the CC-MFC for electricity generation. The closed circuit set up creates a selection pressure in the CC-MFC microbial community. The community develops the ability to transfer electrons to the anode electrode and uses it as an electron acceptor. The OC-MFC bacteria, growing under open circuit conditions, are not adapted for this. A previous study on bioremediation-MFC by Yang et al. (2013) confirms this hypothesis. The authors observed a significant difference between the microbial community of the CC-MFC and OC-MFC with increased number of exoelectrogens in the CC-MFC (Yang et al., 2013).

Biodegradation of phenolic compounds

Phenolic compounds diffused from the anode chamber to the cathode chamber through the Nafion membrane (Figure 4), decreasing the concentration of total phenols in the anode chamber from 158 mg/l to 93 mg/l at the end of the experiment. The concentration of phenolic compounds in the cathode chamber of the S-MFC was 72 mg/l, due to phenol diffusion from the anode chamber. The diffusion coefficient for the total phenols was calculated using data from the S-MFC. The mass balance of total phenols for the sterile system can be expressed as

$$m_{an,0} + m_{cat,0} = m_{an,t} + m_{cat,t} \quad (1)$$

$$c_{an,0}V + 0 = c_{an,t}V + c_{cat,t}V \text{ or } c_{an,t} = c_{an,0} - c_{cat,t} \quad (2)$$

$$\frac{dc_{cat,t}}{dt} = \frac{D_{phenols} \cdot A}{L \cdot V}(c_{an,0} - 2c_{cat,t}), \quad (3)$$

where m is mass, c is concentration, V is volume, $D_{phenols}$ is the average diffusion coefficient of total phenols through the membrane, A is the membrane surface area, L is the membrane thickness, an,0 and cat,0 are anode and cathode chambers at the beginning of the experiment, and an,t and cat,t are the MFC chambers at time t (Kim et al., 2007). The diffusion coefficient of phenolic compounds can be calculated after integration,

$$D_{phenols} = -\frac{VL}{2At} ln\left[\frac{(C_{an,0} - 2c_{cat,t})}{C_{an,0}}\right]. \quad (4)$$

The diffusion coefficient $D_{phenols}$ = (1.280±0.017)·10^{-6} cm^2/s was calculated from measured data applying Equation 4.

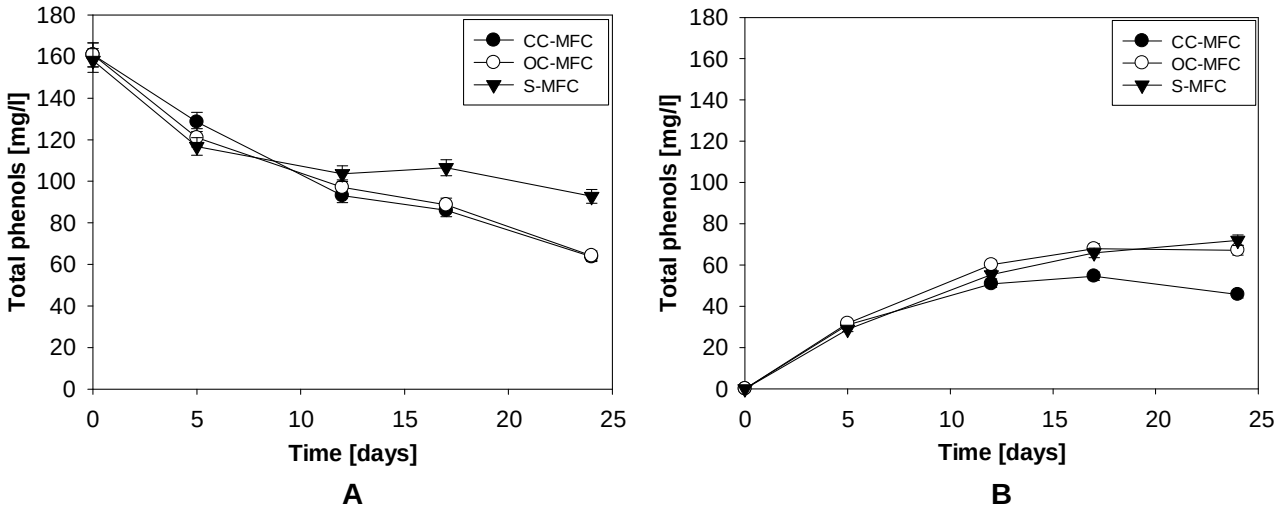

Figure 4: Concentration of total phenols in the anode (A) and cathode (B) chamber.

The concentration of phenolic compounds in the anode chamber of the OC-MFC decreased from 161 mg/l to 64 mg/l which is due to diffusion into the cathode chamber and biodegradation. The final concentration of total phenols in the cathode chamber is similar to the S-MFC (67 mg/l). It was previously reported that oxygen can be transported from the cathode chamber via the Nafion membrane to the anode chamber ($D_{O2} = 2.4 \cdot 10^{-6}$ cm^2/s) (Kim et al., 2007). It is likely that oxygen served as the main electron acceptor for biodegradation of the phenolic compounds in the OC-MFC. Total phenols in the anode chamber of the CC-MFC decreased from 161 mg/l to 64 mg/l. It is the same rate of decrease as in the OC-MFC. This change was also caused by diffusion and biodegradation. Considering the concentration of phenolic compounds in the anode chamber, there's no significant difference between the CC-MFC and OC-MFC. However, the concentration of total phenols in the cathode chamber of the CC-MFC starts decreasing after 16 days of operation and reaches 46 mg/l at the end of the experiment. It is likely that the phenols were transported back to the anode chamber and then biodegraded, supporting further electricity production. Electricity production in the CC-MFC decreased after 16 days of operation (Figure 2), which is likely due to the limited mass transfer of phenolic compounds from the cathode chamber to the anode chamber.

Table 1: Biodegradation of phenolic compounds.

Time [days]	CC-MFC	OC-MFC	S-MFC
	Biodegradation [%]		
0	0	0	0
5	0.87	5.14	9.54
12	10.48	2.27	1.20
17	12.65	2.67	-7.17
24	32.04	18.35	-2.36

The total mass of phenolic compounds, considering the anode and cathode chamber, does not decrease in the S-MFC (Table 1), but decreases in comparison with S-MFC by 18% in the OC-MFC and by 32% in the CC-MFC after 24 days of operation. The microbial community in the CC-MFC used two types of electron acceptors: oxygen transported to the anode chamber and the anode electrode. The presence of the anode electrode as an electron acceptor enhanced the biodegradation of the phenolic compounds by 17% compared with the OC-MFC.

CONCLUSIONS

Electricity was produced in a dual-chamber MFC using groundwater contaminated by phenolic compounds. The maximum power generation reached 2.0 mW/m^2. Bacteria already present in the groundwater were able to biodegrade the phenolic compounds, using the anode electrode as an electron acceptor. Bioremediation of the total phenols was

enhanced by approximately 17% in comparison with an open circuit control system. Phenolic compounds diffused through the Nafion membrane at the rate $(1.280\pm0.017)\cdot10^{-6}$ cm^2/s, which must be taken into account to correctly interpret the biodegradation rate and performance of the MFC design concept. Future research will explore the mass transfer processes, electron acceptors and microbial community present in the system in more detail.

ACKNOWLEDGEMENTS

This study was completed while PH held a Marie Curie Early Stage Researcher Fellowship within the framework of the Marie Curie Initial Training Network ADVOCATE - Advancing sustainable *in situ* remediation for contaminated land and groundwater, funded by the European Commission, Marie Curie Actions Project No. 265063. We would like to thank Dr. Paul Bentley for building the potentiostat, and Helen Emma Mallinson and Dr. Douglas F. Call for advice with the experimental set up.

REFERENCES

Huang, D.-Y.; Zhou, S.-G.; Chen, Q.; Zhao, B.; Yuan, Y.; Zhuang, L. 2011. Enhanced anaerobic degradation of organic pollutants in a soil microbial fuel cell. Chemical Engineering Journal 172:647–653.

Kim, J.R.; Cheng, S.; Oh, S.-E.; Logan, B.E. 2007. Power generation using different cation, anion, and ultrafiltration membranes in microbial fuel cells. Environmental Science & Technology 41:1004–1009.

Logan, B.E. 2008. Microbial fuel cells 1st ed. New Jersey: John Wiley & Sons, Inc.

Lovley, D.R. 2006. Bug juice: harvesting electricity with microorganisms. Nature Reviews. Microbiology 4:497–508.

Luo, H.; Liu, G.; Zhang, R.; Jin, S. 2009. Phenol degradation in microbial fuel cells. Chemical Engineering Journal 147:259–264.

Mohan, S.V.; Chandrasekhar, K. 2011. Self-induced bio-potential and graphite electron accepting conditions enhances petroleum sludge degradation in bio-electrochemical system with simultaneous power generation. Bioresource Technology 102:9532–9541.

Morris, J.M.; Jin, S. 2008. Feasibility of using microbial fuel cell technology for bioremediation of hydrocarbons in groundwater. Journal of Environmental Science and Health. Part A, Toxic/Hazardous Substances & Environmental Engineering 43:18–23.

Morris, J.M.; Jin, S. 2012. Enhanced biodegradation of hydrocarbon-contaminated sediments using microbial fuel cells. Journal of Hazardous Materials 213-214:474–477.

Morris, J.M.; Jin, S.; Crimi, B.; Pruden, A. 2009. Microbial fuel cell in enhancing anaerobic biodegradation of diesel. Chemical Engineering Journal 146:161–167.

Reimers, C.E.; Tender, L.M.; Fertig, S.; Wang, W. 2001. Harvesting energy from the marine sediment-water interface. Environmental science & Technology 35:192–5.

Rizoulis, A.; Elliott, D.R.; Rolfe, S.A.; Thornton, S.F.; Banwart, S.A.; Pickup, R.W.; Scholes, J.D. 2013. Diversity of planktonnic and attached bacterial communities in a phenol-contaminated sandstone aquifer. Microbial Ecology 66:84-95.

Thornton, S.F.; Quigley, S.; Spence, M.J.; Banwart, S.A.; Bottrell, S.; Lerner, D.N. 2001. Processes controlling the distribution and natural attenuation of dissolved phenolic compounds in a deep sandstone aquifer. Journal of Contaminant Hydrology 53:233-267.

Wang, X.; Cai, Z.; Zhou, Q.; Zhang, Z.; Chen, C. 2012. Bioelectrochemical stimulation of petroleum hydrocarbon degradation in saline soil using U-tube microbial fuel cells. Biotechnology and Bioengineering 109:426–433.

Yan, Z.; Song, N.; Cai, H.; Tay, J.-H.; Jiang, H. 2012. Enhanced degradation of phenanthrene and pyrene in freshwater sediments by combined employment of sediment microbial fuel cell and amorphous ferric hydroxide. Journal of Hazardous Materials 199-200:217–225.

Yang, Y.; Xu, M.; He, Z.; Guo, J.; Sun, G.; Zhou, J. 2013. Microbial electricity generation enhances decabromodiphenyl ether (BDE-209) degradation. PLoS ONE 8: e70686. doi:10.1371/journal.pone.0070686.

Zhang, T.; Gannon, S.M.; Nevin, K.P.; Franks, A.E.; Lovley, D.R. 2010. Stimulating the anaerobic degradation of aromatic hydrocarbons in contaminated sediments by providing an electrode as the electron acceptor. Environmental Microbiology 12:1011–1120.

Appendix C

Hedbavna, P., Rolfe, S.A., Huang, W.E., Thornton, S.F., 2016. Biodegradation of phenolic compounds and their metabolites in contaminated groundwater using microbial fuel cells. Bioresource Technology 200, 426–434.

Bioresource Technology 200 (2016) 426–434

Contents lists available at ScienceDirect

Bioresource Technology

journal homepage: www.elsevier.com/locate/biortech

Biodegradation of phenolic compounds and their metabolites in contaminated groundwater using microbial fuel cells

Petra Hedbavna [a,*], Stephen A. Rolfe [b], Wei E. Huang [c], Steven F. Thornton [a]

[a] Department of Civil and Structural Engineering, Kroto Research Institute, Broad Lane, University of Sheffield, S3 7HQ, United Kingdom
[b] Department of Animal and Plant Sciences, Alfred Denny Building, Western Bank, University of Sheffield, S10 2TN, United Kingdom
[c] Department of Engineering Science, Oxford University Begbroke Science Park, Sandy Lane, Yarnton, Kidlington OX5 1PF, United Kingdom

HIGHLIGHTS

- Bioremediation of groundwater contaminated by phenols was examined in MFCs.
- Fermentation of phenols to acetate was a dominant process in the field studied.
- Acetate served as an electron donor in the MFCs and its removal was enhanced.
- Enhanced biodegradation of acetate can speed up the removal of phenols.
- Knowledge of biodegradation pathways of contaminants is critical for BES-remediation.

GRAPHICAL ABSTRACT

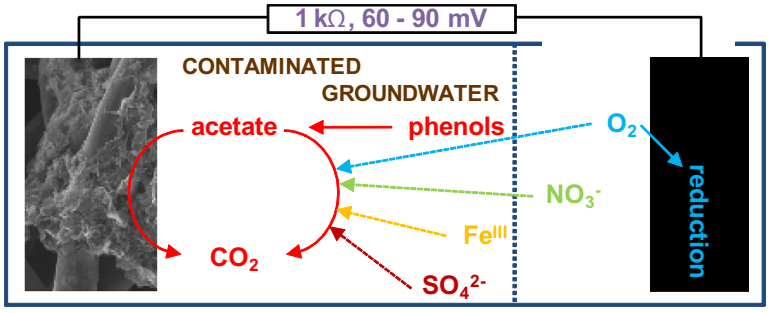

ARTICLE INFO

Article history:
Received 5 August 2015
Received in revised form 21 September 2015
Accepted 22 September 2015
Available online 11 November 2015

Keywords:
Microbial fuel cells
Bioremediation
Groundwater
Phenol
Contaminants

ABSTRACT

This is the first study demonstrating the biodegradation of phenolic compounds and their organic metabolites in contaminated groundwater using bioelectrochemical systems (BESs). The phenols were biodegraded anaerobically via 4-hydroxybenzoic acid and 4-hydroxy-3-methylbenzoic acid, which were retained by electromigration in the anode chamber. Oxygen, nitrate, iron(III), sulfate and the electrode were electron acceptors for biodegradation. Electro-active bacteria attached to the anode, producing electricity (~1.8 mW/m^2), while utilizing acetate as an electron donor. Electricity generation started concurrently with iron reduction; the anode was an electron acceptor as thermodynamically favorable as iron(III). Acetate removal was enhanced by 40% in the presence of the anode. However, enhanced removal of phenols occurred only for a short time. Field-scale application of BESs for *in situ* bioremediation requires an understanding of the regulation and kinetics of biodegradation pathways of the parent compounds to relevant metabolites, and the syntrophic interactions and carbon flow in the microbial community.

1. Introduction

Groundwater contamination is a problem worldwide, potentially causing harm to the environment and human health. *In situ* bioremediation is receiving increasing interest as a potentially more sustainable approach to manage pollutants in contaminated aquifers (Interstate Technology & Regulatory Council, 2011). Various *in situ* bioremediation concepts have been developed for many organic chemicals, recognizing that biodegradation processes and treatment performance are often limited by the availability of electron acceptors for microbial metabolism (Zhang et al., 2010).

* Corresponding author.
E-mail addresses: petra.hedbavna@sheffield.ac.uk, petra.hedbavna@gmail.com (P. Hedbavna).

http://dx.doi.org/10.1016/j.biortech.2015.09.092
0960-8524/

Bioelectrochemical systems (microbial fuel cells and microbial three-electrode systems, BESs) can enhance the biodegradation of organic chemicals such as petroleum hydrocarbons (Mohan and Chandrasekhar, 2011; Morris and Jin, 2012; Morris et al., 2009; Wang et al., 2012), phenol (Friman et al., 2013; Huang et al., 2011; Luo et al., 2009), benzene, toluene and naphthalene (Zhang et al., 2010), and phenanthrene and pyrene (Yan et al., 2012), by providing bacteria with an electrode that acts as an inexhaustible electron acceptor. This has been demonstrated at laboratory scale using pure cultures of bacteria, wastewater, sediment or soil, often amended with nutrients and vitamins. However, the potential role of BES technology in the treatment of contaminated groundwater has been limited to one study of petroleum hydrocarbon-contaminated groundwater (Morris et al., 2009). This is an important knowledge gap in the development of bioelectrochemically-enhanced treatment of groundwater contaminants in terms of both, scientific understanding of the processes involved and engineering applications.

Organic contaminants in groundwater typically occur in mixtures with different potential for biodegradation (Wiedemeier et al., 1999). An example is phenolic compounds, which can enter groundwater from coal-gasification plants and many other industrial processes (Thornton et al., 2001). However, only biodegradation of phenol has been examined in MFCs (Friman et al., 2013; Huang et al., 2011; Luo et al., 2009). The performance of BES technology in the treatment of natural groundwater containing a mixture of phenols (phenol, isomers of cresols and xylenols) and their metabolites, electron acceptors and an indigenous microbial community is to date unknown. The influence of different organic compounds, which may compete with target contaminants as alternative carbon sources for bacteria in biodegradation processes, is of particular interest. This is important as bioremediation may be limited by preferential metabolism of alternative substrates despite an adequate supply of electron acceptors for complete metabolism (Wiedemeier et al., 1999).

Groundwater used in this study was sampled from a plume of phenolic compounds (Thornton et al., 2001). From chemical analysis it is characterized as anaerobic, nitrate depleted, with iron(III) in colloid oxide/hydroxide form and sulfate as electron acceptors. It contained phenol, cresols and xylenols (1.4 mM total concentration), acetate (1.9 mM) and high cell numbers (10^7 cells/mL) (Rizoulis et al., 2013; Thornton et al., 2001). Twenty-five percent of the planktonic microbial community at the depth sampled consists of *Geobacter* sp. (unpublished data), implying that the community could be electro-active (Logan, 2008).

Previous studies of phenol biodegradation in MFCs have demonstrated the basic concept of enhanced bioremediation (Friman et al., 2013; Huang et al., 2011; Luo et al., 2009) but the metabolic pathways and mechanism of phenol removal were not studied. The aim of this study is to examine the chemical and biological processes that occur in an MFC used to treat groundwater contaminated by phenols. We hypothesized that the groundwater microbial community would use the anode of an MFC as an electron acceptor after forming a biofilm on it. *Geobacter* sp. are often dominant in MFCs fed by acetate (Kiely et al., 2011) but can also degrade aromatic compounds (Bond et al., 2002; Zhang et al., 2010). Phenolic compounds and/or acetate could therefore serve as electron donors for electricity production. If the phenols were degraded directly by the electro-active bacteria, the enhanced removal of phenols should occur immediately with current generation. However, exoelectrogens might prefer simpler substrates such as acetate (Kiely et al., 2011). In that case, enhanced removal of phenols could occur after acetate depletion and such MFC-aided biodegradation should be enhanced by syntrophic metabolism within the microbial community.

In this study, we showed that the microbial community in contaminated groundwater can produce electricity using acetate, a fermentation product of phenols, as an electron donor for exoelectrogens. It suggests that syntrophic interactions within microbial community should play an important role in bioelectrochemically-enhanced remediation.

Conceptual models of large-scale BESs have been developed for potential use in the field as described in Aulenta and Majone (2010) and Williams et al. (2010). We designed a field-scale conceptual model of a groundwater MFC based on this literature and additionally on Logan (2010) and Logan et al. (2006). The anode is built as a permeable reactive barrier in contact with the contaminated, oxygen-depleted groundwater whilst the cathode is placed in uncontaminated groundwater where oxygen is provided via a borehole. In our study, we used a laboratory-scale model of this system to better understand the processes controlling the performance of groundwater MFCs. In a field-scale MFC, the natural presence of bacteria at the cathode would potentially allow for the biologically catalyzed reduction of oxygen (Logan et al., 2006). However, in our laboratory system, we simplified the microbiological component by filter-sterilizing the uncontaminated groundwater placed in the cathode chamber. Other aspects of the laboratory MFC were also sought to be relevant to the field scale. For example, we chose to use carbon-cloth electrodes as although they may limit electrode performance to some extent (Logan et al., 2006), carbon cloth would be cost effective at a large scale and is less prone to poisoning than Pt catalysts (Logan, 2010).

2. Methods

2.1. Groundwater

Groundwater samples were collected from different depths in the aquifer (Thornton et al., 2001); uncontaminated water from above the plume at 7 mbgl (meters below ground level) and contaminated groundwater from the plume fringe at 12 mbgl. The groundwater was collected in sterile, nitrogen-purged 2.5 L amber glass bottles, which were filled completely. Samples were stored at 4 °C prior to use in the experiments.

2.2. Microbial fuel cells

H-type dual-chamber MFCs were constructed based on the well-known MFC designs (Logan, 2008) using two 250 mL Schott bottles, joined by a 7.5 cm glass tube (1.5 cm diameter), with a Nafion™ 117 proton exchange membrane (DuPont) between the chambers. The anode chamber was equipped with a 3-port gas-tight screw cap fitted with two ports for separate gas and liquid sampling (Shah et al., 2009) and one port to insert the wire. The sampling ports were covered by 0.22 μm sterile PES filters (Millex®, Merck KGaA) (Shah et al., 2009) and the cathode chamber was closed by a wooden pulp stopper to keep both chambers aseptic. The electrodes were made of carbon cloth (H2315, Freudenberg FCCT SE & Co. KG) with a projected surface area of 50 cm^2.

Three MFCs were created in triplicate or duplicate in an anaerobic chamber. These comprised a closed circuit MFC (CC-MFC), an open circuit control MFC (OC-MFC) and a sterile control MFC (S-MFC). The anode chamber of the CC-MFC and OC-MFC contained 200 ml of contaminated groundwater (12 mbgl). 200 ml of filter-sterilized (bottle-top filter VacuCap 90 PF 0.8/0.2 μm, Pall) contaminated groundwater were added to the anode chamber of the S-MFC. All cathode chambers were filled with 200 mL of filter-sterilized uncontaminated groundwater (7 mbgl). The circuits of the CC-MFC and S-MFC were closed with copper wire connecting a 1 kΩ resistor to the electrodes, whereas the OC-MFC operated

under open circuit conditions. All MFCs were shaken (100 rpm) at 25 °C ± 2 °C for the first 27 days of the 92 day experiment.

The voltage across the resistor was monitored every 10 min with a data logger (NI USB-6251, National Instruments) connected to a computer. Polarization and power curves were generated using a potentiostatic discharge technique (Zhao et al., 2009) when the closed circuit voltage (i.e. electricity production by the MFC) reached a maximum value. The electrical potential of the cathode was measured at the maximum electricity production point against a silver chloride electrode (Ag/AgCl/saturated KCl, 0.197 V vs. SHE at 25 °C) under open and closed circuit conditions (Zhao et al., 2009).

Individual carbon sources were added to the anode chamber of the MFCs later in the experiment (days 56–80) to evaluate the contribution of potential electron donors in electricity production. 4 mL of liquid were removed from the MFCs and replaced by a pure chemical dissolved in ultra pure (ultra high quality, UHQ) water. The concentrations used reflected those in the original groundwater (control: no chemical added, phenol: 213 μmol/L, m- and p-cresol: 185 μmol/L each, 3,4- and 3,5-xylenol: 164 μmol/L each, acetate: 508 μmol/L, 1016 μmol/L and 2033 μmol/L).

The role of the electrode biofilm in electricity production was examined. An electrode from one of the closed circuit MFCs (running for 87 days) was removed and replaced by a sterile electrode from a new sterile MFC (sterile electrode in a mature closed circuit MFC, SE + CC-MFC). The mature electrode was gently washed in filter-sterilized contaminated groundwater (12 mbgl) and put into a new sterile MFC (mature electrode in a sterile MFC, ME + S-MFC).

2.3. Chemical analysis

Groundwater (3–13 mL) for chemical analysis was sampled at approximately 1 week intervals and filtered (0.22 μm sterile PES). The filters were changed for each sampling point. Samples for analysis of dissolved metals were acidified (1% (*v*/*v*) ultra pure nitric acid) and stored with samples for analysis of phenols at 4 °C. Samples for major ion and acetate analysis were stored at −20 °C (Shah et al., 2009). A volume of fresh filter-sterilized groundwater equal in volume to the sample removed, with the same composition as the starting sample, was added to MFCs to maintain the total volume during the experiment.

Phenolic compounds (phenol, isomers of cresols and xylenols) were analyzed by reversed-phase high performance liquid chromatography (HPLC) using a PerkinElmer instrument with a UV detector (wavelength 280 nm) and C18 column (Thermo Scientific™ Hypersil™ ODS-2, particle size 5 μm, 250 mm × 4.6 mm I. D.) and C18 guard column (Thornton et al., 2001). The sample injection loop was 10 μL. The eluent was an 80:20 mixture of 1% (*v*/*v*) acetic acid and acetonitrile, with 1.6 mL/min flow rate, changing to 1.0 ml/min between 4.7 and 5.7 min, followed by a 12 min gradient to a 60:40 ratio for another 4 min. The detection limit was 1 mg/L, with an analytical precision of ±7%.

Organic acid metabolites of phenols were identified using a QStar Elite (AppliedBiosystems) mass spectrometer with ion-spray injection. 0.3 ml fractions of HPLC eluent were collected in Eppendorf tubes between 2 and 6 min elution time. Samples were vacuum dried overnight (SpeedVac Plus, Thermo Scientific™) and re-suspended in 100 μl of 50% methanol and 0.1% formic acid in UHQ water. These fractions were then analyzed on the mass spectrometer.

Major ions and acetate were analyzed using an ion chromatograph (Thornton et al., 2001) (Dionex ICS 3000, Thermo Scientific™) with autosampler and eluent regeneration. The anions and acetate were separated using a Dionex IonPac® AS18 column with a AG18 guard column and 31 mM sodium hydroxide as eluent, at a flow rate of 0.25 mL/min. The cations were separated by a Dionex IonPac® CS16 column with a CG16 guard column and 48 mM methane sulfonic acid as eluent, at a flow rate of 0.42 mL/min. Sample conductivity and pH were measured prior to ion analysis. Dissolved iron was analyzed by ICP-MS (PerkinElmer Elan DRC II) (Shah et al., 2009).

The dissolved oxygen concentration in the MFCs was measured weekly, non-invasively, using a fiber-optic probe and oxygen sensor (Fibox, PreSens) fitted to the inside of MFC chambers. The detection limit was 15 ppb (Shah et al., 2009).

Statistical comparison of CC- and OC-MFC performance (phenolics, metabolite and acetate data) at day 27 and 34 was completed with two-tailed *t*-test ($\alpha = 0.05$) in SigmaPlot 12.5.

2.4. Scanning electron microscopy (SEM)

All carbon cloth anodes were removed from the MFCs at the end of the experiment, drained using a sterile paper tissue, washed gently in filter-sterilized phosphate buffer saline (PBS) and drained again. A 1 cm^2 piece of carbon cloth from the middle of each electrode was prepared for SEM using standard methods (for example Little et al., 1991). The samples were fixed overnight in 0.1 M cacodylate buffer with 3% glutaraldehyde at 4 °C. The specimens were then washed twice in 0.1 M cacodylate buffer with 15 min intervals at 4 °C. Secondary fixation was carried out in 2% osmium tetroxide aqueous for 1 h at room temperature. The washing step was then repeated. All the following steps took place at room temperature. Samples were then dehydrated through a graded series of ethanol (75%, 95%, 100% twice), each for 15 min. Samples were dried over anhydrous copper sulfate for 15 min, removing most of the ethanol. Residual ethanol was then removed by hexamethyldisilazane. Initially, the specimens were placed in a 50/50 mixture of 100% ethanol and 100% hexamethyldisilazane for 30 min, followed by 30 min in 100% hexamethyldisilazane. They were then allowed to air dry overnight before mounting. After drying, the samples were mounted on 12.5 mm diameter stubs and attached with carbon-sticky tabs and then coated in a sputter coater (Edwards S150B) with approximately 25 nm of gold. The specimens were examined in a Philips XL-20 scanning electron microscope at an accelerating voltage of 20 kV.

3. Results and discussion

The biological and chemical processes expected to occur in the MFCs include: (i) biodegradation of phenolic compounds to carbon dioxide via organic metabolites; (ii) bacterial respiration, with the anode and other chemical compounds in the groundwater serving as electron acceptors; (iii) enhanced biodegradation of phenolic compounds in CC-MFC compared with OC-MFC, due to bacterial transfer of electrons to the anode; (iv) reduction of oxygen on the cathode by electron transfer from the anode to the cathode, supporting electricity generation; and (v) diffusion and electromigration of dissolved ions between the chambers.

3.1. Biodegradation of phenolic compounds and their metabolites

Phenolic compounds can be degraded to carbon dioxide, firstly by fermentation to structurally simpler and more easily biodegradable compounds, with subsequent respiration using different electron acceptors (Watson et al., 2003). Fermentation is generally considered rate limiting in the biodegradation of phenols, but is important for the production of acetate in groundwater at the field site under consideration (Thornton et al., 2001; Watson et al., 2005).

In this experiment, phenolic compounds diffused from the anode chamber to the cathode chamber via the membrane along a concentration gradient, as shown in the S-MFC data (Fig. 1AB).

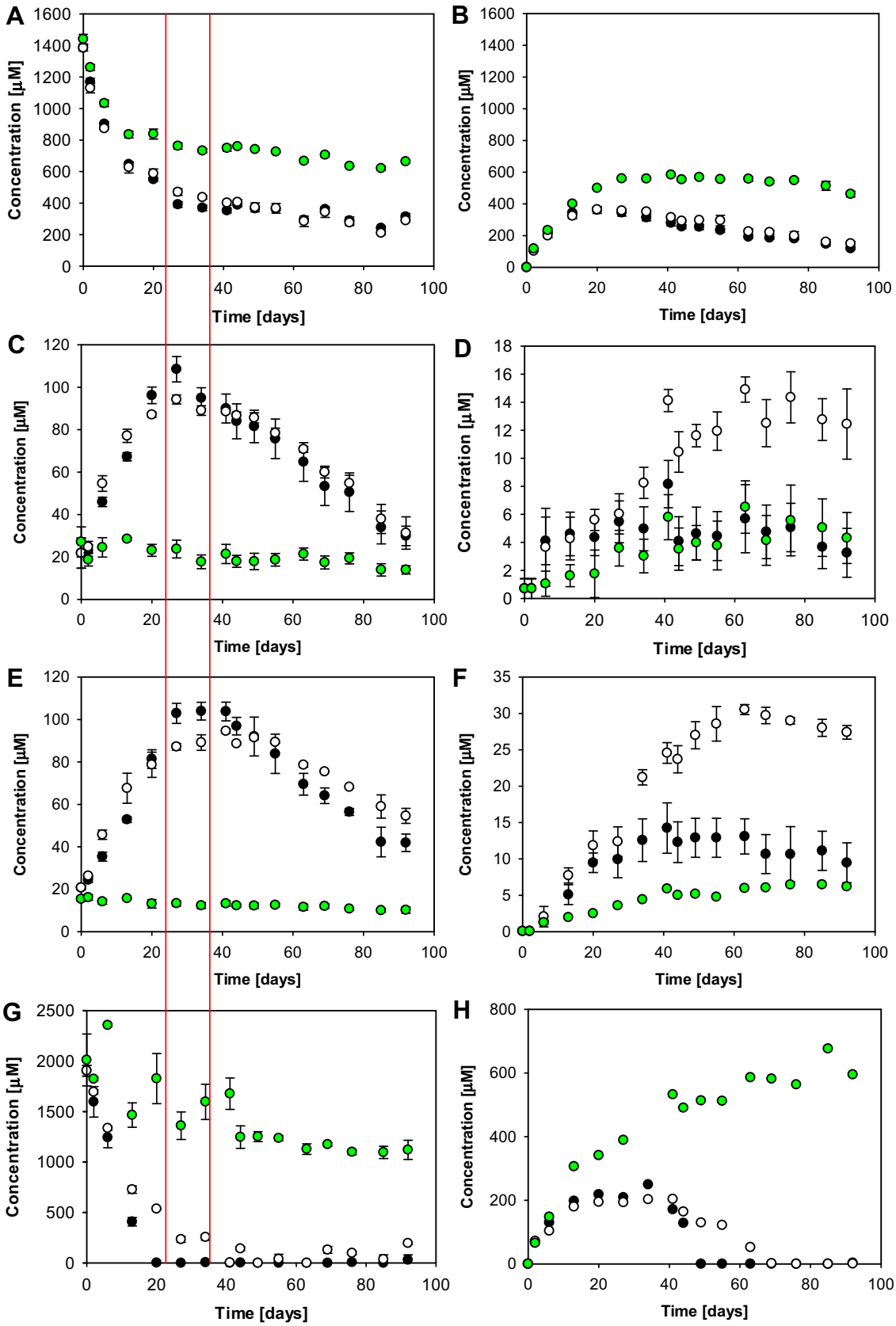

Fig. 1. Changes in concentrations of total phenols (A, B), 4-hydroxybenzoic acid (C, D), 4-hydroxy-3-methylbenzoic acid (E, F) and acetate (G, H) in the anode chamber (left) and cathode chamber (right) of the CC-MFC (black), OC-MFC (white), S-MFC (green). Average data from replicates shown with error bars representing standard deviation. The concentration of individual phenolic compounds was reduced by biodegradation and all are presented as a total concentration in A and B. (For interpretation of the references to color in this figure legend, the reader is referred to the web version of this article.)

The concentration of total phenols in the S-MFC decreased from 1440 μM ± 30 μM to 664 μM ± 8 μM at the end of the experiment. The final concentration of phenols in the cathode and anode chamber of the S-MFC should theoretically be equal. The lower than expected (462 μM ± 18 μM) final concentration of phenols in the cathode chamber of the S-MFC can be explained by their aqueous volatility (Chen et al., 2014). Biodegradation of phenols occurred in the CC- and OC-MFC, shown by the faster decrease in concentration in the anode chamber (Fig. 1AB). At most time points, there was no significant difference in the concentration of phenols between the CC-MFC and OC-MFC. However, the concentration of total phenols was significantly lower ($P < 0.05$) in the CC-MFC than in the OC-MFC at day 27 and 34.

Two metabolites of phenols, 4-hydroxybenzoic acid (4HB acid) and 4-hydroxy-3-methylbenzoic acid (4H3MB acid), referred to as metabolites hereafter, were identified by mass spectrometry and a comparison of their elution times on HPLC (data not shown). Both metabolites were detected at low concentration in the groundwater at the start of the experiment (21 μM ± 7 μM for 4HB acid and 21 μM ± 1 μM for 4H3MB acid). As biodegradation of phenols proceeded, the concentration of metabolites in the anode chamber of the CC- and OC-MFC increased to the maximum value 108 μM ± 6 μM and 104 μM ± 4 μM for 4HB acid and 4H3MB acid, respectively, after ~30 days (Fig. 1CD and EF, respectively). There was a significant difference ($P < 0.05$) in concentration of 4HB acid between the CC- and OC-MFC at day 27, and 4H3MB acid at day 27 and 34. After reaching the peak value, the concentration of metabolites decreased, indicating that the rate of the following metabolic reactions had increased and/or the rate of conversion of phenols to hydroxybenzoic acids had decreased. No significant change in metabolite concentration was observed in the S-MFC.

The metabolites also diffused from the anode chamber to the cathode chamber via the membrane. There was a significant difference in the diffusion rate of metabolites through the membrane between the CC-MFC and OC-MFC, which could have been caused by their electromigration to the anode or faster biodegradation in the CC-MFC. As shown in the text below, electromigration is likely to have affected the diffusion of metabolites within the chambers and therefore through the membrane.

The MFC systems were not stirred after day 27. Diffusion was therefore the main mechanism for mass transfer of chemicals within the anode and cathode chambers in all MFCs. The metabolites in the anode chamber were present in ionic form at pH 8 and therefore susceptible not only to diffusion but also to electromigration induced by the electrical current in the CC-MFC. The electromigration flux, J_E (Acar and Alshawabkeh, 1993), and diffusion flux, J_D (Kim et al., 2007), are given by the following equations, respectively:

$$J_E = D\frac{zFc}{RT}\frac{\Delta E}{\Delta L} \quad (1)$$

$$J_D = -D\frac{\Delta c}{\Delta L} \quad (2)$$

where D is the solute diffusion coefficient, z is the charge of the ion, F is the Faraday constant (96,485 C/mol), R is the universal gas constant (8.314 J/mol K), c is the solute molar concentration, L is the distance, T is the temperature in Kelvin and ΔE is the voltage.

We consider the mass transfer of hydroxybenzoic acids between the electrode and membrane over distance ΔL within the anode chamber at the overall MFC voltage of 60 mV. We assume that the concentration difference Δc in Eq. (2) is small compared with the term $(zFc\Delta E)/(RT)$ in Eq. (1), at 25 °C for an anion with charge −1 and voltage difference of ~30 mV between the electrode and membrane. In this case, electromigration to the electrode is a more significant mass transfer mechanism than diffusion from the electrode. The hydroxybenzoic acids will be therefore attracted to the anode in the CC-MFC, limiting their transfer to and across the membrane, explaining their lower concentration in the cathode chamber in the CC-MFC compared with the OC-MFC. With respect to field application of BES technology, negatively charged metabolites or contaminants could be drawn towards the anode, keeping the biodegrading microorganisms, contaminants, organic metabolites and electron acceptors in close proximity.

Acetate also diffused through the membrane, along the concentration gradient, and was biodegraded in the CC-MFC and OC-MFC (Fig. 1GH). There was a significant difference between the rate of acetate biodegradation in the CC-MFC and OC-MFC; starting at 1905 μM ± 53 μM at day 0, acetate decreased to 536 μM ± 8 μM, 234 μM ± 30 μM and 256 μM ± 31 μM in the OC-MFC at day 20, 27 and 34, respectively, but was not detected in the CC-MFC. During the next 72 days, a smaller amount of acetate was detected in the CC-MFC (0–6 μM) than in the OC-MFC (0–200 μM).

Acetate was biodegraded faster and eventually depleted in the presence of the electrode (Fig. 1G). As the acetate concentration decreased in the CC-MFC, the metabolite concentrations increased faster in the CC-MFC than in the OC-MFC (Fig. 1CE). Metabolite accumulation was higher in the CC-MFC compared with the OC-MFC after acetate depletion at day 27 and 34. At these time points, the concentration of phenols was significantly lower in the CC-MFC than in the OC-MFC (Fig. 1A), showing that biodegradation of phenols was enhanced. It is unclear why this trend was not sustained after day 34.

3.2. Electricity production

Electricity production in the CC-MFC started 5 days after inoculation with contaminated groundwater. The voltage then increased exponentially, reaching a maximum of 90 mV with a resistance of 1 kΩ (Fig. 2A), which was maintained for 11 days. Electricity production then fell rapidly to 11 mV, but could be quickly restored to 60–70 mV by the addition of filter-sterilized contaminated groundwater. The S-MFC did not produce any current; the voltage stayed at −0.17 mV ± 0.30 mV (1 kΩ).

Polarization curves were measured at the point of the highest voltage; the highest power output of the CC-MFC was ~1.8 mW/m^2 of projected electrode surface area, the internal resistance of the systems being 3.9 kΩ, while the OC-MFC produced only ~0.8 mW/m^2. The open circuit voltage in the CC- and OC-MFC reached approximately 550 mV, the potential of the CC-MFC cathode at open circuit being 290 ± 28 mV vs. SHE. Based on the measured cathode potential, cathode material (carbon cloth), increased nitrate concentration in the cathode chamber of the CC-MFC (Section 3.3) and pH 9, it is likely that an anion of hydrogen peroxide was produced on the cathode as a product of oxygen reduction (Song and Zhang, 2008).

To explore which carbon source in the groundwater served as an electron donor for electricity production and the Coulombic efficiency of MFCs, 4 ml of selected chemical compounds dissolved in UHQ water at the concentration found in the groundwater were added to all MFCs. Electricity generation in the CC-MFC did not increase when UHQ water (control), phenol, cresols or xylenols were added (data not shown). The addition of acetate to the MFCs induced a rapid voltage increase, in proportion to the acetate added, with a Coulombic efficiency of 54% (Fig. 2B). This demonstrated that acetate, rather than the contaminants, served as an electron donor for electricity generation.

As electro-active bacteria typically build a biofilm on the electrode (Logan, 2008), we hypothesized that the current generation in the CC-MFC reflected the development of a biofilm on the carbon electrode surface. To test this, a mature electrode (ME) from a working CC-MFC at its highest point of electricity production was removed and put into a sterile MFC (ME + S-MFC), and a sterile

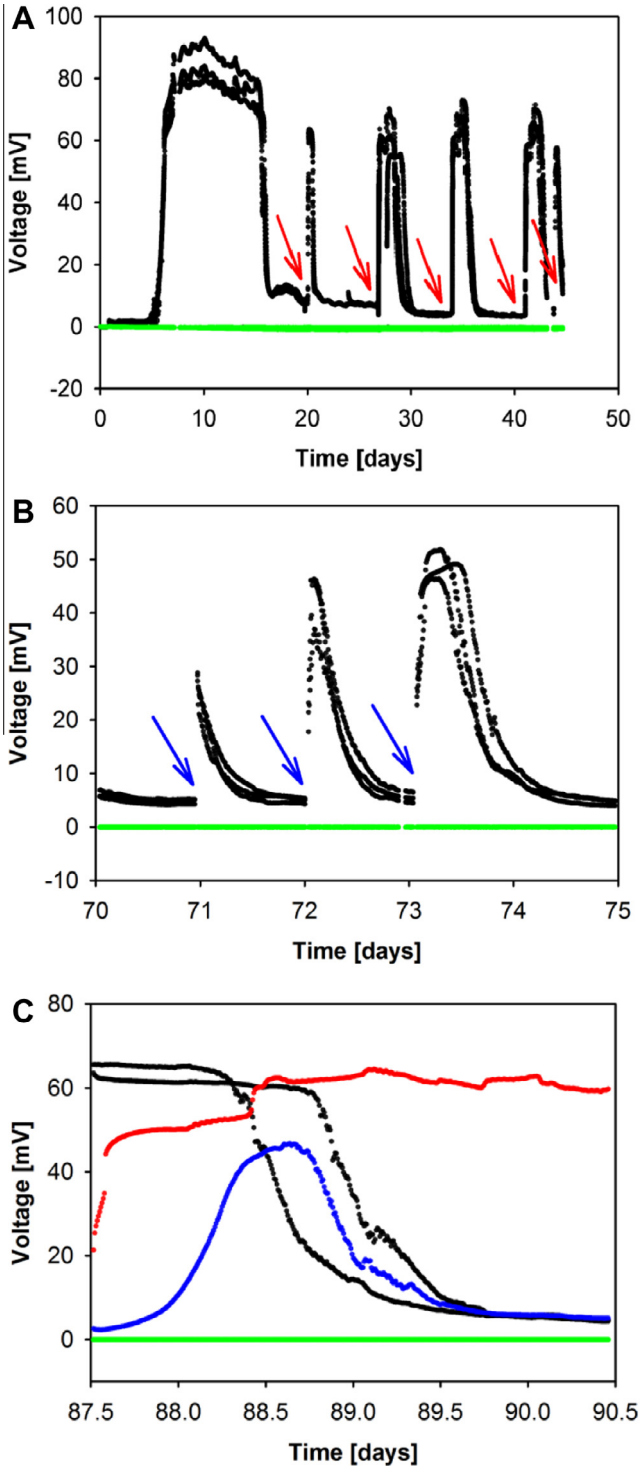

Fig. 2. Electricity production in the CC-MFCs (black), S-MFCs (green), ME + S-MFC (red) and SE + CC-MFC (blue). (A) Start of the experiment, (B) day 70–75, (C) day 87–91. Groundwater addition (red arrow), acetate addition (2.0, 3.4 and 7.7 μmol) (blue arrow). Showing all replicate data. (For interpretation of the references to color in this figure legend, the reader is referred to the web version of this article.)

electrode (SE) placed in the mature CC-MFC (SE + CC-MFC). Electricity production in ME + S-MFC started to increase immediately (Fig. 2C), indicating that current generation required a biofilm community on the electrode. In contrast, current generation was delayed in the SE + CC-MFC, most likely due to the time required for a new biofilm to form on the electrode. This is supported by SEM images of the electrodes at the end of the experiment, 5 days after the electrode exchange. The biofilm on a CC-MFC electrode was mature with a complex 3D structure, whereas only single cells had attached to the electrode fibers in a SE + CC-MFC. The results show that electrogenic biofilm on the electrode produced electricity using acetate derived from fermentation of phenols.

3.3. Electron acceptors

Various electron acceptors were available in the anode chamber. Oxygen diffused via the membrane from the cathode chamber to the anode chamber, as evident from the S-MFC data in Fig. 3AB. Oxygen was not detected in the anode chamber of the CC- or OC-MFC, indicating that it was rapidly consumed by the microbes. The rate of diffusion to the S-MFC containing sterile contaminated groundwater was slower than that reported for pure water (Kim et al., 2007). The chemicals in the groundwater would decrease the oxygen solubility in this water (Stumm and Morgan, 2013), thereby decreasing the apparent oxygen diffusion rate. For the mass balance (Section 3.4), it was assumed that any oxygen entering the anode chamber through the membrane was depleted immediately. Hence, the diffusion coefficient for pure water was used (Kim et al., 2007). The diffusion followed a linear trend as the oxygen concentration in both chambers remained the same, i.e. no oxygen detected in the anode chamber and saturated oxygen concentration in the cathode chamber. The average rate of oxygen transfer into the anode chamber was therefore 4.9 μmol/day.

As with oxygen, nitrate diffused into the anode chamber from the cathode chamber (S-MFC data), where it was used by bacteria (CC- and OC-MFC data) (Fig. 3CD). The calculated nitrate diffusion coefficient was $2.15 \cdot 10^{-7}$ cm^2/s, with an average diffusion of 1.2 μmol/day. The higher concentration of nitrate in the cathode chamber of the CC-MFC was likely due to the oxidation of ammonium or nitrous oxides by hydrogen peroxide which developed on the cathode (Section 3.2).

Iron(III) reduction occurred between days 2 and 13, causing a rapid increase in the concentration of soluble iron, from 11 μM ± 2 μM and 14 μM ± 1 μM to 43 μM ± 6 μM and 43 μM ± 8 μM in the CC-MFC and OC-MFC, respectively (Fig. 3EF). Iron reduction and electricity production started simultaneously (ca. day 5), showing that the anode was an electron acceptor as thermodynamically favorable as iron(III). It is therefore possible that the electro-active bacteria attached to the electrode belonged to iron reducers. *Geobacter* sp., a dominant iron-reducing species in the groundwater studied, could have been the primary exoelectrogenic species using acetate as an electron donor, which is typical for this bacterium (Chae et al., 2009; Logan, 2008). The concentration of soluble iron in the cathode chamber decreased rapidly, probably due to oxidation to iron(III) oxides by oxygen or hydrogen peroxide.

Sulfate reduction occurred between days 41 and 63 in both live MFCs, decreasing the sulfate concentration from 9.4 μM ± 1.7 μM and 7.9 μM ± 0.4 μM in the CC-MFC and OC-MFC, respectively, to 0.8 μM ± 0.2 μM (Fig. 3GH). This was accompanied by the formation of a black precipitate (iron sulfide) in the anode chambers of the CC- and OC-MFC (Morris et al., 2009). The respiration processes were sequential and followed theoretical predictions (Stumm and Morgan, 2013).

3.4. Conceptual model

A conceptual model of the processes occurring within the CC-MFC can be developed from the observed results.

Phenols in the anode chamber are first transformed anaerobically by oxidation or *para*-carboxylation, forming 4HB acid and 4H3MB acid. Both acids can originate from anaerobic biodegradation of phenols. 4HB acid can be produced during *para*-carboxylation of phenol (Boll and Fuchs, 2005) or anaerobic oxida-

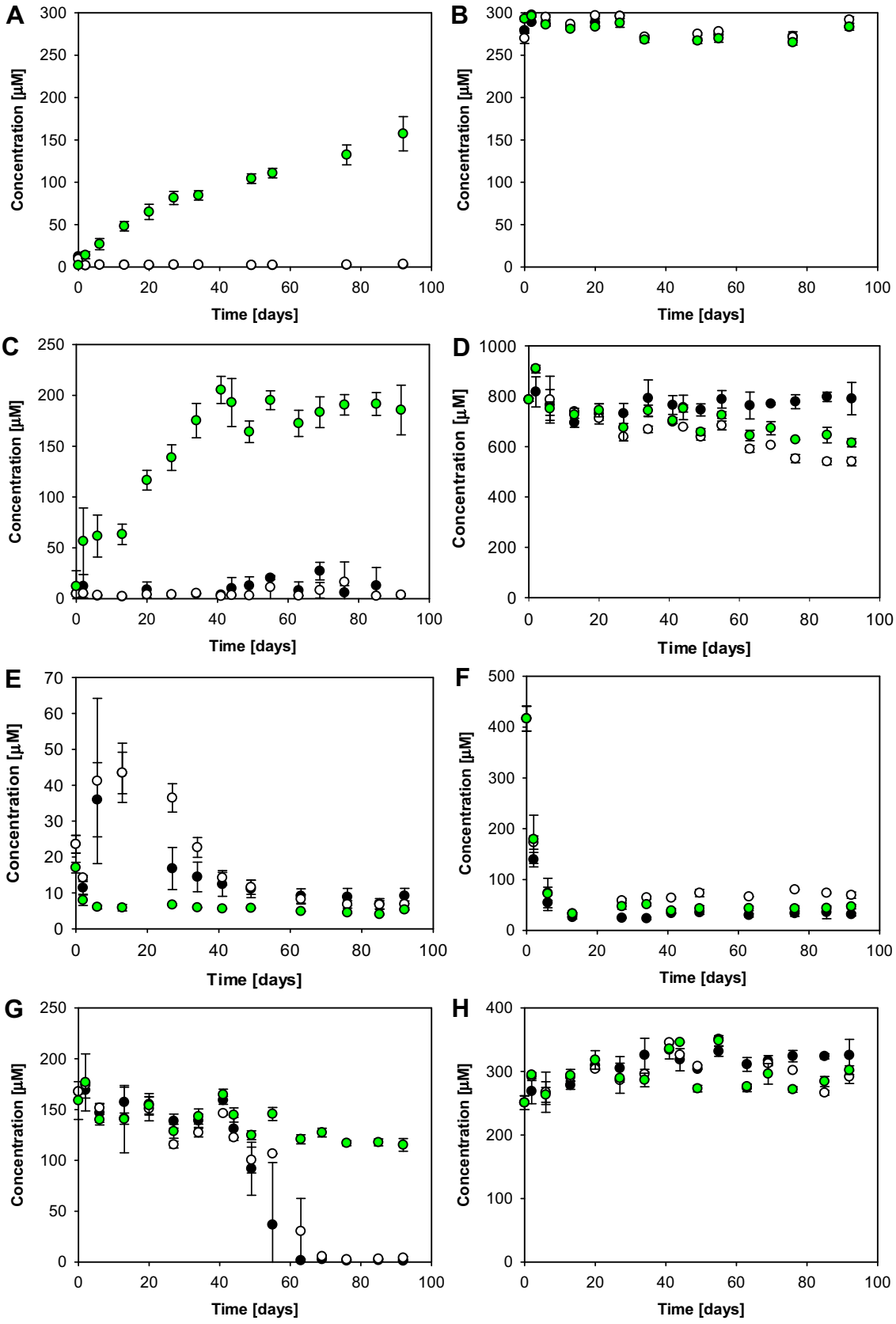

Fig. 3. Changes in concentrations of oxygen (A, B), nitrate (C, D), soluble iron (E, F) and sulfate (G, H) in the anode chamber (left) and cathode chamber (right) of the CC-MFC (black), OC-MFC (white), S-MFC (green). Average data from replicates shown with error bars representing standard deviation. (For interpretation of the references to color in this figure legend, the reader is referred to the web version of this article.)

tion of *p*-cresol (Bossert and Young, 1986), whereas 4H3MB acid is produced by *para*-carboxylation of *o*-cresol (Bisaillon et al., 1991) and presumably also from anaerobic oxidation of 2,4-xylenol. The hydroxybenzoic acids can be then biodegraded to acetyl-SCoA (Boll and Fuchs, 2005) and then acetate, to complete the fermentation of phenols (Madigan et al., 2011). As previously mentioned, fermentation is an important process for biodegradation of phenols in the contaminant plume (Watson et al., 2005). The decreased concentrations of phenols and increased concentrations of hydroxybenzoic acids are evidence of anaerobic biodegradation of phenols in the MFCs. However, it is unclear whether the biodegradation proceeded to acetyl-SCoA and further. The location of fermenting bacteria is also unknown; they could have been present in planktonic or electrode biofilm form.

Acetyl-SCoA is a central compound of metabolism. It can be transformed to acetate and also used to build biomass or enter the TCA cycle, followed by the respiratory chain (Madigan et al., 2011). Respiration was a dominant process in the MFCs and resulted in fast removal of acetate after its transfer to acetyl-SCoA. Acetate is a more metabolically favorable carbon source for bacteria than phenols (Madigan et al., 2011) and was therefore biodegraded more rapidly in the MFCs.

Based on this conceptual model, the mass balance of acetate vs. electron acceptors was calculated and compared with the total amount of acetate available. The measured amount of biodegraded acetate was corrected for diffusion through the membrane, and sampling and additions of groundwater/acetate to the MFCs. If there was more available acetate than electron acceptors, it was assumed that it was used to build biomass. The calculation was done in two parts: the first 20 days of the experiment before acetate depletion and subsequent 72 days when the MFCs were operated under acetate limitation.

Several electron acceptors were present in the MFCs to support respiration. The amount of acetate biodegraded by oxygen, nitrate, iron and sulfate respiration was the same for the CC- and OC-MFC, as calculated from previously presented data using the stoichiometry. Data from electricity production were numerically integrated according to Eq. (3) to obtain the amount of charge Q and subsequently the amount of electrons released from acetate:

$$Q = \int_{t_0}^{t_i} I\,dt = \int_{t_0}^{t_i} \frac{E}{R_{ext}}\,dt \tag{3}$$

where I is the electric current generated between time t_0 and t_i, E is the measured voltage and R_{ext} is the external resistance (Logan, 2008). Eight moles of electrons are produced from one mole of acetate. The CC-MFC biodegraded 1733 μM ± 30 μM, which is 520 μM ± 30 μM more acetate biodegraded compared with the OC-MFC (1213 μM ± 30 μM) during the first 20 days of the experiment (Table 1). This corresponds with the acetate used for electricity production (455 μM ± 30 μM). Hence, the presence of the electrode as an electron acceptor enhanced acetate removal.

The results explain why a peak in electricity production occurred when the removal of phenol reached approximately 90% in a similar study (Luo et al., 2009). Supposedly, phenol was fermented to less complex substrates (e.g. acetate), which were then utilized by exoelectrogens.

Removing a fermentation product such as acetate reduces potential feedback inhibition effects. This can theoretically accelerate fermentation and increase the biodegradation rate of phenols (Kiely et al., 2011). The concentration of total phenols in the CC-MFC was slightly lower than in the OC-MFC at two time points (day 27 and 34) after acetate depletion (Fig. 1). However, it is unclear why this trend was not maintained for the duration of the experiment.

The mass of electron acceptors available in the CC-MFC is significantly higher than in the OC-MFC, shown especially in the results for the latter 72 days of the experiment. The equivalent mass of acetate biodegraded in the CC-MFC should theoretically be higher (1306 μM + 792 μM) than the measured value 1468 μM ± 30 μM (Table 1). This indicates that more electron acceptors were available than needed for complete acetate removal. These electron acceptors could be used for the biodegradation of phenols. The CC-MFC could have therefore biodegraded 180 μM ± 10 μM more phenols than the OC-MFC. This difference between the two MFC set-ups was not observed (Fig. 1); the maximum concentration difference was 80 μM ± 20 μM at day 27. There is potentially a high amount of acetate produced by fermentation of phenols in the MFCs (approximately 1500 μM during the first 20 days and 1700 μM afterwards). As previously stated, it is unclear whether the fermentation of phenols to acetate was complete. Hence, understanding the regulation of fermentation pathways is essential for the future application of BESs for enhanced *in situ* bioremediation of phenols.

The results presented in this study demonstrate that it is crucial to identify compound(s) utilized by exoelectrogens as electron donor(s) to implement bioelectrochemically-enhanced remediation of organic contaminants. Two theoretical scenarios are possible. Firstly, the contaminants can serve directly as electron donors for extracellular electron transfer to the electrode. The presence of the electrode as an electron acceptor will therefore directly enhance their biodegradation rate. In this case, exoelectrogens should be able to transfer electrons to the electrode *and* degrade contaminants. In the second scenario, electro-active bacteria cannot directly degrade contaminants but utilize their metabolites. Our study suggests that the second scenario is more likely to occur.

4. Conclusions

Electro-active bacteria prefer easily biodegradable substrates and are therefore more likely to utilize less complex metabolites of target contaminants rather than the contaminants themselves. Removal of metabolites enhanced by electrode presence can increase the biodegradation rate of targeted organic chemicals. In this case, microbial syntrophic interactions play an important role in contaminant degradation and electricity generation. Hence, knowledge of the biodegradation pathways of the parent com-

Table 1
Mass balance of acetate in the MFCs. The total decrease in acetate results from consumption by different electron acceptors (MFC electrode and O_2, NO_3^-, Fe(III), SO_4^{2-}) and biomass synthesis. Difference in acetate decrease between the CC- and OC-MFC due to electricity production (bold). The total amount of acetate biodegraded in the CC-MFC is lower than the amount of electron acceptors available (italic).

	First 20 days			Next 72 days		
Acetate (μM ± 30 μM)	CC-MFC	OC-MFC	Difference (CC-MFC − OC-MFC)	CC-MFC	OC-MFC	Difference (CC-MFC − OC-MFC)
Total decrease measured	1733	1213	**520**	*1469*	1748	−279
Electrode	455	0	**455**	*792*	0	792
O_2, NO_3^-, Fe(III), SO_4^{2-}	326	326	0	*1306*	1306	0
Biomass	953	888	65	0	442	−442
Theoretically produced from phenols	1516	1402	114	1713	1774	−61

pound to the electron donating metabolite and their regulation, as well as the cell–cell interactions and carbon flow in the microbial community, is critical for successful application of remediation BESs at the field scale.

Acknowledgements

This study was completed while PH held a Marie Curie Early Stage Researcher Fellowship within the framework of the Marie Curie Initial Training Network ADVOCATE – Advancing sustainable *in situ* remediation for contaminated land and groundwater, funded by the European Commission, Marie Curie Actions Project No. 265063. We thank Helen Emma Mallinson, Dr. Gabriella Kakonyi, Dr. Douglas F. Call, Dr. Heather Walker and Prof. Mike Burrell for help with experimental set-up, and Dr. Paul Bentley, Andrew Fairburn, Paul Blackbourn, Chris Hill and Darren Lincoln for technical support. SEM images were acquired at the Department of Biomedical Science at the University of Sheffield.

Appendix A. Supplementary data

Supplementary data associated with this article can be found, in the online version, at http://dx.doi.org/10.1016/j.biortech.2015.09.092.

References

Acar, Y.B., Alshawabkeh, A.N., 1993. Principles of electrokinetic remediation. Environ. Sci. Technol. 27, 2638–2647.
Aulenta, F., Majone, M., 2010. Bioelectrochemical systems for subsurface remediation. In: Rabaey, K., Angenent, L.T., Schröder, U., Keller, J. (Eds.), Bioelectrochemical Systems: From Extracellular Electron Transfer to Biotechnological Application. IWA Publishing, London, New York, pp. 305–326.
Bisaillon, J.G., Lepine, F., Beaudet, R., Sylvestre, M., 1991. Carboxylation of o-cresol by an anaerobic consortium under methanogenic conditions. Appl. Environ. Microbiol. 57, 2131–2134.
Boll, M., Fuchs, G., 2005. Unusual reactions involved in anaerobic metabolism of phenolic compounds. Biol. Chem. 386, 989–997.
Bond, D.R., Holmes, D.E., Tender, L.M., Lovley, D.R., 2002. Electrode-reducing microorganisms that harvest energy from marine sediments. Science 295, 483–485.
Bossert, I.D., Young, L.Y., 1986. Anaerobic oxidation of p-cresol by a denitrifying bacterium. Appl. Environ. Microbiol. 52, 1117–1122.
Chae, K.-J., Choi, M.-J., Lee, J.-W., Kim, K.-Y., Kim, I.S., 2009. Effect of different substrates on the performance, bacterial diversity, and bacterial viability in microbial fuel cells. Bioresour. Technol. 100, 3518–3525.
Chen, Z., Zhao, Y., Bai, J., Li, H., Zhou, R., Hong, M., 2014. Migration and transformation behavior of volatile phenol in the vadose zone. Water Sci. Technol. 70, 685.
Friman, H., Schechter, A., Nitzan, Y., Cahan, R., 2013. Phenol degradation in bioelectrochemical cells. Int. Biodeterior. Biodegradation 84, 155–160.
Huang, D.-Y., Zhou, S.-G., Chen, Q., Zhao, B., Yuan, Y., Zhuang, L., 2011. Enhanced anaerobic degradation of organic pollutants in a soil microbial fuel cell. Chem. Eng. J. 172, 647–653.
Interstate Technology & Regulatory Council, 2011. Green and Sustainable Remediation: State of the Science and Practice. Interstate Technology & Regulatory Council, Washington, DC.
Kiely, P.D., Regan, J.M., Logan, B.E., 2011. The electric picnic: synergistic requirements for exoelectrogenic microbial communities. Curr. Opin. Biotechnol. 22, 378–385.
Kim, J.R., Cheng, S., Oh, S.-E., Logan, B.E., 2007. Power generation using different cation, anion, and ultrafiltration membranes in microbial fuel cells. Environ. Sci. Technol. 41, 1004–1009.
Little, B., Wagner, P., Ray, R., Pope, R., Scheetz, R., 1991. Biofilms: an ESEM evaluation of artifacts introduced during SEM preparation. J. Ind. Microbiol. 8, 213–221.
Logan, B.E., 2008. Microbial fuel cells, 1st ed. John Wiley & Sons Inc, New Jersey.
Logan, B.E., 2010. Scaling up microbial fuel cells and other bioelectrochemical systems. Appl. Microbiol. Biotechnol. 85, 1665–1671.
Logan, B.E., Hamelers, B., Rozendal, R., Schröder, U., Keller, J., Freguia, S., Aelterman, P., Verstraete, W., Rabaey, K., 2006. Microbial fuel cells: methodology and technology. Environ. Sci. Technol. 40, 5181–5192.
Luo, H., Liu, G., Zhang, R., Jin, S., 2009. Phenol degradation in microbial fuel cells. Chem. Eng. J. 147, 259–264.
Madigan, M.T., Martinko, John M., Stahl, D.A., Clark, D.P., 2011. Brock Biology of Microorganisms, 13th ed. Benjamin Cummings, San Francisco.
Mohan, S.V., Chandrasekhar, K., 2011. Self-induced bio-potential and graphite electron accepting conditions enhances petroleum sludge degradation in bio-electrochemical system with simultaneous power generation. Bioresour. Technol. 102, 9532–9541.
Morris, J.M., Jin, S., 2012. Enhanced biodegradation of hydrocarbon-contaminated sediments using microbial fuel cells. J. Hazard. Mater. 213–214, 474–477.
Morris, J.M., Jin, S., Crimi, B., Pruden, A., 2009. Microbial fuel cell in enhancing anaerobic biodegradation of diesel. Chem. Eng. J. 146, 161–167.
Rizoulis, A., Elliott, D.R., Rolfe, S.A., Thornton, S.F., Banwart, S.A., Pickup, R.W., Scholes, J.D., 2013. Diversity of planktonic and attached bacterial communities in a phenol-contaminated sandstone aquifer. Microb. Ecol.
Shah, N.W., Thornton, S.F., Bottrell, S.H., Spence, M.J., 2009. Biodegradation potential of MTBE in a fractured chalk aquifer under aerobic conditions in long-term uncontaminated and contaminated aquifer microcosms. J. Contam. Hydrol. 103, 119–133.
Song, C., Zhang, J., 2008. Electrocatalytic Oxygen Reduction Reaction. PEM Feul Cell Electrocatal. Catal. Layers Fundam. Appl.
Stumm, W., Morgan, J.J., 2013. Aquatic Chemistry: Chemical Equilibria and Rates in Natural Waters. John Wiley & Sons Inc.
Thornton, S.F., Quigley, S., Spence, M.J., Banwart, S.A., Bottrell, S., Lerner, D.N., 2001. Processes controlling the distribution and natural attenuation of dissolved phenolic compounds in a deep sandstone aquifer. J. Contam. Hydrol. 53, 233–267.
Wang, X., Cai, Z., Zhou, Q., Zhang, Z., Chen, C., 2012. Bioelectrochemical stimulation of petroleum hydrocarbon degradation in saline soil using U-tube microbial fuel cells. Biotechnol. Bioeng. 109, 426–433.
Watson, I.A., Oswald, S.E., Mayer, K.U., Wu, Y., Banwart, S.A., 2003. Modeling kinetic processes controlling hydrogen and acetate concentrations in an aquifer-derived microcosm. Environ. Sci. Technol. 37, 3910–3919.
Watson, I.A., Oswald, S.E., Banwart, S.A., Crouch, R.S., Thornton, S.F., 2005. Modeling the dynamics of fermentation and respiratory processes in a groundwater plume of phenolic contaminants interpreted from laboratory- to field-scale. Environ. Sci. Technol. 39, 8829–8839.
Wiedemeier, T.H., Rifai, H.S., Newell, C.J., Wilson, J.T., 1999. Natural Attenuation of Fuels and Chlorinated Solvents in the Subsurface. John Wiley & Sons Inc.
Williams, K.H., Nevin, K.P., Franks, A., Englert, A., Long, P.E., Lovley, D.R., 2010. Electrode-based approach for monitoring in situ microbial activity during subsurface bioremediation. Environ. Sci. Technol. 44, 47–54.
Yan, Z., Song, N., Cai, H., Tay, J.-H., Jiang, H., 2012. Enhanced degradation of phenanthrene and pyrene in freshwater sediments by combined employment of sediment microbial fuel cell and amorphous ferric hydroxide. J. Hazard. Mater. 199–200, 217–225.
Zhang, T., Gannon, S.M., Nevin, K.P., Franks, A.E., Lovley, D.R., 2010. Stimulating the anaerobic degradation of aromatic hydrocarbons in contaminated sediments by providing an electrode as the electron acceptor. Environ. Microbiol. 12, 1011–1020.
Zhao, F., Slade, R.C.T., Varcoe, J.R., 2009. Techniques for the study and development of microbial fuel cells: an electrochemical perspective. Chem. Soc. Rev. 38, 1926–1939.

Appendix D

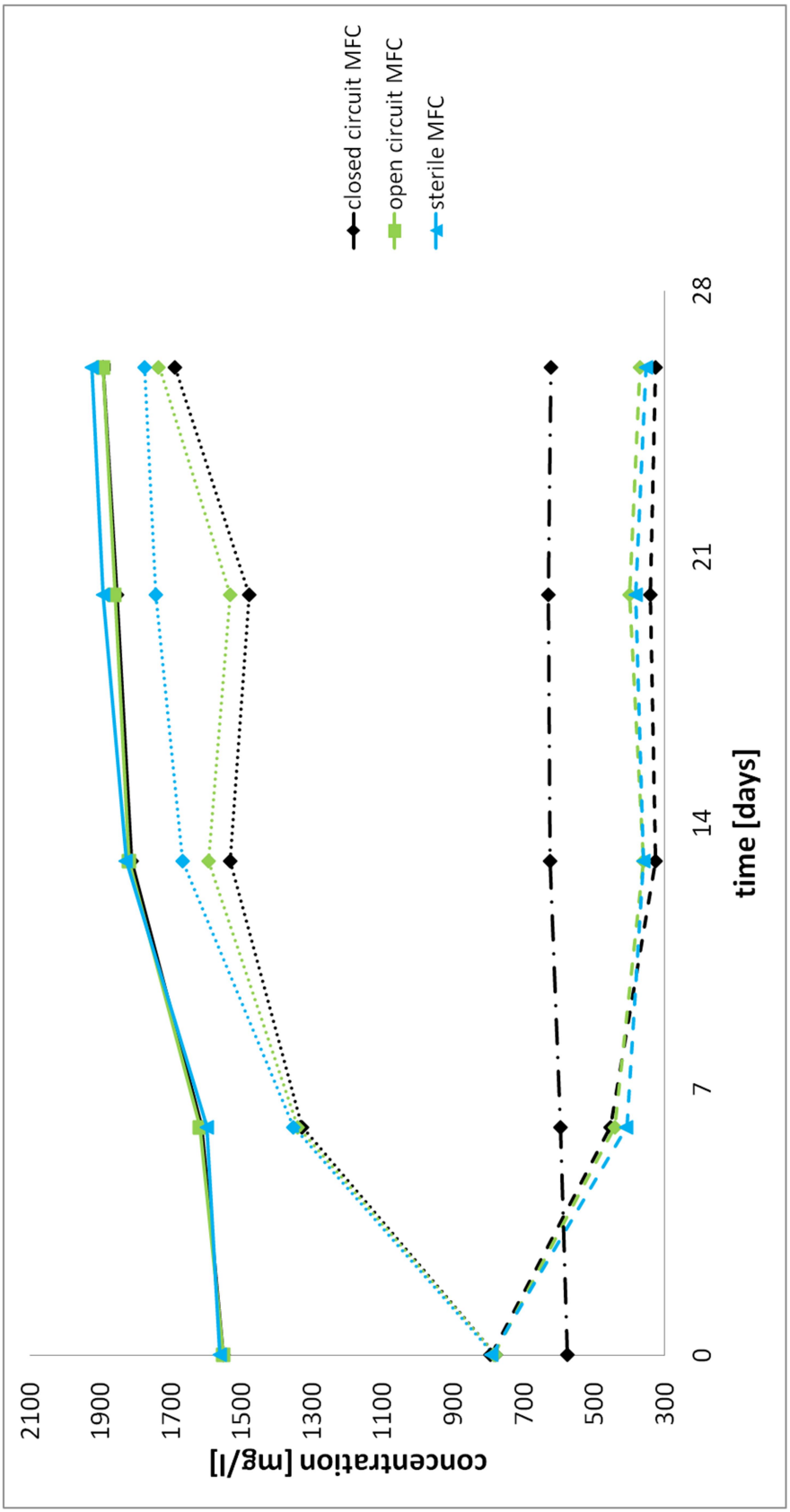

Changes in concentrations of different ions in the anode chamber of the biosludge MFC. Phosphate concentrations - solid line, sodium - dashed, sum of other cations - dotted, sum of other anions - dash + dot. Error bars not shown because their size is not significant.

Appendix E

Oxygen diffusion coefficient

Oxygen diffusion through the membrane was observed in the S-MFC. This is given by

$$c_2 = c_{1,0}\left(1 - e^{-\frac{D_{C_m} A t}{V L_t}}\right) \quad \text{(A1)}$$

where V is the volume of each chamber [cm^3], J_c the flux of oxygen [mg/cm^{3}s], A the membrane area [cm^2], D_{Cm} the diffusion coefficient [cm^2/s] and L_t the membrane thickness [cm], assuming constant oxygen concentration in the cathode chamber $c_{1,0}$ ($c_1 = c_{1,0}$ = 9 mg/cm^3) and no oxygen initially present in the anode chamber ($c_{2,0} = 0$). It was also assumed that no reaction in the anode chamber was consuming oxygen (Kim et al., 2007).

Equation A1 was linearised for easier manipulation

$$\ln\left(\frac{c_{1,0} - c_2}{c_{1,0}}\right) = -\left(\frac{A D_{C_m}}{V L_t}\right) t + E \quad \text{(A2)}$$

where E is the error of the measurement.

The equation (A2) can be simplified to

$$y = -B \cdot t + E \quad \text{(A3)}$$

where

$$y = \ln\left(\frac{c_{1,0} - c_2}{c_{1,0}}\right) \quad \text{(A4)}$$

and

$$B = \left(\frac{A \cdot D_{C_m}}{V \cdot L_t}\right). \quad \text{(A5)}$$

From the measured data

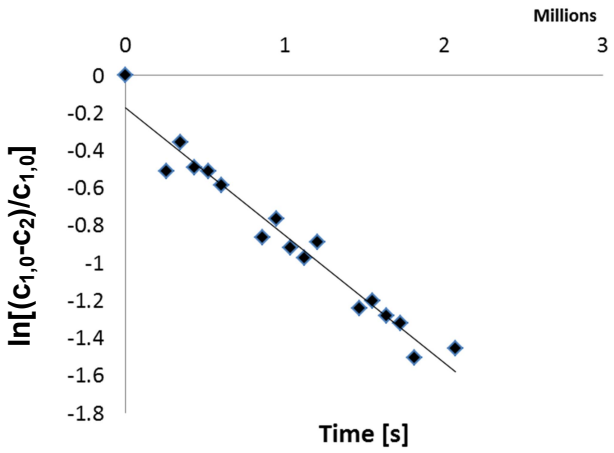

$$y = -7 \cdot 10^{-7} t - 0.1717, \text{R}^2 = 0.9588 \quad \text{(A6)}$$

therefore from equations (A3), (A5), (A6) and parameters of the experiment (V = 200 ml, L_t = 0.019 cm, A = 1.767 cm^2)

$$D_{C_m} = \frac{7 \cdot 10^{-7} \cdot V \cdot L_t}{A} = \frac{7 \cdot 10^{-7} \cdot 200 \cdot 0.019}{1.767} = 1.5 \cdot 10^{-6} cm^2/s.$$

This value is similar to the effective diffusion coefficient through the Nafion membrane measured by Kim et al. (2007) ($2.4 \cdot 10^{-6}$ cm^2/s). The membrane in their experiment was pre-treated by H_2O_2 and H_2SO_4 to increase the membrane permeability (Kim et al., 2007) which can explain the difference.

Appendix F

Phenol

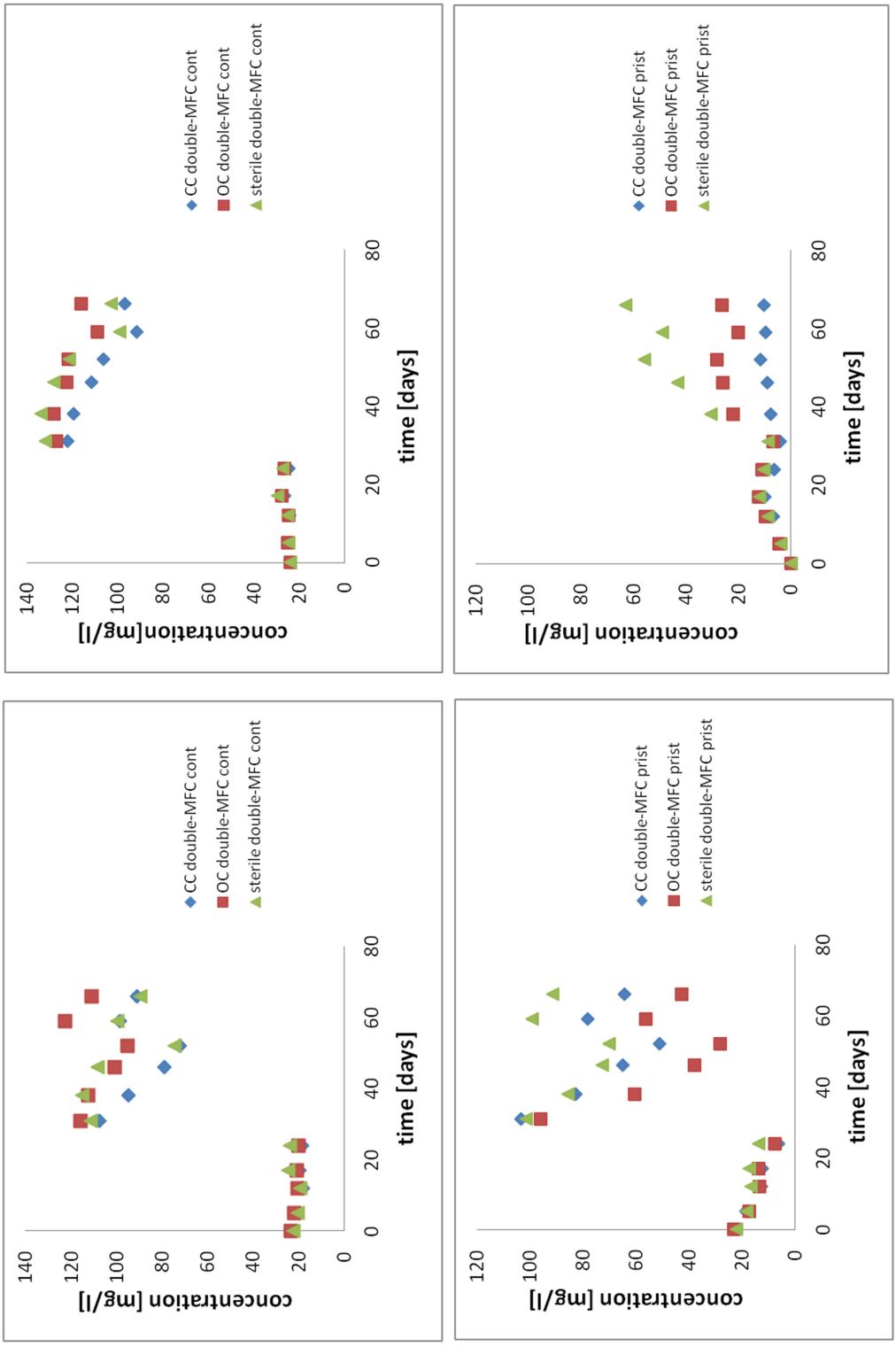

Changes in concentration of phenol in the dual-MFC cont (top), dual-MFC prist (bottom). Anode chamber - left, cathode chamber - right.

Appendix F

Cresols

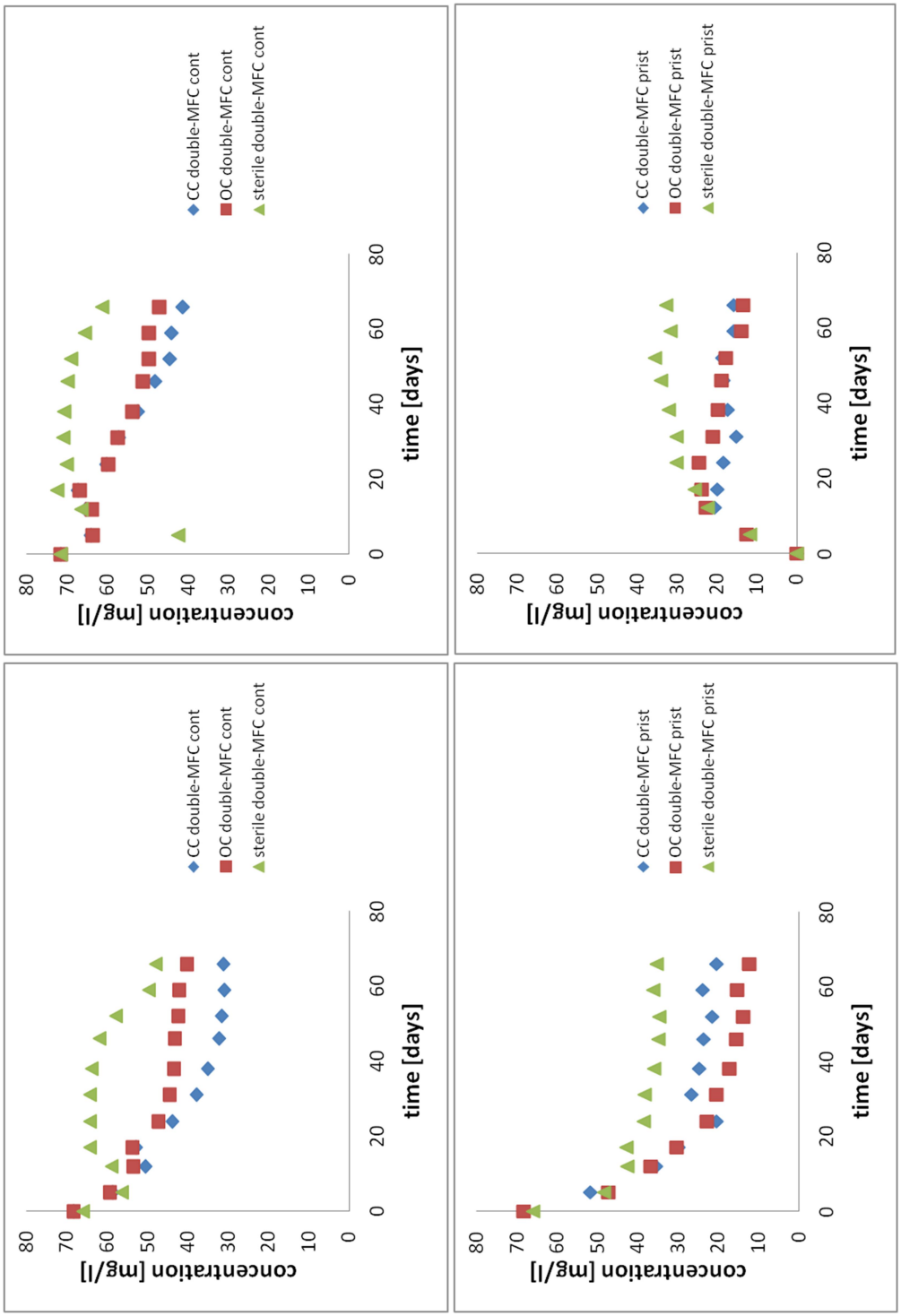

Changes in concentration of cresols in the dual-MFC cont (top), dual-MFC prist (bottom). Anode chamber - left, cathode chamber - right.

Appendix F

Xylenols

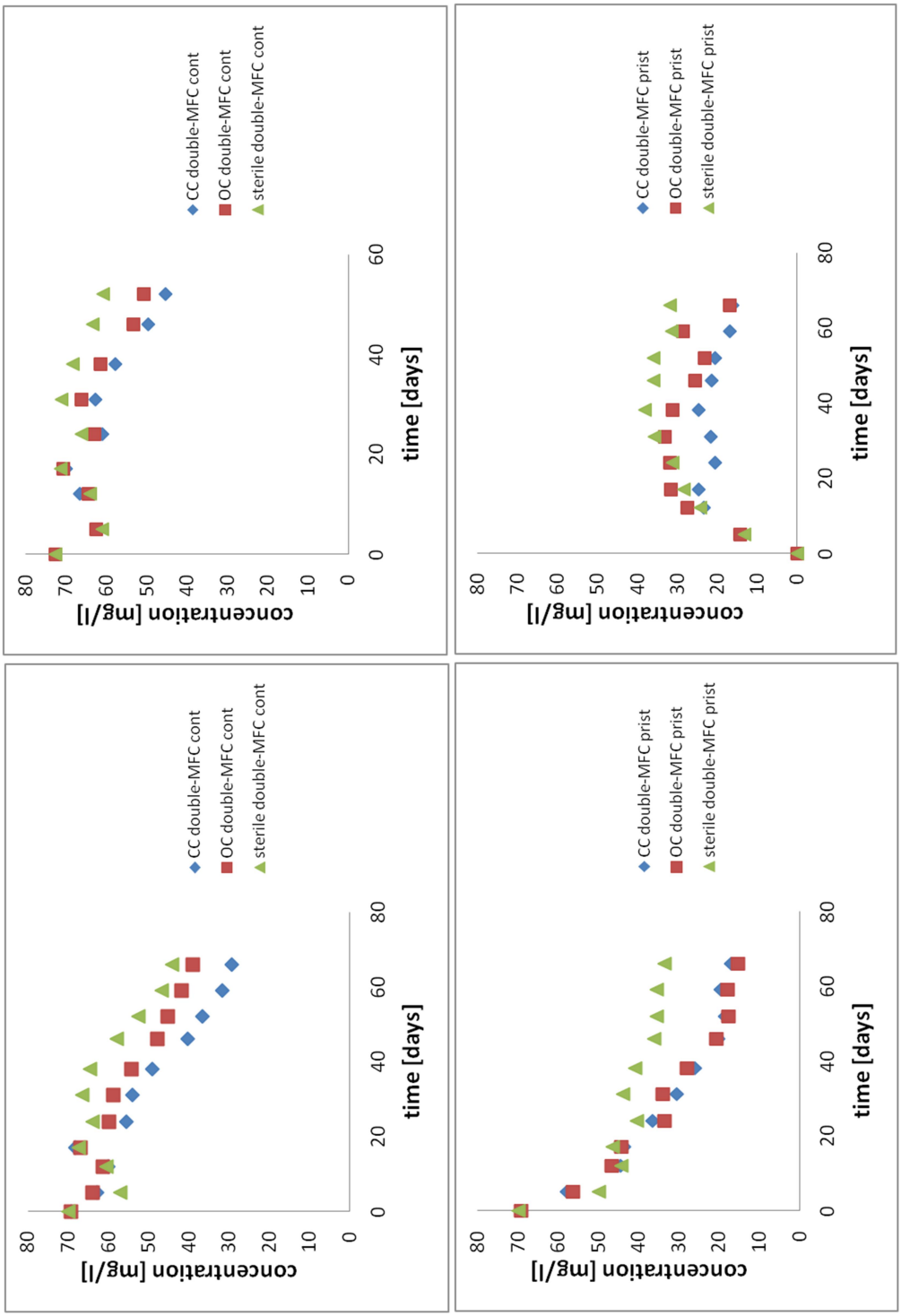

Changes in concentration of xylenols in the dual-MFC cont (top), dual-MFC prist (bottom). Anode chamber - left, cathode chamber - right.

Appendix G

Metabolite 1

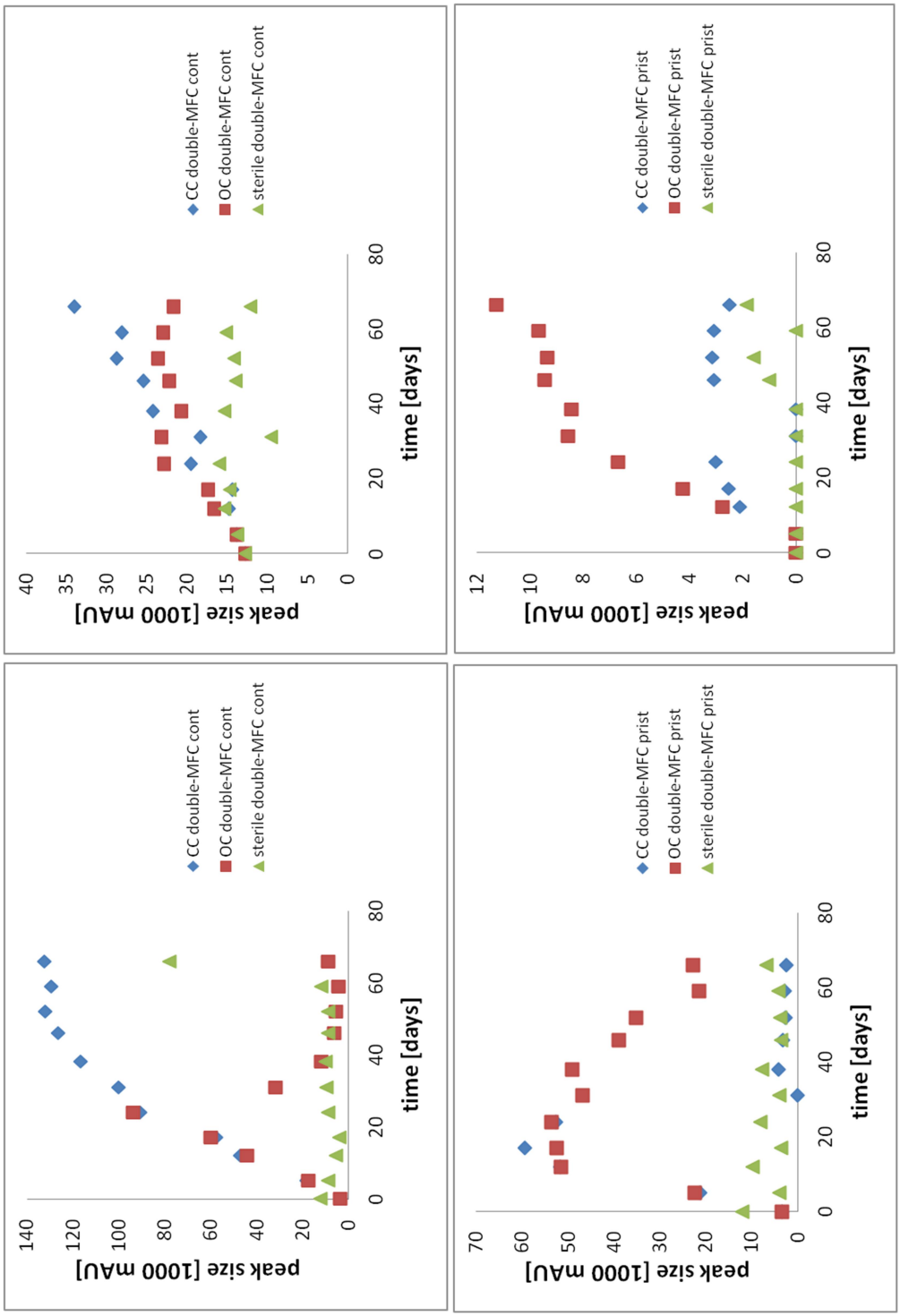

Changes in peak sizes (mAU - milliabsorbance units) of metabolite 1 in the dual-MFC cont (top), dual-MFC prist (bottom). Anode chamber - left, cathode chamber - right.

Appendix G

Metabolite 2

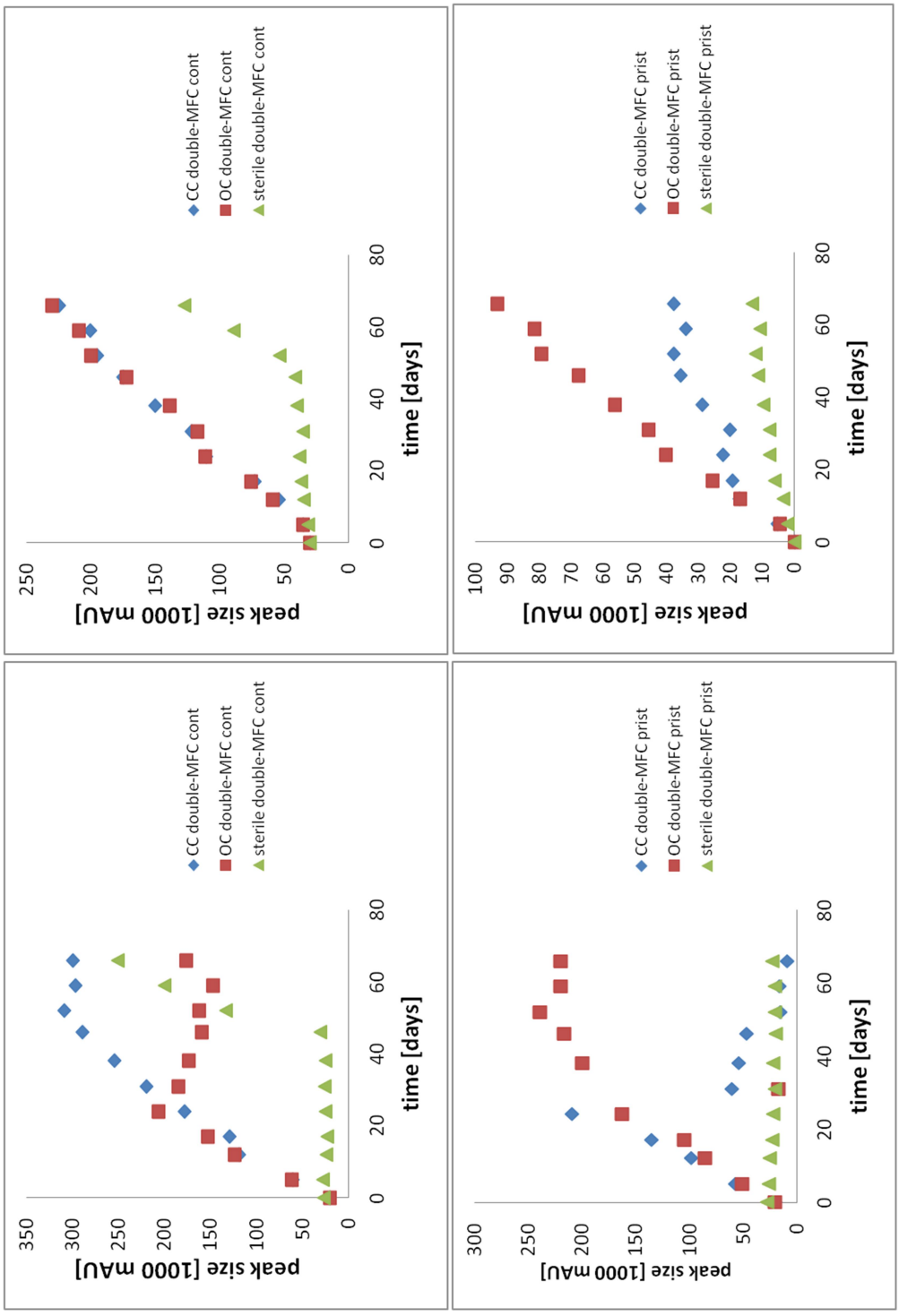

Changes in peak sizes (mAU - milliabsorbance units) of metabolite 2 in the dual-MFC cont (top), dual-MFC prist (bottom). Anode chamber - left, cathode chamber - right.

Appendix H

Mass spectra

metabolite 1

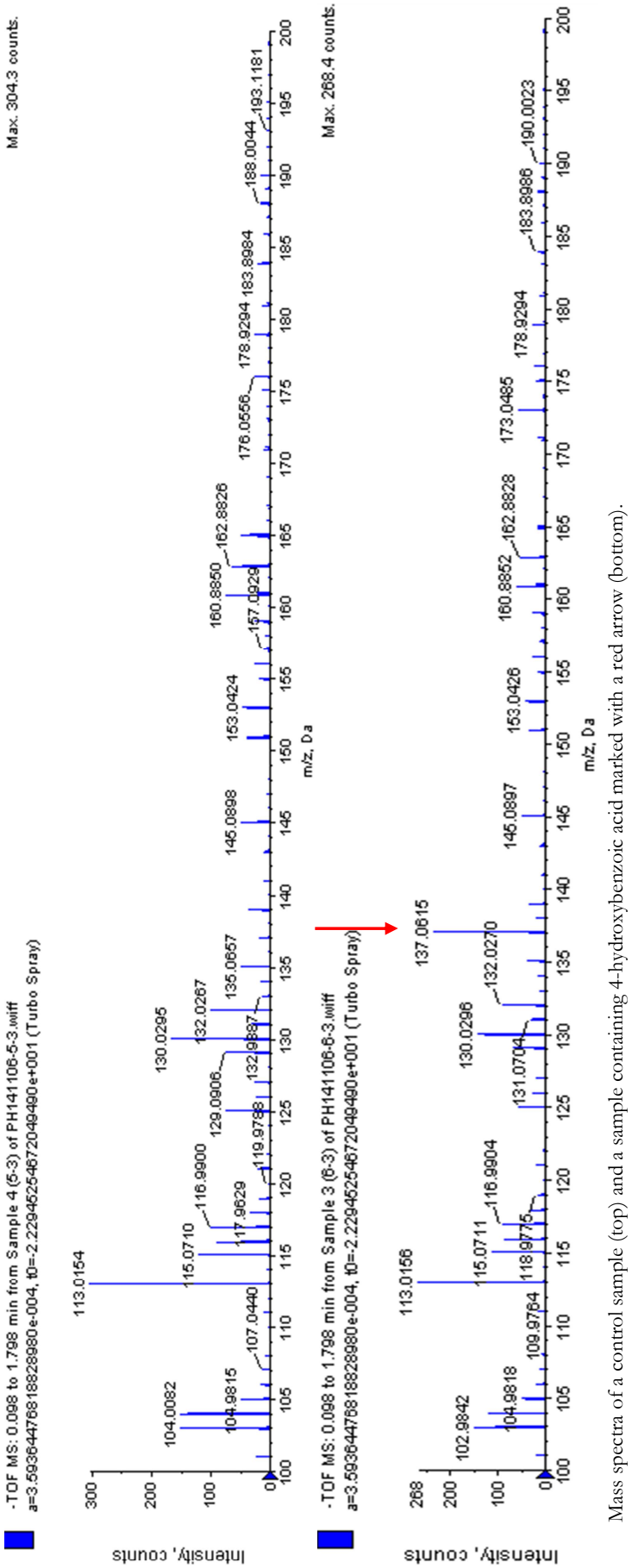

Mass spectra of a control sample (top) and a sample containing 4-hydroxybenzoic acid marked with a red arrow (bottom).

Appendix H

Mass spectra

metabolite 2

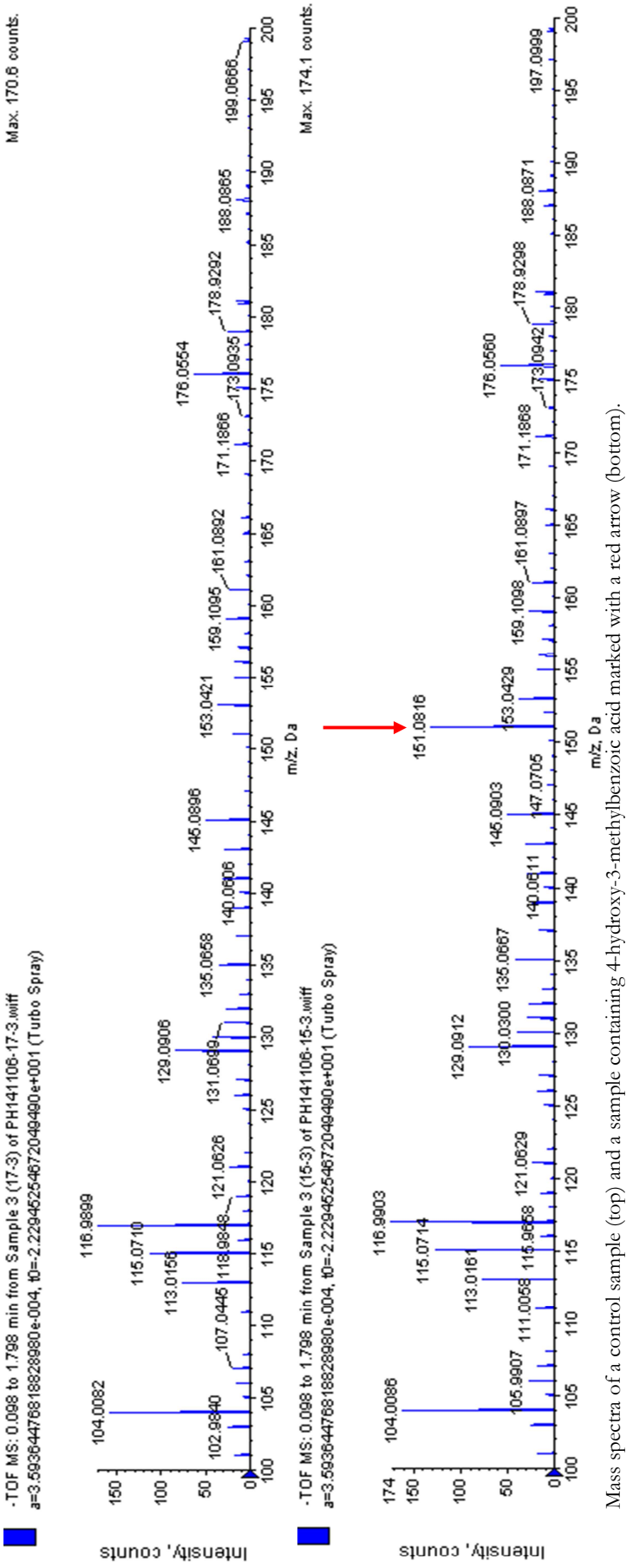

Mass spectra of a control sample (top) and a sample containing 4-hydroxy-3-methylbenzoic acid marked with a red arrow (bottom).

Appendix I

Elution times of the MFC samples and potential metabolites 4-hydroxy-2-methylbenzoic acid and 4-hydroxy-3-methylbenzoic acid

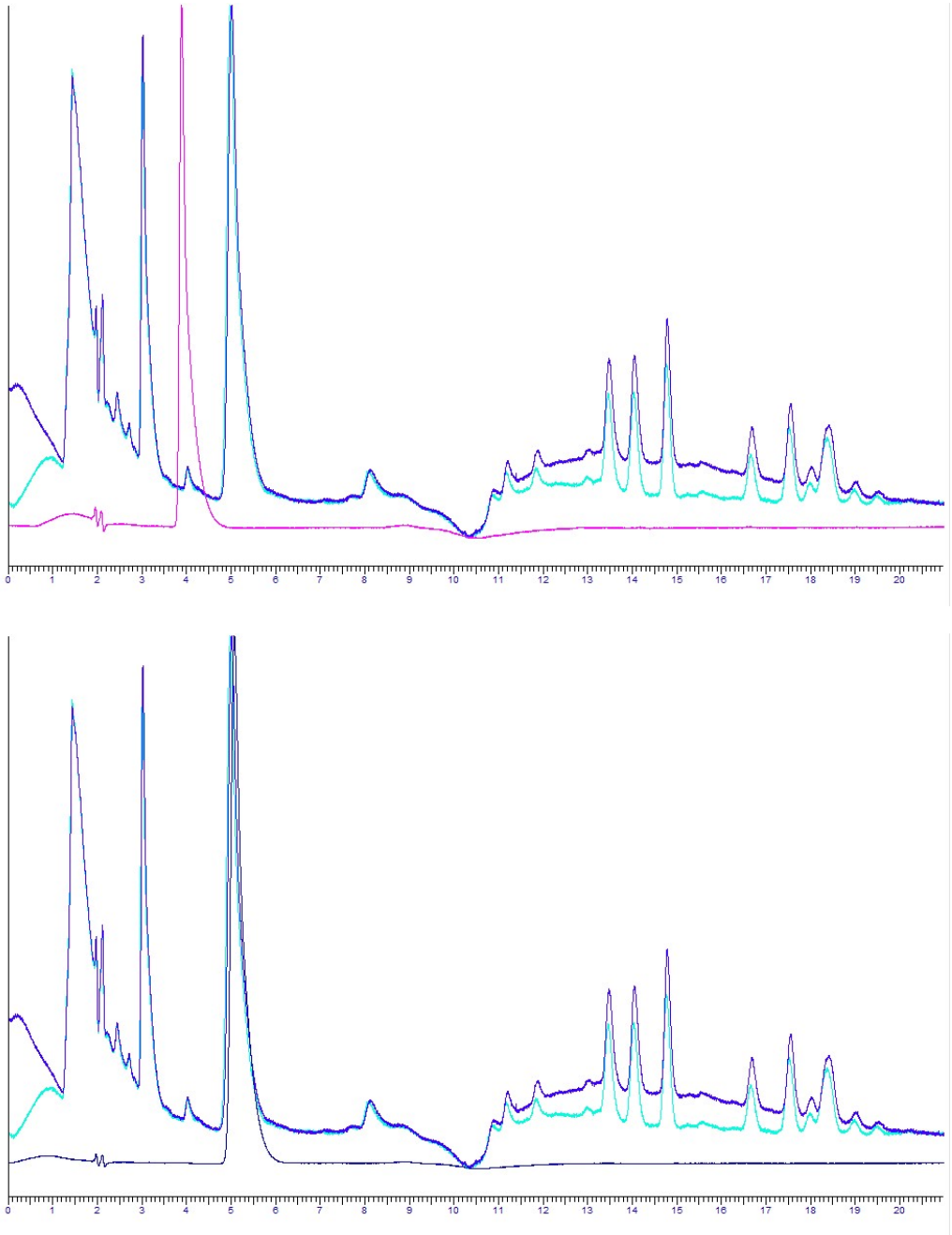

Elution profiles of MFC samples (dark and light blue) and 4-hydroxy-2-methylbenzoic acid (pink) and 4-hydroxy-3-methylbenzoic acid (black).

Appendix J

Electromigration flux J_E (Equation A7) vs. diffusion flux J_D (Equation A8) of metabolites in the anode chamber of the CC-MFC

$$J_E = D\frac{z\cdot F\cdot c}{R\cdot T}\frac{\Delta E}{\Delta L} \quad \text{(A7)}$$

$$J_D = -D\frac{\Delta c}{\Delta L} \quad \text{(A8)}$$

where D is the solute diffusion coefficient, z is the charge of the ion, F is the Faraday constant (96,485 C/mol), R is the universal gas constant (8.314 J/mol·K), c is the solute molar concentration, L is the distance, T is the temperature in Kelvin and ΔE is the voltage.*

For the maximum measured c = $100\cdot10^{-6}$ mol/dm^3, ΔE = 0.03 V and laboratory temperature 298 K

$$\frac{zFc\Delta E}{(RT)} = \frac{-1\cdot96485\cdot100\cdot10^{-6}\cdot0.03}{8.314\cdot298} = -0.117\cdot10^{-3}.$$

For the average concentration c = $0.1\cdot10^{-3}$ mol/dm^3, it was assumed that the metabolite concentration difference between the electrode and membrane (Δc) was significantly smaller than the average metabolite concentration (c) (due to the production of the metabolites in the planktonic microbial community, not only in the electrode biofilm), therefore $\Delta c < 0.1\cdot10^{-3}$ mol/dm^3 and also $\Delta c < -(zFc\Delta E)/(RT)$. In this case, electromigration to the electrode is more significant mass transfer mechanism than diffusion from the electrode.

* Electromigration flux is positive in the direction from the anode to the cathode and negative in the opposite direction.

Appendix K

Representative sequences for dominant OTUs 97% clustering threshold

AB176954|Pseudomonas
GGGGAATATTGGACAATGGGCGAAAGCCTGATCCAGCCATGCCGCGTGTGT
GAAGAAGGTCTTCGGATTGTAAAGCACTTTAAGTTGGGAGGAAGGGCATTA
ACCTAATACGTTAGTGTTTTGACGTTACCGACAGAATAAGCACCGGCTAACTT
CGTGCCAGCAGCCGCGGTAATACGAAGGGTGCAAGCGTTAATCGGAATTAC
TGGGCGTAAAGCGCGCGTAGGTGGTTC

AF100323|Pseudomonas
GGGGAATATTGGACAATGGGCGAAAGCCTGATCCAGCCATGCCGCGTGTGT
GAAGAAGGTCTTCGGATTGTAAAGCACTTTAAGTTGGGAGGAAGGGCATTA
ACCTAATACGTTGGTGTCTTGACGTTACCGACAGAATAAGCACCGGCTAACT
CTGTGCCAGCAGCCGCGGTAATACAGAGGGTGCAAGCGTTAATCGGAATTA
CTGGGCGTAAAGCGCGCGTAGGTGGTTC

AF218076|Sulfurospirillum
GGGGAATATTGCACAATGGAGGAAACTCTGATGCAGCAACGCCGCGTGGAG
GATGACGCATTTCGGTGTGTAAACTCCTTTTATAGGGGAAGATAATGACGGT
ACCCTATGAATAAGCACCGGCTAACTCCGTGCCAGCAGCCGCGGTAATACGG
AGGGTGCAAGCGTTACTCGGAATCACTGGGCGTAAAGGATGCGTAGGCTGG
AAATCAAGTCGAGAGTGAAATCCAACG

AF223382|Geobacter
GGGGAATTTTGCGCAATGGGGGAAACCCTGACGCAGCAACGCCGCGTGAGT
GATGAAGGCTTTCGGGTCGTAAAGCTCTGTCTAGAGGGAAGAAATGATATT
GGGTTAATACCCTGATTTTTTGACGGTACCTCTGAAGGAAGCACCGGCTAAC
TCCGTGCCAGCAGCCGCGGTAATACGGAGGGTGCAAGCGTTGTTCGGAATT
ATTGGGCGTAAAGCGCGTGTAGGCGGTT

AF357915|Desulfuromonas
GGGGAATTTTGCGCAATGGGCGAAAGCCTGACGCAGCAACGCCGCGTGAGT
GATGAAGGTTTTCGGATCGTAAAGCTCTGTCAGAGGGGAAGAAACTCCCGG
GTGATAATAACGCCTGGGCCTGACGGTACCCTCAAAGGAAGCACCGGCTAAC
TCCGTGCCAGCAGCCGCGGTAATACGGAGGGTGCAAGCGTTGTTCGGAATT
ATTGGGCGTAAAGCGCGTGTAGGCGGTT

AJ308319|Azotobacter
GGGGAATATTGGACAATGGGCGAAAGCCTGATCCAGCCATGCCGCGTGTGT
GAAGAAGGTCTTCGGATTGTAAAGCACTTTAAGTTGGGAGGAAGGGCAGTA
AGTTAATACCTTGCTGTTTTGACGTTACCGACAGAATAAGCACCGGCTAACTT
CGTGCCAGCAGCCGCGGTAATACGAAGGGTGCAAGCGTTAATCGGAATTAC
TGGGCGTAAAGCGCGCGTAGGTGGTTC

AY742226|Proteiniphilum
GAGGAATATTGGTCAATGGACGCAAGTCTGAACCAGCCACGTCGCGTGAAG
GAAGACGGCCCTACGGGTTGTAAACTTCTTTTGTAAGGGAATAAAGTGAGTC
ACGGGTGACTTTTTGCATGTACCTTACGAATAAGGATCGGCTAACTCCGTGC
CAGCAGCCGCGGTAATACGGAGGATCCGAGCGTTATCCGGATTTATTGGGT
TTAAAGGGTGCGCAGGCGGGAGATTAA

EF219370|Georgfuchsia
GGGGAATTTTGGACAATGGGCGCAAGCCTGATCCAGCCATTCCGCGTGAGT
GAAGAAGGCCTTCGGGTTGTAAAGCTCTTTCGGCAGGAACGAAACGGTTTG
GGCTAATACCCTGAGCTAATGACGGTACCTGAAGAAGAAGCACCGGCTAACT
ACGTGCCAGCAGCCGCGGTAATACGTAGGGTGCGAGCGTTAATCGGAATTA
CTGGGCGTAAAGCGTGCGCAGGCGGTTT

New.ReferenceOTU0
GGGGAATTTTGGACAATGGGGGAAACCCTGATCCAGCCATGCCGCGTGAGT
GAAGAAGGCCTTCGGGTTGTAAAGCTCTTTCGGCCGGGAAAAAATTGCACG
GATGAACAGTCTGTGTAGATGATGGTACCGGACTAAGAAGCACCGGCTAAC
TACGTGCCAGCAGCCGCGGTAATACGTAGGGTGCGAGCGTTAATCGGAATT
ACTGGGCGTAAAGCGTGCGCAGGCGGTTT

New.ReferenceOTU1
GGGGAATTTTGGACAATGGGCGAAAGCCTGATCCAGCCATTCCGCGTGCAG
GATGAAGGCCCTCGGGTTGTAAACTGCTTTTGTACAGAACGAAAAGGCTCTG
GTTAATACCTGGGGCTCATGACGGTACTGTAAGAATAAGCACCGGCTAACTA
CGTGCCAGCAGCCGCGGTAATACGTAGGGTGCAAGCGTTAATCGGAATTAC
TGGGCGTAAAGCGTGCGCAGGCGGTTT

New.ReferenceOTU11
AGGGAATATTAGTAATGGGCGAAAGCCTGAACTAGCAACACCGCGTGTGCG
AAGAAGGCCTTCGGGTTGTAAAGCACTTTTTGAGAGGATGAGGAAGGACGG
TACTCTCAGAATAAGTCTCGGCTAACTACGTGCCAGCAGCCGCGGTAACACG
TAGGAGGCGAACGTTATCCGGATTTATTGGGCGTAAAGCGCGTGTAGGTGG
TTTGGTAAGTAGAGCGTGAAAGCTCCTG

New.ReferenceOTU16
GAGGAATATTGGACAATGGATGGAAATCTGATCCAGCCATGCCGCGTGCAG
GAAGACAGCCCTATGGGTTTTAAACTGCTTTTATACGGGAGCAATAAGGACT
ATGCGTAGTTTGATGAGAGTACCGTACGAATAAGCACCGGCTAACTCCGTGC
CAGCAGCCGCGGTAATACGGAGGGTGCAAGCGTTATCCGGATTTATTGGGT
TTAAAGGGTGCGTAGGCGGTTTTATAA

New.ReferenceOTU2
GGGGAATTTTGCGCAATGGGCGAAAGCCTGACGCAGCAACGCCGCGTGAGT
GATGAAGGCTTTCGGGTCGTAAAGCTCTGTCGAGGGGAAAGAAGTGTACGG
GGGCTAATATCCTCTGTACTTGACGGTACCCCTAAAGGAAGCACCGGCTAAC
TCCGTGCCAGCAGCCGCGGTAATACGGGGGGTGCAAGCGTTGTTCGGAATT
ATTGGGCGTAAAGCGCGTGTAGGCGGTC

New.ReferenceOTU3
GGGGAATATTGGGCAATGGGGGAAACCCTGACCCAGCGACGTCGCGTGGG
TGACGAAATCCTTCGGGATGTAAAGCCCTGTTGTATGGGAAGATGAAAGAG
ACGGTACCATACGAGGAAGCCCCGGCAAACTACGTGCCAGCAGCCGCGGTA
ATACGTAGGGGGCAAGCGTTGTCCGGAATTACTGGGCGTAAAGCGCACGCA
GGCGGAATATCAAGTCGGTTGTAAAAGGCA

New.ReferenceOTU31
GGGGAATCTTCCGCAATGGACGAAAGTCTGACGGAGCAACGCCGCGTGTAT
GATGAAGGCCTTCGGGTTGTAAAGTACTGTCATTGGGGAAGAATGGTCGCT
ATGAAAATATTGTAGTGACATGACGGTACCCAAGAAGGAAGCCCTGGCTAAC
TACGTGCCAGCAGCCGCGGTAATACGTAGGGGGCAAGCGTTGTCCGGAATC
ATTGGGCGTAAAGGGCGCGTAGGCGGAT

New.ReferenceOTU37
GGGGAATATTGGGCAATGGGGGCAACCCTGACCCAGCAACGCCGCGTGAGT
GAAGAAGGCCTTCGGGTTGTAAAGCTCTGTCGCAGGGGAAGAAAAAAATGA
CGGTACCCTGTGAGGAAGCCCCGGCTAACTACGTGCCAGCAGCCGCGGTAA
TACGTAGGGGGCGAGCGTTGTCCGGAATTACTGGGCGTAAAGGGTGCGTA
GGTGGCTATTTAAGTTGGATGTGAAATCCC

New.ReferenceOTU4
GAGGAATTTTGCGCAATGGGGGAAACCCTGACGCAGCAACGCCGCGTGAGT
GAAGAAGGCTTTCGGGTCGTAAAGCTCTGTCAAGAGGGAAGAAAGTGGGA
GATGGTAATACTGTTTTCTATTGACGGTACCTCTGAAGGAAGCACCGGCTAA
CTCCGTGCCAGCAGCCGCGGTAATACGGGGGGTGCAAGCGTTATTCGGATT
TATTGGGCGTAAAGAGCGCGTAGGCGGTT

New.ReferenceOTU45
CGAGAATATTCCCCAATGGCCGAAAGGCTGAGGGAGCGACGCCGCGTGCGG
GAAGAAGGCCTTCGGGTCGTAAACCGCTTTTACCAAGGACGAAACATGACG
GTACTTGGAGAATAAGAGGTTGCTAACTCTGTGCCAGCAGCAGCGGTAATA
CAGAGACCTCAAGCATTATCCGGATTCATTGGGCGTAAAGGGTCCGCAGGT
GGCTGTTCACGTCAACGGTTAAATTTCAG

New.ReferenceOTU6
GAGGAATTTTGCGCAATGGGGGCAACCCTGACGCAGCAACGCCGCGTGAGT
GAAGAAGGCCTTTGGGTCGTAAAGCTCTGTCAACAGGGAAGAAGTTACAGG
TGTTTAATAGATGTCTGTATTGACGGTACCTGTGGAGGAAGCGCCGGCTAAC
TCCGTGCCAGCAGCCGCGGTAATACGGGGGGCGCAAGCGTTATTCGGAATT
ATTGGGCGTAAAGGGCGCGTAGGCGGTC

New.ReferenceOTU9
GGGGAATCTTGGACAATGGGCGAAAGCCTGATCCAGCAATGTCGCGTGTGT
GAAGAAGGCCTTAGGGTTGTAAAACACTTTCAGCAATGAAGAAGTGGTATTT
GCTAATATCAATATATCATTGACGTTAGTTGCAAAAGAAGTACTGGCTAACTC
TGTGCCAGCAGCCGCGGTAATACAGAGAGTGCAAGCGTTAATCGGAATTAT
TGGGTGTAAAGGGTGTGTAGGTGGAT

Representative sequences for dominant *Geobacter* sp. and *Desulfuromonas* sp. OTUs 99% clustering threshold

AF223382|Geobacter
GGGGAATTTTGCGCAATGGGGGAAACCCTGACGCAGCAACGCCGCGTGAGT
GATGAAGGCTTTCGGGTCGTAAAGCTCTGTCTAGAGGGAAGAAATGATATT
GGGTTAATACCCTGATTTTTTGACGGTACCTCTGAAGGAAGCACCGGCTAAC
TCCGTGCCAGCAGCCGCGGTAATACGGAGGGTGCAAGCGTTGTTCGGAATT
ATTGGGCGTAAAGCGCGTGTAGGCGGTT

AF357915|Desulfuromonas
GGGGAATTTTGCGCAATGGGCGAAAGCCTGACGCAGCAACGCCGCGTGAGT
GATGAAGGTTTTCGGATCGTAAAGCTCTGTCAGAGGGGAAGAAACTCCCGG
GTGATAATAACGCCTGGGCCTGACGGTACCCTCAAAGGAAGCACCGGCTAAC
TCCGTGCCAGCAGCCGCGGTAATACGGAGGGTGCAAGCGTTGTTCGGAATT
ATTGGGCGTAAAGCGCGTGTAGGCGGTT

New.CleanUp.ReferenceOTU0 Geobacter
GGGGAATTTTGCGCAATGGGCGAAAGCCTGACGCAGCAACGCCGCGTGAGT
GATGAAGGCTTTCGGGTCGTAAAGCTCTGTCGAGGGGAAAGAAGTGTACGG
GGGCTAATATCCTCTGTACTTGACGGTACCCCTAAAGGAAGCACCGGCTAAC
TCCGTGCCAGCAGCCGCGGTAATACGGGGGGTGCAAGCGTTGTTCGGAATT
ATTGGGCGTAAAGCGCGTGTAGGCGGTC